Current Oncological Abstract Service

COAS (Monthly)

November 2025, Volume 2 Issue 11

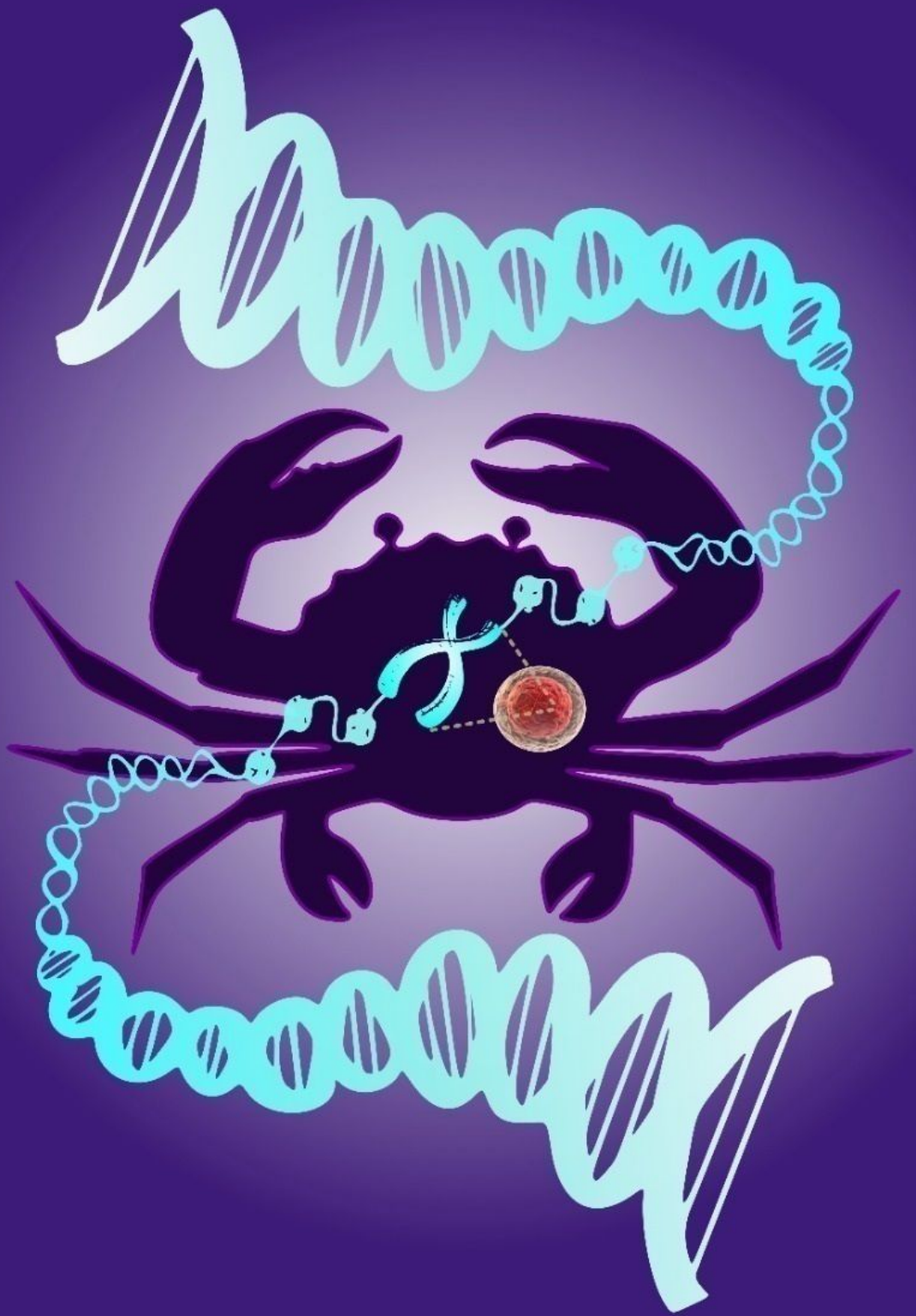

Compiled by:
Chittaranjan National Cancer Institute Library, Kolkata
(An Autonomous Body under Govt. of India, Ministry of Health & Family Welfare)

Current Oncological Abstract Service (COAS)

Monthly

Aims of the Abstracts

The Current Oncological Abstract Service (COAS) aims to provide timely, curated abstracts from a broad spectrum of oncological literature. The objectives of the service are:

1. To deliver concise, up-to-date abstracts of recently published oncological research, covering various subfields such as medical oncology, radiation oncology, anesthesiology, surgical oncology, and hematology.
2. To assist healthcare professionals, researchers, and students in staying informed about the latest advances and trends in oncology.
3. To support clinical and research-based decision-making by providing quick access to relevant, high-impact studies.
4. To foster knowledge exchange across disciplines, promoting a broader understanding of cancer-related topics.

Scope of the Abstracts

1. COAS includes abstracts from areas such as cancer biology, genetics, epidemiology, clinical trials, and treatment modalities (e.g., chemotherapy, immunotherapy, and targeted therapies), as well as patient care practices.
2. Abstracts are sourced from global research publications, offering a comprehensive view of international advancements in oncology.
3. Priority is given to high-impact studies, systematic reviews, meta-analyses, and research with significant implications for clinical practice.
4. In addition to core oncology, abstracts may cover related fields such as molecular biology, pharmacology, palliative care, and psychological support in oncology, reflecting the interdisciplinary nature of cancer care.

Layout

The "Current Oncological Abstract Service" is designed as a targeted information resource that provides clinicians, researchers, and students in oncology with the latest research abstracts and developments in cancer-related fields. It offers a regularly updated collection of abstracts from recently published articles, journals, and reports in oncology to keep users informed about current research trends, treatments, diagnostic methods, and advancements in oncology. The service is delivered monthly via email and as a downloadable PDF available on the CNCI website.

Content Sections - The COAS includes summaries of:

- The latest and most impactful research papers.
- Updates on new treatments, drugs, and clinical trials.
- Abstracts on new diagnostic tools, biomarkers, and techniques.
- Insights into cancer prevention research and epidemiological studies.
- Information on palliative care, patient management, and supportive therapies.

Abstract Formatting Each entry in the Current Oncological Abstract Service (COAS) includes:

- The title of the article or study.
- Authors and publication details.
- A summary focused on key findings and relevance.
- Keywords for easier navigation.
- A direct link to the original source (if online access is available).

User Navigation

- An index organized by cancer types, treatment methods, and research areas to facilitate easy navigation.
- A searchable database on the web platform, allowing users to quickly locate relevant abstracts.

User Engagement

- **Feedback Mechanism**: Users can provide feedback on abstracts and suggest improvements.
- **Personalization**: Users can subscribe to specific categories or topics of interest.

Bibliographical Citation:

Title-The title of the paper is invariably given in English and non-English titles are translated into English.

Author-A maximum of ten author's names are given. In case of more than ten authors, names of first ten authors are given followed by et al.

Details-The title of the paper is followed by volume number, issue number (in parenthesis), pagination and the of publication. Late publication or late receipt of the journals (if any), language(s) and number of references cited in the publication are given in parenthesis.

Abstract-Abstracts are informative and comprehensive. New data or findings are specifically indicated.

Current Oncological Abstract Service (COAS)

Editorial Board Members

Compiled by Central Library, Chittaranjan National Cancer Institute, Kolkata
Published by Chittaranjan National Cancer Institute Library, Kolkata

Current Oncological Abstract Service (COAS)

Monthly Abstracting Journal

VOLUME 2 ISSUE 11 NOVEMBER 2025

Compiler:

Dr. Sanmoy Chakraborty
Assistant **L**ibrary & **I**nformation **O**fficer

&

Mr. Ganesh Gorai
Assistant **L**ibrary & **I**nformation **O**fficer

Phone: 033 2475-9313, 033 3506-0600
Website: https://www.cnci.ac.in/
Email: cnci.library@gmail.com

DTP and Computer Processing:
CNCI Central Library

The purpose of the Current Oncological Abstract Service (COAS) is to provide users with valuable, curated oncology-related abstracts for research, educational, and informational purposes. Access to COAS materials is granted only to authorized users within CNCI, Kolkata. Use of COAS content is restricted to non-commercial, academic, and research-oriented purposes. Every effort is made to present the abstracts accurately but COAS assumes no liability for any errors and omissions.

Current Oncological Abstract Service (COAS)

Monthly Abstracting Journal

VOLUME 2 ISSUE 11 NOVEMBER 2025

Contents

Anesthesiology

25COASNOV01:

Title: Early Effect of Pulmonary Thromboendarterectomy on Right Ventricular–to–Pulmonary Artery Coupling,

Andrej Alfirevic, Mariya Geube, Junhui Mi, Haytham Elgharably, Michael Tong, Andra E. Duncan,

Journal of Cardiothoracic and Vascular Anesthesia, Volume 39, Issue 11, 2025, Pages 2989-2998,
https://doi.org/10.1053/j.jvca.2025.06.011.

Abstract: To assess intraoperative changes in the right ventricular–pulmonary artery coupling ratio, derived using right ventricular free wall strain and invasive pulmonary artery systolic pressure, following pulmonary thromboendarterectomy (PTE). Design Retrospective analysis. Setting Tertiary academic center. Participants Adult patients with chronic thromboembolic pulmonary hypertension. Interventions Pulmonary thromboendarterectomy. Measurements and Main Results Patients were categorized based on the change in the right ventricular–pulmonary artery coupling ratio between pre- and post-bypass assessments: (a) "responders"—an increase in coupling of >0.2; and (b) "non-responders"—either no significant change (≤0.2) or a decrease in coupling of >0.2. Paired t-tests were used to compare coupling, right ventricular free wall strain, and pulmonary artery systolic pressure before and after PTE. Of 67 identified patients, 11 (16%) were classified as responders, while 56 (84%) were classified as non-responders. No significant change in coupling was observed before and after PTE for the entire population (mean difference [95% CI]: 0.03 [– 0.02, 0.08], p = 0.28). The success of the PTE was confirmed by intraoperative reduction of pulmonary artery systolic pressure (mean difference [95% CI]: –15.5 [–19.8, –11.2] mmHg, p < 0.01), improvement in the 6-minute walk test (mean difference [95% CI]: 164 [76, 251] feet, p < 0.01), and a reduction in pulmonary vascular resistance (mean difference [95% CI]: –2.94 [–4.16, –1.71] WU, p < 0.01) at 6 months post-PTE. Conclusion In the majority of patients, despite successful PTE, early measurement of the coupling ratio may not show improvement. Immediate intraoperative hemodynamic or echocardiographic parameters lack the predictability to detect "responders" to surgical success.

Keywords: chronic thromboembolic pulmonary hypertension; pulmonary thromboendarterectomy; coupling ratio; right ventricular performance; right ventricular free wall strain; pulmonary artery systolic pressure

25COASNOV02:

Title: Characteristics Associated with Mortality in 623 Patients Who Received Recombinant Factor VIIa for Bleeding in Cardiac Surgery,

Allianna Mitchell, Kaitlyn Lorbiecki, Cheen Alkhatib, Andrew Gessouroun, Jianghua He, Jaromme Kim, Sara Zoubek, Morgan Whisenhunt, Trip Zorn, Brigid C. Flynn,

Journal of Cardiothoracic and Vascular Anesthesia, Volume 39, Issue 11, 2025, Pages 2948-2952,
https://doi.org/10.1053/j.jvca.2025.07.024.

Abstract: Activated recombinant factor VII (rFVIIa) has been used to treat cardiac surgical bleeding in an off-label manner. Due to the high risk of mortality with ongoing hemorrhage, assessing the risk of potential thrombotic effects of rFVIIa administration is important. This report analyzes the characteristics associated with mortality in patients who received very-low-dose rFVIIa for nonsurgical bleeding. Design A retrospective cohort study. Setting A tertiary care hospital. Participants There were 7,724 patients who had cardiac surgery from January 2012 to January 2025 with 623 receiving rFVIIa. The average dose of rFVIIa given was 18 μg/kg (min-max, 6-55 μg/kg). Interventions rFVIIa was administered perioperatively in doses of 0.5- to 1-mg aliquots. Measurements and Main Results Of the 623 patients, 66 died and 557 survived. The median dose of rFVIIa given was not different in survivors versus nonsurvivors (2.17 v 2.79 mg, respectively; p = 0.001). Procedure type was associated with mortality (p = 0.004) as patients receiving rFVIIa for heart transplant, ventricular assist device, or other complex procedure had a mortality rate of 29.5%. with the majority of these being in ventricular assist device patients. Those who underwent aortic procedures (n = 250) had a mortality rate of 12.4%. Of the 103 patients undergoing coronary artery bypass grafting who received rFVIIa, all but one patient survived. Mortality was higher in patients who had emergent or urgent surgical procedures (p < 0.001), preoperative cardiogenic shock (p = 0.021), longer cardiopulmonary bypass time (p = 0.005), postoperative cardiac arrest (p = 0.001), and received more blood products (p < 0.001). There were no associations between mortality and stroke (p = 0.071) or infections (p = 1.00). Conclusion rFVIIa can be administered to cardiac surgical patients with characteristics associated with mortality that are similar to cardiac surgical patients who did not receive rFVIIa.
Keywords: factor VIIa; cardiac surgery; bleeding; coagulopathy

25COASNOV03:
Title: Usefulness of the Recruitment-to-Inflation Ratio and Pulmonary Compliance for Assessing Pulmonary Recruitability in Cardiac Surgery Patients: A Prospective Study,
Jenny Carvalho Badas, Jaime Guembe, Celia Novials, Giulia Scandurra, Leo Jaubert, Denis Schmartz,
Journal of Cardiothoracic and Vascular Anesthesia,Volume 39, Issue 11,2025,Pages 2970-2977,
https://doi.org/10.1053/j.jvca.2025.08.014.
Abstract: To evaluate in cardiac surgery patients the potential for alveolar recruitment at 3 perioperative time points—after intubation, after cardiopulmonary bypass (CPB), and on arrival in the intensive care unit (ICU)—by collecting pulmonary compliance values and calculating the recruitment-to-inflation (R/I) ratio. Design An interventional cohort single-center study conducted in a department of anaesthesiology and critical care and an ICU Setting This interventional study was conducted in 41 patients undergoing noncomplex cardiac surgery. Ventilatory mechanics, blood gas analysis, and hemodynamic parameters were measured before, during, and after a lung recruitment maneuver (LRM) (3 minutes at a positive end-expiratory pressure [PEEP] of 12 cmH2O). The R/I ratio was calculated retrospectively at 3 time points. Participants The study included patients scheduled for elective, nonurgent cardiac surgery requiring cardiopulmonary bypass (CPB), including coronary artery bypass grafting (CABG), valve replacement, and valve repair. Interventions

R/I ratio measurement. Measurements and Main Results The proportion of recruitable patients (those with an R/I >0.5) decreased over time, from 61% (25 patients) postintubation (IOT), to 29% (12 patients) post-CPB and 17% (7 patients) in the ICU. After recruitment, lung compliance at all 3 time points was significantly higher in recruitable patients (R/I >0.5) compared to nonrecruitable patients (R/I <0.5) ($p < 0.01$). At all 3 time points, compliance before LRM did not differ significantly between the recruitable and nonrecruitable groups. Of the 123 LRMs performed in 41 patients, 11 (9%) were interrupted because of hemodynamic intolerance (defined as a >20% drop in mean arterial pressure). Conclusions In this study, an R/I ratio >0.5 identified up to 60% of patients as potentially recruitable. This parameter is particularly valuable given that PaO2, partial pressure of oxygen in arterial blood (PaO2), PaO2:fraction of inspired oxygen ratio, and prerecruitment compliance did not predict a positive recruitment response. Further studies are needed to assess the utility of the R/I ratio in individualizing PEEP settings and reducing pulmonary complications in cardiac surgery patients.

Keywords: cardiac surgery; pulmonary compliance; recruitment; R/I ratio

25COASNOV04:

Title: Hemolysis Index and Cardiopulmonary Bypass Time as Predictors of Cardiac Surgery-associated Acute Kidney Injury: An Observational Cohort Study,

Michela Di Pierro, Matteo Pozzi, Marta Frazzei, Benedetta Fumagalli, Marco Casati, Silvia Mariani,

Journal of Cardiothoracic and Vascular Anesthesia, Volume 39, Issue 11, 2025, Pages 2953-2962,
https://doi.org/10.1053/j.jvca.2025.07.038.

Abstract: Acute kidney injury (AKI) is a common and serious complication of cardiac surgery, often linked to the use and duration of cardiopulmonary bypass (CPB). The Hemolysis Index (HI) has been proposed as a surrogate marker of hemolysis and a potential predictor of cardiac surgery-associated AKI (CS-AKI). This study was designed to evaluate the associations between CPB time and HI with the onset of CS-AKI. Design An observational cohort study; retrospective analysis of prospectively collected data. Setting A single-center, Italian university tertiary care hospital. Participants Patients admitted to the cardiothoracic intensive care unit (ICU) following cardiac surgery between 2019 and 2023. Interventions HI was measured at ICU admission. CS-AKI and its severity were defined using the Kidney Disease: Improving Global Outcomes creatinine-based criteria. Associations between HI, CPB duration, and CS-AKI were assessed using logistic regression analyses, adjusting for the Cleveland Clinic Score. Measurements and Main Results A total of 1,195 patients were included in the analysis. Median age was 70 years (interquartile range [IQR] 62-75), and 310 patients (26%) were female. Median CPB duration was 110 minutes (IQR 80-140), and median HI at ICU admission was 25 (IQR 15-42). HI showed a moderate correlation with CPB duration ($r = 0.367$, $p < 0.001$). CS-AKI occurred in 103 patients (9%). In multivariable analysis, both HI and CPB time were independently associated with CS-AKI (odds ratio per 10-unit increase in HI 1.52, 95% confidence interval 1.04-2.18, $p = 0.027$; odds ratio per hour of CPB 1.32, 95% confidence interval 1.08-1.63, $p < 0.001$). Conclusions

HI and CPB time were independently associated with CS-AKI. The utility of incorporating these parameters into CS-AKI predictive models warrants further evaluation.
Keywords: cardiac surgery; acute kidney injury; hemolysis; cardiopulmonary bypass

25COASNOV05:
Title: The Prevalence and Prognostic Implications of Elevated Pulmonary Vascular Resistance in Septic Patients,
Hongmin Zhang, Beijun Gao, Ye Liu, Xiaoting Wang, Qing Zhang,
Journal of Cardiothoracic and Vascular Anesthesia,Volume 39, Issue 11,2025,Pages 2999-3008,
https://doi.org/10.1053/j.jvca.2025.06.012.
Abstract: Pulmonary vascular resistance (PVR) elevation is a critical factor contributing to acute right ventricular (RV) dysfunction. This study was designed to investigate the prevalence and prognostic significance of this condition in septic patients. Design An observational study. Setting A tertiary hospital intensive care unit. Participants A total of 638 septic patients. Intervention None. Measurements and main results Hemodynamic, echocardiographic, and prognostic data were collected. PVR was estimated using tricuspid regurgitation and RV outflow tract velocity-time integral. A PVR value exceeding 2.0 Wood units (WU) was considered abnormal. RV systolic dysfunction (RVSD) was determined by tricuspid annular plane systolic excursion, fractional area change, or RV S' velocity. Patients were categorized into four groups: (1) normal RV function (n = 205); (2) isolated RVSD (n = 76); (3) isolated PVR elevation (n = 195), and (4) RVSD + PVR elevation (n = 162). Cox regression analysis revealed that the presence of combined RVSD and PVR elevation was independently associated with 30-day mortality (hazard ratio [HR]: 2.907, 95% confidence interval [CI]: 1.385-6.100, p = 0.005). Conversely, neither isolated RVSD nor isolated PVR elevation was significantly associated with 30-day mortality (HR: 0.617, 95% CI: 0.168-2.274, p = 0.468; HR: 1.074, 95% CI: 0.469-2.461, p = 0.865, respectively). Subgroup analysis revealed that, compared with PVR ≤2.0 WU, PVR >2.0 WU was associated with 30-day mortality in patients with RVSD (HR: 3.878, 95% CI: 1.139-13.203, p = 0.030), but not in those with normal RV systolic function (HR: 1.632, 95% CI: 0.793-3.358, p = 0.183). Conclusions In septic patients, the combination of elevated PVR and RVSD was an independent predictor of 30-day mortality. However, neither PVR elevation nor RVSD alone was significantly associated with 30-day mortality. Further studies are warranted to elucidate the complex interplay between these factors in septic patients and explore potential therapeutic interventions.
Keywords: sepsis; echocardiography; pulmonary vascular resistance; prognosis

25COASNOV06:
Title: Augmented Reality-aided Rescue Ultrasound Curriculum for Perioperative Crisis Management,
Peva F. Gbagornah, Chau Tran, Jacqueline Hannan, Shirin Saeed, Nadav Levy, Christopher Kim,
Journal of Cardiothoracic and Vascular Anesthesia,Volume 39, Issue 11,2025,Pages 3020-3029,

https://doi.org/10.1053/j.jvca.2025.06.027.

Abstract: To develop anesthesiology residents' proficiency in ultrasound for managing hemodynamically unstable patients using an augmented reality-aided multimodal competency-based curriculum (rescue ultrasound [RUS] curriculum). Design This prospective study used a quasi-experimental design, involving a nonrandomized, pre-post intervention assessment of the novel competency-based RUS curriculum. Setting This study was conducted at a university hospital. Participants This single-center prospective study involved 10 attending anesthesiologists for baseline ultrasound data, 8 residents completing traditional training, and 15 residents completing the novel RUS curriculum. Interventions This study enrolled third-year categorical anesthesia (CA-3) residents to evaluate the impact of a novel RUS curriculum. Competency benchmarks were defined using performance metrics derived from motion metrics data, with expert results as a reference. The study utilized task trainers and augmented reality (HoloLens) to teach RUS skills, and clinical transferability of the curriculum's impact was evaluated through a standardized scenario with a simulated hemodynamically unstable patient. The time taken to request ultrasound was compared between the RUS-trained residents and the non-RUS-trained residents using the Mann-Whitney U test. Measurement and Results Curriculum-trained residents averaged 72.3 seconds (standard deviation = 23.2) for ultrasound calls, compared with 294.9 seconds (standard deviation = 110.6) for nontrained residents. The motion metrics-derived data (path length, acceleration, and time) of curriculum-trained residents were comparable with those of experts. Conclusion An augmented reality-aided multimodal RUS curriculum was developed as a training modality. After completion of training, residents integrated ultrasound into clinical practice at an earlier stage of hemodynamic instability and developed RUS skills that were comparable with experts' performance.

Keywords: rescue ultrasound; perioperative crisis management; residency training

25COASNOV07:

Title: Extracorporeal Cardiopulmonary Resuscitation in Hypothermic Cardiac Arrest: Severe Hypoglycemia Does Not Preclude Survival With Good Neurologic Outcome,

Michał P. Pluta, Tomasz Darocha, Hubert Hymczak, Anna Witt-Majchrzak, Ewelina Nowak, Konrad Mendrala,

Journal of Cardiothoracic and Vascular Anesthesia,Volume 39, Issue 11,2025,Pages 3038-3043,
https://doi.org/10.1053/j.jvca.2025.06.006.

Abstract: Prolonged hypoglycemia can cause irreversible brain damage. Clinicians may thus be reluctant to initiate extracorporeal cardiopulmonary resuscitation in hypothermic cardiac arrest patients with severe hypoglycemia. The aim of this study was to evaluate the survival rate with good neurologic outcomes of patients with hypothermic cardiac arrest and severe hypoglycemia. Design Retrospective study. Setting Multicenter study based on data from the HELP Registry. Participants Adult victims of accidental hypothermia with a core temperature ≤28°C and cardiac arrest who had undergone extracorporeal rewarming between January 2014 and June 2024 were included in the study. Interventions Patients with initial blood glucose concentration <3 mmol/L (<54 mg/dL) (severe hypoglycemia) were compared with those with glucose level ≥3 mmol/L (≥54 mg/dL). Survival to hospital discharge with

favorable neurologic outcome was considered the primary outcome. Measurements and Main Results The study population consisted of 127 patients, of whom 21 (17%) presented with glucose concentration <3 mmol/L (<54 mg/dL) on admission to the hospital. By hospital discharge, 8 of 21 patients (38%) with severe hypoglycemia had survived in good neurologic condition. The lowest blood glucose level in a patient who survived without neurologic deficit was 0.9 mmol/L (16 mg/dL). There was no statistically significant difference in survival rates between patients with and without severe hypoglycemia (38% v 43%, p = 0.7). Conclusions In patients with hypothermic cardiac arrest, severe hypoglycemia on admission to the hospital does not rule out survival with good neurologic outcomes after extracorporeal rewarming.

Keywords: accidental hypothermia; cardiac arrest; extracorporeal cardiopulmonary resuscitation; hypoglycemia; brain injury

25COASNOV08:

Title: The Use of Tris-hydroxymethyl Aminomethane in Patients Following Cardiac Surgery: A Retrospective Investigation,

M.A. Radosevich, P.M. Wieruszewski, A.M. LeMahieu, E.D. Wittwer,

Journal of Cardiothoracic and Vascular Anesthesia,Volume 39, Issue 11,2025,Pages 3030-3037,
https://doi.org/10.1053/j.jvca.2025.07.020.

Abstract: To compare the metabolic and hemodynamic parameters of cardiac surgery patients following the receipt of tris-hydroxymethyl aminomethane (THAM) or sodium bicarbonate alone for the treatment of postoperative metabolic acidosis. Design Retrospective chart review. Setting Single, high-volume academic cardiac surgery center. Participants A total of 2,066 adult patients who underwent cardiac surgical procedures utilizing cardiopulmonary bypass were included. Interventions The receipt of THAM or sodium bicarbonate within the first 12 hours following cardiac surgery. Measurements and Main Results The laboratory and hemodynamic parameters of cardiac surgery patients who received THAM or sodium bicarbonate for the treatment of metabolic acidosis were compared. Examples of these variables include pH, bicarbonate, PaCO2, sodium, potassium, mean arterial pressure, and vasopressor needs. Secondary outcomes included acute kidney injury, mortality, mesenteric ischemia, and intensive care unit and hospital length of stay. THAM administration was associated with significantly higher pH and mean arterial pressure compared with sodium bicarbonate alone, without contributing to hypernatremia, hypercarbia, hyperkalemia, acute kidney injury, or mortality.

Keywords: Metabolic acidosis; cardiac surgery; sodium bicarbonate; tris-hydroxymethyl aminomethane; THAM; tromethamine

25COASNOV09:

Title: Ultrasound-Guided Stellate Ganglion Block Regulates Inflammatory Cytokines and Improves Short-Term Outcome after Cardiac Surgery with Cardiopulmonary Bypass: A Randomized Clinical Trial,

Hongyuan Lv, Xiaocui Lv, Zhichao Ai, Zihao Huang, Hong Yu, Xin Yu,

Journal of Cardiothoracic and Vascular Anesthesia, Volume 39, Issue 11, 2025, Pages 3044-3052,
https://doi.org/10.1053/j.jvca.2025.06.024.

Abstract: To evaluate the effectiveness of left stellate ganglion block (SGB) for inflammatory cytokines and short-term outcomes in cardiac surgery with cardiopulmonary bypass (CPB). Design Prospective, randomized, double-blinded clinical trial. Setting Single academic center hospital. Participants We included patients aged 18 to 70 scheduled for cardiac surgery with CPB. Interventions Before anesthesia induction, the patients who were allocated to either the SGB group or the control group received SGB using either 0.5% ropivacaine or 0.9% saline. Measurements and Main Results The primary outcome was the inflammatory cytokine concentration before (T0) and 6 hours (T1), 24 hours (T2), and 5 days (T3) after the block. Secondary outcomes included the incidence of SIRS 24 hours after surgery, immune function at each time point, intraoperative and postoperative complications, 30-day mortality, intensive care unit and hospital stay, and hospitalization costs. The analysis included 25 SGB and 25 control patients. Compared with the control group, the SGB group significantly inhibited elevated TNF-α concentration at 6 hours and 24 hours after the block ($p < 0.05$). SGB significantly reduced the SIRS 24 hours after surgery, decreased the neutrophil percentage at 6 hours after the block, and increased the lymphocyte percentage at 5 days after the block. Additionally, SGB decreased the incidence of ventricular fibrillation after reperfusion, postoperative delirium, and the occurrence of Clavien-Dindo grade III-IV. Conclusions SGB effectively improves short-term outcomes in patients with cardiac surgery and CPB, possibly through modulating the neuro-endocrine-immune network to normalize sympathetic nervous system activity and stabilize perioperative tumor necrosis factor-α concentration.

Keywords: ultrasonography; nerve block; stellate ganglion; inflammatory cytokines; cardiac surgery; outcome

25COASNOV10:

Title: REMOTE Study: Feasibility and Effectiveness of Telemedicine-based Echocardiography Mentoring in Intensive Care,

Hannah Conway, Rachel Evley, Hakeem Yusuff, Rachel Wong, Gary Lau,Journal of Cardiothoracic and Vascular Anesthesia, Volume 39, Issue 11, 2025, Pages 3009-3019,
https://doi.org/10.1053/j.jvca.2025.07.019.

Abstract: To evaluate the feasibility, effectiveness, and user experiences of real-time remote mentoring for echocardiography in intensive care settings using the Remote Education, Augmented Communication, Training and Supervision (REACTS) telemedicine platform. Design Single center, mixed-methods feasibility study with convergent parallel design. Setting Adult intensive care unit at Glenfield Hospital, University Hospitals of Leicester NHS Trust. Participants Fifteen practitioners (12 novices, 3 accredited) participated between June 2020 and June 2021. Interventions Implementation of the REACTS platform for remote echocardiography mentoring with the Philips Lumify handheld ultrasound device. Measurements and Main Results Quantitative analysis demonstrated consistently high mean image quality scores (1.57-2.00/2.00) and mean report accuracy (1.86-2.00/2.00) across all echocardiographic views. All planned sessions were successfully completed with minimal

connectivity interruptions. The teaching effectiveness evaluation consistently yielded high mean scores (5.87-6.00/6.00). Thematic analysis revealed four key themes: “accessibility of expertise,” “educational value,” “technical considerations,” and “implementation challenges.” Conclusions Real-time remote mentoring for critical care echocardiography is technically feasible and educationally valuable in the intensive care setting. Although implementation challenges exist, particularly regarding technical infrastructure and scheduling, these appear surmountable with appropriate planning. Remote mentoring shows promise as a potential strategy to address current disparities in echocardiography training and supervision.

Keywords: remote mentoring; critical care ultrasound; telemedicine; medical education; point-of-care ultrasound

25COASNOV11:

Title: Effect of Combination of Subcutaneous Lidocaine With Two Different Doses of Nitroglycerin Versus Subcutaneous Lidocaine Alone for Ultrasound-guided Radial Artery Cannulation: A Randomized Controlled Trial,

Saras Singh, Rajnish Kumar, Nishant Sahay, Shagufta Naaz,

Journal of Cardiothoracic and Vascular Anesthesia,Volume 39, Issue 11,2025,Pages 2933-2939,

https://doi.org/10.1053/j.jvca.2025.05.046.

Abstract: (s) To estimate the first-attempt and overall-attempt success rates of radial artery cannulation and to compare the diameters and cross-sectional area (CSA) of the radial artery before and 5 minutes after subcutaneous administration of different doses of nitroglycerin with lidocaine. Design A double-blinded, randomized controlled study. Setting A single-center study conducted in a tertiary care hospital. Participants All adult patients aged 18 to 70 years of either sex belonging to American Society of Anesthesiologists physical status classes I, II, or III. Interventions Group C: 0.25 mL of 2% lidocaine + 0.25 mL of normal saline Group T1: 0.25 mL of 2% lidocaine + 0.25 mL of nitroglycerin 250 μg. Group T2: 0.25 mL of 2% lidocaine + 0.25 mL of nitroglycerin 500 μg. Measurements and Main Results The nitroglycerin groups (500 μg and 250 μg) had higher first-attempt success rates (77.1% and 82.6%) compared with the lidocaine group at 51.1% ($p = 0.002$, chi-square: 12.61). This could be because the subcutaneous nitroglycerin injection increased the CSA of the radial artery greater than lidocaine (7.13 ± 4.41 mm2 and 5.81 ± 4.69 mm2 v 1.33 ± 3.93 mm2; analysis of variance $F = 25.4$, $p < 0.001$). Conclusions Subcutaneous infiltration of nitroglycerin before cannulation improved the first-attempt success rate in adult patients and a comparable overall attempt success rate was obtained even with lower doses of nitroglycerin. There was an increase in the diameters of the radial artery, which would have improved the success rate.

Keywords: arterial cannulation; radial artery dimension; subcutaneous nitroglycerin; success rates; ultrasound-guided cannulation

25COASNOV12:

Title: Ipsilateral High Thoracic Ultrasound-Guided Erector Spinae Plane Block for Post-Thoracotomy Shoulder Pain in Thoracic Cancer Surgeries: A Randomized Controlled Clinical Trial,

Tamer A. Kotb, Algohary Moussa Tantawy, Essam Mahran, Osama Mahmoud Mahmoud Elbosraty,
Journal of Cardiothoracic and Vascular Anesthesia,Volume 39, Issue 11,2025,Pages 3053-3059,
https://doi.org/10.1053/j.jvca.2025.07.034.
Abstract: To assess the safety and efficacy of ultrasound-guided high thoracic erector spinae plane block (HT-ESPB) in the management of post-thoracotomy ipsilateral shoulder pain (PTISP). Design Randomized, double-blind, parallel-group, controlled, clinical trial. Setting The National Cancer Institute. Participants Seventy-six adult patients undergoing thoracic cancer surgery. Interventions Patients were randomized into two equal groups: A control group received thoracic epidural analgesia (TEA) alone (TEA group), and a study group received ultrasound-guided HT-ESPB plus TEA (ESPB group). Measurements and Main Results Outcomes included the incidence of PTISP, time to first rescue analgesia and total rescue analgesic doses for ISP, intraoperative fentanyl consumption, heart rate, mean arterial pressure, oxygen saturation, and complications. The ESPB group had a significantly lower incidence of ISP in the first postoperative hour compared to the TEA group (60.5% v 97.4%, $p < 0.001$). The ESPB group also exhibited lower postoperative visual analog scale scores, longer time to first rescue analgesia, and a reduced number of rescue analgesic doses for ISP, as well as lower heart rate and mean arterial pressure. No significant complications were reported. Conclusions Ultrasound-guided HT-ESPB is a safe and efficacious strategy for the management of PTISP. It demonstrated a significant reduction in the incidence and severity of ISP and postoperative analgesic requirements when compared to TEA alone. This approach enhanced hemodynamic stability without significant complications.
Keywords: high thoracic erector spinae plane block; post-thoracotomy shoulder pain; thoracic cancer; ultrasound

25COASNOV13:
Title: Discharge to Nonhome Locations and Association With Long-term Survival After Cardiac Surgery in Australia and New Zealand Intensive Care Units: A Retrospective Multicenter Cohort Study,
Catherine Bartlett, Ryan Ruiyang Ling, Ashwin Subramaniam, David Pilcher, Mahesh Ramanan,
Journal of Cardiothoracic and Vascular Anesthesia,Volume 39, Issue 11,2025,Pages 2978-2988,
https://doi.org/10.1053/j.jvca.2025.06.017.
Abstract: Nonhome discharge (NHD) after cardiac surgery has increased in Australia and New Zealand, but its effect on long-term survival is unclear. This study aimed to assess whether NHD, compared with home discharge (HD), was associated with decreased survival up to 4 years after surgery. Additional included evaluating the effects of discharge location, age, surgery types, and emergency status on long-term survival. Design We conducted a retrospective, multicenter, registry-based study (2018–2023). Setting We included 74 intensive care units (ICUs) across Australia and New Zealand that submitted data to the Australia New Zealand Intensive Care Society Adult Patient Database. Participants Adults (≥16 years) who underwent valvular surgery, coronary artery bypass grafting, or both and

survived hospital discharge. Interventions None. Measurements and Main Results The study involved 92,865 patients, of whom 13,444 (14.5%) experienced NHD. NHD locations comprise rehabilitation centers, aged care facilities, mental health units, acute hospitals, and other settings. Survival up to 4 years was analyzed using Cox proportional hazards models. NHD was associated with reduced survival compared with HD (hazard ratio, 1.91; 95% confidence interval, 1.75-2.09), with the strongest association within the first 12 months after discharge. The association between NHD and reduced survival was notably greater for patients younger than 65 years (hazard ratio, 2.58; 95% confidence interval, 2.20-3.03) compared with those 65 years or older (hazard ratio, 1.71; 95% confidence interval, 1.54-1.89; pinteraction < 0.001). No significant differences existed between the NHD locations. Survival rates after NHD, compared with HD, were lower across all included surgery types, including emergency and elective procedures. Conclusions NHD after cardiac surgery is associated independently with decreased long-term survival, with the highest risk observed within the first year.

Keywords: nonhome discharge; discharge location; cardiac surgery; long-term survival; intensive care; critical care

25COASNOV14:

Title: Preoperative Rectus Femoris Muscle Characteristics as Predictors of Postoperative Walking Ability in Elderly Cardiac Surgery Patients: A Prospective Observational Study,

Ryo Abe, Junji Shiotsuka, Keita Aida, Naoki Tani, Shohei Ono, Naoyuki Kimura, Shigehiko Uchino, Masamitsu Sanui,

Journal of Cardiothoracic and Vascular Anesthesia,Volume 39, Issue 11, 2025, Pages 2963-2969,
https://doi.org/10.1053/j.jvca.2025.07.041.

Abstract: Postoperative walking ability has been identified as a crucial prognostic indicator for older patients undergoing major cardiac surgeries. This study was designed to investigate the predictive value of preoperative lower extremity muscle mass and muscle echo intensity for postoperative walking ability in older patients undergoing cardiac surgeries. Design A prospective observational study. Setting A single-center study conducted at a university hospital. Participants A total of 109 elective cardiac surgery patients, 65 years of age or older, were prospectively enrolled. Interventions Preoperative muscle mass and quality of the rectus femoris were assessed using muscle cross-sectional area and echo intensity on ultrasound images, respectively. Measurements and Main Results The primary outcome of interest was the walking distance achieved in a 6-minute walk test after cardiac surgery. Multiple regression analysis was performed to identify factors independently associated with 6-minute walk distance after surgery. Higher muscle cross-sectional area and lower echo intensity of the rectus femoris, measured by ultrasonography, were associated with a significantly longer 6-minute walk distance upon discharge. Higher muscle mass and lower echo intensity were also significantly associated with shorter hospital length of stay. Conclusions The preoperative measurement of cross-sectional area and echo intensity of the quadriceps muscles can be used as a predictor of postoperative 6-minute walk distance in elderly patients undergoing cardiac surgery.

Keywords: ultrasonography; cardiac surgery; 6-minute walk distance; cross-sectional area of quadriceps muscles; muscle echo intensity

25COASNOV15:

Title: Dose-Dependent Changes in Clot Firmness in Thromboelastometry After Administration of Fibrinogen Concentrate: A Retrospective Observational Study,

Stanislaw Vander Zwaag, Imre Kukel, Kinga Towarek-Nocon, Jakob Labus, Ali Taghizadeh-Waghefi, Jens Fassl,

Journal of Cardiothoracic and Vascular Anesthesia, Volume 39, Issue 11, 2025, Pages 2940-2947,
https://doi.org/10.1053/j.jvca.2025.07.025.

Abstract: Introduction Viscoelastic point-of-care diagnostics are crucial in cardiac surgery. In the FIBTEM assay of rotational thromboelastometry (ROTEM), guidelines suggest target maximum clot firmness values to reduce perioperative bleeding. The fibrinogen doses required to meet these targets remain unclear. This study analyzed the dose-response relationship between fibrinogen concentrate (FC) and clot strength at 5 minutes (A5) and assessed the predictive value of A5 for postoperative hypofibrinogenemia. Design Single-center retrospective observational study. Setting Tertiary academic cardiac hospital. Participants 180 cardiac patients operated on between May 31, 2022, and August 31, 2024. Interventions Patients underwent 2 intraoperative ROTEM examinations and received coagulation factors. Measurements and Main Results Linear regression was used to examin the relationship between the FC dose and A5 changes. Receiver operating characteristic curves assessed the value of A5 in predicting hypofibrinogenemia and bleeding. Weight-based and estimated blood volume–based FC dosing closely correlated with A5 changes. Each 10 mg/kg increase in FC increased A5 by a mean of 1.37 mm (95% confidence interval [CI], 1.12-1.53 mm) for total body weight, 1.20 mm (95% CI, 1.08-1.33 mm) for ideal body weight, and 1.02 mm (95% CI, 0.9-1.13 mm) for lean body weight, as well as 8.857 mm (95% CI, 7.910-9.818 mm) per mg per mL of estimated blood volume. A5 ≤12 mm predicted hypofibrinogenemia (sensitivity, 77%; specificity, 94%). No thresholds predicted excessive blood loss. Conclusions Body weight–based fibrinogen dosing allows predictions of the mean changes in A5. Total, ideal, and lean body weights yielded similar correlation coefficients.

Keywords: cardiac surgery; rotational thromboelastometry; coagulation; fibrinogen

25COASNOV16:

Title: The association between volatile anaesthetic exposure and postoperative complications following bariatric surgery: A multicentre retrospective cohort study,

Karam Azem, Philip Heesen, Eitan Mangoubi, Sharon Orbach-Zinger, Roussana Aranbitski, Shai Fein, Benjamin Zribi,

Journal of Clinical Anesthesia,Volume 107,2025,112020,
https://doi.org/10.1016/j.jclinane.2025.112020.

Abstract: Despite the effectiveness of bariatric surgery for severe obesity, reoperation and acute kidney injury (AKI) remain significant complications. The impact of volatile anaesthetics on postoperative outcomes is unclear, and current guidelines lack evidence-based recommendations for anaesthetic selection. We investigated the association between

cumulative volatile anaesthetic exposure and postoperative complications following bariatric surgery. Methods This multicentre retrospective study included patients undergoing laparoscopic bariatric procedures at four Israeli centres (January 2017–May 2025). Volatile anaesthetic exposure was quantified as age-adjusted minimum alveolar concentration-hours (MAChr). We examined associations with reoperation (within 30 days) and AKI (within 7 days) and compared agent-specific effects using mixed-effects logistic regression. Results A total of 16,685 patients were included in the final analysis. Reoperation occurred in 122 patients (0.7 %) and AKI in 96 patients (0.6 %). Higher total MAChr exposure was independently associated with increased reoperation (OR 1.75, 95 % CI 1.35, 2.26; P < 0.001), and AKI (OR 1.35, 95 % CI 1.05, 1.70; P = 0.015). While isoflurane and sevoflurane showed comparable associations with reoperation risk, only sevoflurane increased AKI risk (OR 1.53, 95 % CI 1.20, 1.90; P < 0.001) versus no association with isoflurane (OR 0.89, 95 % CI 0.55, 1.38; P = 0.630), with a significant difference between these agents (P = 0.012). Conclusion Cumulative volatile anaesthetic exposure was independently associated with increased postoperative complications following bariatric surgery. The association with reoperation rate appears to be a class effect, while sevoflurane, but not isoflurane, is associated with an increased risk of AKI. However, these observational associations may be influenced by residual confounding. These hypothesis-generating findings require prospective validation before clinical recommendations can be made.
Keywords: Bariatric surgery; Anaesthetics, inhalation; Postoperative complications; Acute kidney injury; Reoperation

25COASNOV17:

Title: Impact of neoadjuvant chemotherapy on the efficacy of sugammadex for neuromuscular block reversal in ovarian cancer patients: A prospective cohort study,

Xi Huang, Xiaolan Gu, Lingxi Xing, Qinyu Bao, Rong Gao, Lianbing Gu,
Journal of Clinical Anesthesia,Volume 107,2025,112012,
https://doi.org/10.1016/j.jclinane.2025.112012.

Abstract: Study To investigate the impact of neoadjuvant chemotherapy (NAC) on the efficacy of sugammadex for neuromuscular block reversal in ovarian cancer patients. Design This is a prospective cohort study. Setting Operating room, post-anesthesia care unit (PACU), and wards of a university-affiliated teaching hospital. Patients Among the 43 patients who underwent cytoreductive surgery, 21 patients received 3 to 6 cycles of NAC with paclitaxel and carboplatin and were classified as the “Chemo group”, while 22 patients did not receive NAC before surgery and were classified as the “Non-chemo group”. Intervention During the surgery, intermittent injections of rocuronium were given based on the quantitative monitoring results of neuromuscular block. After the surgery, the patient was transferred to the PACU. Upon the reappearance of the second twitch response in train-of-four stimulation (T2), both Chemo group and Non-chemo group were given an intravenous dose of 2 mg/kg of sugammadex to reverse the rocuronium-induced neuromuscular block. Measurements The primary outcome of the study is the time from sugammadex administration to train-of-four ratio (TOFr) ≥ 0.9. The secondary outcomes include: onset time, clinical duration, recovery index, extubation time, duration of PACU stay, the average dosage of rocuronium. Main results After the administration of sugammadex, the time to TOFr ≥0.9 was longer in Chemo

group compared to Non-chemo group(5.87 ± 2.20 vs 3.22 ± 1.34 min, p < 0.001). The recovery index [2.25 (1.38, 3.00) vs 1.38 (0.75, 2.06) min, p = 0.020] and extubation time [7.50 (5.34, 10.22) vs 4.45 (4.83, 6.61) min, p = 0.002] were also longer in Chemo group. In the Chemo group, the onset time [2.5 (2.0, 4.75) vs 1.75 (1.44, 2.31) min, p = 0.001] was prolonged, the clinical duration [(39.29 ± 10.29 vs 46.23 ± 5.91 min, p = 0.011)] was shortened, and the average dosage of rocuronium (10.35 ± 2.27 vs 8.51 ± 0.69 μg·kg−1·min−1, P = 0.002) was increased compared to Non-chemo group. There was no significant difference in the duration of PACU stay between the two groups. Conclusion The study indicated that in patients who underwent NAC, the time from sugammadex administration to TOFr ≥0.9, the recovery index, and the extubation time were prolonged. Additionally, these patients experienced an textended onset time, a shortened clinical duration, and an increased average dosage of rocuronium.

Keywords: Sugammadex; Neoadjuvant chemotherapy; Neuromuscular block; Rocuronium

25COASNOV18:

Title: Comparison of three different methods of postoperative analgesic effects in laparoscopic major liver resection (systemic analgesia vs. erector spinae plane block vs. quadratus lumborum block): A randomized controlled trial,

Yu Jeong Bang, Seung Yeon Yoo, RyungA Kang, Justin Sangwook Ko, Ji-Hye Kwon, Gyu-Seong Choi, Jong Man Kim, Tae Soo Hahm, Gaab Soo Kim,

Journal of Clinical Anesthesia,Volume 107,2025,112019,
https://doi.org/10.1016/j.jclinane.2025.112019.

Abstract: This study compared the analgesic effect of single-shot erector spinae plane block (ESPB) or posterior quadratus lumborum block (QLB) versus systemic analgesia alone after laparoscopic major liver resection. Methods This randomized controlled trial was conducted at a single referral center between August 2022 and January 2024. 114 patients undergoing laparoscopic major liver resection were randomized to one of three groups: control, ESPB, or QLB (1:1:1). The control group received systemic analgesia without regional anesthesia, whereas both ESPB and QLB groups received an additional regional anesthesia using 40 mL of 0.5 % ropivacaine. The primary outcome was cumulative opioid consumption within 24 h post-surgery. Secondary outcomes included cumulative opioid consumption, pain intensity, and recovery parameters during 72 h post-surgery. Results Cumulative opioid consumption (median [IQR]) within 24 h post-surgery was not significantly different among the groups (control, 35 mg [25, 53]; ESPB, 32 mg [21, 44]; QLB, 29 mg [22, 40]; adjP > 0.99). Cumulative opioid consumption at 1 and 48 h also did not significantly differ among the three groups (adjP = 0.336 and 0.732) but was significantly lower at 72 h post-surgery (adjP = 0.032). Pain at rest during the postanesthesia care unit (PACU) stay and at 48 h post-surgery was lower in ESPB and QLB versus control, while pain when coughing in both block groups was reduced only during the PACU stay. Conclusions Neither ESPB nor posterior QLB resulted in a significant decrease in cumulative opioid consumption within 24 h after laparoscopic major liver resection.

Keywords: Erector spinae plane block; Quadratus lumborum block; Peripheral nerve block; Postoperative pain; Regional anesthesia; Laparoscopic liver resection

25COASNOV19:

Title: Safety and feasibility of intraoperative high PEEP titrated to the lowest driving pressure during anesthesia for minimally invasive abdominal surgery – Interim analysis of GENERATOR,

Tom D. Vermeulen, Galina Dorland, Liselotte Hol, Sunny Nijbroek, Ary Serpa Neto, Arthur R.A. Bouwman,

Journal of Clinical Anesthesia,Volume 107,2025,112014,
https://doi.org/10.1016/j.jclinane.2025.112014.

Abstract: The optimal level of positive end–expiratory pressure (PEEP) during minimally invasive abdominal surgery is uncertain. Intraoperative ventilation with individualized high PEEP and recruitment maneuvers can be used to keep the driving pressure (ΔP) low, but can also lead to hypotension. In addition, the resulting ΔP and feasibility of individualized high PEEP in minimally invasive abdominal surgery is unclear. Methods Planned interim analysis on safety and feasibility of 'Driving Pressure During General Anesthesia for Minimally Invasive Abdominal Surgery' (GENERATOR), an ongoing randomized clinical trial that compares individualized high PEEP, titrated to the lowest ΔP, with a standard low PEEP ventilation strategy with respect to postoperative pulmonary complications. The primary endpoint for this analysis was the proportion of patients with intraoperative hypotension. Secondary endpoints were other intraoperative complications, ventilation variables and feasibility parameters. Results From December 2023 to July 2024, 181 patients were enrolled. Data for analysis were available for 177 patients, of which 87 patients were randomized to individualized high PEEP and 90 to standard low PEEP. Intraoperative hypotension was similar between the individualized high PEEP vs standard low PEEP group (11.5 vs 11.1 %, relative risk ratio 1.0 [95 % CI 0.5–2.4], p = 1.00), while vasopressor use was higher in the intervention group. The median difference in ΔP between both groups was 6 cm H2O. Protocol compliance was 81.6 % in the individualized high PEEP group vs 97.8 % in the standard low PEEP group; most instances of non–compliance in the individualized high PEEP group concerned a level of PEEP that was too high. Discussion In minimally invasive abdominal surgery, a ventilation strategy using individualized high PEEP was not associated with a higher incidence of hypotension, but did show an increased use of vasopressors. The intervention was highly feasible, and led to a lower ΔP. These interim findings warrant confirmation in the main analysis of GENERATOR. Funding This research was funded by ZonMW, grant number 10390012110091.

Keywords: Hypotension; Positive end−expiratory pressure; PEEP; Driving pressure; Minimally invasive abdominal surgery; Surgery; Ventilation

25COASNOV20:

Title: Postoperative erector spinae plane block does not reduce morphine consumption after lumbar spinal fusion: A randomized controlled trial,

Diana Zamudio, Laura Fernández, Andrea Rodríguez, David Delgado,

Journal of Clinical Anesthesia, Volume 107,2025,112022,
https://doi.org/10.1016/j.jclinane.2025.112022.

Abstract: Postoperative pain management following spinal fusion surgery remains challenging, with opioids being the mainstay of treatment despite their potential adverse

effects. The erector spinae plane block (ESPB) has emerged as a promising regional anesthetic technique, but its efficacy in lumbar spinal fusion surgery remains controversial. Methods In this randomized, double-blind, controlled trial, we enrolled adult patients undergoing elective open posterior lumbar arthrodesis between December 2021 and July 2024. Patients were randomized to receive either bilateral ultrasound-guided ESPB with levobupivacaine (ESPB group) or no block (control group) at the end of surgery. The primary outcome was morphine consumption during the first 24 postoperative hours. Secondary outcomes included 48-h morphine consumption, pain scores at different time points, functional recovery milestones, opioid-related side effects and block complications. Results Ninety-three patients completed the study. No significant differences in 24-h (18 mg [IQR 11–28] vs 21 mg [IQR 13–34], P = 0.258) or 48-h morphine consumption were observed between the ESPB and control groups. The ESPB group demonstrated lower pain scores at initial evaluation, 6 h, and 12 h postoperatively, as well as earlier initial mobilization, shorter urinary catheter duration, and reduced incidence of dizziness. Subgroup analyses revealed superior pain control and earlier mobilization with ESPB in transforaminal lumbar interbody fusion procedures and multilevel surgeries. No block-related complications were reported. Conclusions Although postoperative bilateral ultrasound-guided ESPB provided statistically significant improvements in early pain scores and mobilization, these differences did not translate into reduced morphine consumption or meaningful clinical benefits in patients undergoing lumbar spinal fusion surgery. The optimal role of this technique in spine surgery remains to be determined.

Keywords: Erector spinae plane block; Lumbar spinal fusion; Postoperative analgesia; Randomized controlled trial; Patient-controlled analgesia

25COASNOV21:

Title: Development and validation of machine learning predictive models for gastric volume based on ultrasonography: A multicentre study,

Jie Liu, Shiqi Li, Minhui Li, Guifei Li, Niannian Huang, Bin Shu, Jie Chen, Tao Zhu, He Huang, Guangyou Duan,

Journal of Clinical Anesthesia, Volume 107, 2025,112010,
https://doi.org/10.1016/j.jclinane.2025.112010.

Abstract: Aspiration of gastric contents is a serious complication associated with anaesthesia. Accurate prediction of gastric volume may assist in risk stratification and help prevent aspiration. This study aimed to develop and validate machine learning models to predict gastric volume based on ultrasound and clinical features. Methods This cross-sectional multicentre study was conducted at two hospitals and included adult patients undergoing gastroscopy under intravenous anaesthesia. Patients from Centre 1 were prospectively enrolled and randomly divided into a training set (Cohort A, n = 415) and an internal validation set (Cohort B, n = 179), while patients from Centre 2 were used as an external validation set (Cohort C, n = 199). The primary outcome was gastric volume, which was measured by endoscopic aspiration immediately following ultrasonographic examination. Least absolute shrinkage and selection operator (LASSO) regression was used for feature selection, and eight machine learning models were developed and evaluated using Bland-Altman analysis. The models' ability to predict medium-to-high and high gastric

volumes was assessed. The top-performing models were externally validated, and their predictive performance was compared with the traditional Perlas model. Main results Among the 793 enrolled patients, the number and proportion of patients with high gastric volume were as follows: 23 (5.5 %) in the development cohort, 10 (5.6 %) in the internal validation cohort, and 3 (1.5 %) in the external validation cohort. Eight models were developed using age, cross-sectional area of gastric antrum in right lateral decubitus (RLD-CSA) position, and Perlas grade, with these variables selected through LASSO regression. In internal validation, Bland-Altman analysis showed that the Perlas model overestimated gastric volume (mean bias 23.5 mL), while the new models provided accurate estimates (mean bias −0.1 to 2.0 mL). The models significantly improved prediction of medium-high gastric volume (area under the curve [AUC]: 0.74–0.77 vs. 0.63) and high gastric volume (AUC: 0.85–0.94 vs. 0.74). The best-performing adaptive boosting and linear regression models underwent externally validation, with AUCs of 0.81 (95 % confidence interval [CI], 0.74–0.89) and 0.80 (95 %CI, 0.72–0.89) for medium-high and 0.96 (95 %CI, 0.91–1) and 0.96 (95 %CI, 0.89–1) for high gastric volume. Conclusions We propose a novel machine learning-based predictive model that outperforms Perlas model by incorporating the key features of age, RLD-CSA, and Perlas grade, enabling accurate prediction of gastric volume.

Keywords: Aspiration; Gastric volume; Machine learning; Prediction; Ultrasound

25COASNOV22:

Title: Myocardial injury and short- and long-term outcomes after oncological surgery: A large-scale retrospective cohort study,

Shaoyong Wu, Xiong Song, Yi Li, Jingxiu Huang, Xiao Ke, Chenyang Feng, Wei Xing, Fei Cao, Weian Zeng,

Journal of Clinical Anesthesia, Volume 107, 2025, 112002,
https://doi.org/10.1016/j.jclinane.2025.112002.

Abstract: Myocardial injury after noncardiac surgery (MINS) significantly contributes to perioperative mortality, yet its incidence and prognostic value in patients undergoing oncological surgery remain inadequately characterized. Methods In this retrospective cohort study, we analyzed 6277 adults (mean age 58.9 years; 60.0 % male) undergoing intermediate-to-high-risk oncological surgeries between September 2013 and September 2022 with postoperative high-sensitivity troponin I (hsTnI) measurements. Dose-response relationships between peak hsTnI and the outcomes of 30-day mortality and 30-day major adverse cardiovascular events (MACE) were modeled using multivariable Cox regression with restricted cubic splines. MINS was defined as an ischemic hsTnI elevation >26 ng/L. Long-term (365-day) mortality was analyzed using both 30-day landmark analysis and flexible parametric survival model (FPSM) to account for potential time-varying effects. Results Each standard deviation increase in log-transformed hsTnI was associated with a twofold higher risk of 30-day mortality (adjusted hazard ratio [aHR] 2.33, 95 % CI: 1.94–2.80; $P < 0.001$) and a nearly fourfold higher risk of 30-day MACE (aHR 3.91, 95 % CI: 3.47–4.42; $P < 0.001$). After excluding 22 patients with nonischemic troponin elevations, MINS occurred in 19.1 % of patients, with 98.7 % being asymptomatic. MINS independently predicted 30-day mortality (aHR 7.10, 95 % CI: 4.21–11.97; $P < 0.001$) and accounted for 53.8 % of the population-attributable risk. Adding MINS modestly improved the C-index for

30-day mortality prediction (0.831 vs. 0.797; ΔC-index, 0.034; P = 0.090) but significantly improved risk reclassification (net reclassification improvement, 31.51 %) and discrimination (integrated discrimination improvement, 0.037). Landmark analysis showed an 8.1-fold increased risk within 30 days and a sustained 1.8-fold risk from day 31 to 365. FPSM confirmed a sustained excess mortality hazard throughout the year. Conclusions MINS is common, largely asymptomatic, and strongly associated with both early and late mortality after oncological surgery. Routine troponin monitoring may help identify high-risk patients for intervention.
Keywords: High-sensitivity troponin I; Myocardial injury; Noncardiac surgery; Postoperative complications; Oncology; Prognosis

25COASNOV23:

Title: Ultrasound assessment of the effects of three different fasting regimens of clear fluids on gastric fluid volume in children,

Xiaofang Liu, Xianjun Li, Junxia Wang, Liang Zhao, Chunhong Duan, Dongmei Li, Bin Zhang,

Journal of Clinical Anesthesia, Volume 107, 2025, 112025,
https://doi.org/10.1016/j.jclinane.2025.112025.

Abstract: Two-hour minimum fasting policy for clear fluids before surgery may prolong fasting and cause negative experiences for children. One-hour minimum and/or liberal fasting policies for clear fluids can significantly shorten the fasting time. However, their effectiveness and safety remain inadequately validated. This study investigated the effects of the above three regimens on the gastric fluid volume (GFV) before anesthesia induction in children. Methods This prospective randomized controlled trial involved 147 children (1–13 years old, ASA I or II) undergoing elective tonsillectomy and adenoidectomy and were randomly allocated to three groups: Group 2: fasting clear fluids for a minimum of 2 h, Group 1: fasting clear fluids for a minimum of 1 h, and Group 0: liberal fluid fasting. Water intake was measured within 6 h before surgery. The primary outcome was GFV before anesthesia induction. Secondary outcomes included water intake behavior and adverse events. Results Among the three groups, there was no evidence for differences in GFVs. The total water intake volume within 6 h before surgery was 80.0 (IQR: 40.0–160.0) mL for Group 2, 150.0 (IQR: 72.5–300.0) mL for Group 1, and 85.0 (IQR: 40.0–180.0) mL for Group 0. The total number of water intake episodes was 1.0 (1.0–2.5), 2.5 (1.0–4.0), and 2.0 (1.0–3.0) for Group 2/1/0, respectively. The last water intake volume before surgery in Group 2/1/0 was 60 (IQR: 30–100) mL, 60 (IQR: 30–100) mL, and 40 (IQR: 20–60) mL, respectively. There were no increases in adverse events among groups. Conclusion Compared to fasting with clear fluids for 2 h, the 1-h and liberal fluid fasting regimens do not increase GFV in children before induction. Trial registration: This prospective randomized controlled trial was registered at the Chinese Clinical Trial Registration (No. ChiCTR2300078309; Date: December 5, 2023).
Keywords: Fasting regimen; Gastric fluid volume; Ultrasound; Children

25COASNOV24:

Title: Impact of Palliative Care on Psychosocial and Spiritual Outcomes in the Neonatal Intensive Care Unit,

Matthew Lin, Clara Horner, Kaytlin Butler, Olivia Bosworth, Taylor Kiernan, Jordan Nelson, Kristyn Pierce,

Journal of Pain and Symptom Management,Volume 70, Issue 5,2025,Pages 470-480.e2,
https://doi.org/10.1016/j.jpainsymman.2025.07.028.

Abstract: Context Pediatric palliative care (PPC) consultation for infants with life-limiting conditions provides parents and caregivers with opportunities to participate in advance care planning, shared decision-making, and to receive appropriate psychosocial and spiritual supports. Objectives To evaluate the impact of PPC consultation on spiritual, psychosocial, and communication outcomes for infants that died in the NICU. Methods Retrospective chart review of infants who died in a level IV NICU over a 10-year period (2014–2024). Mann-Whitney U and Chi-square or Fisher's exact tests were used to evaluate demographic and medical differences between infants with and without PPC consultation. Regression analyses were used to evaluate the impact of PPC on psychosocial, spiritual, and communication outcomes after adjusting for relevant covariates. Results There were significant medical and demographic differences between infants with PPC and no PPC consultation. Infants with PPC consultation had significantly higher odds of referral to child life, participation in memory making activities, documentation of family meetings and advance care planning discussions, and a higher incidence rate ratio of NICU social work visits and family meetings during their admission after adjusting for potential confounders. Conclusion PPC consultation is associated with improved psychosocial, spiritual, and communication support utilization for seriously ill NICU infants and their families.

Keywords: Pediatric palliative care; neonatology; pediatrics

25COASNOV25:

Title: Timely Documentation of CPR Codes and Medical Treatment Preferences in the EHRs of Nursing Homes,

Gary Y.C. Yeung, Martin Smalbrugge, Martine C. de Bruijne, Mariska Bot, Hylco Bouwstra, Nienke Fleuren, Karlijn J. Joling,

Journal of Pain and Symptom Management,Volume 70, Issue 5,2025,Pages 427-436.e1,
https://doi.org/10.1016/j.jpainsymman.2025.07.022.

Abstract: Context Timely documentation of cardiopulmonary resuscitation (CPR) code and medical treatment preferences in electronic health records (EHR) is important for translating advance care planning conversations into actionable medical orders. Objectives To examine documentation rates of CPR code and medical treatment preferences within the recommended first six weeks of admission in Dutch nursing homes (NHs) from 2017 to 2022. Methods This retrospective cohort used EHR from 74 Dutch NHs. We assessed the prevalence of documented CPR codes and medical treatment preferences within six weeks of admission, and the median days until first documentation. To examine whether timely documentation odds improved annually, logit generalized estimating equation models - accounting for clustering of residents within NHs– were used, stratified by NH care type, and adjusted for resident factors. Results We included 163,180 residents. CPR code and medical

treatment preferences was documented within 6 weeks of admission for 88% and 64% of the residents, respectively. The median time to first documentation were 0.5-2 days across care types. Overall, between 2017 and 2022, timely documentation of CPR code increased from 82% to 92% and for medical treatment preferences from 56% to 70%. Recent admission year was associated with higher odds of timely documentation for both type of orders in psychogeriatric and somatic care, and for CPR in rehabilitation care. Conclusion Most residents had documented CPR code and medical treatment preference within the recommended six weeks of admission, with rates improving from 2017 to 2022. The improvement coincided with a national quality indicator introduced in 2018 and the COVID-19 pandemic.
Keywords: Advance care planning; physician treatment order; electronic health record; nursing homes; cardiopulmonary resuscitation code

25COASNOV26:
Title: Clinician Perspectives on Open Notes in Oncology Palliative Care: A Mixed-Methods Study,
Joanna Veazey Brooks, Delisia Chapman-Brown, Amanda Thimmesch, Elizabeth Wulff-Burchfield, Christian Sinclair, Daniel English, Heather Nelson-Brantley,
Journal of Pain and Symptom Management, Volume 70, Issue 5, 2025, Pages 410-421,
https://doi.org/10.1016/j.jpainsymman.2025.07.014.
Abstract: Context The 21st Century Cures Act Interoperability and Information Blocking Rule (IBR) has the laudable goal of increased transparency in sharing health information with patients and informed decision-making by patients, yet strategies to support IBR implementation are sparse. Without evidence-based guidelines, health systems and palliative care clinicians have been left to navigate implementation of the IBR on their own. Objectives We sought to understand clinician perspectives and experiences with the IBR in oncology and palliative care. Methods We used a convergent parallel mixed method design with clinician surveys and interviews. Results 29 clinicians from one institution participated in the study. Three themes emerged from the data: 1) specialty-specific worry about harm; 2) documentation changes in response to the IBR; and 3) sharing notes as a helpful tool. We found that clinicians see benefits and concerns around the IBR. Oncology clinicians worried more about the sensitivity of test results while palliative care clinicians worried more about the sensitivity of information included in documentation of family meetings and of prognostic information. Conclusion Findings from our study indicate that clinicians' experience with the IBR is more nuanced than the initial worry expressed by clinicians in editorials. Additionally, our study shows the importance of capturing specialty-specific experiences with the IBR, as concerns can differ. Future research should continue to examine clinician and organizational practices around implementation of the IBR to identify best practices for maximizing patient and clinician benefit while minimizing unintended harm.
Keywords: Information blocking rule; oncology palliative care; open notes; patient communication

25COASNOV27:
Title: Depression and Cancer Pain: Mediating Roles of Anxiety and Pain Beliefs,

Eun-Jung Shim, Hyeju Ha, Chan-Woo Yeom, Kyung-Lak Son, Won-Hyoung Kim, Bong-Jin Hahm,
Journal of Pain and Symptom Management, Volume 70, Issue 5, 2025, Pages 481-489,
https://doi.org/10.1016/j.jpainsymman.2025.07.030.
Abstract: Context The psychological mechanisms linking depression and pain in cancer remain unclear despite consistent evidence of their strong association. Objectives To investigate psychological pathways underlying the relationship between depression and pain, mediated by anxiety and pain-related beliefs. Methods The participants were 140 adults with a confirmed cancer diagnosis, recruited from three university hospitals in South Korea between April 2024 and May 2025. Participants completed self-report questionnaires, including the M. D. Anderson Symptom Inventory, Hospital Anxiety and Depression Scale, and the Pain Beliefs and Perceptions Inventory. Results A serial-parallel mediation analysis revealed no significant direct effects of depression on pain severity. However, a significant indirect effect was observed through anxiety and the belief that pain is persistent (Time) (b = 0.101, 95% CI [0.032, 0.185]). This pathway differed significantly from other indirect effects. Higher depression levels were associated with greater anxiety, which, in turn, was associated with a stronger belief that pain is persistent, and ultimately, with higher pain severity. Conclusion Depression may indirectly contribute to greater pain severity in patients with cancer patients through anxiety and the belief that pain is persistent. These findings underscore the need to address emotional distress and maladaptive pain beliefs in the psychological management of cancer-related pain.
Keywords: Anxiety; depression; neoplasms. pain; and pain perception

25COASNOV28:
Title: The Association of Filial Piety and Financial Toxicity With Surrogate Decisional Conflict Among Adult Children of ICU Patients With Cancer,
Xiaochun Wu, Yali Tang, Jieling Chen,
Journal of Pain and Symptom Management, Volume 70, Issue 5, 2025, Pages 437-446,
https://doi.org/10.1016/j.jpainsymman.2025.07.023.
Abstract: Context Filial piety, a Confucian cultural value, is deeply rooted in the parent-child relationship in Chinese and many other Asian cultures. Adult children often experience decisional conflict when making decisions for their critically ill parents. However, the quantitative relationship between filial piety and surrogate decisional conflict has yet to be explored. Objective To examine the associations of both financial toxicity and filial piety with surrogate decisional conflict among adult children of intensive care unit (ICU) patients with cancer. Methods A cross-sectional survey was conducted in an ICU of a tertiary hospital in Guangzhou, China. A sample of 180 adult children serving as surrogates for patients with cancer completed the survey after the patients had been admitted to the ICU for at least 4 days. The measures included the family version of the Decision Conflict Scale, the Filial Piety Values Scale for Children of Patients with Advanced Cancer, and the Comprehensive Scores for Financial Toxicity. Multiple regression analysis was conducted to examine factors associated with surrogate decisional conflict. Results The adult children of ICU patients with cancer experienced a high level of surrogate decisional conflict. Surrogate decisional conflict was associated with more siblings (β=0.183,p=0.017), lower levels of filial piety

(β=−0.177,p=0.018) and severe financial toxicity (β=−0.159,p=0.045). Conclusion Healthcare providers are recommended to provide culturally sensitive support for Chinese adult children making decisions for their parents with cancer in the ICU, such as offering strategies to mitigate the negative impact of financial toxicity and helping surrogates clarify their filial piety values to relieve decisional conflict.

Keywords: Decisional conflict; Surrogate; financial toxicity; filial piety

25COASNOV29:

Title: Early Supportive and Nutritional Care For Adults With Pancreatic Cancer: A Pilot Study,

Yu Chen Lin, Kea Turner, Sahana Rajasekhara, Dae Won Kim, Tiago Biachi de Castria, Oliver T. Nguyen,

Journal of Pain and Symptom Management, Volume 70, Issue 5, 2025, Pages 490-502,
https://doi.org/10.1016/j.jpainsymman.2025.07.032.

Abstract: Context Individuals diagnosed with advanced pancreatic cancer face a poor prognosis, heightening the importance of interventions aimed at improving quality of life. Quality of life for individuals with pancreatic cancer is highly influenced by symptom burden and nutritional status. Programs are needed that coordinate palliative and nutrition care for this population. Objectives To address this gap, we conducted a single-arm feasibility trial of Support Through Remote Observation and Nutrition Guidance Plus Supportive Care (STRONG+), a 12-week team-based digital intervention to reduce malnutrition and improve quality of life for individuals with advanced pancreatic cancer. Methods Participants initiating palliative chemotherapy were referred for early and ongoing dietitian-led nutrition counseling and supportive care visits led by a palliative care specialist during the first three months of chemotherapy. Participants also logged food intake daily and completed patient-reported outcome assessments monthly, data that was shared with the dietitian and palliative care specialist through a web-based dashboard. Feasibility and acceptability outcomes were compared against prespecified benchmarks. Preliminary effectiveness was evaluated based on change in patient outcomes between baseline and last follow-up at 16 weeks using linear and ordered logistic regression models. Outcomes included malnutrition risk assessed using the Patient-Generated Subjective Global Assessment Short Form and health-related quality of life measured using the FACT-G. Qualitative data obtained through interviews with participants, their caregivers, and clinicians was analyzed for themes.Results Among the 83 eligible patients who were invited to participate in the study, 50 patients consented to participate. A total of 12 individuals withdrew or died prior to study conclusion. Participants who completed the study (N = 38) had a mean age of 65. Feasibility benchmarks were achieved for participant recruitment (60% vs. benchmark: 50%), attrition (24% vs. benchmark: 30%), study assessment completion (84% vs. benchmark: 70%), and adherence to nutritional counseling (68% vs. benchmark: 60%) and supportive care visits (61% vs. benchmark: 60%). Participants found the overall intervention to be highly acceptable (94% vs. benchmark: 70%). Caregivers also rated the intervention as highly satisfactory (87%). Compared to baseline, participants saw decreased malnutrition risk (P < .001) and improved general health-related quality of life (P = .009) at the end of the study (16 weeks). Participants cited benefits of the intervention including increased knowledge about self-managing nutrition and

improved symptom management. Participants provided recommendations for intervention refinement, such as providing recipes and more hands-on nutrition instruction. Conclusion Study findings suggest the intervention may be feasible and acceptable. Future research is needed to refine the intervention and test the intervention in a fully powered trial. Because the study focused on patients initiating palliative chemotherapy who may benefit from nutrition counseling, findings may be limited in generalizability to all individuals with pancreatic cancer.

Keywords: Early supportive care; Nutrition; Quality of life; Pancreatic cancer; Feasibility; Intervention

25COASNOV30:

Title: UK consensus statement on priorities to support the process of withdrawal of veno-venous extracorporeal membrane oxygenation,

Rebecca Lewis, Emma Jackson, Patrick Collins, Emilia Tomarchio, Christopher Remmington,

British Journal of Anaesthesia, Volume 135, Issue 5,2025, Pages 1223-1230,
https://doi.org/10.1016/j.bja.2025.07.091.

Abstract: Patients with acute severe respiratory failure receiving veno-venous extracorporeal membrane oxygenation (VV-ECMO) have high mortality risk. Management of the process of VV-ECMO withdrawal is challenging, especially in awake patients. Yet there is no guidance to guide clinicians to manage these morally distressing and ethically ambiguous decisions. The study aimed to establish consensus-based priorities for management of the process of VV-ECMO withdrawal to reduce practice variability and improve care quality. Methods Our process for generating priority statements for consideration at our consensus meeting included semi-structured interviews and a scoping review. We recruited healthcare professionals with experience in VV-ECMO withdrawal to participate in interviews and a consensus meeting led by an independent facilitator. Using modified nominal group technique, participants discussed and voted on statements, categorising them as essential, desirable, or not required. A subsequent voting round identified key priorities for future research. Results During our item generation process, we interviewed 12 healthcare professionals with VV-ECMO expertise and identified 41 publications (21 empiric studies and 20 opinion pieces) focused on ECMO withdrawal. We developed 16 priority statements from this data, of which 17 participants representing seven UK ECMO centres considered eight as essential, six desirable, one not required; one was without consensus. Areas for future research highlighted were developing a standardised framework for managing disagreements; creating tools to enhance communication and documentation of information provided; and designing quality improvement strategies to ensure consistency in the clinical and technical aspects of VV-ECMO withdrawal. Conclusions Using rigorous methods, we have established consensus on eight essential and six desirable priorities for management of VV-ECMO withdrawal and three future research priorities. These consensus-based priorities should be viewed as a developmental step towards a standardised approach to support patients, family members, and clinicians through this challenging clinical situation.

Keywords: consensus; end-of-life care; extracorporeal membrane oxygenation; moral distress; veno-venous-ECMO; withdrawal

25COASNOV31:

Title: Association of peripheral nerve blocks with increased postoperative pain and opioid use in orthopaedic surgery: a single-centre retrospective cohort study,

Ashley R. Chung, Rory Vu Mather, Rodrigo Gutierrez, Ran Liu, Chee Fai A. Leung, Mae Zhang,

British Journal of Anaesthesia,Volume 135, Issue 5,2025,Pages 1286-1296,
https://doi.org/10.1016/j.bja.2025.05.030.

Abstract: Peripheral nerve blocks have become popular in orthopaedic surgeries to improve acute postoperative pain. However, studies are mixed on their effectiveness in decreasing postoperative opioid consumption. A more comprehensive analysis is necessary to understand if peripheral nerve blocks reduce postoperative opioid exposure and risk for opioid dependence. Methods This retrospective cohort study evaluated electronic health record data for adults undergoing orthopaedic surgery with general anaesthesia from 2016 to 2020 at the Massachusetts General Hospital. Linear models were fitted on propensity-weighted data to characterise the association between single injection peripheral nerve blocks and clinical outcomes. Our primary outcomes were maximum pain score and cumulative opioid dose, quantified in morphine milligram equivalents, administered in the PACU. Post-discharge outcomes associated with pain and opioid consumption were also evaluated. Results Among 22 956 patients, peripheral nerve block administration was associated with lower maximum pain scores and lower probability of opioid administration in the PACU. However, it was associated with higher maximum pain scores and a 22.7% increase in opioid consumption during the hospital stay. Peripheral nerve blocks were associated with an increase in opioid prescriptions at 30 days after discharge, but no increase at 90 or 180 days, and with decreased chronic pain diagnoses 1 yr after operation. Conclusions Although single injection peripheral nerve blocks were effective in reducing immediate postoperative pain and opioid consumption, they were associated with greater opioid consumption that could increase the risk for opioid dependence. Standardised protocols to mitigate the risk for rebound pain could help minimise postoperative opioid exposure.

Keywords: chronic postsurgical pain; opioid dependence; peripheral nerve block; rebound pain; regional anaesthesia

25COASNOV32:

Title: Association of labour epidural analgesia exposure with infant neurodevelopment: secondary analysis of a prospective cohort study,

Shiyao Tao, Yiyuan Chen, Siyu Chen, Jie Chen, Rui Qin, Yangqian Jiang, Hong Lv, Jiangbo Du, Yuan Lin, Tao Jiang, Zhibin Hu,

British Journal of Anaesthesia,Volume 135, Issue 5,2025,Pages 1240-1248,
https://doi.org/10.1016/j.bja.2025.07.084.

Abstract: Evidence regarding the safety of labour epidural analgesia for infant neurodevelopment remains scarce. We conducted a secondary analysis of the Jiangsu Birth Cohort (JBC) to assess the association between labour epidural analgesia exposure and infant neurodevelopment across five domains: cognition, receptive communication, expressive communication, fine motor, and gross motor. Methods This secondary analysis included singleton vaginal births from data prospectively collected between 1 November 2017 and 1

October 2022. At 1 yr of age, trained paediatricians assessed infant neurodevelopment using the Bayley Scales of Infant and Toddler Development Screening Test, Third Edition (Bayley–III Screening Test). Infants with raw scores below domain-specific thresholds were classified as 'emerging or at risk'. Associations between maternally self-selected labour epidural analgesia exposure and infant neurodevelopment were analysed using generalised linear models adjusted for confounders. Results Among 1811 mother–infant dyads, 1224 (67.6%) received labour epidural analgesia. Labour epidural analgesia exposure was not associated with classification as emerging or at risk in any domain (cognition: adjusted risk ratio [aRR] 1.24; 95% confidence interval [CI] 0.89–1.74, P=0.205; receptive communication: aRR 0.78; 95% CI 0.58–1.04, P=0.095; expressive communication: aRR 1.03; 95% CI 0.59–1.81, P=0.904; fine motor: aRR 0.75; 95% CI 0.38–1.50, P=0.417; gross motor: aRR 0.89; 95% CI 0.57–1.38, P=0.594). The duration of labour epidural analgesia was also not associated with neurodevelopmental outcomes. Conclusions Our findings do not support an association between labour epidural analgesia exposure and increased neurodevelopmental risk at 1 yr of age. These results provide valuable insights, although the CIs and risk ratios underscore the need for larger studies with careful interpretation of clinical significance.

Keywords: Bayley–III Screening Test; birth cohort; labour epidural analgesia; neurodevelopment; obstetric anaesthesia

25COASNOV33:

Title: Effect of intraoperative paravertebral or intravenous lidocaine infusion on postoperative complications and inflammation after lung resection surgery: a randomised controlled trial,

Francisco de la Gala, Elena de la Fuente, Patricia Piñeiro, Almudena Reyes, Patricia Duque,

British Journal of Anaesthesia, Volume 135, Issue 5,2025, Pages 1297-1306,
https://doi.org/10.1016/j.bja.2025.05.059.

Abstract: The potential for the anti-inflammatory effects of lidocaine to reduce complications after lung resection has not been evaluated. We assessed whether intraoperative i.v. or paravertebral lidocaine, compared with remifentanil, reduced complications after lung resection. We also quantified pulmonary and systemic inflammatory responses. Methods This single-centre study randomised participants undergoing lung resection (video-assisted thoracoscopy) to receive continuous infusion of either (1) i.v. lidocaine and paravertebral saline, (2) paravertebral lidocaine and i.v. saline, or (3) remifentanil and paravertebral saline. The primary outcome was the proportion of participants with all-cause complications (Clavien–Dindo classification). Cytokines were measured in bronchoalveolar lavage fluid before and after one-lung ventilation and in plasma during the first 24 h. Results In 154 patients (mean age 65 yr; 42% female), fewer major (Clavien–Dindo Grade ≥III) complications were recorded in participants randomised to intraoperative paravertebral (two of 49; 4.1%) or i.v. (two of 54; 3.7%) lidocaine, compared with six of 51 (11.8%) participants who received remifentanil (P=0.037). Severe complications were less likely with lidocaine from either i.v. or paravertebral sources, compared with remifentanil (odds ratio: 0.44 [95% confidence interval: 0.22–0.88]). Pulmonary complications occurred in 23/103 (22.3%) participants allocated to intraoperative lidocaine from either i.v. or

paravertebral routes, compared with 23/51 (45.1%) participants who received remifentanil (odds ratio: 0.35 [95% confidence interval: 0.17–0.72]; P=0.004). Cytokine levels after one-lung ventilation were lower with lidocaine treatment. Conclusions Intraoperative lidocaine infusion administered either intravenously or through paravertebral catheter reduces the incidence and severity of complications after lung resection surgery compared with remifentanil. Lidocaine might confer this benefit through reducing systemic and lung inflammation.

Keywords: inflammation; lidocaine; paravertebral; postoperative complications; thoracic anaesthesia

25COASNOV34:

Title: Predictive validity of chronic obstructive pulmonary disease phenotypes in inpatient elective surgery: a population-based study,

Ashwin Sankar, Julian F. Daza, Joseph S. Munn, Daniel I. McIsaac, Duminda N. Wijeysundera,

British Journal of Anaesthesia, Volume 135, Issue 5, 2025, Pages 1307-1315,
https://doi.org/10.1016/j.bja.2025.07.036.

Abstract: Chronic obstructive pulmonary disease (COPD) is prevalent among surgical patients, yet guidance for its preoperative assessment remains limited. Whether previously defined COPD phenotypes influence outcomes after surgery is unknown. Methods Population-based retrospective cohort of older adults (≥65 yr) with COPD who underwent inpatient elective surgery in Ontario, Canada. Candidate COPD phenotypes included: advanced COPD with home oxygen; COPD with frailty; COPD with frequent exacerbation; COPD with cardiovascular comorbidity; both asthma and COPD; and COPD alone. Nested Cox proportional hazards models examined the added performance of COPD phenotype when added to a baseline model (age, sex, procedural risk, Surgical Outcome Risk Tool) in predicting survival in the year after surgery using model fit, discrimination, calibration, and net benefit analyses. Results A total of 116 757 patients with COPD underwent inpatient elective surgery; the most common phenotypes included: COPD alone (41.8%), COPD with cardiovascular comorbidity (31.6%), and COPD with frailty (21.8%). There were significant differences in survival between phenotypes when added to the baseline model: advanced COPD (adjusted hazard ratio [aHR] 5.59) and COPD with frailty (aHR 3.56) were associated with markedly decreased survival, while COPD with frequent exacerbation (aHR 1.45) and COPD with cardiovascular comorbidity (aHR 1.35) were associated with moderately decreased survival vs COPD alone. Addition of COPD phenotype improved model fit (likelihood ratio test P<0.001), discrimination (C-index 0.775 vs 0.720), calibration (integrated calibration index 0.035 vs 0.043), and net benefit across all decision thresholds. Conclusion COPD phenotypes are predictive of postoperative survival and improve perioperative risk stratification. These findings support phenotype-based assessment in the preoperative evaluation of patients with COPD.

Keywords: chronic obstructive pulmonary disease; clinical epidemiology; perioperative medicine; predictive validity; preoperative assessment; respiratory medicine; risk stratification

25COASNOV35:

Title: The cutaneous sympathetic blockade associated with labour epidural analgesia: a quasi-experimental study conducted during labour and after delivery,

Giulia M.V. Iacona, Aimee R. Rolph, Hugo F.M. Manteigas, Paul H. Strutton, David A. Low, Christopher J. Mullington,

British Journal of Anaesthesia, Volume 135, Issue 5, 2025, Pages 1231-1239,
https://doi.org/10.1016/j.bja.2025.07.077.

Abstract: The mechanisms contributing to epidural-related maternal hyperthermia remain unclear. One explanation is that blockade of cholinergic sympathetic nerves prevents active vasodilation and sweating. However, it is not known how labour epidural analgesia affects cutaneous sympathetic function. The aim of this study was to test the hypothesis that labour epidural analgesia inhibits cholinergic and noradrenergic function in the lower, but not the upper, limbs. Methods Twenty women (mean age [range]:33 yr [21-48]) receiving epidural analgesia had upper and lower limb cutaneous sympathetic skin responses assessed during labour (epidural) and after delivery (control). Responses were evoked with auditory stimuli delivered through headphones. Sudomotor skin responses (cholinergic function) were recorded with Ag/AgCl electrodes on the hand and foot (median [range]). Vasomotor skin responses (noradrenergic function) were recorded with laser Doppler flowmetry on the finger and toe (median [range]). Results Sudomotor skin response amplitude was less during labour in both the hand (epidural: 0.05 mV [0.00–1.87] vs control: 0.69 mV [0.02–3.73]; P=0.013) and the foot (epidural: 0.00 mV [0.00–0.92] vs control: 0.53 mV [0.05–2.79]; P<0.001). Vasomotor skin response reduction rate was less during labour in the toe (epidural: 6.3% [0.0–41.8] vs control: 18.2% [0.0–53.3]; P<0.001) but was not different between visits in the finger (epidural: 7.9% [0.0-29.9] vs control: 5.0% [0.0-29.8]; P=0.242). Conclusions Labour epidural analgesia can inhibit cholinergic sympathetic outflow to 90% of the body surface. Cholinergic sympathetic blockade could prevent women offloading heat generated during labour. The distribution of cutaneous sympathetic blockade varied among individuals. Cholinergic sympathetic blockade distribution is a potential contributing factor to epidural-related maternal hyperthermia.

Keywords: body temperature; epidural analgesia; epidural-related maternal fever; epidural-related maternal hyperthermia; labour; pregnancy; sympathetic nervous system; thermoregulation

25COASNOV36:

Title: Society for Perioperative Assessment and Quality Improvement: a narrative review of best practices for perioperative management of patients with bleeding disorders,

Maleka Khambaty, Jean M. Connors, Erin S. Grawe, David L. Hepner, Mandeep Kumar, Barbara Slawski,

British Journal of Anaesthesia, Volume 135, Issue 5, 2025, Pages 1269-1278,
https://doi.org/10.1016/j.bja.2025.07.090.

Abstract: Patients with bleeding disorders comprise a population at elevated risk of adverse events in the perioperative period. Patients might have been previously diagnosed with bleeding disorders or be suspected of having an underlying bleeding disorder. Because of the

rarity of these diseases, perioperative management of these patients requires carefully orchestrated multidisciplinary care to prevent adverse outcomes. We present a practical and clinically relevant approach to patients with suspected and known inherited bleeding disorders. For patients with more common bleeding disorders such as von Willebrand disease (vWD), haemophilias, and factor deficiencies, we detail recommendations for perioperative laboratory evaluation and factor and blood product supplementation. We also provide an overview of the diagnosis and perioperative management of less common conditions such as inherited platelet function disorders and disorders of fibrinogen and fibrinolysis. We discuss best practices with regards to availability of specialist expertise and timely phlebotomy, laboratory, and pharmacy resources. A detailed and individualised plan coupled with close communication amongst the perioperative team will help improve care for patients with bleeding disorders undergoing surgery.

Keywords: bleeding disorders; factor deficiency; fibrinogen; haemophilia; inherited platelet disorders; perioperative management

25COASNOV37:

Title: Use and effectiveness of directed, closed-loop communication in the operating theatre: mixed methods analysis of simulated clinical emergencies,

Henrietta Lee, Alan F Merry, Robyn Woodward-Krohn, Jennifer M. Weller,

British Journal of Anaesthesia, Volume 135, Issue 5,2025,Pages 1279-1285,
https://doi.org/10.1016/j.bja.2025.05.015.

Abstract: Effective team performance requires clear communication. Closed-loop communication has improved outcome measures across a range of clinical contexts. We explored the use and effectiveness of directed, closed-loop communication in the operating theatre. We hypothesised that directed, closed-loop communication would increase the proportion of requested actions that were completed. We explored actions completed with closed-loop and directed communication, request type, communication efficiency, and professional differences. Methods The study involved a mixed methods conversational analysis of eight operating theatre emergency simulations. Results Of 150 requests for action, 12% used closed-loop and directed communication together and were associated with higher action completion rates than when neither or one strategy alone was used (100% vs 81%, P=0.030), 19% used closed-loop (with or without directed) communication and were associated with higher action completion rate than when closed-loop was not used (97% vs 80%, P=0.023), and 45% used directed (with or without closed-loop) communication and were not associated with a significant difference in action completion rate compared with when not used (86% vs 81%, P=0.256). We identified inefficiencies in response to requested tasks, including in time-critical tasks, such as no verbal response, repetition of request, or an initial response but no action. Conclusions Directed, closed-loop communication in simulated operating theatre emergencies was associated with increased task completion but was infrequently used. Inefficiencies and dropped requests have implications for team performance and patient safety. Our findings support implementing context-specific interventions to improve task management in operating theatre emergencies through improved communication clarity.

Keywords: closed-loop communication; directed communication; operating theatre; patient safety; task management; team communication; team performance

25COASNOV38:

Title: Genetic variants associated with chronic postsurgical pain: evidence from the China Surgery and Anaesthesia Cohort study,

Jie Song, Yanan Zhang, Huolin Zeng, Yanjie Dong, Wenwen Chen, Lei Yang, Yu Zeng,

British Journal of Anaesthesia,Volume 135, Issue 5,2025,Pages 1257-1268,
https://doi.org/10.1016/j.bja.2025.07.078.

Abstract: Chronic postsurgical pain (CPSP) is one of the most common surgery-related complications and significantly impacts patient' quality of life. However, studies exploring the underlying genetics of postsurgical pain remain limited. Methods This study was based on 17 025 individuals from the China Surgery and Anaesthesia Cohort. We used the Brief Pain Inventory to measure pain intensity prospectively after surgery. CPSP was defined as a dichotomous (yes, no) or continuous (based on pain intensity) variable across surgeries (abdomen, thorax, head and neck, limbs and superficial body regions and other body areas) at 3 months, and persistent pain at various postsurgical follow-up assessments. Genome-wide association analyses were conducted in 9022 individuals with genotyping data. Results We identified 16 independent genome-wide significant loci associated with CPSP. Multiple approaches, including gene mapping, annotation, and multiomics colocalisation, prioritised several potential risk genes, such as ASTN1, RSU1, and C1QL3, involved in neuronal migration, extracellular signal-regulated kinase/mitogen-activated protein kinase signalling, and synaptic function. The single nucleotide polymorphism-based narrow-sense heritability was estimated to be 13.7% (5.1–22.4%) for CPSP defined as a continuous variable. The polygenic risk scores of post-traumatic stress disorder, pain all over the body, multisite chronic pain, and opioid dependence were associated with CPSP at a nominal significance level. Conclusions This study enhances our understanding of the genetic predisposition to chronic postsurgical pain.

Keywords: ASTN1; chronic postsurgical pain; genetics; ERK signalling; NOS2

25COASNOV39:

Title: Navigating care: a multicentre US survey of health literacy in paediatric perioperative care,

Anushree Doshi, Anita Akbar Ali, Chinyere Egbuta, Tessa Mandler, Kaitlyn Pellegrino, Shanique Kilgallon,

British Journal of Anaesthesia,Volume 135, Issue 5,2025,Pages 1249-1256,
https://doi.org/10.1016/j.bja.2025.07.086.

Abstract: Health literacy is a critical determinant of patient outcomes and adherence to medical recommendations across healthcare settings, but it remains unexplored in the paediatric perioperative care. We evaluated the prevalence of limited health literacy among caregivers of paediatric patients undergoing surgery using the validated Newest Vital Sign tool. Methods A cross-sectional survey was conducted in 2023 across multiple paediatric institutions: Children's Hospital of Philadelphia, Arkansas Children's Hospital, Boston Children's Hospital, Children's Colorado, Children's Nebraska, and Nemours Children's

Health. Caregivers completed the Newest Vital Sign tool (available in English and Spanish) and provided patient data via an online database. Data analysis used Pearson's $\chi 2$ test or Fisher's exact test for categorical variables and Wilcoxon rank sum test for non-normally distributed continuous variables. Results Of the 1400 caregivers surveyed, 16% demonstrated limited or possibly limited health literacy. Factors significantly associated with limited health literacy included younger age, lower educational attainment, non-White ethnicity, primary language other than English, and underrepresented minority status ($P<0.001$). Conclusions This multicentre study found that 16% of caregivers had limited health literacy, with higher rates among certain groups. These findings underscore a potential barrier to equitable access to care and highlight the need for further research and interventions aimed at reducing health literacy disparities and improving patient engagement in perioperative care.

Keywords: health literacy; healthcare disparities; paediatric anaesthesia; patient safety; perioperative care; social determinants of health

25COASNOV40:

Title: Title: Impact of Music Intervention or Usual Care on Sedative Exposure During a Spontaneous Awakening Trial among Intensive Care Unit Patients Receiving Mechanical Ventilation: A Prospective Randomized Feasibility Study,

Justin R. Culshaw and Christopher A. Droege and Elsira M. Pina and Neil E. Ernst and Dalton J. Kuebel and Eric W. Mueller,

Journal of Intensive Care Medicine,volume 40,number 11,pages 1177–1185,year 2025, https://doi.org/https://doi.org/10.1177/08850666251343799,

Abstract: Purpose of Research: The objective of this study was to determine if protocolized music intervention paired with spontaneous awakening trial (SAT) is a feasible intervention for mechanically ventilated and sedated intensive care unit (ICU) patients to reduce overall sedation exposure. Major Findings: Patients were admitted to the medical ICU (MICU) or surgical ICU (SICU), mechanically ventilated for at least 24 h with anticipated duration of at least 72 h, and with hearing optimized to baseline disposition. Patients were excluded if they had a specified prior to admission diagnosis, traumatic or medical encephalopathy, or need for deep sedation. Eligible patients were randomized to music intervention or usual care during SAT. Patients in the music intervention group underwent a second randomization to Commercial Music Intervention (CMI) or Preference Music Intervention (PMI).The primary outcome was sedation exposure via sedation intensity score (SIS), an aggregate of the frequency and intensity of sedatives from disparate drug classes such as opioids, anxiolytics, antipsychotics, and others, which was summed for exposure comparison. The usual care group had significantly higher median SIS compared to the music intervention group (4 [IQR 4.9-6.4] vs 3 [IQR 3.1-4.2], $P = .0006$). Patients who received PMI had significantly higher mean SIS compared to the CMI group (5 ± 2.4 vs 2.3 ± 1.7, $P = .0002$). Compared to usual care, the music intervention group had a higher percentage of delirium-free ICU days (37% vs 22%, $P = .009$) and a higher percentage of CPOT scores at goal (69% vs 52%, $P = .002$), but no difference in percentage of goal sedation scores (64% vs 67%, $P = .7$). Conclusions: Protocolized music intervention paired with daily spontaneous awakening trial is a feasible routine intervention for mechanically ventilated patients. Future studies are needed to confirm if this intervention may reduce overall sedation requirements.

25COASNOV41:

Title: Title: Lung Ultrasound Score and Bronchiolitis: What can be Predicted in a Single Center Experience,

Matteo D'Alessandro and Tommaso Bellini and Marta Bustaffa and Benedetta Chianucci and Francesca Ridella and Daniele Franzone and Emanuela Piccotti,

Journal of Intensive Care Medicine,volume 40,number 11,pages 1186–1192,year 2025,
https://doi.org/https://doi.org/10.1177/08850666251344465,

Abstract: To evaluate the presence of pulmonary infiltrates on admission among patients with intracranial hemorrhages, further refining on etiology and the agreement between ultrasonography and chest radiography. Materials and Methods Prospective analysis of patients with aneurysmal subarachnoid hemorrhage (SAH) and intracerebral hemorrhage (ICH), during a 3-month period in a single center, utilizing a standardized protocol of lung ultrasonography. Clinical and ancillary testing data were also collected. Results 44 patients were studied, 30 (68.18%) with ICH, and 14 (31.81%) with SAH. Among patients with ICH, 73.3% had B-lines detected in the assessment, and in the SAH group, 57.14% had presence of lung B-lines. Etiologically, 43% of patients with ICH and 7.1% with SAH had findings suggestive of neurogenic pulmonary edema. 13% of ICH patients and 28.5% in the SAH group had assessments consistent with cardiogenic pulmonary edema. Findings between chest radiography and lung ultrasonography showed poor agreement. Conclusion Sonographic lung infiltrates in patients with severe brain injuries are common, reaching up to two-thirds of ICH admissions and the majority of SAH cases. The etiology varied, with presumed neurogenic pulmonary edema leading the incidence in the ICH cohort, and with cardiogenic pulmonary edema being the most common culprit within SAH patients.

25COASNOV42:

Title: Title: Propofol-associated Hypertriglyceridemia: Development and Multicenter Validation of a Machine-Learning-Based Prediction Tool,

Jiawen Deng and Kiyan Heybati and Keshav Poudel and Guozhen Xie and Eric Zuberi and Vinaya Simha and Hemang Yadav,

Journal of Intensive Care Medicine,volume 40,number 11,pages 1159–1168,year 2025,
https://doi.org/https://doi.org/10.1177/08850666251342559,

Abstract: Purpose: To develop and validate an explainable machine learning (ML) tool to help clinicians predict the risk of propofol-associated hypertriglyceridemia in critically ill patients receiving propofol sedation. Methods: Patients from 11 intensive care units (ICUs) across five Mayo Clinic hospitals were included if they met the following criteria: a) ≥ 18 years of age, b) received propofol infusion while on invasive mechanical ventilation for ≥24 h, and c) had a triglyceride level measured. The primary outcome was hypertriglyceridemia (triglyceride >400 mg/dL) onset within 10 days of propofol initiation. Both COVID-inclusive and COVID-independent modeling pipelines were developed to ensure applicability post-pandemic. Decision thresholds were chosen to maintain model sensitivity >80%. Nested leave-one-site-out cross-validation (LOSO-CV) was used to externally evaluate pipeline performance. Model explainability was assessed using permutation importance and SHapley Additive exPlanations (SHAP). Results: Among 3922 included patients, 769 (19.6%) developed propofol-associated hypertriglyceridemia, and 879 (22.4%) had COVID-19 at ICU

admission. During nested LOSO-CV, the COVID-inclusive pipeline achieved an average AUC-ROC of 0.71 (95% confidence interval [CI] 0.70–0.72), while the COVID-independent pipeline achieved an average AUC-ROC of 0.69 (95% CI 0.68–0.70). Age, initial propofol dose, and BMI were the top three most important features in both models. Conclusion: We developed an explainable ML-based tool with acceptable predictive performance for assessing the risk of propofol-associated hypertriglyceridemia in ICU patients. This tool can aid clinicians in identifying at-risk patients to guide triglyceride monitoring and optimize sedative selection.

25COASNOV43:

Title: Title: Mortality Predictors in Stroke Patients Requiring Mechanical Ventilation: A Multicenter Prospective Observational Study,

Vadim Ershov and Andrey Belkin and Vladimir Gorbachev and Alexey Gritsan

Journal of Intensive Care Medicine,volume 40,number 11,pages 1169–1176,year 2025,
https://doi.org/https://doi.org/10.1177/08850666251342731,

Abstract: Patients with acute severe stroke requiring mechanical ventilation represent a significant clinical challenge. Identification of mortality predictors is necessary to improve outcomes. Methods: Fourteen hospitals located around Russia participated in this prospective multicenter observational clinical study. Patients admitted to ICU between November 1, 2017, and November 1, 2019 with confirmed cerebral stroke, aged 18 to 90 years, and requiring mechanical ventilation were included. The impact of various clinical factors on mortality during the 28-day period after stroke was assessed. Results: A total of 1289 patients were included in the registry, and 1144 met the study criteria. The 28-day mortality rate for stroke patients on mechanical ventilation was 64.3%. The most common indications for mechanical ventilation were impaired consciousness (75.7%) and hypoxemia (60.9%). In the cohort of strokes with NIHSS severity greater than 20 points, hypoxemia at the start of ventilation (OR 1.85 [1.21; 2.81], P = 0.004) and the use of hyperventilation mode (OR 1.46 [1.02; 2.06], P = 0.0336) were associated with increased mortality. Pressure-controlled mode as the primary ventilation method (OR 0.36 [0.21; 0.60], P < 0.001) and ICP monitoring (OR 0.23 [0.12; 0.44], P < 0.001) were associated with decreased mortality. Infectious complications were associated with longer mechanical ventilation and ICU stay (P < 0.001). The relationship between probable mortality and the severity of neurological deficit on the NIHSS scale at the start of mechanical ventilation is non-linear. A critical threshold was reached at 16 points NIHSS, where a trend of increasing probable mortality emerged. Conclusion: The identified predictors of mortality in stroke patients requiring mechanical ventilation are essential for decision-making in this cohort. They include hypoxemia, hyperventilation (used to control intracranial hypertension), volume-controlled (VC) versus pressure-controlled (PC) initial ventilation, and the use of clinical methods for monitoring ICP alone versus invasive monitoring.

Cancer Research

25COASNOV1:

Title: Triple Combination of Recombinant Methioninase and the Anti-parasitic Drugs Ivermectin, and Chloroquine Selectively Eradicates Pancreatic Cancer Cells While Sparing Normal Fibroblasts

Yohei Asano, Qinghong Han, Shukuan Li et.al.

Anticancer Research November 2025, 45 (11) 4791-4802
https://doi.org/10.21873/anticanres.17828

Abstract: Pancreatic cancer is a recalcitrant disease which often presents with few symptoms in the early stages and is frequently diagnosed with distant metastases, limiting treatment options and resulting in a poor prognosis. Recombinant methioninase (rMETase), which targets cancer-specific methionine addiction, has shown synergistic efficacy with numerous types of chemotherapy against all major cancer types. Ivermectin and chloroquine, anti-parasitic drugs, are showing promise against cancer. The present study investigates in vitro the potential synergy of rMETase combined with ivermectin and chloroquine, two agents with multiple anticancer mechanisms, as a novel treatment strategy for metastatic pancreatic cancer.Materials and Methods: The human pancreatic-cancer cell line MiaPaCa-2 and normal human fibroblasts Hs27 were cultured in 96-well plates (1×103 cells/well) for 24 h. Cell viability was assessed using the WST-8 reagent following 72-h treatment with rMETase, ivermectin, or chloroquine to determine their 30% inhibitory concentration (IC30) values. To evaluate synergy, cells were treated with each drug alone or double or triple combinations at their respective IC30 concentrations. Additionally, to evaluate the optimal order of the combination therapy, MiaPaCa-2 cells were divided into four groups and sequentially treated for 72 h as follows: (1) untreated control; (2) the triple-drug combination therapy alone; (3) rMETase followed by the triple-drug combination therapy; (4) the triple-drug combination therapy followed by rMETase.Results: The IC30 value of rMETase was 0.39 U/ml, ivermectin was 4.41 μM, and chloroquine was 3.29 μM on MiaPaCa-2 cells. The triple combination of these agents at their IC30 concentrations significantly inhibited MiaPaCa-2 cell growth compared to monotherapies or dual combinations, indicating a synergistic efficacy. In contrast, the same combination had minimal impact on Hs27 cells at the IC30 values determined for MiaPaCa-2. Regarding the treatment sequence, triple-drug combination therapy and triple-drug combination treatment followed by rMETase treatment significantly inhibited cell proliferation more than rMETase followed by the triple-drug combination treatment.Conclusion: The combination of rMETase, ivermectin, and chloroquine exhibited a selective cytotoxic synergy against pancreatic-cancer cells while sparing normal fibroblasts. Furthermore, the order of treatment may also affect efficacy. This triple combination treatment may offer a novel and effective first-line therapeutic approach for pancreatic cancer.

Keywords: Recombinant methioninase (rMETase)ivermectin, chloroquine combination treatment synergy, pancreatic cancer, normal fibroblasts, methionine addiction, Hoffman effect.

25COASNOV2:

Title: Clearance of TP53 Mutations in ctDNA Reflects Therapeutic Response in

Advanced Pancreatic Cancer Patients

Young Koog Cheon, Sang Hoon Lee, Dong Wook Kim et.al.

Anticancer Research November 2025, 45 (11) 4891-4907;
https://doi.org/10.21873/anticanres.17836

Abstract: TP53 is one of the most frequently altered genes in pancreatic ductal adenocarcinoma (PDAC), yet its clinical significance as a predictive biomarker for treatment response remains unclear. The aim of study was to evaluate the feasibility of repeated ctDNA analysis and explore its potential relevance in predicting treatment outcomes by profiling the molecular evolution of PDAC patients during the 1st course of palliative chemotherapy.Materials and Methods: We investigated the association between TP53 alterations and treatment outcomes in 19 patients with advanced PDAC who received either FOLFIRINOX or gemcitabine plus nab-paclitaxel. TP53 mutation status was assessed using next-generation sequencing (NGS) of circulating tumor DNA (ctDNA) obtained before and after treatment.Results: Among 21 chemotherapy-naive patients with advanced PDAC, 19 were evaluable for treatment response, with an objective response rate of 52.6%. Baseline ctDNA analysis detected Tier 1/2 mutations in 100% of samples, with TP53 (52%) and KRAS (27%) as frequent alterations. KRAS mutations were significantly more common in responders than non-responders (67% vs. 11%, p=0.040). Post-chemotherapy ctDNA analysis revealed that 42% of TP53-mutated patients showed complete clearance of these mutations, correlating with partial radiologic responses. Novel mutations such as BRCA2 and PBRM2 emerged after treatment. CA 19-9 levels decreased significantly in responders but not in non-responders. Gene Ontology analysis highlighted a post-treatment shift toward hypoxia response, chromatin remodeling, and Wnt pathway activation, suggesting clonal adaptation and potential drug resistance.Conclusion: Dynamic changes in ctDNA, particularly the disappearance of TP53 mutations, serve as a sensitive biomarker for chemotherapy response in advanced PDAC, even when traditional markers like CA 19-9 are unreliable. Longitudinal ctDNA profiling offers a promising approach to guide early treatment evaluation and may inform therapeutic strategies targeting resistant subclones.

Keywords: Pancreatic ductal adenocarcinomaTP53 mutationcirculating tumor DNApredictive biomarker

25COASNOV3

Title: Efficacy and Safety of Chemoimmunotherapy in Patients With Advanced Non-small Cell Lung Cancer With Pre-existing Interstitial Pneumonia and Low PD-L1 Expression

Aosa Sasada, Hayato Kawachi, Tadaaki Yamada et.al.

Anticancer Research November 2025, 45 (11) 5045-5057;
https://doi.org/10.21873/anticanres.17845

Abstract: Establishing the suitability of initiating immune checkpoint inhibitor (ICI) therapy in patients with lung cancer and coexisting interstitial pneumonia (IP) is challenging. Real-world evidence on the efficacy and safety of ICIs in such patients is urgently needed to inform clinical practice.Patients and Methods: This retrospective study evaluated the effects of ICI administered to 79 patients with advanced or recurrent non-small cell lung cancer (NSCLC) and programmed death ligand 1 (PD-L1) tumor proportion scores of 1-49%, who had pre-existing IP. These patients received first-line therapy comprising an ICI with

chemotherapy or chemotherapy alone at 18 institutions in Japan between March 2017 and June 2022.Results: Twelve patients received ICI plus chemotherapy (chemoimmunotherapy group) as first-line treatment, and 67 received chemotherapy alone (chemotherapy group). Only brain metastases were significantly more frequent in the chemoimmunotherapy group; no other differences in patient backgrounds between the two groups were observed. Overall survival (OS) and progression-free survival did not differ between the two groups. After propensity score matching, chemoimmunotherapy significantly prolonged OS compared to chemotherapy alone (25.3 months vs. 9.6 months, p=0.033), without significant differences in incidences of severe adverse events, including pneumonitis. In the analysis of patients who received ICI up to second-line treatment, ICI therapy was associated with prolonged OS compared to non-ICI treatment (29.8 months vs. 16.3 months, p=0.012).Conclusion: Early use of immunotherapy for patients with advanced NSCLC with low PD-L1 expression and coexisting IP may improve prognosis.

Keywords: Immune checkpoint inhibitor, combination therapy, interstitial pneumonia, non-small cell lung cancer, programmed death ligand 1propensity score, retrospective study

25COASNOV4

Title: The Posterior First Approach in Robot-assisted Radical Prostatectomy for Prostate Cancer Reduces Positive Surgical Margins on the Bladder Neck Side

Yasushi Nakai, Nobumichi Tanaka, Kenta Onishi et.al.

Anticancer Research November 2025, 45 (11) 5177-5184
https://doi.org/10.21873/anticanres.17857

Abstract: There is limited data comparing outcomes and quality of life between the conventional robot-assisted radical prostatectomy (RARP) (anterior approach) and the posterior first approach RARP. In the present study, we evaluated the differences between conventional and posterior first approach RARP.Patients and Methods: This study enrolled consecutive patients who underwent conventional RARP (n=255) and posterior first approach RARP (n=107). Propensity scores were calculated, and patients were matched in a 1:1 ratio based on these scores. The quality of life (QOL), continence, and perioperative outcomes were evaluated in the two groups.Results: Using propensity matching, 99 patients were included in each group. The number of patients (75%) whose bladder necks were preserved in the posterior first approach RARP group was significantly higher (p<0.001) than that in the conventional RARP group (42%). Positive surgical margin on the side of the bladder neck in the posterior first approach group (1%) was not significantly (p=0.03) detected compared to that in the conventional group (8%). There was no significant difference in QOL score at 12 months after RARP or in continence rate within 12 months after RARP.Conclusion: Compared to the conventional approach, the posterior first approach RARP can preserve the bladder neck and reduce the incidence of positive surgical margins at the bladder neck side.

Keywords: Robot surgery, prostatectomy, quality of life, urinary incontinence, surgical margin

25COASNOV5

Title: Role of Ubiquitin-specific Protease 1 in the Pathogenesis and Treatment of Adult T-Cell Leukemia

Chie Ishikawa And Naoki Mori

Anticancer Research November 2025, 45 (11) 4827-4840;
https://doi.org/10.21873/anticanres.17831

Abstract: We previously reported the therapeutic potential of pimozide against adult T-cell leukemia (ATL) caused by human T-cell leukemia virus type 1 (HTLV-1). Pimozide inhibits ubiquitin-specific protease 1 (USP1). In this study, we investigated the functional significance of USP1 and its potential as a therapeutic target for ATL treatment.Materials and Methods: Cellular processes, including proliferation, metabolism, apoptosis, and the expression of USP1 and related regulatory proteins, were assessed.Results: HTLV-1-infected T cells showed aberrant USP1 protein expression, and USP1 knockdown significantly inhibited their proliferation. Similarly, treatment with pimozide and the USP1 inhibitor SJB3-019A reduced USP1 expression, inhibiting cell proliferation and survival. SJB3-019A decreased the expression of c-Myc, a USP1 target, resulting in G1 cell cycle arrest. Furthermore, it induced caspase-mediated apoptosis by suppressing anti-apoptotic proteins, as well as mitochondrial dysfunction, ROS production, endoplasmic reticulum stress, and DNA damage. SJB3-019A led to a reduction in the critical glycolytic enzyme LDHA, decreasing lactate levels. Additionally, SJB3-019A inhibited the expression of polo-like kinase 1, another USP1 target and a kinase upstream of LDHA and c-Myc. SJB3-019A also suppressed β-catenin expression and IκBα, RelA, and Akt phosphorylation, indicating NF-κB/Akt inhibition.Conclusion: Our study supports the clinical potential of USP1 inhibitors as a novel therapy for ATL.

Keywords: Adult T-cell leukemiaubiquitin-specific protease 1human T-cell leukemia virus type 1SJB3-019A

25COASNOV6

Title: Prognostic Impact of Additional Resection of Bile Duct Margins in Radical Resection for Perihilar Cholangiocarcinoma

Katsunori Sakamoto, Yoichiro Uchida, Kentaro Kadono et.al.

Anticancer Research November 2025, 45 (11) 5095-5107;
https://doi.org/10.21873/anticanres.17850

Abstract: During radical resection in patients with perihilar cholangiocarcinoma, the prognostic impact of additional resection of bile duct to achieve negative surgical margin in case of that of positive initial frozen margin is unclear. This study aimed to investigate the prognostic impact of margin status of additional bile duct resection in patients undergoing radical surgery for perihilar cholangiocarcinoma with initially positive bile duct cut-end margins.Patients and Methods: This retrospective study used data from 100 patients who underwent bile duct resection with major hepatectomy for the radical resection of perihilar cholangiocarcinoma at the Kyoto University Hospital between January 2010 and March 2024. Patients with 90-day postoperative mortality or no pathological evidence of invasive carcinoma were excluded. The status of bile duct surgical margin was classified into three types: negative by the initial division of the bile duct (initial negative group), negative by additional resection (secondary negative group), and positive (positive group).Results: Out of the 100 patients, 72 had negative margins at the initial bile duct division, 21 achieved negative margins after additional resection, and seven had persistently positive margins. Both the secondary negative group and positive group had significantly shorter recurrence rates compared to the initial negative group (median time to recurrence; 13.6 vs. 10.5 vs. 24.2

months; p=0.009 and p=0.003, respectively). Multivariate analyses identified bile duct margin status as an independent predictor of recurrence, but not of overall survival.Conclusion: Achieving a negative bile duct margin at the initial division is crucial for improving recurrence outcomes in perihilar cholangiocarcinoma. Surgical strategies should prioritize in obtaining a negative margin from the outset to enhance long-term disease control.

Keywords: Perihilar cholangio, carcinoma, surgical margin, frozen sections

25COASNOV7

Title: Gamma Knife Radiotherapy of Brain Metastasis Resection Cavities: Outcome Analysis of a Single-center Cohort

Àlex Godó Jiménez, Gero Wieger, Stefanie Brehmer et.al.

Anticancer Research November 2025, 45 (11) 5019-5029;
https://doi.org/10.21873/anticanres.17843

Abstract: Stereotactic radiotherapy (SRT), including stereotactic radiosurgery (SRS) and fractionated stereotactic radiotherapy (FSRT), is the current standard adjuvant treatment after resection of brain metastases (BM). In the era of immunotherapy and targeted systemic therapies enabling effective extracranial control, achieving durable intracranial outcomes has become increasingly important. Intraoperative radiotherapy (IORT) is an emerging alternative to Gamma Knife-based irradiation. We aimed to assess the clinical outcome of BM resection cavities treated with Gamma Knife SRT (GK-SRT), for retrospective comparison to a cohort treated with IORT.Patients and Methods: This retrospective single-center analysis included all patients who received GK-SRT to the resection cavity after complete surgical removal of BM. A total of 41 cavities from 37 patients were evaluated. Local control (LC), distant intracranial control (DIC), and overall survival (OS) were calculated, and the potential influence of whole-brain radiotherapy (WBRT) as part of the adjuvant treatment on OS was analyzed.Results: With a median follow-up of 19.3 months, the 1-year LC was 93.3%. The 1-year DIC was 54.1%, and the median OS was 27.3 months. Median cavity volume was 5.89 cm3; the median interval from surgery to GK-SRT initiation was 24.5 days, and to subsequent systemic treatment 59.0 days. DIC, but not LC, was significantly associated with OS, with better DIC correlating with longer survival. WBRT as part of the adjuvant regimen did not confer a significant survival benefit.Conclusion: Adjuvant GK-SRT to the resection cavity is an effective treatment with excellent local control. Nonetheless, challenges remain regarding distant intracranial progression and overall survival.

Keywords: Brain metastases, Gamma Knife, resection cavity, stereotactic radiosurgery, fractionated stereotactic radiotherapy

25COASNOV8

Title: Senolytic Elimination of Senescent Ovarian Clear Cell Carcinoma Cells Induced by CEP-1347 With the BH3 Mimetic Navitoclax

Yasufumi Ito, Kazuki Nakamura, Yurika Nakagawa-Saito et.al.

Anticancer Research November 2025, 45 (11) 4841-4851;
https://doi.org/10.21873/anticanres.17832

Abstract: Ovarian clear cell carcinoma (OCCC) is a subtype of epithelial ovarian cancer

characterized by infrequent TP53 mutations. We recently reported that the MDM4 inhibitor CEP-1347 effectively activated the p53 – p21 axis and inhibited the proliferation of OCCC cells with wild-type TP53. We also recently found that CEP-1347 induced senescence-like phenotypes in glioma stem cells and sensitized them to senolytics, such as BH3 mimetics represented by navitoclax. In the present study, we investigated whether CEP-1347 induced senescence-like phenotypes in OCCC cells and if combinations with BH3 mimetics enhanced the anti-cancer activity of CEP-1347 by promoting senolysis in OCCC cells.Materials and Methods: Senescence-like phenotypes were analyzed using microscopy, flow cytometry, and western blotting. Combined effects with senolytics were evaluated using cell death assays, colony formation assays, and western blot analysis.Results: CEP-1347 induced cellular senescence in OCCC cells with wild-type TP53. Furthermore, in combination with senolytics, particularly navitoclax, CEP-1347 strongly induced apoptotic death in these OCCC cells under conditions that were not toxic to normal cells.Conclusion: CEP-1347 induced cellular senescence in OCCC cells with wild-type TP53. The combination of CEP-1347 with senolytics, such as navitoclax, represents a rational strategy to ensure the selective elimination of senescent OCCC cells and enhance therapeutic efficacy.

Keywords: Clear cell ovarian cancer, ABT-263KT7515, cellular senescence.

25COASNOV9

Title: Mouse model of prenatal valproic acid exposure: Effects on cortical morphogenesis and behavioral outcomes across environmental conditions

Mizuki Tanizaki, Takuma Matsui, Rei Sugiyama et.al.

Toxicology Letters, Volume 413, November 2025, 111719
https://doi.org/10.1016/j.toxlet.2025.09.004

Abstract: Autism spectrum disorder is a developmental disability characterized by impaired social communication and repetitive behaviors, and environmental and genetic factors are involved in its onset. The use of the antiepileptic drug valproic acid (VPA) during pregnancy is associated with neural tube defects and developmental disorders in the fetus. In this study, we aimed to identify abnormalities in cortical morphogenesis owing to prenatal VPA exposure and to elucidate the abnormalities in brain function associated with these abnormalities, particularly by comparing multiple and single environments. Pregnant mice were administered a single dose of 400 mg/kg/day of VPA on embryonic day 12, and the morphogenesis and behavioral characteristics of the fetal and newborn mouse brains were analyzed. Prenatal VPA exposure caused an increase in cell proliferation and morphological abnormalities in microglia. In the single-housing environment, a decrease in spontaneous locomotor activity and psychomotor activity, and an increase in anxiety-like behavior and abnormal social interactions, were observed. In the multiple-housing environment, no effect on spontaneous activity was detected, however, an effect on social interactions and social proximity was observed. These findings provide valuable insights into the effects of environmental factors during the fetal period on the risk of developmental disorders. Moreover, they indicate that developmental disorder-like behavior is also affected by the environment.

25COASNOV10

Title: Role of phthalates in breast cancer initiation, progression and drug rersistance: A

scoping review and recommendations

L. Benoit, C. Tomkiewicz, S. Bortoli et.al.

Toxicology Letters, Volume 413, November 2025,

https://doi.org/10.1016/j.toxlet.2025.111721

Abstract: Phthalates are endocrine-disrupting chemicals (EDCs) with implications in breast cancer (BC). This review synthesizes epidemiological and experimental data to evaluate the role of phthalates in BC initiation, progression, and therapeutic resistance. We performed a scoping review using bibliographic citations from PubMed, Clinical Trials.gov, Embase, Cochrane Library, and Web of Science databases. MeSH terms for breast cancer and phthalates were combined and not restricted to the English language. The search was performed from 2010 to July 2024. The primary outcome was to determine the role of phthalates in BC. Two hundred and forty-seven articles were screened from 2010 to 2024. Of the 90 studies included, 23 were reviews, 24 were epidemiologic and 43 were experimental. Epidemiological evidence is mixed, with certain studies identifying a correlation between high cumulative exposure to specific phthalates, such as dibutyl phthalate, and increased BC risk, particularly in estrogen receptor-positive subtypes. Conversely, other studies reported no significant associations. Experimental investigations have demonstrated that phthalates disrupt estrogenic signaling, induce BC cell proliferation, and potentiate metastasis. Additionally, phthalates contribute to chemoresistance by modulating drug metabolism and altering gene expression. Given the persistent exposure to phthalates this review calls for public health interventions and recommendations.

25COASNOV11

Title: Bisphenol A exposure promotes proliferation and invasion capabilities of bladder cancer cells: Insights from gene expression and pathway analysis

Bo Cong, He Liu, Minghui Sun et.al.

Toxicology Letters, Volume 413, November 2025,

https://doi.org/10.1016/j.toxlet.2025.09.002

Abstract: Bisphenol A (BPA), a synthetic organic compound widely used in plastic products, toys, water pipes, and flame retardants, has been linked to the onset and progression of various cancers. This study explores the association between BPA and bladder cancer using bioinformatics approaches. We applied the ssGSEA algorithm to calculate BPA-related scores in TCGA-BLCA cohort and classify patients based on this. GO and KEGG pathway enrichment analyses identified key pathways associated with BPA-related genes. Prognostic genes were screened through differential expression, Cox regression, and Lasso regression, leading to the construction of a prognostic model. Pathway enrichment suggested that BPA exposure promotes bladder cancer progression by modulating the Epithelial-Mesenchymal Transition pathway. In vitro experiments demonstrated that exposure to 10^{-7} μM BPA significantly enhanced the proliferation and invasion of bladder cancer cells, with Western blot confirming that BPA induces the EMT phenotype in a dose-dependent manner. These findings suggest the involvement of the BPA-mediated regulatory network in bladder cancer progression, thereby providing novel insights into the molecular mechanisms underlying BPA-induced bladder cancer development upon environmental exposure.

25COASNOV12

Title: The association between urinary levels of organic phosphorus insecticide exposure and subclinical thyroid disorders

Gaohui Wei, Yi Shen, Xian Wang et.al.

Toxicology Letters,Volume 413, November 2025,
https://doi.org/10.1016/j.toxlet.2025.111723

Abstract: Objective: Studies have shown that exposure to organophosphorus pesticides (OPPs) may disrupt thyroid endocrine function in animal models and in agroforestry practitioners, leading to subclinical hyperthyroidism (SHyper). However, the relationship between exposure to OPPs and SHyper in the general population remains unclear. This research aims to investigate the relationship between OPPs exposure and SHyper in the general population.Methods: This was a retrospective cross-sectional study based on data collected from three cycles of the National Health and Nutrition Examination Survey (NHANES, 2001–2010), which ultimately analyzed 3425 participants who met the inclusion criteria. The study period is particularly relevant because it reflects the era of widespread chlorpyrifos (CPF) use in the United States before its subsequent ban, thereby providing important historical context for understanding OPP exposure levels. OPPs exposure was estimated by measuring urinary composition of two OPPs metabolites (3,5,6-trichloropyridinol and paranitrophenol). Logistic regression models were employed to assess the correlation between OPPs metabolites and SHyper. Subgroup analyses were conducted based on gender, age, body mass index (BMI), and household income, and interactions with OPPs were investigated. The two metabolites were categorized into quartiles, and trend analysis was performed. Restrictive cubic spline models were used to fit the relationship between the two metabolites and the risk of SHyper. Sensitivity analyses were conducted by excluding participants who consumed alcohol and those with iodine deficiency to validate the model's stability.Results: Adjusted logistic regression analyses revealed significant positive associations between both para-nitrophenol (PNP) and 3,5,6-trichloropyridinol (TCPy) with subclinical hyperthyroidism (SHyper). Participants in the second, third, and highest quartiles of PNP exposure exhibited a progressively increased risk of SHyper compared to those in the lowest quartile.Stratified analyses demonstrated that TCPy's association with SHyper was particularly pronounced in specific subgroups: individuals aged 12–64 years, males, those with household incomes < $20,000/year, and participants with obesity (BMI ≥30 kg/m²). Similarly, PNP was consistently associated with elevated SHyper risk across all stratified populations. Sensitivity analyses confirmed the robustness of these associations, as the relationships between PNP/TCPy and SHyper persisted even after excluding alcohol consumers or iodine-deficient individuals.Conclusions: Our study suggests that exposure to OPPs is associated with an increased risk of SHyper, an association reflected by the observed correlations between urinary metabolites (PNP and TCPy) and SHyper.

25COASNOV13

Title: Distinct responses of the constitutive androstane receptor NR1I3 to indole-containing metabolites of bacterial origin

Ryuya Narita, Misaki Kaito, Takashi Kondo et.al.

Toxicology Letters, Volume 413, November 2025
https://doi.org/10.1016/j.toxlet.2025.111724

Abstract: The constitutive androstane receptor (CAR, NR1I3) has been recognised as a nuclear receptor for various xenobiotics, such as barbiturates and dietary polyphenols. In this study, the CAR responded to internal metabolites produced by intestinal bacteria from the dietary amino acid tryptophan. We screened 15 indole-containing compounds in HepG2 cells using a luciferase reporter assay and found that three of them, tryptamine, indole-3-pyruvic acid, and indole-3-ethanol, significantly increased transcriptional activity of both mouse and human CAR. The estimated EC50 values of these compounds at the micromolar concentration order, which were close to those found in the host sera and tissues. Importantly, 3-methyl indole (skatole) inhibited mouse CAR activity to a lesser extent than androstanol, an inverse agonist of mouse CAR. Considering this, we investigated the transactivation mechanisms of these compounds in terms of their nuclear translocation. Indole-3-pyruvic acid and diindolylmethane slightly but not significantly increased the nuclear translocation of mouse CAR, whereas skatole significantly increased nuclear translocation. This is in contrast to the observation that androstanol does not induce nuclear translocation. Tryptamine is produced by Ruminococcus gnavus and skatole by Lactobacillus spp. Our findings suggest that the CAR can be positively or negatively regulated by indole-containing metabolites, depending on the composition of the gut microbiota.

25COASNOV14

Title: A core physiologically based toxicokinetic (PBTK) model for exposure assessment of multiple environmental phenols

Jeong Weon Choi, Seungho Lee, Jangwoo Lee et.al.

Toxicology Letters: Volume 413, November 2025

https://doi.org/10.1016/j.toxlet.2025.111722

Abstract: Environmental phenols are widely used in consumer products and are of increasing concern due to their potential endocrine-disrupting effects. Physiologically based toxicokinetic (PBTK) models offer a powerful tool for estimating human exposure by translating biomonitoring data into external intake values. However, conventional PBTK models are typically chemical-specific and resource-intensive. In this study, we developed a core human PBTK model capable of describing the absorption, distribution, metabolism, and excretion (ADME) of four groups of environmental phenols—parabens (MeP, EtP, PrP), bisphenols (BPA, BPS), triclosan (TCS), and benzophenone-3 (BP-3)—based on shared toxicokinetic characteristics.The model was calibrated and validated using human volunteer data and applied to urinary biomonitoring data from 3787 Korean adults in the Korean National Environmental Health Survey (KoNEHS 2015–2017). Estimated daily intakes (EDIs) for MeP, EtP, PrP, and BPA were estimated via reverse dosimetry and compared with values derived from the conventional fractional urinary excretion (Fue) method. Median EDIs derived from the PBTK model were 3.7, 4.8, 0.4, and 0.02 μg/kg-bw/day for MeP, EtP, PrP, and BPA, respectively, and showed good agreement with Fue based estimates.The core model successfully captured blood and urinary concentration profiles across multiple phenols, demonstrating its potential as a practical and scalable framework for exposure assessment. Furthermore, the model was used in a reverse dosimetry framework to estimate human exposure levels from urinary biomonitoring data. This approach can be particularly valuable when chemical-specific models are unavailable, offering an efficient alternative for interpreting biomonitoring data in environmental health risk assessment.

25COASNOV15

Title: Physiologically based toxicokinetic models in aggregate exposure: A review

L. Lamon, A. Paini, M. Siccardi et.al.

Toxicology Letters, Volume 413, November 2025,
https://doi.org/10.1016/j.toxlet.2025.111725

Abstract: This literature review explores the application of Physiologically Based Kinetic (PBK) models in aggregate exposure (AE) assessment across different chemical classes. It builds on the screening of 1119 publications and the identification of 40 relevant articles. The most frequently studied chemicals include volatile organic compounds and plant protection products, with metals, personal care products, persistent organic pollutants and plasticisers also represented. Most studies reported in this review are applied to human populations and build on human biomonitoring (HBM) data to enhance model reliability. However, some studies use animal models (primarily rat models) and apply cross-species extrapolation to the human AE scenario. Occupational exposure is taken into consideration as part of the AE scenario in a few studies. Many of the reviewed studies are designed in support of chemical risk assessment (CRA), illustrating the wide applicability of PBK models. The review discusses the joint role of HBM data and PBK model in AE scenarios, highlighting its importance for a reliable risk assessments. The studies identified and discussed in this review suggest a broad interpretation of AE. The diversity across case reported studies is attributed to varying interpretations and existing definitions of AE. Finally, the roles of forward and reverse dosimetry in refining AE assessments are discussed, highlighting their importance for future research. This scoping review provides a comprehensive overview of PBK model applications in addressing AE, serving as a valuable foundation for future research and development aimed at advancing human health protection towards the Next-Generation Risk Assessment (NGRA).

25COASNOV16

Title: Studying APAP metabolism in a cohort of intoxicated patients using HRMS-based profiling: Detection of catechol and delayed thiomethyl metabolites

Thomas Gicquel, Romain Pelletier, Eva Gorrochategui et.al.

Toxicology Letters, Volume 413, November 2025
https://doi.org/10.1016/j.toxlet.2025.111727

Abstract: Acetaminophen (APAP) overdose is one of the most important causes of drug-induced liver injury worldwide. Hepatotoxicity induced by APAP is mainly caused by the production of N-acetyl-p-benzoquinone imine (NAPQI), a highly reactive intermediate. Although, the medical management of APAP intoxication is well known, research is still ongoing to identify markers that could help to predict adverse issues after APAP intoxication. In this study, we aimed to study APAP biotransformation pathways in a cohort of patients with proven acute APAP intoxication to identify new biomarkers using state-of-the-art high-resolution mass spectrometry (HRMS) methodologies that could help improve the diagnosis of intoxication as well as patient follow-up. We used a cohort of 37 patients whom blood plasma samples were stratified according to the collection time after APAP intoxication. Our results showed that direct phase II metabolites from glucuronidation and sulfation pathways remain the main markers of APAP consumption. Our study also revealed that several oxidative pathways produce significant metabolites (including catechol ones) that could also

help to monitor the intoxication and the elimination of the hepatotoxic NAPQI. In particular, significant levels of thiomethyl metabolites derived from the glutathione-NAPQI conjugates could be detected with a delay in their kinetics of appearance.

25COASNOV17

Title: Follicular and neural toxic effect of prolonged exposure of synthetic dye fast green FCF (E143)–Insights from zebrafish model

Gokul Sudhakaran, P. Snega Priya, Raghul Murugan et.al.

Toxicology Letters, Volume 413, November 2025

https://doi.org/10.1016/j.toxlet.2025.111726

Abstract: This study highlights the toxic effects of prolonged exposure of synthetic food dye fast green FCF (E143) in zebrafish and the cumulative consequences of such exposure on multiple biological systems mainly neural and reproductive. Chronic exposure to FCF at concentrations of 0.1 %, 0.3 %, and 0.5 % led to a reduction in acetylcholinesterase (AChE) activity and an increase in malondialdehyde (MDA) levels, indicating impaired neuronal function. The disruption in the production of key antioxidant enzymes, including catalase (CAT), lactate dehydrogenase (LDH), superoxide dismutase (SOD), and nitric oxide (NO), further supported the link between elevated reactive oxygen species (ROS) levels and increased oxidative stress and lipid peroxidation (LPO). Histopathological analysis using H&E, MTS, Toluidine blue, and PAS staining revealed significant changes in the brain, liver, and ovaries of FCF-exposed zebrafish, suggesting potential neurological damage, hepatotoxicity, and reproductive disturbances, particularly arrest of follicular maturation. High-performance liquid chromatography (HPLC) analysis confirmed bioaccumulation of FCF in the ovaries. Gene expression analysis of SOD1, CAT, NF-κB, TNF-α, IL-1β, BCL2, BAX, MBP, and Syn2a provided molecular evidence of disrupted antioxidant defenses, impaired myelin formation, altered synaptic function in the brain, inflammatory responses, and increased apoptosis in the ovaries. This study is crucial for understanding the potential risks to zebrafish and provides insights into the broader implications for consumer health when exposed to similar food dyes in the environment.

25COASNOV18

Title: Dysregulation of immune checkpoint LAG3 in mice exposed to silica

Meixiu Duan, Youliang Zhao, Yaqian Qu et.al.

Toxicology Letters, Volume 413, November 2025

https://doi.org/10.1016/j.toxlet.2025.111729

Abstract: Silica exposure can cause silicosis, and its pathogenesis is not fully understood. This study investigates the role of immune checkpoint lymphocyte activation gene 3 (LAG3) in silicosis. Mice were intratracheally exposed to silica, and tissues were collected and analyzed after 7 and 28 days. Additionally, peripheral blood samples were also collected from silicosis patients. The mRNA and protein expression levels of LAG3 in various tissues were quantified using qRT-PCR and western blot techniques. The localization of LAG3 in the lung, spleen, thymus and hilar lymph nodes was visualized by immunochemistry. Our data showed that silica exposure induced systemic changes in LAG3 expression in an organ-specific manner. In mouse lungs, LAG3 levels were significantly upregulated after silica exposure. In mouse spleen, LAG3 expression changed only during early stage of silica

exposure. In mouse thymus, the level of LAG3 decreased during early stage of silica exposure but reversed to increase during late stage. In mouse hilar lymph nodes, expression of LAG3 increased significantly. A marked increase in the concentration of soluble LAG3 was observed in the plasma of mice exposed to silica. Plasma soluble LAG3 levels in silicosis patients were found to be significantly higher than healthy controls. These findings suggest that LAG3 may be involved in the pathogenesis of silicosis and that immune disorders in lung tissue may further affect systemic immune homeostasis.

25COASNOV19

Title: Constitutive androstane receptor activation modulates YAP expression and activity through ubiquitination and sumoylation

Fengting Liang, Shuaishuai Zhang, Wenhong Zhou et.al.

Toxicology Letters, Volume 413, November 2025

https://doi.org/10.1016/j.toxlet.2025.111728

Abstract: Constitutive Androstane Receptor (CAR) is a member of the nuclear receptor superfamily that significantly contributes to the metabolism of endogenous and exogenous substances and the homeostatic regulation of the body. Yes-associated protein (YAP) is a core component of the Hippo signaling pathway. We have previously demonstrated that CAR activation interacts with YAP and induces the nuclear translocation of YAP, although the specific binding site and regulatory mechanism remain unclear. In this study, we identified the ligand-binding domain (LBD) of CAR as essential for its interaction with YAP, while the WW domain (Tryptophan- Tryptophan domain) of YAP was found to be crucial for CAR binding. We further explored the impact of CAR activation on YAP post-translational modifications. CAR agonism inhibited YAP ubiquitination but promoted its SUMO1 modification, and had no effect on acetylation, glycosylation, and methylation. Notably, CAR activation enhanced the K63-linked ubiquitination of YAP, facilitating its nuclear translocation, and this effect was dependent on the E3 ligase TRAF6. Furthermore, PIAS4 was identified as a key SUMO E3 ligase, promoting YAP SUMO1 modification upon CAR activation. These findings provide new insights into how CAR regulates YAP activity through post-translational modifications, contributing to the understanding of CAR's role in liver regeneration.

25COASNOV20

Title: Pre-clinical safety assessments of gadobutrol in diabetes-induced neuropathy: In vivo, in vitro and in silico studies

Batuhan Bilgin, Munevver Gizem Hekim, Muhammed Adam et.al.

Toxicology Letters, Volume 413, November 2025,

https://doi.org/10.1016/j.toxlet.2025.111733

Abstract: Due to its vascular complications, patients with diabetes mellitus (DM) are exposed to gadobutrol in imaging. However, the safety concerns of gadobutrol to diabetes-induced neuropathy, a common complication of DM, remain unclear as a scientific gap. This study aimed to investigate the effects of gadobutrol on hypersensitivity in a streptozotocin (STZ)-induced diabetic neuropathy model in mice and its effects on cytotoxicity and genotoxicity in high glucose (HG)-induced neuropathy in dorsal root ganglion (DRG) neurons. Adult (6–8 weeks old) BALB/c male mice were intraperitoneally administered STZ

(150 mg/kg) and hot plate, cold plate, von Frey, and rota rod tests were performed 21 days after blood glucose levels rose above 250 mg/dL (N = 40). Gadobutrol was administered intravenously. DRG neurons were isolated from neonatal Sprague-Dawley rats and HG (45 mmol/L) was administered. Subsequently, 3-(4,5-dimethylthiazol-2-yl)-2,5-diphenyl-2H-tetrazolium bromide (MTT) and comet assay were performed on gadobutrol-treated and HG-exposed DRG neurons. Furthermore, molecular docking analysis was performed between gadobutrol and catalase (CAT). STZ + gadobutrol showed a statistically significant increase in sensitivity in hot plate, cold plate and von Frey assays compared to STZ ($p = 0.0013$, $p = 0.0019$ and $p = 0.0189$, respectively). HG + gadobutrol showed statistically significant increases in cytotoxicity and genotoxicity compared to HG. The binding affinity of gadobutrol to CAT was determined as − 8.59 kcal/mol. The results of this study suggest for the first time that gadobutrol can exacerbate diabetes-induced neuropathy. Further clinical studies are needed to elucidate these results, which may pose a new safety concern for patients with diabetic neuropathy.

25COASNOV21

Title: Individual and mixed effects of PFAS on osteoporosis: Insights from epidemiological and bioinformatic approaches

Wei Wei, Hongjin Huo, Xinxi Song et.al.

Toxicology Letters, Volume 413, November 2025,
https://doi.org/10.1016/j.toxlet.2025.111731

Abstract: This cross-sectional study investigated the associations between individual and mixed exposure to per- and polyfluoroalkyl substances (PFAS) and osteoporosis, and explored potential biological mechanisms in 2764 U.S. adults. Multivariable logistic regression and weighted quantile sum (WQS) regression were applied to examine associations between individual and mixed PFAS exposure and osteoporosis. Restricted cubic spline (RCS) was used to assess dose-response relationships. Mediation analysis was used to evaluate the mediated effects of neutrophil-to-lymphocyte ratio (NLR). Five PFAS compounds (PFOA, perfluorooctanoic acid; PFOS, perfluorooctane sulfonic acid; PFHxS, perfluorohexane sulfonic acid; PFDeA, perfluorodecanoic acid; PFNA, perfluorononanoic acid) with > 80 % detection rates were selected for investigation in this study. Individual exposure to PFOA, PFOS, PFHxS and PFNA were associated with increased lumbar osteoporosis risk (OR Ln-PFOA = 1.963, 95 %CI: 1.433, 2.687, OR Ln-PFOS = 1.422, 95 %CI: 1.061, 1.907, OR Ln-PFHxS = 1.530, 95 %CI: 1.141, 2.052, OR Ln-PFNA = 1.597, 95 %CI: 1.218, 2.094). Dose-response relationships were observed for PFOA and PFHxS, particularly in women and young adults. WQS regression demonstrated that mixed PFAS exposure increased osteoporosis risk (OR = 1.198, 1.077–1.318) and decreased bone mineral density (BMD, β = −0.017, −0.026 to −0.008), with PFOA contributing most significantly (41–48 % weight). NLR partially mediated these associations. Bioinformatic analyses further identified osteoporosis-related targets and pathways, with inflammation emerging as a key mechanistic link in these associations. Our findings demonstrated a significant association between PFAS exposure and osteoporosis risk, underscoring the importance of reducing PFAS exposure in mitigating bone disease burden.

25COASNOV22

Title: Role of inflammatory response in benzo[a]pyrene-induced noradrenergic axon degeneration in mouse brain

Yousra Reda, Cai Zong, Akane Ikoma et.al.

Toxicology Letters, Volume 413, November 2025,
https://doi.org/10.1016/j.toxlet.2025.111737

Abstract: Environmental pollution is a major contributor to neurotoxicity and could explain various nervous system dysfunctions. The polycyclic aromatic hydrocarbon (PAH) benzo[a]pyrene (B[a]P) is widely present in the environment, including air polluted with combustion or cigarette smoke, and considered to be involved in the development of neurodegenerative disorders. Our previous study demonstrated that B[a]P decreased noradrenergic axon density and upregulated proinflammatory cytokines in the mouse brain. The aim of this study was to explore the hypothesis that B[a]P induced neurodegeneration through signals related to inflammatory response in the brain and that sulforaphane (SFN), a naturally present antioxidant and anti-inflammatory compound, can protect against B[a]P-induced neurotoxicity. Adult male mice (C57Bl/6JJcl) were exposed to B[a]P at 0, 0.87, 2.74 or 8.67 μg which is approximately equivalent to (0.037,0.117 and 0.37 mg/kg) by pharyngeal aspiration once a week, with subcutaneous injection of SFN at 0 or 25 mg/kg body weight daily for 4 weeks. Neurotoxicity was evaluated by morphological examination of noradrenergic axon density and the positive stained Iba-1 microglia in the hippocampal areas CA1 and CA3. Moreover, we also analyzed the expression of various genes in the same tissues. At 8.67 μg, B[a]P significantly increased brain weight. Sulforaphane protected against B[a]P-induced neurotoxicity, including brain weight gain, decreased noradrenergic axon density, and microglial activation in the hippocampus. Sulforaphane also suppressed B[a]P-induced upregulation of Nf-κB and Il-6. These findings demonstrate that SFN effectively protected against B[a]P-induced neuroinflammation and axonal degeneration and suggest that B[a]P-induced neurodegeneration is mediated through brain inflammatory response.

25COASNOV23

Title: Challenges and solutions in measuring commonly used biomarkers for drug-induced liver injury in a liver-on-a-chip platform

Qiang Shi, Laura K. Schnackenberg, Lijun Ren et.al.

Toxicology Letters, Volume 413, November 2025
https://doi.org/10.1016/j.toxlet.2025.111735

Abstract: Liver-on-a-chip (liver-chip) is designed to better maintain in vitro-cultured hepatic cells and improve the prediction of drug-induced liver injury (DILI). Albumin, urea, alanine aminotransferase (ALT), aspartate aminotransferase (AST), and lactate dehydrogenase (LDH) are proposed translational biomarkers for the prediction of DILI using liver microphysiological systems (MPS), including liver-chip. However, the performance of commonly-used assays for these biomarkers in liver MPS may vary. While using the Emulate® liver-chip, we observed that the activity of ALT, but not AST, measured using the extensively validated International Federation of Clinical Chemistry and Laboratory Medicine (IFCC) Reference Procedure, spontaneously and remarkably decreased in the perfusing medium after 24 h. Furthermore, ALT and AST activity remained largely below the

detection limit (5 U/L) after acetaminophen treatment when their protein concentrations were increased by approximately 20-fold, as determined by an enzyme-linked immunosorbent assay (ELISA). The protein concentrations of ALT and AST, but not activity, showed good correlation with LDH activity, which was nearly eliminated after a freeze-thaw cycle. For viability of non-parenchymal cells, an unusually high background signal, largely attributable to CultureBoost and fetal bovine serum in the perfusion medium, prevented the use of LDH activity assays; however, LDH ELISA appeared to be a useful alternative. Of two widely used urea assays, the enzymatic approach was profoundly affected by medium supplements, wherein sample dilution increased the limit of detection, making it impossible to observe drug-induced urea inhibition. By contrast, the chemical assay offered adequate and improved specificity and sensitivity. For albumin, an ELISA had to be adopted, since routinely used dye-binding methods were not sensitive enough. These findings provide a plausible explanation for some controversies in the literature and highlight the significance of establishing reliable and reproducible assays for translational DILI biomarkers in liver MPS.

25COASNOV24

Title: Application of an in vitro reconstructed human skin coculture with THP-1 on cosmetics in skin sensitization

Bo Wang, Hongyu Ma , Yuying Cheng et.al.

Toxicology Letters,Volume 413, November 2025
https://doi.org/10.1016/j.toxlet.2025.111738

Abstract: Sensitivity testing for cosmetic formulations mainly involves human patch tests. Cell models, including KeratinoSensTM, ARE-Nrf2 luciferase LuSens and h-CLAT, can predict chemical sensitization according to the OECD 442E standard.Objective: The aim of this study was to identify a potential approach for the assessment of the sensitization potential of cosmetics using skin models cocultured with THP-1 cells.Methods: We identified the surface markers CD54 and CD86 in THP-1 cells using flow cytometry and enzyme-linked immunosorbent assays (ELISAs); detected the relative secretion of IL-18, MTT and 7AAD; and evaluated tissue and cell viability. Adverse reactions were analysed using the human patch test.Results: The relative level of IL-18 secretion after exposure to cinnamyl aldehyde, 2,4-dinitrochlorobenzene, propyl gallate and coumarin was less than 0.79. The relative fluorescence intensity of CD54 was greater than 150, and that for CD86 was greater than 200. Using RFI CD54 $\geq$ 150, RFI CD86 $\geq$ 200 or RS IL-18 $\leq$ 0.79 as the potential sensitization standard, an 18-item cosmetic formulation caused sensitization. Moreover, a 23-item cosmetic formulation caused sensitization in the human patch test. The sensitivity to the products in the in vitro test reached 56.52 %, compared with 75 % for the cleaning products.Conclusion: RFI CD54/CD86 and IL-18 may serve as a new approach to evaluate potential sensitization to cosmetics. In vitro SkinEthic and THP-1 cell coculture combined with the human patch test may better predict potential sensitization to cosmetics.

25COASNOV25

Title: Geniposide induces hepatotoxicity via the bile acid-induced activation of NLRP3 inflammasome and regulation of the FXR/PERK/TXNIP pathway

Zhinan Jin, Shenghui Cheng, Baoyue Liu et.al.

Toxicology Letters, Volume 413, November 2025,

https://doi.org/10.1016/j.toxlet.2025.111740

Abstract: Gardenia jasminoides, as a widely used traditional Chinese medicine, excessive consumption of it may lead to severe liver injury. As the main hepatotoxic component in Gardenia jasminoides, the specific mechanism by which geniposide (GE) causes liver injury remains elusive. In this study, we conducted a systematic investigation of the effects of GE on bile acid (BA) metabolism and related signal transduction and inflammatory pathways in healthy Sprague-Dawley (SD) rats after oral administration of a 13-fold clinical equivalent dose (450 mg/kg) for 5 days. It is noteworthy that GE administration altered the content and composition of BAs and disrupted BA metabolism. At the same time, the expressions of farnesoid X receptor (FXR) and its downstream proteins bile salt export pump (BSEP) and sodium taurocholate cotransporting polypeptide (NTCP) are significantly inhibited. In addition, the inhibition of FXR will increase the signal transduction of the protein kinase R-like endoplasmic reticulum kinase (PERK)-thioredoxin-interacting protein (TXNIP)-nod-like receptor family pyrin domain-containing 3 (NLRP3) inflammasome axis, thereby triggering cysteine protease-1 (caspase-1), leading to the release of inflammatory factors and worsening liver injury. The addition of the FXR agonist obeticholic acid (OCA) effectively reversed the expressions of the above proteins and mRNA, and alleviated the liver injury caused by GE by restoring BAs homeostasis and regulating the inflammatory pathway. Conclusion: GE causes severe liver injury by affecting bile acid metabolism and inflammatory pathways, and the inhibition of FXR is a crucial factor.

25COASNOV26

Title: PFOA exposure causes kidney injury via disruption of lipid metabolism mediated by PPARα signaling pathway: An integrated analysis

Yuanyuan Wu, Yuhong Jiang, Zhonghua Fan et.al.

Toxicology Letters, Volume 413, November 2025,
https://doi.org/10.1016/j.toxlet.2025.111736

Abstract: Perfluorooctanoic acid (PFOA) is a persistent organic pollutant (POP) that can accumulate in living organisms and cause damage to multiple organs and systems in the human body. The kidney is viewed as a key organ affected by PFOA, but the exact mechanism by which PFOA exposure causes kidney damage remains unclear. We selected data from 13,804 participants aged > 12 years old from the National Health and Nutrition Examination Survey (NHANES) database from 2003 to 2018 to analyze the relationship between PFOA and kidney injury. In addition, in the animal experiment, twenty adult male SD rats were divided into four groups randomly: one control group and three PFOA-treated groups. The experiment lasted 28 days, during which time water consumption and urine output were recorded daily. Kidney tissue samples were collected at the end of the experiment. Biochemical assays, RT-qPCR and Western blotting techniques were used to investigate the toxic effects of PFOA exposure on the kidney. Analysis of NHANES data shows a positive correlation between serum PFOA and uric acid (UA) with a β-value of 0.23 (95 % CI: 0.18–0.27) in Model 2. In animal studies, PFOA significantly affected rats' water intake (increased at 5 mg/kg/d, decreased at 20 mg/kg/d) and urine output (5 > 1.25 > 20 mg/kg/d > control). Renal biochemical analyses revealed significantly lower total cholesterol (TC) (1.25, 20 mg/kg/d groups) and triglyceride (TG) (1.25, 5 mg/kg/d groups) in PFOA-exposed rats. The peroxisome proliferator-activated receptors (PPAR) pathway-related

gene/protein levels were significantly altered, such as 900 differentially expressed genes (DEGs) in the 20 mg/kg/d group and upregulated ACOT1 in all PFOA groups. In conclusion, the present study confirms that exposure to PFOA leads to increased oxidative catabolism of fatty acids and impaired renal lipid metabolism. These findings provide an important basis for elucidating the potential health hazards of PFOA.

25COASNOV27

Title: Bisphenol A exposure associates with colorectal cancer metastasis and immunosuppression: A five-year cohort study

Xiaoming Shen, Chuanqing Bao

Toxicology Letters, Volume 413, November 2025,
https://doi.org/10.1016/j.toxlet.2025.111732

Abstract: Bisphenol A (BPA) is a widespread endocrine-disrupting chemical found in consumer products. While BPA exposure has been associated with various health risks, its specific impact on colorectal cancer (CRC) progression and underlying mechanisms remain poorly understood.Methods: In this five-year retrospective cohort study, we analyzed 63 CRC patients selected from an initial cohort of 574. Urinary BPA was quantified using HPLC-MS/MS, and patients were stratified into normal (n = 15), low (n = 30), and high (n = 18) BPA exposure groups. Flow cytometry and immunohistochemistry profiled immune cell populations in blood and tumor tissues. Multivariate regression analyses identified relationships between BPA exposure, metabolic parameters, and clinical outcomes.Results: BPA levels showed significant inverse correlations with HDL/LDL ratio ($p = 0.010$) and positive correlations with BMI ($p = 0.028$). Patients with high BPA exposure demonstrated significantly higher rates of metastasis (61.1 % vs. 10 % in low exposure and 0 % in normal exposure groups, $p < 0.001$) and shorter overall survival (median 20 months vs. 51 months in low exposure group, $p = 0.034$). Flow cytometric analysis revealed dose-dependent reductions in circulating CD8 + T cells, CD4 + T cells, and NK cells with increasing BPA exposure. Immunohistochemical analysis showed pronounced decreases in tumor-infiltrating CD8 + T lymphocytes correlating with BPA exposure levels ($p = 0.0027$). High BPA exposure was also significantly associated with increased post-surgical infection rates (OR=1.9, 95 % CI: 1.1–3.1).Conclusion: These preliminary findings suggest BPA exposure represents a potential risk factor for CRC progression, likely mediated through metabolic alterations and immunosuppression within the tumor microenvironment. Environmental exposures may significantly influence cancer outcomes through immune-metabolic pathways, though further validation in larger cohorts is warranted.

25COASNOV28

Title: Association between volatile organic compound exposure and elevated total immunoglobulin E: Risk factor screening in mixed exposure scenarios and potential biological mechanisms

Xianhao Wang, Xinyue Wang, Ruxu Yan et.al.

Toxicology Letters, Volume 413, November 2025,
https://doi.org/10.1016/j.toxlet.2025.111730

Abstract: Environmental pollutants are increasingly recognized as important modulators of immune function, yet the influence of volatile organic compound (VOC) exposure on

immunoglobulin E (IgE) levels remains poorly characterized. Using data from the National Health and Nutrition Examination Survey (NHANES) 2005–2006, we systematically evaluated the association between VOC metabolites and total IgE levels through five statistical approaches combined with machine learning algorithms. Mediation analyses were conducted to examine the role of inflammatory markers in these associations. Finally, functional enrichment analyses were employed to identify potential pathways and key molecular targets. Our analyses consistently demonstrated significant positive associations between VOC exposure and elevated total IgE levels. 2-aminothiazoline-4-carboxylic acid (ATCA), N-Acetyl-S-(2-cyanoethyl)-L-cysteine (CYMA), and N-Acetyl-S- (3-hydroxypropyl)-L-cysteine (HPMA) emerged as robust risk factors. Mediation analysis revealed that eosinophil (EOS) counts accounted for 15.89–29.03 % of the observed associations between VOC metabolites and total IgE levels. TNF and IL-17 signaling pathways were significantly enriched. Integrated analyses confirmed VOC exposure as a significant environmental risk factor for elevated total IgE levels, primarily driven by ATCA, CYMA, and HPMA, with inflammatory responses as a plausible mechanism.

25COASNOV29

Title: Human serum albumin-adduct biomarkers to prove human poisoning with methanethiol

Chenglong Zhang, Ruiqin Yang, Shuai Liu et.al.

Toxicology Letters, Volume 413, November 2025,
https://doi.org/10.1016/j.toxlet.2025.111741

Abstract: Exposure to methanethiol (MT) presents a significant challenge in public healthcare and could be a concern in the context of terrorist attacks. Therefore, reliable verification procedures for MT intoxication are essential for forensic, toxicological, and clinical purposes. We developed and validated a bioanalytical method for the simultaneous detection and identification of biomarkers indicative of MT exposure. Neat human serum albumin (HSA) and human plasma were incubated with MT to form adducts, which served as references. Subsequently, HSA and human plasma were subjected to proteolysis using two proteases, resulting in the formation of disulfide adducts detected as adducts of the single amino acid cysteine (MT-Cys), the dipeptide cysteine-proline (MT-Cys34Pro), and the tripeptides aspartic acid-isoleucine-cysteine (AspIleCys514-MT) and cysteine-proline-phenylalanine (MT-Cys34ProPhe). The adducts were analyzed using a sensitive ultra-performance liquid chromatography-quadrupole exactive orbitrap-high resolution mass spectrometry (UPLC-Q Exactive Orbitrap-HRMS) method operating in full scan mass spectrometry (Full MS) and parallel reaction monitoring (PRM) mode. Time- and concentration-dependent adduct formation during exposure was investigated. The limits of detection (LODs) for the adducts ranged from 20 ng/mL to 2 µg/mL, corresponding to the MT concentrations in plasma. Adducts at Cys34 exhibited the lowest LOD (20 ng/mL MT in plasma), the fastest adduct formation (20 min), and superior stability in plasma at 37 °C. The applicability of the method was demonstrated by the successful detection of adducts in sample from MT-poisoned patient, establishing the method as a reliable bioanalytical procedure for forensic and toxicological analysis.

25COASNOV30

Title: Is lychee-associated encephalopathy in children a straightforward case of toxicity or a complex metabolic and environmental cascade?

Richa Soni, Santasabuj Das, Gopal Shankar Sahni et.al.

Toxicology Letters, Volume 413, November 2025,
https://doi.org/10.1016/j.toxlet.2025.111742

Abstract: Every year, annual outbreaks of AES occur in lychee-growing regions: previously healthy children suddenly succumb to Acute Encephalitis Syndrome (AES). Initial suspicions pointed towards the seemingly innocent lychee fruit and its inherent toxins, Hypoglycin A and MCPG. However, the toxin-alone hypothesis is challenged by the fact that lychees are safely consumed globally. This discrepancy suggests that the development of severe illness is not caused by the toxins alone but requires specific host vulnerabilities, such as malnutrition, and co-factors like the consumption of unripe fruit on an empty stomach. This has prompted the consideration of alternative hypotheses. These include the role of pesticide contamination in orchards, potential bat-borne viral infections, and environmental stressors that may shift with seasons and geography. The striking differences in illness patterns observed in Bihar (India), Bangladesh, and Vietnam further complicate the picture. Moreover, documented reports of children falling ill with AES without any reported lychee consumption cast doubt on a singular explanation. This review delves into the heart of this enduring medical enigma, critically dissecting the compelling arguments and critical caveats surrounding each potential cause. This review critically evaluates the evidence for the multifaceted theories behind lychee-associated AES and challenges established assumptions. The analysis indicates a multifactorial etiology is responsible for this recurring childhood tragedy.

25COASNOV31

Title: Differentiating the in vitro toxicity of solid-surface composite dust: A comparison of material components and abrasive particles

W. Kyle Mandler, Walter McKinney, Chaolong Qi et.al.

Toxicology Letters,Volume 413, November 2025
https://doi.org/10.1016/j.toxlet.2025.111743

Abstract: Workers fabricating solid-surface composite (SSC) materials like Corian® are exposed to airborne particulate matter (PM) containing aluminum trihydrate (ATH) and potentially abrasive particles from sanding tools, leading to concerns about respiratory health effects like pulmonary fibrosis. However, the relative toxicological contributions of the SSC material versus the sandpaper abrasives remain unclear. Objective: This study aimed to compare the in vitro cellular responses induced by respirable dust generated from sanding SSC with different commercial sandpapers (aluminum oxide [Al2O3], ceramic, silicon carbide [SiC]) to the responses elicited by ATH and corresponding abrasive analogue particles.Methods: Respirable dust (PM with an aerodynamic diameter less than 5 µm) was generated from sanding Corian® using the three sandpaper types via a fluidized bed generator coupled with a cyclone separator. Human monocytic THP-1 cells, differentiated into macrophage-like cells, were exposed for 48 h to suspensions of these SSC dusts, ATH, or Al2O3, ceramic, and SiC abrasive analogue particles (10 µg/well). Cytotoxicity (LDH release), apoptosis (Caspase 3/7 activity), necrosis (propidium iodide uptake), cell cycle distribution, and nuclear morphology (including mono-, bi-, multi-, and micronucleation) and

the Nuclear Division Index were assessed. Results: Exposure to SSC dusts generated with any sandpaper type, as well as ATH, resulted in significant increases in apoptosis compared to controls. However, these exposures did not cause significant LDH release or alterations in cell cycle progression or mitotic indices. Conversely, the Al2O3, ceramic, and SiC abrasive analogue particles induced significant disruptions in cell cycle (S phase population reduction) and mitosis (increased multinucleation, micronucleation, and NDI), alongside apoptosis (Al2O3, SiC) or necrosis (ceramic, SiC), but also caused minimal LDH release.Conclusion: Under these in vitro conditions, the apoptotic response to respirable SSC sanding dust appears primarily driven by components inherent to the SSC material itself, consistent with the effects of ATH. This response profile was distinct from the cell cycle arrest and mitotic disruption prominently caused by the abrasive analogue particles. These findings suggest the intrinsic properties of SSC material components are key drivers of initial macrophage responses in vitro, differing significantly from the effects of the abrasive materials alone.

25COASNOV32

Title: Toxicological evaluation of 4-methylimidazole: Research advances, health concerns and regulatory perspectives

Shikha, Keerti Gautam, Muskan Sharma

Toxicology Letters, Volume 413, November 2025

https://doi.org/10.1016/j.toxlet.2025.111747

Abstract: This review provides a comprehensive analysis of the toxicology, mechanistic pathways, and regulatory evaluations of 4-methylimidazole (4-MI), a nitrogen-containing compound formed during caramel coloring production and industrial synthesis. The study aimed to consolidate evidence on health risks and clarify regulatory inconsistencies. Experimental models show that 4-MI induces hepatotoxicity via oxidative stress, mitochondrial dysfunction, and inflammation, leading to liver cell damage. Neurotoxicity includes behavioral changes, brain mitochondrial injury, and teratogenic effects. Reproductive toxicity has been observed in rodents and zebrafish, impairing sperm function, hormone production, and embryonic development. Although cytotoxic and genotoxic effects—such as DNA damage and chromosomal aberrations—have been reported, standard mutagenicity assays largely remain negative, contributing to regulatory uncertainty. California classifies 4-MI as a possible carcinogen with strict exposure limits, while EFSA finds genotoxic evidence insufficient. Emerging studies also link 4-MI to disruptions in glucose and lipid metabolism, raising concerns about chronic low-dose dietary exposure. Overall, these findings highlight significant public health risks and the urgent need for further toxicodynamic research to inform harmonized regulations and more accurate risk assessments.

25COASNOV33

Title: Evaluating the role of glutathione reductase in aspartame-induced liver hepatocellular carcinoma: A molecular network and prognostic approach

Wenhui Sun, Siyan Huo, Shitian Li et.al.

Toxicology Letters, Volume 413, November 2025

https://doi.org/10.1016/j.toxlet.2025.111748

Abstract: This study aims to elucidate the molecular mechanisms underlying aspartame-

associated liver hepatocellular carcinoma (LIHC) by identifying glutathione reductase (GSR) as a key molecular target. Through a combination of network toxicology analysis and Mendelian randomization, GSR was implicated as a critical protein involved in the pathogenesis of aspartame-associated LIHC. Functional annotation using Gene Ontology (GO) and Kyoto Encyclopedia of Genes and Genomes (KEGG) pathways revealed that GSR is predominantly involved in energy metabolism, particularly lipid metabolism and glycolysis, both of which are central to tumorigenesis in LIHC. Elevated GSR expression was observed in LIHC tumor tissues, correlating with poor clinical outcomes including reduced overall survival (OS) and recurrence-free survival (RFS). Furthermore, genetic analyses revealed significant alterations in GSR, including mutations and copy number variations, in various cancer types, with specific relevance to immune regulatory gene networks. Molecular dynamics simulations demonstrated a robust binding affinity between aspartame and GSR, with favorable binding interactions, suggesting a stable protein-ligand complex. Additionally, functional assays confirmed that GSR modulates tumor cell proliferation via regulation of glycolytic enzyme activity, indicating its pivotal role in metabolic reprogramming during LIHC progression. These findings collectively highlight GSR as a promising biomarker and therapeutic target in the context of aspartame-associated hepatocellular carcinoma, with implications for targeted intervention in cancer treatment.

25COASNOV34

Title: Embryo-fetal developmental toxicity and toxicokinetics studies of YWS20045 orally administered to pregnant rats

Haonan Li , Peng Yue, Qing Shao et.al.

Toxicology Letters, Volume 413, November 2025
https://doi.org/10.1016/j.toxlet.2025.111749

Abstract: This study aimed to explore the embryo-fetal developmental toxicity and concurrent toxicokinetic characteristics of YWS20045 in rats. Pregnant rats were divided into a solvent control group, three YWS20045 dose groups (4, 16 and 32 mg/kg), and a positive control group (3.5 mg/kg cyclophosphamide). Oral administration was conducted from gestation day (GD) 6–17. Results showed that all dose groups exhibited loose stools, with the high dose group experiencing significant maternal toxicity, including perianal soiling, reduced food intake, weight loss, increased dead fetuses on GD20 and mortality. YWS20045 crossed the placental barrier and accumulated in fetuses at all doses. Doses of 4 mg/kg and above significantly increased fetal rib deformities, affecting fetal growth and development. Toxicokinetic analysis revealed non-proportional increases in Cmax and AUC(0-t) of YWS20045 and its metabolite with dose. The drug was primarily distributed in the liver and lungs, with maternal metabolite mainly in the lungs. Therefore, the relatively safe oral dose of YWS20045 for maternal rats in the embryonic-fetal developmental toxicity study was determined to be 16 mg/kg or lower, whereas doses of 4 mg/kg and above were found to adversely affect fetal growth and development. These findings provide a critical basis for evaluating the reproductive safety of YWS20045 in clinical use.

25COASNOV35

Title: Microplastics as vectors for environmental contaminants in the food chain: Assessing the combined toxicological effects and bioavailability

Jia Du, Linlin Qiu, Qingwei Zhou et.al.
Toxicology Letters, Volume 413, November 2025
https://doi.org/10.1016/j.toxlet.2025.111734
Abstract: The global proliferation of microplastics (MPs) and nanoplastics (NPs) has raised concerns not only for their persistence in ecosystems but also for their role as transport agents of environmental contaminants through food chains. This review provides a comprehensive analysis of the mechanisms driving the sorption and desorption of diverse pollutants—including hydrophobic organics, metals, additives, and microbial agents—onto plastic particles, emphasizing how polymer composition, particle size, environmental aging, and eco-corona formation influence these interactions. Particular attention is paid to the transfer of MPs/NPs across trophic levels and their documented presence in various food items consumed by humans. The paper evaluates how ingestion may lead to desorption of contaminants in gastrointestinal environments, with in vitro studies demonstrating variable bioaccessibility depending on physicochemical and digestive conditions. Furthermore, the review synthesizes findings on cellular and systemic toxicity, highlighting how exposure to MPs/NPs—alone or in combination with other contaminants—can disrupt oxidative balance, immune responses, metabolic regulation, and reproductive health. Notably, combined exposures often result in synergistic or antagonistic effects, contingent on concentration, particle properties, and biological context. The potential for translocation of smaller particles and their associated chemicals across epithelial barriers introduces an additional vector of concern for internal exposure. Methodological variability in contamination assessment, limited real-world exposure data, and unresolved questions regarding long-term health consequences underscore the need for standardization and further investigation. This review aims to inform future risk assessments by integrating current knowledge of contaminant transport, bioavailability, and co-toxicological effects related to MPs/NPs in environmental and food systems.

25COASNOV36

Title: Toxicity of humectants propylene glycol and vegetable glycerin in electronic nicotine delivery systems

Yehao Sun, Karen Lin, Felix Effah et.al.
Toxicology Letters, Volume 413, November 2025
https://doi.org/10.1016/j.toxlet.2025.111739
Abstract: E-cigarettes and other electronic nicotine delivery systems (ENDs) remain a significant public health risk. Although deployed as tobacco smoking cessation tools, e-cigarettes have gained greater popularity among non-smokers, specifically adolescents and young adults. Previous research has focused primarily on the toxicities associated with nicotine, flavorings, and other chemicals generated from e-cigarette liquid aerosolization; however, little attention has been given to the two primary and most abundant chemicals found in most e-cigarette liquids – propylene glycol (PG) and vegetable glycerin (VG).Purpose: The purpose of this review is to assess the toxicity associated with PG/VG in e-cigarettes to inform future ENDS regulations.Methods: Database searches were performed using PubMed for relevant literature published from 1/1/2014–9/1/2025. Cited articles about the prevalence, toxicities, and public perceptions of PG/VG.Results: Toxicity associated with PG/VG inhalation is primarily due to thermal degradation byproducts (TDBs) generated by

PG/VG-containing e-liquids. More specifically, high-power ENDS devices with sub-ohm power capabilities generate aerosols with larger mass and higher concentrations of TDBs. The most common TDBs identified in e-cigarette aerosols include formaldehyde, acetaldehyde, acrolein, acetone, acetoin/diacetyl, as well as benzene. These TDBs, along with other chemical adducts, contribute significantly to the e-cigarette aerosols' potential to cause oxidative stress, airway inflammation, and increase risks for cancer. Mechanistically, the toxicity associated with e-cigarette aerosols is mediated through the activation of the NF-κB and MAPK pathways, as well as the dysfunction of ion channels responsible for mucus hydration. These effects of e-cigarette aerosol exposures, whether induced by TDBs or other chemicals, can be affected by factors involved in the aerosolization process, including the ratio of PG/VG, the device power, and the resistance of the coil.Conclusions: E-cigarettes are often considered a harm-reduction alternative to combustible cigarettes due to PG and VG's FDA designation as "Generally Recognized as Safe" (GRAS) for consumption. However, when heated and inhaled, mixtures of PG/VG in e-cigarette liquids have their toxicities independent of the other constituents of e-liquids. Future regulations that focus on the PG/VG ratios, set limits on thermal degradation byproducts, and establish exposure thresholds for e-cigarette aerosols will help reduce toxic exposures associated with PG/VG inhalation. As such, further research is needed on PG/VG alone to understand its long-term health effects better and to inform evidence-based public health policies.

25COASNOV37

Title: A systematic review on the effect of microplastics on the hypothalamus-pituitary-ovary axis based on animal studies

Saeed Shahsavari, Behrouz Akbari-Adergani, Hamed Shafaroodi et.al.

Toxicology Letters, Volume 413, November 2025
https://doi.org/10.1016/j.toxlet.2025.111745

Abstract: Humans are exposed to microplastics through three routes: oral, dermal, and respiratory. These tiny polymer particles enter the body and accumulate in various organs. One of the most sensitive organs to microplastics is the female reproductive system. In this review, manuscripts that investigated the effects of various microplastics on the hypothalamic-pituitary-ovarian axis in laboratory animals were collected with relevant keywords. This axis plays an important role in the function of the female reproductive system. Effects on endpoints of this axis, including hormonal changes, gene expression, and histopathological changes, were assessed. The most studied microplastic was polystyrene. Hormone levels were measured in all studies. In almost all studies, 17β-estradiol was decreased. Apoptosis and oxidative stress-induced damage in the ovaries were also observed in some studies. The results summarized from the manuscript emphasize the adverse effects of microplastics, especially polystyrene microplastics, on the female reproductive system following exposure.

25COASNOV38

Title: Translational regulation in stress biology

Naomi R. Genuth & Andrew Dillin

Nature Cell Biology volume 27, pages1609–1621 (2025)
https://doi.org/10.1038/s41556-025-01765-z

Abstract: Organisms must constantly respond to stress to maintain homeostasis, and the successful implementation of cellular stress responses is directly linked to lifespan regulation. In this Review we examine how three age-associated stressors—loss of proteostasis, oxidative damage and dysregulated nutrient sensing—alter protein synthesis. We describe how these stressors inflict cellular damage via their effects on translation and how translational changes can serve as both sensors and responses to the stressor. Finally, we compare stress-induced translational programmes to protein synthesis alterations that occur with age and discuss whether these changes are adaptive or deleterious to longevity and healthy ageing.

25COASNOV39

Title: Nuclear mechanics as a determinant of nuclear pore complex plasticity

C. Patrick Lusk, Kimberly J. Morgan & Megan C. King

Nature Cell Biology volume 27, pages1622–1631 (2025)
https://doi.org/10.1038/s41556-025-01768-w

Abstract: Thousands of nuclear pore complexes (NPCs) cover the nuclear surface of mammalian cells and establish selective transport conduits that biochemically segregate the nucleoplasm and cytoplasm. Although the molecular composition and structure of archetypical NPCs are well understood, distinct NPCs composed of varying nucleoporins exist in different cell types and even within individual cells. Furthermore, the integration of NPCs within mechanosensitive networks impacts their dilation state. However, whether (and how) the dilation or compositional plasticity of NPCs impacts their primary role as selective transport channels remains unclear. Based on our current understanding of NPC plasticity, we propose here that nuclear membrane tension and the resulting dilation of nuclear pores is a determinant of the compositional plasticity of NPCs, thus providing a framework to interpret how nucleoporins may influence cell fate decisions and explain the tissue-specificity of some NPC-related diseases.

25COASNOV40

Title: NOX1 and NPY1R mark regional colon stem cell populations that serve as cancer origins in vivo

Maxime Gasnier, Tanysha Chi-Ying Chen et.al.

Nature Cell Biology volume 27, pages1632–1646 (2025)
https://doi.org/10.1038/s41556-025-01763-1

Abstract: Current colorectal cancer mouse models either lack colon specificity, limiting progression towards more advanced disease, or preclude evaluation of resident stem cells as cancer origins. Here we report the identification of NOX1 and NPY1R as cell-surface markers enriched in LGR5+ stem cells predominantly within the caecum and exclusively within the middle and distal colorectum, respectively. Selective dysregulation of Wnt signalling in NOX1+ or NPY1R+ stem cells using CreERT2 mouse lines drives colon cancer initiation, predominantly within the caecum and rectum respectively, establishing these stem cell populations as important sources of colon cancer. Selective conditional activation of Wnt signalling and oncogenic Kras in combination with loss of TRP53 in these stem cell compartments resulted in the development of advanced, invasive cancers. This study establishes CreERT2 drivers as valuable tools for studying stem cell contributions to colon

cancer.

25COASNOV41

Title: Antagonistic stem cell fates under stress govern decisions between hair greying and melanoma

Yasuaki Mohri, Jialiang Nie, Hironobu Morinaga et.al.

Nature Cell Biology volume 27, pages1647–1659 (2025)
https://doi.org/10.1038/s41556-025-01769-9

Abstract: The exposome, an individual's lifelong environmental exposure, profoundly impacts health. Somatic tissues undergo functional decline with age, exhibiting characteristic ageing phenotypes, including hair greying and cancer. However, the specific genotoxins, signals and cellular mechanisms underlying each phenotype remain largely unknown. Here we report that melanocyte stem cells (McSCs) and their niche coordinately determine individual stem cell fate through antagonistic, stress-responsive pathways, depending on the type of genotoxic damage incurred. McSC fate tracking in mice revealed that McSCs undergo cellular senescence-coupled differentiation (seno-differentiation) in response to DNA double-strand breaks, resulting in their selective depletion and hair greying, and effectively protecting against melanoma. Conversely, carcinogens can suppress McSC seno-differentiation, even in cells harbouring double-strand breaks, by activating arachidonic acid metabolism and the niche-derived KIT ligand, thereby promoting McSC self-renewal. Collectively, the fate of individual stem cell clones—expansion versus exhaustion—cumulatively and antagonistically governs ageing phenotypes through interaction with the niche.

25COASNOV42

Title: Edge curvature drives endoplasmic reticulum reorganization and dictates epithelial migration mode

Simran Rawal, Pradeep Keshavanarayana et.al.

Nature Cell Biology volume 27, pages1660–1675 (2025)
https://doi.org/10.1038/s41556-025-01729-3

Abstract: From single-cell extrusion to centimetre-sized wounds, epithelial gaps of various sizes and geometries appear across organisms. Their closure involves two orthogonal modes: lamellipodial crawling at convex edges and purse string-like movements at concave edges. The mechanisms driving this curvature-dependent migration remain unclear. Here we perform an intracellular cartography to reveal that in both micropatterned and naturally arising gaps, the endoplasmic reticulum (ER) undergoes edge curvature-dependent morphological reorganizations, forming tubules at convex edges and sheets at concave edges. This reorganization depends on cytoskeleton-generated protrusive and contractile forces. Mathematical modelling reveals that these morphologies minimize strain energy under their respective geometric regime. Functionally, ER tubules at the convex edge favour perpendicularly oriented focal adhesions, supporting lamellipodial crawling, while ER sheets at the concave edge favour parallelly oriented focal adhesions, supporting purse string-like movements. Altogether, ER emerges as a central mechanotransducer, integrating signals from cytoskeletal networks to orchestrate two orthogonal modes of cell migration.

25COASNOV43

Title: Membrane receptors cluster phosphatidylserine to activate LC3-associated phagocytosis

Emilio Boada-Romero, Clifford S. Guy, Gustavo Palacios et.al.

Nature Cell Biology volume 27, pages1676–1687 (2025)
https://doi.org/10.1038/s41556-025-01749-z

Abstract: LC3-associated phagocytosis (LAP) represents a non-canonical function of autophagy proteins in which ATG8-family proteins (LC3 and GABARAP proteins) are lipidated onto single-membrane phagosomes as particles are engulfed by phagocytic cells. LAP plays roles in innate immunity, inflammation and anticancer responses, and is initiated following phagocytosis of particles that stimulate Toll-like receptors (TLR) and Fc receptors as well as following engulfment of dying cells. However, how this molecular process is initiated remains elusive. Here we report that receptors that engage LAP enrich phosphatidylserine (PS) in the phagosome membrane via membrane-proximal domains that are necessary and sufficient for LAP to proceed. Subsequently, PS recruits the Rubicon-containing PI3-kinase complex to initiate the enzymatic cascade leading to LAP. Manipulation of plasma membrane PS content, PS binding by Rubicon or the PS-clustering domains of receptors prevents LAP and delays phagosome maturation. Therefore, the initiation of LAP represents a novel mechanism of PS-mediated signal transduction following ligation of surface receptors.

25COASNOV44

Title: Chaperone-mediated autophagy regulates neuronal activity by sex-specific remodelling of the synaptic proteome

Rabia R. Khawaja, Ernesto Griego, Kristen Lindenau et.al.

Nature Cell Biology volume 27, pages1688–1707 (2025)
https://doi.org/10.1038/s41556-025-01771-1

Abstract: Chaperone-mediated autophagy (CMA) declines in ageing and neurodegenerative diseases. Loss of CMA in neurons leads to neurodegeneration and behavioural changes in mice but the role of CMA in neuronal physiology is largely unknown. Here we show that CMA deficiency causes neuronal hyperactivity, increased seizure susceptibility and disrupted calcium homeostasis. Pre-synaptic neurotransmitter release and NMDA receptor-mediated transmission were enhanced in CMA-deficient females, whereas males exhibited elevated post-synaptic AMPA-receptor activity. Comparative quantitative proteomics revealed sexual dimorphism in the synaptic proteins degraded by CMA, with preferential remodelling of the pre-synaptic proteome in females and the post-synaptic proteome in males. We demonstrate that genetic or pharmacological CMA activation in old mice and an Alzheimer's disease mouse model restores synaptic protein levels, reduces neuronal hyperexcitability and seizure susceptibility, and normalizes neurotransmission. Our findings unveil a role for CMA in regulating neuronal excitability and highlight this pathway as a potential target for mitigating age-related neuronal decline.

25COASNOV45

Title: MAPL regulates gasdermin-mediated release of mtDNA from lysosomes to drive pyroptotic cell death

Mai Nguyen, Jack J. Collier, Olesia Ignatenko et.al.
Nature Cell Biology volume 27, pages1708–1724 (2025)
https://doi.org/10.1038/s41556-025-01774-y
Abstract: Mitochondrial control of cell death is of central importance to disease mechanisms from cancer to neurodegeneration. Mitochondrial anchored protein ligase (MAPL) is an outer mitochondrial membrane small ubiquitin-like modifier ligase that is a key determinant of cell survival, yet how MAPL controls the fate of this process remains unclear. Combining genome-wide functional genetic screening and cell biological approaches, we found that MAPL induces pyroptosis through an inflammatory pathway involving mitochondria and lysosomes. MAPL overexpression promotes mitochondrial DNA trafficking in mitochondrial-derived vesicles to lysosomes, which are permeabilized in a process requiring gasdermin pores. This triggers the release of mtDNA into the cytosol, activating the DNA sensor cGAS, required for cell death. Additionally, multiple Parkinson's disease-related genes, including VPS35 and LRRK2, also regulate MAPL-induced pyroptosis. Notably, depletion of MAPL, LRRK2 or VPS35 inhibited inflammatory cell death in primary macrophages, placing MAPL and the mitochondria–lysosome pathway at the nexus of immune signalling and cell death.

25COASNOV46

Title: Microtubule architecture connects AMOT stability to YAP/TAZ mechanotransduction and Hippo signalling

Giada Vanni, Anna Citron, Ambela Suli et.al.
Nature Cell Biology volume 27, pages1725–1738 (2025)
https://doi.org/10.1038/s41556-025-01773-z
Abstract: Cellular mechanotransduction is a key informational system, yet its mechanisms remain elusive. Here we unveil the role of microtubules in mechanosignalling, operating downstream of subnuclear F-actin and nuclear envelope mechanics. Upon mechanical activation, microtubules reorganize from a perinuclear cage into a radial array nucleated by centrosomes. This structural rearrangement triggers degradation of AMOT proteins, which we identify as key mechanical rheostats that sequester YAP/TAZ in the cytoplasm. AMOT is stable in mechano-OFF but degraded in mechano-ON cell states, where microtubules allow AMOT rapid transport to the pericentrosomal proteasome in complex with dynein/dynactin. This process ensures swift control of YAP/TAZ function in response to changes in cell mechanics, with experimental loss of AMOT proteins rendering cells insensitive to mechanical modulations. Ras/RTK oncogenes promote YAP/TAZ-dependent tumorigenesis by corrupting this AMOT-centred mechanical checkpoint. Notably, the Hippo pathway fine-tunes mechanotransduction: LATS kinases phosphorylate AMOT, shielding it from degradation, thereby indirectly restraining YAP/TAZ. Thus, AMOT protein stability serves as a hub linking cytoskeletal reorganization and Hippo signalling to YAP/TAZ mechanosignalling.

25COASNOV47

Title: Cholesterol sensing by the SCAP–FAM134B complex regulates ER-phagy and STING innate immunity

Boran Li, Dongheng Zhou, Xinyi Wang et.al.

Nature Cell Biology volume 27, pages1739–1756 (2025)
https://doi.org/10.1038/s41556-025-01766-y

Abstract: The endoplasmic reticulum (ER) is central to cholesterol biosynthesis and trafficking, yet paradoxically maintains low cholesterol levels, enabling it to sense fluctuations that impact various signalling pathways. However, the role of ER cholesterol in cellular signalling remains unclear. Here we show that the ER-phagy receptor FAM134B interacts directly with both cholesterol and SCAP, a key regulator of cholesterol biosynthesis. When ER cholesterol is high, FAM134B and SCAP are sequestered by cholesterol-tightened interactions, halting ER-phagy, STING activation and cholesterol synthesis. Under low cholesterol conditions, FAM134B dissociates from SCAP, allowing SCAP to activate SREBP2 and upregulate cholesterol synthesis, while FAM134B either facilitates ER-phagy through oligomerization or aids STING trafficking to activate innate immune responses. These findings reveal that the SCAP–FAM134B complex senses ER cholesterol levels, regulating both ER-phagy and immune signalling, with implications for diseases linked to cholesterol imbalance.

25COASNOV48

Title: A subset of transposable elements as mechano-response enhancer elements in controlling human embryonic stem cell fate

Tongyu Sun, Yueyuan Xu, Nicole Angel et.al.

Nature Cell Biology volume 27, pages1785–1796 (2025)
https://doi.org/10.1038/s41556-025-01770-2

Abstract: Transposable elements (TEs), constituting half of the human genome, are essential for development and diseases. While the regulation of TE activity by cellular intrinsic mechanisms is well documented, their response to microenvironmental signals, particularly mechanical cues involving numerous biological processes, remains unknown. Here we show that various TE families, notably LTR7, undergo transcriptomic, epigenetic and three-dimensional genome changes in response to matrix mechanical cues in human embryonic stem cells. Interestingly, LTR7s act as ‘mechano-response enhancer elements’ (MREEs), controlling the gene expression and cell fate of human embryonic stem cells. Mechanistically, mechano-effectors YAP/TEAD1 control LTR7’s epigenetic activity by engaging with BRD4. Furthermore, YAP recruits CTCF, a key genome architecture protein, to facilitate long-range interactions between gene promoters and TEs as MREEs. In particular, a mechano-responsive LTR7 element is a distal enhancer for FAM189A2, thereby inhibiting definitive endoderm differentiation. These findings highlight the underappreciated role of TEs as MREEs that control human cell fate and gene expression.

25COASNOV49

Title: Remodelling bivalent chromatin is essential for mouse peri-implantation embryogenesis

Yanhe Li, Jincan He, Yingdong Liu et.al.

Nature Cell Biology volume 27, pages1797–1811 (2025)
https://doi.org/10.1038/s41556-025-01776-w

Abstract: Bivalency regulates developmental genes during lineage commitment. However, mechanisms governing bivalent domain establishment, maintenance and resolution in early

embryogenesis remain unclear. Here we comprehensively trace bivalent chromatin remodelling throughout mouse peri-implantation development, revealing bifurcated establishment modes that partition epiblast and primitive endoderm regulatory programmes. We identify transiently maintained bivalent domains (TB domains) enriched in the epiblast, where gradual resolution fine-tunes pluripotency progression. Through targeted screening in embryos, we uncover 22 TB domain regulators, including the essential factor ZBTB17. Genetic ablation or degradation of ZBTB17 causes peri-implantation arrest. Mechanistically, ZBTB17 collaborates with KDM6A/B to resolve bivalency by removing H3K27me3 and priming the activation of key pluripotency genes. Remarkably, TB domain dynamics are evolutionarily shared in human pluripotent transitions, with ZBTB17 involvement despite species differences. Our work establishes a framework for bivalent chromatin regulation in early mammalian development and elucidates how its resolution precisely controls lineage commitment.

25COASNOV50

Title: Two microbiome metabolites compete for tRNA modification to impact mammalian cell proliferation and translation quality control

Wen Zhang, Kuldeep Lahry, Denis Cipurko et.al.

Nature Cell Biology volume 27, pages1812–1826 (2025)

https://doi.org/10.1038/s41556-025-01750-6

Abstract: The microbiome affects eukaryotic host cells via many metabolites, including the well-studied queuine as substrate for host tRNA queuosine modification. The microbial metabolite pre-queuosine 1 (preQ1) is produced in the bacterial tRNA queuosine biosynthesis pathway, with unknown effects on host cell biology. Here we show that preQ1 strongly represses cell proliferation in both human and mouse cells. Queuine reverses this effect by competing with preQ1 to modify the same tRNA. PreQ1 is detectable in the plasma and tissues of mice, and its injection suppresses tumour growth in a mouse cancer model. Mechanistically, preQ1 reduces cognate tRNA levels specifically, as well as codon-dependent translation of housekeeping genes. We identify the endoplasmic reticulum-localized inositol-requiring enzyme 1 (IRE1) ribonuclease as the enzyme responsible for the selective degradation of preQ1-modified tRNAs on translating ribosomes. Our results identify two microbial metabolites competing for host tRNA modification, which elicits translation quality control and impacts cell proliferation.

25COASNOV51

Title: Defining heterogeneity in core regulatory circuitry reveals HOXB3 condensation as a potential target in glioblastoma

Chuanxia Zhang, Yijing He, Xiudan Zhan et.al.

Nature Cell Biology volume 27, pages1848–1862 (2025)

https://doi.org/10.1038/s41556-025-01758-y

Abstract: Glioblastoma (GBM) exhibits marked heterogeneity, yet therapeutic strategies effectively targeting this variability remain inadequately developed. Here we employed single-cell CUT&Tag analysis to investigate H3K27ac modifications, uncovering pronounced heterogeneity within the core regulatory circuitry (CRC) of GBM. Notably, we observed heterogeneous condensation states of CRC factors, particularly HOXB3, which are

shaped by its intrinsically disordered regions and interactions with RUNX1, driving the phenotypic manifestations. Leveraging these findings, we synthesized the peptide P621-R9, which effectively disrupted HOXB3 condensation, altered chromatin structure and reduced transcription at super-enhancer-associated oncogenic sites in GBM cells exhibiting HOXB3 condensation. Treatment with P621-R9 selectively diminished tumourigenic potential in GBM patient-derived xenograft models characterized by HOXB3 condensates, but showed no efficacy in the models lacking these condensates. These results highlight the critical role of CRC condensation in GBM heterogeneity and suggest that peptide-based targeting of distinct GBM subpopulations could represent an avenue for therapeutic exploration.

25COASNOV52

Title: Integrated spatial transcriptome and metabolism study reveals metabolic heterogeneity in human bladder cancer

Yu Lu, Fangdie Ye, Xuedan Han et.al.

Cancer Gene Therapy volume 32, pages1177–1190 (2025)

https://doi.org/10.1038/s41417-025-00947-z

Abstract: Bladder cancer (BC) is a malignancy that originates from the cells lining the bladder and is one of the most common cancers of the urinary system, capable of occurring in any part of the bladder. However, the molecular mechanisms underlying the malignant transformation of BC have not been systematically studied. This study integrated cutting-edge techniques of spatial transcriptomics (ST) and spatial metabolomics (SM) to capture the transcriptomic and metabolomic landscapes of both BC and adjacent normal tissues. ST results revealed a significant upregulation of genes associated with choline metabolism and glucose metabolism, while genes related to sphingolipid metabolism and tryptophan metabolism were significantly downregulated. Additionally, significant metabolic reprogramming was observed in BC tissues, including the upregulation of choline metabolism and glucose metabolism, as well as the downregulation of sphingolipid metabolism and tryptophan metabolism. These alterations may play a crucial role in promoting tumorigenesis and immune evasion of BC. The interpretation of ST and SM data in this study offers new insights into the molecular mechanisms underlying BC progression and provides valuable clues for the prevention and treatment of BC.

25COASNOV53

Title: MALNC: a new mutant NPM1/IDH2R140 and PML-RARA-associated lncRNA with impact on AML cell proliferation, maturation and drug response

Elisabetta Cozzi, Anne Neddermeyer, Xiangfu Zhong et.al.

Cancer Gene Therapy volume 32, pages1191–1205 (2025)

https://doi.org/10.1038/s41417-025-00954-0

Abstract: As the non-coding genome remains poorly characterized in acute myeloid leukemia (AML), we aimed to identify and functionally characterize novel long non-coding RNAs (lncRNAs) relevant to AML biology and treatment. We first identified lncRNAs overexpressed in AML blasts and, among them, discovered a novel transcript, which we named myeloid and AML-associated intergenic long non-coding RNA (MALNC). MALNC is overexpressed in AML, particularly in cases with the PML-RARA fusion or IDH2R140/NPM1 co-mutations, and is associated with a distinct gene expression profile.

Functional studies showed that MALNC knockout impairs AML cell proliferation and colony formation, enhances ATRA-induced differentiation, and sensitizes cells to arsenic trioxide. Transcriptomic analysis revealed that MALNC loss alters the expression of retinoic acid pathway genes, and chromatin binding studies showed that MALNC binds to genes related to the retinoic acid and Rho GTPase pathways. In conclusion, we have identified MALNC as a novel lncRNA that promotes leukemic cell proliferation, counteracts ATRA-induced differentiation, and modulates drug sensitivity in AML.

25COASNOV54

Title: Characterization of tertiary lymphoid structure identifies competitive binding of CD40 and STING with TRAF2 driving IRF4-mediated B cell activation in esophageal squamous cell carcinoma

Yujia Zheng, Donglai Chen, Yi Xu et.al.

Cancer Gene Therapy volume 32, pages1206–1217 (2025)

https://doi.org/10.1038/s41417-025-00944-2

Abstract: Esophageal squamous cell carcinoma (ESCC) is a highly aggressive malignancy with a dismal prognosis. Hitherto, little has been known regarding the clinical implications of tertiary lymphoid structures (TLS) and its biological mechanisms of antitumor effect on treatment-naïve ESCC. We herein identified the presence of TLS as an independent factor for favorable survival. By characterizing the immune infiltration and genomic profiles based on transcriptomic datasets, we found TLS abundant in enriched B cells with IRF4 as a signature gene. Increased expression of IRF4 and its positive correlation with STING in activating tumor-infiltrating B cells were also investigated using a single-cell RNA sequencing dataset. CD40 as a co-regulator of IRF4 and TLS formation, in vitro experiments were conducted to further demonstrate the competitive binding relationships between CD40 and STING with TRAF2 in promoting IRF4 expression and B cell activation via the non-canonical NF-kB signaling pathway, in which CD40 reduced STING ubiquitination while promoting its phosphorylation. Our data provided deeper insights into the potential role of activated B cells and TLS in ESCC, with implications for the development of biomarkers and therapeutic targets.

25COASNOV55

Title: NRF2-SOX4 complex regulates PSPH in hepatocellular carcinoma and modulates M2 macrophage differentiation

Chi-Neu Tsai, Ming-Chin Yu, Yun-Shien Lee et.al.

Cancer Gene Therapy volume 32, pages1218–1232 (2025)

https://doi.org/10.1038/s41417-025-00951-3

Abstract: Hepatocellular carcinoma (HCC) progression is tightly linked to metabolic reprogramming and immune evasion. However, the transcriptional networks driving these processes remain misunderstood. Here, we identified a novel regulatory axis wherein the transcription factor SOX4 formed a stress-responsive complex with NRF2, as confirmed by co-immunoprecipitation and proximity ligation assay. This process was orchestrated via p62-mediated disruption of the KEAP1–SOX4 complex. The SOX4–NRF2 complex directly activated Phosphoserine Phosphatase (PSPH) transcription—as revealed by luciferase reporter and chromatin immunoprecipitation—enhancing serine biosynthesis and downstream

metabolites critical for oxidative phosphorylation (OXPHOS) and redox balance. Inhibition of SOX4 or NRF2 impaired PSPH expression, exacerbated oxidative damage—marked by elevated 4-hydroxynonenal—and increased sensitivity to sorafenib treatment in HCC cells. Furthermore, PSPH-driven metabolites, particularly serine, fostered M2-like macrophage polarization, thereby potentially contributing to the promotion of an immunosuppressive tumor microenvironment. Analysis of HCC specimens from TCGA and clinical cohorts confirmed that high SOX4/NRF2/PSPH expression was correlated with increasing M2 macrophage infiltration and poor patient prognosis. Our findings revealed a previously unrecognized SOX4–NRF2–PSPH regulatory loop that coupled cancer metabolism with immune modulation. Targeting this axis may offer a promising therapeutic avenue to simultaneously disrupt metabolic support and immune evasion in HCC.

25COASNOV56

Title: Pentagamavunone-1 targets excessive MYCN/NCYM expression mediated by mitotic arrest to suppress hepatocellular carcinoma proliferation

Dhania Novitasari, Ikuko Nakamae, Noriko Yoneda-Kato et.al.

Cancer Gene Therapy volume 32, pages1233–1244 (2025)

https://doi.org/10.1038/s41417-025-00956-y

Abstract: Hepatocellular carcinoma (HCC) is a common liver cancer often diagnosed at an advanced stage. While chemotherapies such as sorafenib is effective for some patients, others show poor responses, necessitating new treatments. Overexpression of MYCN/NCYM was recently shown to contribute to the development of HCC. This study investigated the effects of Pentagamavunone-1 (PGV-1), a curcumin analog with strong antiproliferative properties, on HCC cells expressing MYCN/NCYM. PGV-1 was more effective than curcumin and sorafenib in inhibiting HCC cell proliferation by inducing mitotic arrest, oxidative stress, and senescence. In MYCN-positive JHH-7 cells, PGV-1 treatment increased phosphorylation of aurora A, cyclin B1, and PLK1. PGV-1 also suppressed MYCN/NCYM transcription and destabilized MYCN protein by inducing phosphorylation at Ser54 and Thr58. In a xenograft model, PGV-1 significantly reduced tumor formation and growth. These findings highlight PGV-1's potential as a targeted therapy for MYCN-overexpressing HCC, warranting further development.

25COASNOV57

Title: Targeting MTPN sensitizes pancreatic cancer of wild-type BRCA1/2 to Cisplatin-based chemotherapy

Zhuoxin Wang, Xinyang Huang, Tingting Bai et.al.

Cancer Gene Therapy volume 32, pages1245–1258 (2025)

https://doi.org/10.1038/s41417-025-00925-5

Abstract: The clinical application of combination chemotherapy with cisplatin is unsatisfactory for most pancreatic cancer patients with wild-type BRCA1/2 or PALB2 due to resistance. Genes associated with cisplatin resistance in patients without BRCA1/2 or PALB2 mutations should be pursued. Through bioinformatics analysis, we found that Myotrophin (MTPN) expression was correlated with that of nuclear factor kappa B (NF-κB), a protein involved in the regulation of cisplatin sensitivity. Immunohistochemistry revealed that MTPN was more highly expressed in human pancreatic cancer tissues than in normal tissues. MTPN

promoted the malignant biological behaviors of pancreatic cancer (PC) cells and activated the epithelial-mesenchymal transition process. Furthermore, MTPN was found to induce cisplatin resistance in PC cells and upregulate BRCA1/2 while promoting DNA repair. The enhancing effects of MTPN on cisplatin resistance and BRCA1/2 up-regulation were abolished by an inhibitor of IκBα phosphorylation. These studies suggested that MTPN may increase cisplatin resistance by activating IκBα to regulate BRCA1/2 expression. In summary, targeting MTPN could be a potential therapeutic strategy, as MTPN knockdown increased the sensitivity to cisplatin-based chemotherapy in pancreatic cancer with wild-type BRCA1/2.

25COASNOV58

Title: Integration of humanized ROBO1 CAR in PD-1 locus in natural killer cells delivers synergistic tumor-killing effect against non-small cell lung cancer

Jia-Hao Tao, Jun Zhang, Chun-Yan Tang et.al.

Cancer Gene Therapy volume 32, pages1259–1275 (2025)

https://doi.org/10.1038/s41417-025-00957-x

Abstract: Lung cancer is the most common cancer and one of the leading causes of cancer-related deaths in the world, however, the treatment of non-small cell lung cancer (NSCLC) is still limited, and it is a clinically urgent problem. ROBO1 is an important surface receptor on tumor cells, but the role of humanized chimeric antigen receptor (CAR) modified natural killer (NK) cells targeting ROBO1 in NSCLC is rarely explored. Furthermore, the role of PD-1 in NK cell killing tumor cells remains controversial. In this study, we identified the expression pattern of ROBO1 in lung squamous cell carcinoma (LUSC) by searching biological information databases. We constructed hROBO1-CAR-NK-92 cells and performed functional identification.We inserted the hROBO1-CAR at the PD-1 locus and performed functional detection in vitro and in vivo. The results showed that ROBO1 expression was significantly increased in LUSC. After inserting the hROBO1-CAR sequence at the PD-1 locus, the PD-1-KO-hROBO1-CAR-NK-92 cells had the best long-term killing ability and cytokine secretion ability, and had a significant inhibitory effect on tumor growth in the mouse xenograft model. We also observed that the long-term killing ability of PD-1-KO-hROBO1-CAR-NK-92 cells was achieved by inhibiting cell senescence via knocking out PD-1. These studies proposed ROBO1 as a key target for CAR-NK therapy in NSCLC and integrated hROBO1 CAR in PD-1 locus in NK cells, resulting in synergistic tumor killing effects in NSCLC, presenting a new treatment strategy for solid tumor treatment.

25COASNOV59

Title: A novel GM-CSF-encoding oncolytic adenovirus induces profound autophagy and promotes viral replication to enhance anti-tumor efficacy

Heng Cao, Jiaqi Ye, Xiaojiao Li et.al.

Cancer Gene Therapy volume 32, pages1276–1291 (2025)

https://doi.org/10.1038/s41417-025-00962-0

Abstract: Granulocyte-macrophage colony-stimulating factor (GM-CSF) acts as a double-edged sword in cancer by enhancing both anti- and pro-tumorigenic immune cells. In this study, two oncolytic adenoviruses were engineered to modulate GM-CSF expression using different strategies: one with the CMV promoter (oAd-CMV-GM-CSF) and the other using the endogenous viral E3 promoter (oAd-GM-CSF). The impacts of these modifications on

transgene expression, cytotoxicity, viral replication, and apoptosis were assessed both in vitro and in vivo. The results demonstrated that oAd-CMV-GM-CSF produced significantly lower GM-CSF levels than oAd-GM-CSF, interestingly oAd-CMV-GM-CSF exhibited increased cytotoxicity and apoptosis compared to oAd-GM-CSF and control groups. The further study showed oAd-CMV-GM-CSF induced profound autophagy through the activation of the Janus kinase 2/Signal Transducer and Activator of Transcription 2 (JAK2/STAT2) signaling pathway. The use of autophagy and JAK-2 inhibitors, Chloroquine (CQ) and AG-490, respectively, significantly mitigated the apoptosis induced by oAd-CMV-GM-CSF. In addition, oAd-CMV-GM-CSF presented a faster viral replication and production of more active progeny virus than oAd-GM-CSF, which could be inhibited by CQ. oAd-CMV-GM-CSF augments propagation of the progeny viruses and induces immunogenic cell death(ICD) in A549 and PANC-1 cells. In vivo oAd-CMV-GM-CSF had stronger anti-tumor effect than oAd-GM-CSF in immunodeficient model and immune-competent model. Our findings indicate that oAd-CMV-GM-CSF induces more profound autophagy and promoting viral replication to enhance the anti-tumor efficacy.

25COASNOV60

Title: Documentation of patient withdrawals, retention strategies, and postwithdrawal data practices in cancer clinical trials

Alexander B. Karol MD, Rodrigo Paredes MD, Anna Argulian BS et.al.

Cancer, Volume131, Issue19, 2025
https://doi.org/10.1002/cncr.70106

Abstract: The withdrawal of patients from cancer clinical trials with unspecified rationale introduces selection bias, compromises study validity, and reduces generalizability. Excluding these data can lead to informative censoring, masking treatment toxicity, or inflating efficacy estimates. Whereas regulatory agencies emphasize documenting reasons for withdrawal and retaining data after withdrawal, adherence to these guidelines is unclear, raising concerns about trial integrity. The objectives of this study were to determine the prevalence of withdrawal with unspecified rationale, evaluate retention strategies, and assess data-retention practices after patient withdrawal in contemporary cancer clinical trials.Methods: This cross-sectional study included 300 completed phase 3 clinical trials registered on ClinicalTrials.gov between 2014 and 2024 that evaluated systemic or local anticancer therapies with available protocols. The primary outcome was the proportion of patients who withdrew without a specified rationale. Secondary outcomes included the prevalence of protocol-stated retention strategies and postwithdrawal data-retention practices.Results: Of 165,674 enrolled patients, 106,915 discontinued participation. Of those, 15.8% (n = 16,842) withdrew without a specified rationale. Nearly all protocols (99.6%; n = 299) required documenting the reasons for withdrawal; however, the median proportion of withdrawals without a specified rationale per trial was 7.5% (range, 0%–64.4% withdrawals; 25th to 75th percentile, 4.5%–10.5%). Most withdrawals were patient-initiated (60.1%), retention strategies were absent in 68.0% of trial protocols, and 32.3% of protocols failed to specify retention practices for data collected after withdrawal.Conclusions: A substantial proportion of patients in phase 3 cancer trials withdraw without a specified rationale. Inconsistent withdrawal documentation practices, limited use of a retention strategy, and unclear postwithdrawal data policies highlight the need for standardized approaches to

improve trial quality.

25COASNOV61

Title: Medical marijuana policies, opioid prescriptions, and adverse events among patients undergoing cancer resection surgery

Ju-Chen Hu PhD, Kenneth Karan MPH, Hao Zhang PhD et.al.

Cancer, Volume131, Issue19, 2025
https://doi.org/10.1002/cncr.70107

Abstract: Opioid use and adverse events among cancer patients may change with access to medical marijuana. This study investigated the impacts of medical marijuana legalization (MML) since 2016.Methods: Using a difference-in-differences approach and 2016 to 2022 private insurance claims data, this cross-sectional study included patients (aged 18–64 years) undergoing resection surgery for newly diagnosed (female) breast, colorectal, or lung cancer in 27 states without MML as of 2016. MML policies were classified into (1) no MML, (2) MML without dispensaries (after MML effective date and before the first state-licensed dispensary opened), and (3) MML with dispensaries. Outcomes included during the 6 months postdiagnosis: (1) any opioid prescription, (2) any short-acting oxycodone, hydrocodone, hydromorphone, or morphine prescription ("strong opioids"), (3) any short-acting tramadol or codeine prescription ("weak opioids"), and (4) total morphine milligram equivalents among patients with opioid prescriptions, (5) any all-cause, and (6) any pain-related emergency department visits or hospitalizations.Results: The sample (N = 34,911) included 24,592 patients with breast, 8510 colorectal, and 1809 lung cancer. Compared to no MML, MML with dispensaries was associated with reduced any strong short-acting opioids prescription use (difference = −4.6; 95% CI, −8.6 to −0.5 percentage points [pp]; p = .028) and increased any all-cause adverse hospital events (difference = 2.6; 95% CI, 0.7−4.5 pp; p = .006). MML without dispensaries was associated with increased any weak opioid prescription use (difference = 1.2; 95% CI, 0.5−2 pp; p = .002).Conclusions: MML policies may have affected the type of opioid prescribed and increased adverse hospital events among patients with cancer and resection surgery. Additional investigation of medical marijuana's impact on cancer pain management is warranted.

25COASNOV62

Title: Unveiling the impact of chemotherapy in patients with breast cancer: A longitudinal study on peripheral inflammation, multimodal magnetic resonance imaging, and cognition

Rob Colaes MSc, Gwen Schroyen PhD, Ahmed Radwan MD et.al.

Cancer, Volume131, Issue19, 2025
https://doi.org/10.1002/cncr.70095

Abstract: The pathophysiology of chemotherapy-induced cognitive impairment (CICI) remains unclear. Besides direct neurotoxicity, chemotherapy may trigger peripheral proinflammatory responses leading to neuroinflammation and neuronal injury. This longitudinal study investigated changes in peripheral inflammatory and neuronal markers, and multimodal magnetic resonance imaging measures from pre-to post-chemotherapy, and their potential role in CICI.Methods: This study included 32 women receiving chemotherapy for early breast cancer (C+), 35 patients not exposed to chemotherapy (C–), and 46 healthy

women (HC) age- and education-matched. Participants were assessed at diagnosis (T0), 3 months post-chemotherapy (T1), and 1 year post-chemotherapy (T2), or at matched intervals. Differences over time were assessed in cognitive outcomes, peripheral inflammatory and neuronal markers, and multimodal magnetic resonance imaging measures, reflecting white matter (WM) lesions, magnetic resonance spectroscopy metabolites, WM microstructure, and the diffusion tensor imaging along the perivascular space (DTI-ALPS) index. To investigate changes in WM structure, the authors performed a longitudinal fixel-based analysis on multi-shell diffusion-weighted images. Associations between peripheral inflammation and WM microstructure were explored, as well as their relationship to both subjective and objective cognitive outcomes.Results: This study observed alterations after chemotherapy in subjective and objective cognition, inflammatory profiles, neurofilament light chain, the DTI-ALPS index, and WM microstructure within the left inferior longitudinal fasciculus and in the genu of the prefrontal corpus callosum. Alterations in peripheral inflammatory profiles were associated with worse performance in objective cognition, but not with changes in WM microstructure.Conclusion: Peripheral inflammatory responses and alterations in WM microstructure are potential key mechanisms underlying CICI.

25COASNOV63

Title: Remnant cholesterol and systemic inflammation as synergistic predictors of cancer risk: A 16-year prospective cohort study

Hongxue Xu MD, Peipei Liu MD, Shuohua Chen PhD et.al.

Cancer, Volume131, Issue20, 2025
https://doi.org/10.1002/cncr.70096

Abstract: Remnant cholesterol (RC), a marker of triglyceride-rich lipoproteins, has been implicated in cardiovascular disease via inflammatory pathways, but its role in cancer development remains unclear. This study investigated the independent and joint effects of RC and systemic inflammation on long-term cancer risk.Methods: The authors analyzed data from 136,158 participants in the Kailuan cohort who were free from cancer and cardiovascular disease at baseline. RC was calculated as total cholesterol minus high-density lipoprotein cholesterol and low-density lipoprotein cholesterol. High-sensitivity C-reactive protein (hs-CRP) was used to assess systemic inflammation. Incident cancer cases were identified during a median follow-up of 16.18 years. Cox proportional hazards models, interaction analyses, mediation analysis, and cross-lagged panel models were used to assess the relationships between RC, hs-CRP, and cancer.Results: A total of 7080 incident cancers were recorded. Compared with the lowest quartile of RC (Q1), participants in the highest quartile (Q4) had a significantly increased risk of overall cancer (hazard ratio [HR], 1.188; 95% confidence interval [CI], 1.108–1.273), lung cancer (HR, 1.349; 95% CI, 1.179–1.543), and colorectal cancer (HR, 1.775; 95% CI, 1.443–2.184). Participants with both high RC and high hs-CRP had the highest risk (HR, 1.332; 95% CI, 1.268–1.400). Mediation analysis revealed that RC mediated 8.31% of the hs-CRP–cancer relationship, and vice versa. Cross-lagged models confirmed a bidirectional temporal association.Conclusion: RC and systemic inflammation act synergistically and bidirectionally to increase cancer risk, supporting a metabolic–inflammatory axis in carcinogenesis. These findings identify novel, potentially modifiable targets for early cancer risk stratification and prevention.

25COASNOV64

Title: Opioid prescribing trends and pain scores among adult patients with cancer in a large health system

Laura Van Metre Baum MD, MPH, Pamela R. Soulos MPH, Madhav KC PhD et.al.

Cancer, Volume131, Issue20, 2025
https://doi.org/10.1002/cncr.70027

Abstract: Opioid stewardship policies could adversely affect pain management for patients with cancer. Yet patients with cancer are also at risk for opioid-related harms. This study sought to determine trends in opioid prescribing by clinical stratum and pain for patients with cancer from 2016 to 2020.Methods: A retrospective study was conducted of opioid-naive adults with newly diagnosed cancer from 2016 to 2020 (N = 10,232) in a large Connecticut health system. Logistic regression was used to calculate changes in the predicted probability of opioid prescribing from 2016 to 2020. Two subpopulations were examined: patients treated surgically (n = 4405) and patients with metastatic cancer (n = 2158). Flowsheet pain scores for patients with metastatic cancer were used to stratify by no pain (all scores, 0) versus any pain. The main outcomes were new (≥1 prescription in the 0–6 months after diagnosis) and additional (0–6 and 7–9 months) opioid prescriptions.Results: A decline was observed in the predicted probability of new (71.1% to 64.6%; p < .001) and additional prescribing (27.2% to 24.2%; p = .07 [not significant]) declined. Among surgical patients, the predicted probability of new opioid prescribing fell (96.0% to 88.6%; p < .001), whereas additional prescribing was stable (13%). For patients with metastatic cancer with pain, new opioid prescribing was stable (56%). For those reporting no pain, the predicted probability of new opioid prescribing declined from 61.6% to 36.1% (p < .001).Conclusions: In the context of widespread policy changes, this study showed a modest decline in new and additional opioid prescribing for patients with cancer. In metastatic cancer, prescribing remained stable for patients reporting pain and declined steeply for those reporting no pain.

25COASNOV65

Title: Liver-directed therapies for colorectal liver metastases

Andrew D. Folkerts MD, Lauren M. Janczewski MD, MS, Ryan P. Merkow

Cancer, Volume131, Issue20, 2025
https://doi.org/10.1002/cncr.70097

Abstract: Colorectal cancer is the third most common cancer diagnosed in the United States, with an anticipated 53,000 deaths from this disease in 2025. Greater than one in five patients will present with synchronous colorectal liver metastases (CRLMs), and 25%–30% will develop CRLMs during the course of the disease. In addition, the rate of liver-specific recurrence is high, with recurrences in 50%–75% of patients who previously underwent resection for liver metastasis. Surgical resection remains the cornerstone of treatment for resectable CRLM, but a significant proportion of CRLMs are unresectable on presentation. Unique treatment strategies have been developed to expand treatment options and improve outcomes. Today, there are multiple established therapies in routine practice as well as novel therapies that are currently under development with promising results to date. Each therapy has its own goals ranging from reducing the chances of locoregional recurrence, supporting an effort to convert unresectable disease burden into potentially resectable tumors, and salvage options with the goal of extending survival. Because most liver-directed therapies are

complementary, it is also important to understand how each option affects other therapies to develop a coordinated treatment strategy. Specifically, it is essential to understand the indications, limitations, and outcomes of each option when making multidisciplinary treatment decisions. In this article, the authors review the current landscape of liver-directed therapies and briefly discuss promising emerging treatment options.

25COASNOV66

Title: 5-fluoro-deoxyglucose PET/CT response after neoadjuvant chemotherapy predicts long-term outcomes in soft tissue sarcomas: Results from a prospective trial

Edward Y. Cheng MD, Andrea P. Espejo Freire MD, Juan C. Manivel MD et.al.

Cancer, Volume131, Issue20, 2025
https://doi.org/10.1002/cncr.70129

Abstract: Only 30%–40% of high-grade sarcomas respond to initial chemotherapy, which can have significant toxicities. Computed tomography imaging alone has limitations in evaluating treatment response. Imaging with 5-fluoro-deoxyglucose–positron emission tomography/computed tomography (FDG-PET/CT), which evaluates tumor metabolism, offers an alternative. This study examined whether early changes in the maximum standardized uptake value (SUVmax) after neoadjuvant chemotherapy can be used to predict outcomes in high-grade sarcomas.Methods: This prospective trial assessed whether changes in the SUVmax after one or four cycles of pegylated-liposomal doxorubicin plus ifosfamide could predict progression-free survival (PFS), overall survival (OS), and histologic response. Fifty-six patients were required for 90% power. Metabolic response was defined as a reduction ≥40% in the SUVmax from baseline after either cycle 1 (delta 1) or cycle 4 (delta 2).Results: Sixty-nine patients were enrolled (2006–2013) with a median follow-up of 8.1 years. The 10-year PFS rate was 74% versus 42% for delta 1 responders versus nonresponders (p = .0082), respectively; and 69% versus 33% for delta 2 responders versus nonresponder (p = .0015), respectively. The 10-year OS rate was 73% versus 58% for delta 1 responders versus nonresponder (p = .28), respectively; and 81% versus 37% for delta 2 responders versus nonresponder (p = .00026), respectively. Of 46 delta 1 nonresponders, 23 met criteria at delta 2. A positron emission tomography response was correlated with histologic necrosis. At last follow-up, 31 patients (44.9%) were alive and disease free, and 10 (14.5%) were alive with sarcoma. Five patients developed secondary malignancies.Conclusions: An SUVmax reduction verified on FDG-PET/CT imaging after neoadjuvant chemotherapy was a strong predictor of long-term outcomes. Metabolic imaging at treatment completion identified responders, supporting continued therapy in initially nonresponsive patients and guiding personalized treatment strategies.

25COASNOV67

Title: Lobular breast cancer statistics, 2025

Angela N. Giaquinto MSPH, Rachel A. Freedman MD, MPH, Lisa A. Newman MD et.al.

Cancer, Volume131, Issue20, 2025
https://doi.org/10.1002/cncr.70061

Abstract: Breast cancer statistics and clinical trial data largely reflect ductal carcinoma, the dominant histologic subtype, concealing important differences for invasive lobular carcinoma (ILC), the second most common subtype.Methods: Nationally representative cancer registry

data from the National Cancer Institute and Centers for Disease Control and Prevention were used to report on the incidence and outcomes of ILC by age, race, and ethnicity among women in the United States.Results: In 2021 incidence of ILC was 14 per 100,000 women, which accounted for 10.6% of breast cancer diagnoses. Rates increased from 2012 through 2021 in all racial ethnic groups, ranging from 2.5% annually in American Indian/Alaska Native women to 4.4% annually in Asian American/Pacific Islander women. White women have the highest incidence overall (14.7 per 100,000), and in every age group, followed by Black women (11 per 100,000), although American Indian/Alaska Native women have the second-highest rates among those <50. Compared to ductal carcinoma, survival for ILC is slightly higher in the first 7 years after diagnosis and similar at 10 years overall, but lower for ILC for regional- and distant-stage disease, perhaps in part due to its unique metastatic pattern.Conclusion: ILC has distinctive characteristics that can contribute to delayed detection, resistance to therapy, and poorer prognosis for advanced disease. Differentiating ILC from ductal carcinoma in research and clinical trials could help identify risk factors, facilitate treatment efficacy, and lead to better understanding of metastatic mechanisms, thus improving outcomes for the increasing number of affected women.

25COASNOV68

Title: Genome-wide association analysis identifies fucosyltransferase 2 variants associated with pancreatic intraductal papillary mucinous neoplasms

Apostolos Gaitanidis MD, PHD, Carlos Fernandez-del Castillo MD, Shravya Srinivas Rao MD et.al.

Cancer, Volume131, Issue20, 2025
https://doi.org/10.1002/cncr.70114

Abstract: Intraductal papillary mucinous neoplasms (IPMNs) are common pancreatic cystic neoplasms. Observation or surgical resection in patients with high-risk IPMNs is recommended because there is a risk of malignant transformation leading to pancreatic adenocarcinoma. Risk factors for the development of IPMNs are not well characterized. The authors hypothesized that common genetic variants are associated with development of IPMNs.Methods: Individuals were enrolled and genotyped as part of the Mass General Brigham Biobank, and individuals with IPMNs were identified retrospectively using electronic medical records. Single nucleotide variants (SNVs) with a minor allele frequency ≥5% were examined for an association with IPMNs. SNVs that surpassed the significance threshold ($p < 5e-08$) were further examined in a validation cohort.Results: Of 68,931 individuals, 2525 (3.6%) had IPMNs. After genome-wide association analysis, a genetic locus at chromosome 19 was identified as associated with IPMNs. The lead SNVs were reference SNVs rs681343 (19:49206462; odds ratio, 1.01; $p = 1.04e-8$) and rs601338 (19:49206674; odds ratio, 1.01; $p = 1.06e-8$). This result was verified in an independent cohort of 5014 individuals. The rs601338 variant is in a noncoding exon of fucosyltransferase 2 (FUT2) and causes replacement of a normal codon with a stop codon and termination of protein translation. FUT2 codes the FUT2 enzyme, an important enzyme in the Lewis antigen system.Conclusions: FUT2 variants are associated with the development of pancreatic IPMNs. FUT2 and rs601338 have important functions in mucin synthesis, biliopancreatic duct homeostasis, carcinoembryonic antigen, and cancer antigen 19-9 regulation, which provide a biologically plausible role in IPMN pathogenesis.

25COASNOV69

Title: Risk of second primary malignancies after adjuvant chemotherapy for colon cancer

Tomas Buchler MD, PhD, Monika Ambrozova MSc (Eng), Ondrej Majek PhD et.al.

Cancer, Volume131, Issue20, 2025
https://doi.org/10.1002/cncr.70116

Abstract : Advances in adjuvant chemotherapy have improved survival in patients with stage II–III colon cancer (CC). However, concerns have emerged regarding the risk of second and subsequent primary malignancies (SPMs) based on preclinical data and registry-based studies. This study evaluated the incidence of SPMs among CC survivors in relation to adjuvant chemotherapy type.Methods: This retrospective, population-based cohort study included 18,383 patients with stage II–III CC who were treated between 2010 and 2022. Patients were categorized based on three adjuvant treatments: (1) no chemotherapy, (2) fluorouracil or capecitabine alone, and (3) fluorouracil or capecitabine with oxaliplatin. Standardized incidence ratios (SIRs) for SPMs were calculated using national cancer registry data.Results: In an analysis of all 18,383 patients with stage II and III CC who had up to 11.5 years of follow-up, those who received with fluorouracil or capecitabine plus oxaliplatin had a higher overall risk of SPMs (SIR, 1.5; 95% confidence interval, 1.4–1.6) compared with SIRs of 1.1 (95% confidence interval, 1.0–1.2) in patients who did not receive chemotherapy or who received treatment without oxaliplatin. This elevated risk persisted across both stages and was most pronounced for colorectal SPMs. At 10 years, the cumulative SPM incidence reached 14.6% in the oxaliplatin group versus 12.5% and 11.0% in the other two groups, respectively. Oxaliplatin-treated patients had the highest second CC risk (SIR, 2.2).Conclusions: Oxaliplatin-based adjuvant chemotherapy was associated with a heightened long-term risk of SPMs, particularly second colorectal cancers. These findings highlight the need for risk-adapted survivorship care strategies.

25COASNOV70

Title: Racial differences in kidney cancer histology and outcome: A nationwide study from the UroCCR Cohort

Xiaofan Lu PhD, Jean-Christophe Bernhard MD, PhD, Gaëlle Margue MD et.al.

Cancer, Volume131, Issue20, 2025
https://doi.org/10.1002/cncr.70120

Abstract: Racial differences in renal cell carcinoma (RCC) have been well described in U.S. cohorts, particularly for common histologic subtypes. However, such differences remain underexplored in European populations, especially for rare RCC subtypes and within universal health care settings. We aimed to characterize racial differences in RCC histology, renal comorbidities, and clinical outcomes in France, and to investigate potential molecular underpinnings.Methods: A total of 9404 patients were analyzed from the UroCCR national registry (1987–2024), including 338 Black and 9066 non-Black individuals with nephrectomy-confirmed diagnoses. Clinical features, histologic subtypes, and outcomes were compared between groups. Transcriptomic differences between Black and White individuals were assessed using publicly available single-nucleus and bulk RNA-sequencing data from nonneoplastic renal tissue.Results: Clear-cell RCC was less common in Black patients (47.6% vs. 68.8%), whereas papillary, translocation, and fumarate hydratase–deficient RCC

subtypes, as well as angiomyolipoma, were more prevalent (all odds ratios ≥ 2). Black patients were diagnosed younger, with smaller, earlier-stage tumors, and underwent partial nephrectomy more frequently. No difference in disease-specific survival was observed; however, distant recurrence-free survival was longer in Black patients (hazard ratio, 0.54; p = .019), likely reflecting earlier diagnosis. Race was not associated with survival after adjusting for clinical factors. Transcriptomic profiling revealed upregulation of adipogenic and angiogenic programs in White individuals and enrichment of hemoglobin- and chemokine-related pathways in Black individuals. Limitations include retrospective design and race classification.Conclusion: Distinct racial patterns in RCC histology and renal biology may inform subtype susceptibility. These findings support ancestry-informed strategies in RCC diagnosis and research.

25COASNOV71

Title: Multilevel challenges and adaptations to patient navigation programs for colorectal cancer screening and follow-up: Findings from the Accelerating Colorectal Cancer Screening and follow-up through Implementation Science consortium

Gloria D. Coronado PhD, Priyanka Gautom PhD, MPH, Jennifer L. Schneider et.al.

Cancer, Volume131, Issue20, 2025
https://doi.org/10.1002/cncr.70121

Abstract: Patient navigation services can substantially boost participation in colorectal cancer screening and follow-up. As part of the Accelerating Colorectal Cancer Screening and follow-up through Implementation Science (ACCSIS) consortium, this study describes facilitators, barriers, and context-specific adaptations to sustainably deliver navigation in diverse settings.Methods: Qualitative interviews were conducted with patient navigators and ACCSIS research project team members between February and August 2024; interviews were recorded, transcribed, and analyzed via rapid methods.Results: Seventeen patient navigators and eight research project team members (from six research projects) were interviewed. The navigation programs varied in scope: supporting initial screenings, follow-ups for abnormal stool tests, or both. Common facilitators were training navigators via multiple teaching methods and integrating navigators directly into clinic teams. Common barriers were high staff turnover, lack of sustainable funding for navigator positions, limited clinic resources and inadequate electronic health record tools, difficulty in contacting patients, and problems in accessing endoscopy services. Common adaptations made to improve programs included providing gift bags or drop boxes to make stool testing more appealing to patients, adjusting how often and how navigators were trained, evaluating clinic and specialist capacity before implementation, allowing navigators to schedule colonoscopies directly, and establishing partnerships that reduced colonoscopy costs and shortened wait times.Conclusions: Identified barriers to patient navigation program implementation might be addressed by providing ongoing navigator training via multiple delivery modes; applying best practices for engaging clinic teams, gastroenterology practices, and community partners; building centralized repositories of navigation training and patient-facing materials; and securing consistent funding via billing and institutional support.

25COASNOV72

Title: Unravelling a clinical role of peripheral blood leukemia stem cells at diagnosis in

chronic myeloid leukemia patients: Final results of prospective FLOWERS study
Anna Sicuranza PhD, Paola Pacelli PhD, Adele Santoni MD et.al.
Cancer, Volume131, Issue20, 2025
https://doi.org/10.1002/cncr.70122
Abstract: The authors previously demonstrated that in peripheral blood (PB) of chronic myeloid leukemia (CML), patients' leukemia stem cells (LSCs) CD26+ are detectable by flow cytometry at diagnosis, during tyrosine kinase inhibitor (TKI) therapy, and during treatment-free remission.Methods: This study presents results of a prospective multicenter study including 242 newly diagnosed CML patients monitored for PB CD26+ leukemic stem cells (LSCs) quantification from diagnosis up to 24 months of TKI treatment.Results: The bulk of CD26+ LSCs at diagnosis varied between patients with a median value of 7.14 cells/μL. During TKI treatment, it has been observed their consistent and rapid reduction without statistical differences according to type of first-line TKI. Instead, a significant correlation between a low amount of CD26+ LSCs at diagnosis and an optimal molecular response at 3, 12, and 24 months was documented ($p = .03$, $p = .004$, and $p = .009$, respectively). Three tertiles of CD26+ LSCs correlating to molecular response were identified: <3.21 cells/μL; between 3.21 and 19.21 cells/μL; and >19.21 cells/μL. The incidence of patients with optimal response was higher in the first CD26+ LSCs tertile respect to the third one ($p = .027$, $p = .015$, and $p = .079$, respectively) at all time points (3, 12 and 24 months).Conclusions : This study demonstrated a correlation between the amount of CD26+ LSCs at diagnosis and the molecular response, suggesting that the number of CD26+ LSCs at diagnosis could represent an additional tool for predicting TKI response.

25COASNOV73
Title: Incidence of chronic medical conditions among survivors of adolescent and young adult cancer compared to a population without cancer
Theresa H. M. Keegan PhD, MS, Renata Abrahão MD, MSc, PhD, Jessica Chubak PhD et.al.
Cancer, Volume131, Issue20, 2025
https://doi.org/10.1002/cncr.70125
Abstract: Few studies have assessed the burden of chronic medical conditions in adolescent and young adult (AYA) cancer survivors. This study estimated the risk of these conditions among AYA survivors compared to a matched cohort without cancer.Methods: This retrospective cohort study included 2-year survivors (n = 14,917) of 11 common AYA (15–39 years) cancers diagnosed at the integrated health care organizations of Kaiser Permanente (KP) Southern and Northern California during 2006–2020. A comparison cohort (n = 149,164) without cancer (matched 10:1 by age, sex, calendar year, and KP site) was included. Cumulative incidence (CMI) accounting for death as a competing risk was calculated. Poisson regression estimated the incidence rate ratio (IRR) of each condition in cancer survivors versus the matched cohort, adjusting for age, sex, and race/ethnicity.Results: The 5-year CMI was highest for thyroid (17.4%), respiratory (6.6%), cardiovascular (5.0%), and liver (4.8%) diseases. At 10 years, the CMI of any condition was 39% in survivors versus 26% in the matched cohort. Survivors had a 2-fold increased risk of being diagnosed with any medical condition (IRR, 2.0; 95% confidence interval [CI], 1.9–2.0) as well as two or more conditions (IRR, 2.3; 95% CI, 2.2–2.5). Risk was highest among survivors of hematologic cancers and those diagnosed with distant stage disease. Elevated risks were observed within

all sociodemographic groups of this insured population.Conclusion: AYAs with cancer had a higher risk of chronic medical conditions compared to those without cancer. Long-term surveillance, risk mitigation through lifestyle modifications and effective disease management are crucial to reduce premature mortality.

25COASNOV74

Title: Inflammation and dimensions of fatigue in women with early stage breast cancer: A longitudinal examination

Julienne E. Bower PhD, Arielle Radin PhD, Patricia A. Ganz MD et.al.

Cancer, Volume131, Issue20, 2025

https://doi.org/10.1002/cncr.70038

Abstract: Fatigue is a common and long-lasting side effect of cancer. Although fatigue is a multidimensional symptom, biologic mechanisms of fatigue dimensions have not been identified.Methods: Women recently diagnosed with early stage breast cancer (n = 192) completed assessments before and after adjuvant therapy and at 6-month, 12-month, and 18-month posttreatment follow-up visits. At each assessment, women completed the Multidimensional Fatigue Symptom Inventory and provided blood for protein markers of inflammation (tumor necrosis factor [TNF] alpha [TNF-α], soluble tumor necrosis factor receptor type II [sTNF-RII], interleukin 6 [IL-6], and C-reactive protein [CRP]). Mixed-effect linear models examined within-person and between-person associations between inflammatory markers and dimensions of fatigue. Results: Analyses demonstrated a positive within-person association between general fatigue and TNF-α (b = 1.67; p = .037), sTNF-RII (b = 2.77; p = .002), and IL-6 (b = 0.86; p = .010) when controlling for age, race, education, body mass index, and cancer stage. Similarly, there was a positive within-person association between physical fatigue and TNF-α (b = 1.58; p = .007), sTNF-RII (b = 2.38; p < .001), and CRP (b = 0.43; p = .007). Conversely, there were negative within-person associations between emotional fatigue and TNF-α (b = −1.92; p = .004) and sTNF-RII (b = −2.10; p = .006). General and physical fatigue were positively associated with CRP at the between-person level (b = 0.82, p = .024 for general; b = 0.71; p = .012 for physical). No significant associations between mental fatigue and inflammatory makers were found.Conclusions: The current findings identified distinct dimensions of fatigue associated with inflammatory activity in women with breast cancer and highlighted individual variability in inflammatory markers as a key predictor of fatigue symptoms.

25COASNOV75

Title: Association between medication burden and acute care use in older metastatic prostate cancer patients on androgen receptor signaling inhibitors

Michael A. Liu MD, MPH, Rohit Raghunathan MS, Karie Runcie MD et.al.

Cancer, Volume131, Issue21, 2025

https://doi.org/10.1002/cncr.70163

Abstract: Management of metastatic prostate cancer often requires combining androgen deprivation therapy (ADT) with novel androgen receptor signaling inhibitors (ARSIs). Although these agents improve survival, older patients may face acute care utilization from medication burden, reflected in polypharmacy and nonadherence.Methods: Using SEER-Medicare data, the authors identified patients ≥66 years old with de novo metastatic prostate

cancer prescribed abiraterone, enzalutamide, or apalutamide (2010–2017). Polypharmacy was defined by the Youden index (≥8 medications). ARSI adherence was measured by medication possession ratio (≥0.8) from initiation to discontinuation, assessed over 6 months. Acute care use was defined as any inpatient hospitalization or emergency visit within 6 months. Demographic characteristics were compared by t-tests/χ2. Negative binomial regression estimated incidence rate ratios (IRRs) for acute care use.Results: Among 2697 patients (mean age, 75 years), most were White (80.3%), married (63.1%), and received prior ADT (85.3%). Polypharmacy was present in 50.6% of patients before ARSI initiation, whereas ARSI nonadherence in the 6 months post-initiation was 34.0%. Polypharmacy and adherence were not significantly associated. In adjusted analyses controlling for demographic, clinical, and treatment factors, both polypharmacy (IRR, 1.59; 95% confidence interval [CI], 1.28–1.98) and ARSI nonadherence (IRR 2.50; 95% CI, 2.00–3.03) independently prognosticated higher acute care use.Conclusions: Medication burden, as characterized by suboptimal adherence and polypharmacy, is an independent risk factor for acute care use among older adults initiating ARSI treatment for metastatic prostate cancer. These findings highlight an opportunity for potential interventions to reduce downstream acute care use.

25COASNOV76

Title: A tour of leukemia progress in 2025, viewed through the MD Anderson leukemia research lens

Hagop M. Kantarjian MD, Gautam Borthakur MD, Naval Daver MD et.al.

Cancer, Volume131, Issue21, 2025

https://doi.org/10.1002/cncr.70113

ABSTRACT: Advances in the prognostication, monitoring, and treatment of both the acute and chronic leukemias have led to drastically improved outcomes over the past 2 decades. With the advent of targeted therapies, including antibodies such as blinatumomab and inotuzumab and small molecule inhibitors, such as the BCR::ABL1 tyrosine kinase inhibitors, Bruton tyrosine kinase inhibitors, and venetoclax, the treatment landscape of leukemia has drastically changed, improving survival outcomes while relying less on overall chemotherapy intensity in many leukemia types. This progress has allowed the categorization of more leukemia types as favorable (i.e., chronic lymphocytic leukemia, younger acute lymphoblastic leukemia [patients younger than 60 years], and Philadelphia chromosome-positive acute lymphoblastic leukemia) in addition to the traditional favorable subtypes of acute promyelocytic leukemia, core-binding factor acute myelocytic leukemia, chronic myelocytic leukemia, and hairy cell leukemia. Advancements in the treatment of TP53-mutated, MECOM-rearranged, and treated secondary AML are still needed to improve outcomes in these adverse risk groups. The authors also review the recent progress in the treatment of the acute and chronic leukemias.

25COASNOV77

Title: Cost-effectiveness of office-based, magnetic resonance imaging-guided transperineal versus transrectal prostate biopsy: An economic analysis of the PREVENT trial

Mitchell M. Huang MD, Conor B. Driscoll MD, Nicole Handa MD et.al.

Cancer, Volume131, Issue21, 2025

https://doi.org/10.1002/cncr.70118

Abstract: As antimicrobial resistance increases, safer alternative approaches to prostate biopsy are needed. PREVENT was a multi-institutional, randomized controlled trial comparing transperineal (TP) biopsy without antibiotic prophylaxis versus transrectal (TR) biopsy with targeted prophylaxis. The authors conducted a secondary cost-effectiveness analysis of PREVENT.Methods: The authors designed a Markov model with a simulated cohort of 1000 biopsied men. They assessed the short-term cost-effectiveness over a 2-week period, comparing relative costs in US dollars and utility measured in quality-adjusted life years (QALYs). The strategies they compared were office-based, magnetic resonance imaging-guided biopsy using two approaches: (1) TP without antibiotics; or (2) TR with targeted antibiotic prophylaxis. Analysis was from a health care payer perspective using a willingness-to-pay (WTP) threshold of $100,000/QALY. Probabilistic sensitivity analysis was performed with 5000 Monte Carlo simulations.Results: Compared to TR, TP was dominant, offering lower cost and higher utility per patient. This finding was robust to sensitivity analyses with TP having >89% probability of cost-effectiveness regardless of WTP threshold. TP remained dominant when real-world infection rates were used. TP biopsy needed to prevent >0.5% infections compared to TR to maintain cost-effectiveness. Per 1000 patients, TP biopsy prevented 16 infections, and the additional cost to prevent a single infection was $3.18/patient.Conclusions:In this model, TP biopsy was more cost-effective than TR from a health care payer perspective. In the setting of increasing concerns about the risk of infection from traditional TR biopsy, these findings suggest that office-based TP biopsy is a more cost-effective population-level alternative.

25COASNOV78

Title: Intersection of Black race and carbohydrate antigen 19-9 nonproduction underpins worse pathologic response to neoadjuvant therapy in pancreatic cancer

Mary P. Martos MD, MPH, Erin M. Dickey MD, MBS, Kawther Abdilleh PhD et.al.

Cancer,Volume131, Issue21, 2025

https://doi.org/10.1002/cncr.70130

Abstract: Black patients with pancreatic ductal adenocarcinoma (PDAC) are less likely to have a major pathologic response (MPR) after neoadjuvant chemotherapy (NAC). Data suggest lower baseline carbohydrate antigen 19-9 (CA 19-9) among Black patients. Whether CA 19-9 nonproduction contributes to racial differences in NAC response was evaluated, and the biological mechanisms underlying the reduced response in CA 19-9 nonproducers (CAnonprod) were investigated.Methods: Black and White patients with PDAC who received ≥2 NAC cycles and pancreatectomy at seven centers were reviewed. Patients were categorized as CA 19-9 producers (CAprod; CA 19-9 > 5 U/mL) or CAnonprod (CA 19-9 ≤ 5 U/mL). Univariable and multivariable models assessed CAnonprod rates by race and the association of CAnonprod with MPR. The Pancreatic Cancer Action Network's SPARK platform was queried for genomic data. Differentially mutated genes were identified by Fisher exact test; differentially expressed gene analysis used an absolute fold change of ≥2 and an adjusted p value of <.05.Results: Among 415 patients (385 CAprod and 30 CAnonprod), Black patients comprised more CAnonprod than CAprod (50% vs. 13%; p < .01). MPR rates were lower among CAnonprod versus CAprod (8% vs. 26%; p = .03). CA nonproduction was associated with decreased odds of an MPR (odds ratio [OR], 0.21; 95%

CI, 0.04–0.99), and Black race was associated with increased odds of CA 19-9 nonproduction (OR, 8.7; 95% CI, 3.8–19.7). CAnonprod had higher rates of SWI/SNF alterations than CAprod (52% vs. 34%; p < .01; p-adjusted, not significant). LIPF was downregulated and CTCFL was upregulated in CAnonprod.Conclusions: CA 19-9 nonproduction is more prevalent in Black patients, and potentially mediates lower rates of MPR. CAnonprod have a distinct molecular profile, which suggests a biological basis for racial differences in chemoresponsivity.

25COASNOV79

Title: Prostate-specific membrane antigen positron emission tomography/computed tomography imaging as a precision diagnostic at prostate cancer recurrence after radical prostatectomy: Modeling long-term survival

Kemal Caglar Gogebakan PhD, Zizi Elsisi MS, Felipe Montano-Campos et.al.

Cancer, Volume131, Issue21, 2025
https://doi.org/10.1002/cncr.70131

Abstract: Prostate-specific membrane antigen positron emission tomography/computed tomography (PSMA-PET/CT) is affecting the management of patients with prostate cancer with biochemical recurrence after radical prostatectomy. The long-term outcomes of tailoring salvage treatment on the basis of PSMA-PET/CT status remain to be determined.Methods: A decision-analytic model was developed to project incremental life-years of strategies that allocate treatments at biochemical recurrence after radical prostatectomy on the basis of PSMA-PET/CT status (PSMA-metastatic vs. PSMA-nonmetastatic). Modeled treatments are local/regional (radiation) or systemic (hormone therapy and doublet therapy), administered immediately or delayed. PSMA-metastatic status was assumed to lead to treatment intensification, whereas PSMA-nonmetastatic status would lead to deintensification. To project survival, data on progression to metastasis from a clinical cohort were combined with registry data on postmetastasis survival. Because of the lack of data on long-term treatment benefits by PSMA status, survival was projected by varying the hazard ratio (HR) for disease-specific death among PSMA-metastatic versus PSMA-nonmetastatic patients under delayed or local/regional regimens (HR1) and under immediate systemic regimens (HR2).Results: Mean life-years are projected to be 15.5 under the non–PSMA-tailored strategy, and mean incremental life-years range from 0.38 to 0.81 depending on HR1 and HR2. A greater benefit is projected when PSMA-metastatic status is more adverse under salvage regimens that do not include systemic agents.Conclusions: This decision-analytic modeling study projects that PSMA-PET/CT–guided management at biochemical recurrence after radical prostatectomy yields a modest survival benefit under the specified model inputs and assumptions regarding treatment distributions. These findings may complement emerging data on the corresponding economic costs and health-related quality of life.

25COASNOV80

Title: Proteolysis-targeting chimeras in cancer therapy: Targeted protein degradation for next-generation treatment

Yamile Abuchard Anaya BS, Mariana Barragan BS, Ricardo Pequeno Bracho BS et.al.

Cancer, Volume131, Issue21, 2025
https://doi.org/10.1002/cncr.70132

Abstract: Proteolysis-targeting chimeras (PROTACs) have the potential to revolutionize cancer treatment by specifically targeting and degrading oncogenic proteins. Using the ubiquitin-proteasome system, PROTACs allow the selective degradation of disease-causing proteins, including those traditionally deemed "undruggable" by conventional small-molecule inhibitors. By catalytically eliminating rather than inhibiting proteins, PROTACs provide sustained target suppression with lower doses and reduced toxicity. Their bifunctional design linking a protein of interest to an E3 ligase drives targeted ubiquitination and subsequent proteasomal degradation. Recent progress demonstrates promise in treating solid and hematologic malignancies, with several candidates advancing to clinical trials. This review provides a comprehensive overview of developing PROTACs, from understanding their mechanism to clinical applications, and highlights their emerging role in overcoming drug resistance and advancing the limits of cancer treatment. In addition, the authors discuss the challenges of optimizing PROTACs, including issues related to pharmacokinetics, E3 ligase compatibility, and the delivery of PROTACs to tumors. With their modularity, adaptability, and precision, PROTACs represent a next-generation platform for personalized cancer therapy across various patient groups.

25COASNOV81

Title: County-level medical debt and treatment initiation among individuals newly diagnosed with cancer

Jingxuan Zhao PhD, MPH, Marcelo Perraillon PhD, Roxanne M. Clark MPH et.al.

Cancer, Volume131, Issue21, 2025
https://doi.org/10.1002/cncr.70133

Abstract: The high costs of cancer care may lead to medical debt for patients and families. This study examined the association of county-level medical debt and timely treatment initiation among individuals newly diagnosed with cancer.Methods: Individuals aged 19 years and older who were newly diagnosed with acute leukemias, diffuse large B-cell lymphoma, Hodgkin lymphoma, female breast cancer, colorectal cancer, and lung cancer with consecutive enrollment in the same insurance type from the month of diagnosis through 90 days afterward were identified from the 2012–2021 Colorado Central Cancer Registry linked to the Colorado All-Payer Claims Database with information about county-level medical debt from the Urban Institute (N = 35,789). The exposure was the county-level share of adults with medical debt in collections, categorized in four quartiles (Q1–Q4). The outcome was timely treatment initiation—defined as the receipt of any cancer-directed treatment within 90 days after cancer diagnosis. The association of county-level medical debt and time to treatment initiation was examined by using multivariable Cox models.Results: Higher county-level medical debt was associated with lower likelihood of timely treatment initiation for all selected cancers combined (Q4 [counties with the highest medical debt rate; n = 8652] vs. Q1 [counties with the lowest medical debt rate; n = 9042]: hazard ratio [HR], 0.916; 95% confidence interval [CI], 0.871–0.963; p for trend = .001), for female breast cancer (Q4 vs. Q1: HR, 0.910; 95% CI, 0.847–0.978; p for trend = .011), and among individuals aged 19–64 years with private health maintenance organization plans (Q4 vs. Q1: HR, 0.790; 95% CI, 0.699–0.893; p for trend = .002) or Medicaid coverage (Q4 vs. Q1: HR, 0.869; 95% CI, 0.786–0.960; p for trend = .013).Conclusions: Policies aimed at preventing and alleviating medical debt could be effective strategies for improving access to timely

treatment.

25COASNOV82

Title: Understanding the role of neighborhood deprivation in racial disparities in triple-negative breast cancer

Lauren E. Barber PhD, MSc, Maret L. Maliniak PhD, MPH, Jasmine M. Miller-Kleinhenz PhD et.al.

Cancer, Volume131, Issue21, 2025
https://doi.org/10.1002/cncr.70138

Abstract: US Black women are twice as likely to be diagnosed with triple-negative breast cancer (TNBC), an aggressive subtype, as White women. Adverse neighborhood characteristics may contribute to the disparity. This study examined neighborhood deprivation in relation to TNBC, according to race and rurality.Methods: The authors identified 40,095 non-Hispanic Black and White women diagnosed with invasive breast cancer in 2010–2017 in the Georgia Cancer Registry. The Neighborhood Deprivation Index (NDI), a composite measure, was calculated using 2011–2015 block group-level American Community Survey data. County-level rurality was measured via Georgia Department of Public Health data. We estimated multivariable odds ratios (ORs) and 95% confidence intervals (CIs) for the associations between NDI, in quintiles, and each breast cancer subtype (TNBC, HER2-enriched, luminal B vs. luminal A breast cancer), overall, and according to race and rurality.Results: Compared to least deprived neighborhoods, living in the most deprived neighborhoods was associated with a 33% (OR, 1.33; 95% CI, 1.19–1.48) increased odds of TNBC versus luminal A breast cancer. Race and rurality did not modify the association. However, estimates were less pronounced among non-Hispanic Black women (OR, 1.18; 95% CI, 1.00–1.39 vs. OR, 1.40; 95% CI, 1.18–1.65 among non-Hispanic White women) and women living in urban counties (OR, 1.33; 95% CI, 1.18–1.50 vs. OR, 1.52; 95% CI, 1.15–2.03 in rural counties).Conclusions: In this study, neighborhood deprivation was associated with increased odds of TNBC, regardless of race or rurality. Given Black women are more likely to live in deprived neighborhoods, neighborhood deprivation may contribute to racial disparities in TNBC occurrence.

25COASNOV83

Title: Optimizing Wilms tumor 1 thresholds for measurable residual disease monitoring in acute myeloid leukemia: Improved sensitivity and concordance with nucleophosmin 1 in a single-center validation study

Sabrina Barriere MD, Céline Bourgne PhD, Thomas Tassin PharmD et.al.

Cancer, Volume131, Issue21, 2025
https://doi.org/10.1002/cncr.70140

Abstract: In acute myeloid leukemia (AML), measurable residual disease (MRD) assessment is essential for predicting relapse and guiding therapy decision-making. Nucleophosmin 1 (NPM1) mutations are reliable MRD markers but apply to only ~30% of patients with AML. Wilms tumor 1 (WT1) expression monitoring is applicable to a broader population but the European LeukemiaNet (ELN) threshold of 50 WT1 copies per 104 ABL copies (0.5%) may be too high, which limits sensitivity.Methods: With WT1 expression data from 100 healthy controls, this study established a revised WT1 threshold of seven copies per 104 ABL copies

(0.07%). Its performance was retrospectively validated against NPM1 in 308 paired follow-up samples from 63 patients with NPM1-mutated AML, and against the core binding factor (CBF) β-MYH11 fusion transcripts in 83 samples from 12 patients. Statistical analyses included concordance, sensitivity/specificity, survival estimates, and model comparison with the Akaike information criterion.Results: Compared to the ELN cutoff, the revised threshold showed higher concordance with NPM1 (78.6% vs. 73%) and sensitivity (54% vs. 24%; $p < .0001$) and acceptable specificity (91% vs. 98%; $p = .002$). In survival analyses, the seven-copy cutoff demonstrated stronger prognostic value than the ELN threshold, particularly after consolidation therapy. In the CBFB::MYH11 cohort, the two thresholds showed similar concordance but WT1 positivity with the revised cutoff preceded relapse in selected patients.Conclusions: In AML, the revised WT1 threshold of seven copies per 104 ABL copies enhanced MRD sensitivity while maintaining specificity, improving concordance with NPM1, and showing prognostic relevance. These findings support the clinical value of locally optimized WT1 thresholds, and highlight the need for prospective multicenter validation and harmonization of WT1-based MRD monitoring.

25COASNOV84

Title: Phase 1 clinical trial of the ataxia telangiectasia and Rad3-related inhibitor berzosertib with irinotecan in patients with advanced solid tumors (ETCTN 9938)

Liza C. Villaruz MD, Jingxiao Jin MD, Hong Wang PhD et.al.

Cancer, Volume131, Issue21, 2025
https://doi.org/10.1002/cncr.70157

Abstract: Ataxia telangiectasia and Rad3-related (ATR) inhibition with berzosertib potentiates the efficacy of irinotecan in preclinical models. The authors hypothesize that this combination is well tolerated, modulates the DNA damage response to irinotecan, and is associated with clinical activity in advanced solid tumors. Methods: In this phase 1 study (NCT02595931), berzosertib 60–270 mg/m2 was administered with irinotecan 180 mg/m2 every 2 weeks in a 4-week cycle. The primary end point was determination of the maximum tolerated dose and recommended phase 2 dose (RP2D). Antitumor activity, pharmacokinetics, and pharmacodynamics were secondary end points.Results: Sixty-three patients were enrolled, the majority with colorectal cancer (49%) or pancreatic cancer (21%). Median number of prior lines of therapy was four (range, 2–7). Two dose-limiting toxicities, both febrile neutropenia, occurred among 45 patients treated with berzosertib 270 mg/m2 and irinotecan 180 mg/m2. The most common treatment-related grade ≥3 toxicities were lymphopenia (30%), neutropenia (29%), and anemia (25%). Two partial responses occurred in patients with pancreatic cancer and ataxia telangiectasia mutated (ATM) alterations: 32% decrease in an ATM E11828/ATM K1109* tumor lasting 15.8 months and 57% decrease in an ATM R3008H/germline ATM R1882* tumor lasting 13.6 months. Induction of DNA damage markers γH2AX and pNBS1 was observed in one tumor biopsy obtained post berzosertib and irinotecan combination treatment compared with post irinotecan alone.Conclusion: Berzosertib 270 mg/m2 and irinotecan 180 mg/m2 was the RP2D. The combination is associated with manageable side effects and promising disease activity in ATM mutant solid tumors.

25COASNOV85

Title: Evaluating portal-enabled elicitation of patients' health-related values in solid tumor oncology: A qualitative content analysis

Carrie Sha MD, Erin Santos MD, Jaime Gilliland MA et.al.

Cancer, Volume131, Issue21, 2025
https://doi.org/10.1002/cncr.70159

Abstract: Electronic patient portals are increasingly used to improve care and patient–clinician communication. Portal-elicited health-related values (HRVs) were evaluated as to whether they contain themes similar to those arising from nurse-led in-person discussions. Methods: HRV questionnaires, consisting of seven questions, were sent by portal to patients of five solid tumor clinics from July 2023 to August 2024. Applying a theoretical framework generated from prior analysis of in-person nurse-led discussions with patients about their HRVs, questionnaires were coded via thematic content analysis.Results: A total of 1556 HRV questionnaires were sent to individual patients. Of 852 unique patients who returned questionnaires with response to at least one question, a random subset of 200 patients' responses (167 gastrointestinal cancers, 33 genitourinary cancers) were analyzed by an interdisciplinary team. Analysis identified five themes consistent with those previously identified from in-person discussions: cancer as threat/disruption; expression of personhood and desire to retain a sense of self; communication with loved ones and the medical team as a tool for maintaining individual agency; connection to others as core to social identity and a source of individual strength; and sources of meaning and fulfillment. Uniquely identified by our analysis of portal responses were elements of financial toxicity and spiritual and existential well-being.Conclusion: Elicitation of patient values through the electronic portal provides valuable insights into the HRV of patients with solid tumors. The electronic portal captures values comparable to those elicited in in-person discussions, supporting efforts to scale such initiatives while preserving the content of patients' reports as a basis for discussion of their HRVs with clinicians.

25COASNOV86

Title: Disparities in cancer clinical trials among low- and middle-income countries: A 20-year analysis

Fanny G. A. Cascelli MD, Milene C. Mitsuyuki MD, Gustavo Werutsky MD et.al.

Cancer, Volume131, Issue21, 2025
https://doi.org/10.1002/cncr.70067

Abstract: There are suspected disparities in clinical research (CR) development among low- and middle-income countries (LMICs). This study investigated differences in number and complexity of clinical trials (CTs) and how economic growth (EG) might contribute to these disparities.Methods: For countries classified as LMICs in 2000, number, proportion of phase 1-2/3 and independent/pharma-sponsored CTs were documented. For correlations with EG, correlation coefficients (CC) were produced, indicating very weak, weak, moderate, strong, and very strong correlation.Results: A total of 16,977 CTs were identified. Asian countries China and South Korea experienced strong EG and increases in CTs (very strong CC). South/Southeast Asian countries had strong EG but modest increases in CTs (variable CC). Most East European countries and West Asian/Southeast European Turkey experienced robust EG and increases in CTs (moderate to strong and very strong CC, respectively).

South/North American Argentina, Brazil, and Mexico had inconsistent EG but increases in CTs (weak to moderate CC). Among African countries, Egypt showed strong EG with a corresponding increase in CTs (strong CC), whereas South Africa had a weak CC. Most LMICs, except for China and South Korea, relied heavily on pharma-sponsored CTs, with a persistently low proportion of early-phase (1-2) compared to late-phase (3) CTs.Conclusion: CR development has been unequal among LMICs. Strong EG could be a contributing factor but only to some extent. Only China and South Korea meaningfully developed independent and high–complexity CR. These data reinforce the need for initiatives to support cancer research in LMICs.

25COASNOV87

Title: Efficacy, safety and predictive biomarker of third-generation tyrosine kinase inhibitors with azacitidine in myeloid blast phase of chronic myeloid leukemia

Mei Bao MD, Xiao S. Zhang MD, Zong R. Li MD et.al.

Cancer, Volume131, Issue22, 2025

https://doi.org/10.1002/cncr.70166

Abstract: Objective: To evaluate the efficacy, safety, and predictive biomarker of a third-generation tyrosine kinase inhibitor (3G-TKI; ponatinib or olverembatinib) combined with azacitidine in chronic myeloid leukemia (CML) in myeloid blast phase. Methods: We conducted a single-center, prospective study combining 3G-TKI with azacitidine in 28-day cycles. The primary end point was a major hematologic response (MaHR) by cycle 2. The trial is registered in Chinese Clinical Trial Registry (ChiCTR2200055887)Results: In total, 37 patients were studied. The median follow-up was 30 months (interquartile range, 24–40 months). Twenty-five patients achieved a MaHR by cycle 2, 30 returned to chronic phase. Ten patients underwent transplantation. The patients who underwent transplantation had higher 3-year probability of survival compared with nontransplanted patients (50%; [95% confidence interval (CI), 9%–37%] versus 18% [95% CI, 3%–33%]; p = .01). The regimen was well tolerated. In adjusted logistic/Cox regression analyses, KRAS mutation was significantly associated with a lower MaHR rate (odds ratio, 0.1; 95% CI, 0–0.8; p = .03), worse progression-free survival (PFS; hazard ratio [HR], 3.1; 95% CI, 1.1–8.6; p = .04), and worse survival (HR, 8.2; 95% CI, 2.5–26.8; p < .001); PTPN11 mutation was associated with worse PFS (HR, 5.1; 95% CI, 1.2–22.2; p = 0.03) and worse survival (HR, 9.6; 95% CI, 2.2–41.5; p = .002); and increasing numbers of non-ABL1 mutations were associated with worse PFS (HR, 1.2; 95% CI, 1.0–1.3; p = .04). Transcriptomic analysis revealed that patients who did not achieve a MaHR experienced activation of cancer-, metabolism-, oxidative phosphorylation-related pathways. The KRAS signaling pathway was significantly activated in patients who lost MaHR during treatment.Conclusions: 3G-TKI with azacitidine is an effective and safe therapy providing more chance to receive a transplantation for CML in myeloid blast phase. Potential biomarkers associated with outcomes were identified.

25COASNOV88

Title: MYC amplification and MYC protein expression are poor prognostic markers in pediatric and young adult osteosarcoma

Matthew R. Nagy MD, MPH, Olivia Puopolo BS, Erin Alston MD et.al.

Cancer: Volume 131, Issue 22, 2025

https://doi.org/10.1002/cncr.70161

Abstract: Prognostication in pediatric and young adult osteosarcoma is typically limited to metastatic status at diagnosis and tumor necrosis after chemotherapy. Despite a complex genomic landscape, few molecular biomarkers are used clinically. This study evaluates the prognostic relevance of MYC amplification and MYC protein expression.Methods: This study analyzed 105 patients with high-grade osteosarcoma. MYC copy number was assessed via targeted sequencing, and MYC protein expression was assessed via immunohistochemistry H score. Amplification (AMP) was defined as >7 copies; high expression (EXP) was defined as an H score of >150. Correlation between AMP and EXP was calculated, and overall survival (OS) was analyzed with Kaplan–Meier and Cox models.Results: Among the 105 patients (42% female; median age, 14 years; interquartile range, 11–17 years), 16% had AMP, 22% had high EXP, and 8% had both AMP and high EXP. MYC copy number positively correlated with protein expression ($r = 0.53$; $p < .0001$). With accounting for metastatic status, AMP and high EXP had lower OS (AMP vs. non-AMP: 3-year OS, 27% vs. 74%; adjusted hazard ratio [HR], 3.4; high EXP vs. low EXP: 35% vs. 77%; adjusted HR, 4.9; both $p < .0001$). Patients with both AMP and high EXP had markedly lower survival compared to those with non-AMP and low EXP (3-year OS, 0% vs. 79%; adjusted HR, 17.7; $p < .0001$).Conclusions: MYC amplification and high protein expression both independently and concurrently predict poor survival in pediatric and young adult osteosarcoma, beyond metastatic status. Incorporating MYC status into risk stratification may enhance prognostic accuracy and inform targeted therapeutic development.

25COASNOV89

Title: The association between human papillomavirus type 16 seropositivity and oropharyngeal cancer among men living with HIV

Ashley J. Duff MPH, Anna Junkins PhD, Li Chen PhD et.al.

Cancer: Volume 131, Issue 22, 2025
https://doi.org/10.1002/cncr.70167

Abstract: There are no methods for the early detection of human papillomavirus–driven oropharyngeal squamous cell carcinoma (HPV+OPSCC); however, HPV16 E6 seropositivity has been identified as a promising screening marker. Although people living with HIV have a higher risk of developing HPV+OPSCC, few studies have evaluated the association between HPV16 antibodies and HPV+OPSCC. Methods: The association between HPV16 seropositivity (L1, E1, E2, E4, E6, and E7) and OPSCC was assessed among 2331 men living with HIV (MLWH) aged ≥40 years who had blood specimens banked within the Tennessee Center for AIDS Research biorepository between 2001 and 2019; some samples were collected before OPSCC diagnosis, and others after. The association between HPV16 seropositivity and OPSCC was analyzed via univariable logistic regression. Results: One hundred and thirty-five HPV16 E6 seropositive cases and 11 OPSCC cases were identified. HPV16 E6 seropositivity was associated with a 14-fold higher odds of OPSCC (odds ratio [OR], 14.04; 95% CI, 4.23–46.61; $p < .001$); five of the 11 OPSCC cases were HPV16 E6 seropositive (sensitivity, 45%; 95% CI, 17%–77%) compared to 6% of controls (specificity, 94%; 95% CI, 93%–95%). Seroreactivity against HPV16 E1 (OR, 7.14; 95% CI, 1.52–33.67; $p = .013$), HPV16 E2 (OR, 16.43; 95% CI, 4.94–54.65; $p < .001$), and HPV16 E7 (OR, 13.84; 95% CI, 3.99–48.11; $p < .001$) was also significantly associated with OPSCC. HPV16 E6

antibodies were detectable up to 9 years before and 19 years after OPSCC diagnosis. Conclusions: Among MLWH, HPV16 E6 antibodies are strongly associated with OPSCC, yet point estimates of the sensitivity and specificity of HPV16 E6 antibodies for OPSCC were lower compared to studies in populations without HIV.

25COASNOV90

Title: The impact of multicancer early detection tests on cancer stage shift: A 10-year microsimulation model

Jagpreet Chhatwal PhD, Jade Xiao PhD, Andrew K. ElHabr et.al.

Cancer: Volume 131, Issue 22, 2025
https://doi.org/10.1002/cncr.70075

Abstract: Early detection of cancer improves survival following diagnosis. However, routine screening is limited to a few cancer types. Multicancer early detection (MCED) tests could revolutionize cancer screening by simultaneously detecting multiple cancer types. This study evaluates the potential impact of an MCED test on stage shift in the US general population. Methods: A microsimulation model of 14 solid tumor cancer types that account for nearly 80% of cancer incidence and mortality was developed. The model was calibrated to reproduce annual incidence rates reported in the Surveillance, Epidemiology, and End Results database. Cancer diagnosis could arise from standard-of-care procedures or annual MCED testing. MCED sensitivities were derived from a large, multicenter, prospective, case control study. Ten-year disease progression was simulated for 5 million US adults aged 50 to 84 years. The primary outcome was stage shift resulting from MCED testing. Results: Over 10 years, supplemental MCED testing led to a 10% increase in Stage I diagnoses, 20% increase in Stage II diagnoses, 34% increase in Stage III diagnoses, and 45% decrease in Stage IV diagnoses, relative to the standard of care alone. The largest absolute reductions in Stage IV diagnoses were in lung (400 vs. 765 per 100,000), colorectal (96 vs. 236), and pancreatic (89 vs. 211) cancer. The largest relative reductions were in cervical (83%), liver (74%), and colorectal (59%) cancer. Conclusion: MCED testing has the potential to substantially reduce late-stage cancer diagnoses, improve outcomes across multiple cancer types, and address a critical gap in screening.

25COASNOV91

Title: Race-related subsequent breast events after ductal carcinoma in situ: A Surveillance, Epidemiology, and End Results–based analysis

Alzina Koric PhD, Shu Jiang PhD, Ying Liu MD et.al.

Cancer: Volume 131, Issue 22, 2025
https://doi.org/10.1002/cncr.70164

Abstract: The risk of subsequent ductal carcinoma in situ (DCIS) or invasive breast cancer (IBC) has been evaluated in either breast after a DCIS diagnosis; this study modeled competing risks of ipsilateral and contralateral DCIS or IBC subtypes by self-reported race. Methods: A cohort of 198,827 women diagnosed with primary unilateral DCIS between 2000 and 2022 was identified from the US Surveillance, Epidemiology, and End Results tumor registries. Competing subdistributional hazard ratio (sHR) models were used to estimate DCIS or IBC laterality-associated risks overall and for the estrogen receptor (ER+) or progesterone receptor (PR+) overexpressing (ER+/PR+) and ER−PR− expressing tumor

subtypes. Cox models were used for subanalysis to estimate the overall risk of a second event (DCIS or IBC). Results: Within an average of 10 (±6.1) years of follow-up after the initial DCIS, 16,148 women had a subsequent event (25.7% DCIS; 74.3% IBC). Overall, compared with White women, Black women had an elevated risk of IBC for either tumor subtype, whereas Asian and Hispanic women had an elevated risk of ER−PR− IBC. For tumor aggressiveness by laterality, Black women had an elevated IBC risk in either breast for ER−PR− (sHR, 1.82; 95% CI, 1.53–2.17 in the ipsilateral breast; sHR, 1.512; 95% CI, 1.24–1.86 in the contralateral breast), as did Hispanic and Asian women in the ipsilateral breast only (with stronger association vs. ER+/PR+) (phet = .0001). Conclusions: These contemporary data reflect treatment patterns since 2000, which show an elevated risk of subsequent breast tumors in either breast among Black women after DCIS.

25COASNOV92

Title: A phase 2 trial of a "sandwich" strategy: Sequential CD22/CD19 chimeric antigen receptor T-cells therapy combined with autologous hematopoietic stem cell transplantation in patients with Philadelphia chromosome–negative B-cell acute lymphoblastic leukemia

Chong-Sheng Qian MD, PhD, Zi-Hao Wang MS, Zheng Li MD et.al.

Cancer: Volume 131, Issue 22, 2025
https://doi.org/10.1002/cncr.70168

Abstract: The relapse after chimeric antigen receptor (CAR) T-cell therapy remains a critical challenge, and the optimal timing and treatment strategies for CAR T urgently need to be explored. Autologous hematopoietic stem cell transplantation (auto-HSCT) demonstrates comparable leukemia-free survival (LFS) and overall survival (OS) in patients who rapidly achieve MRD-negative complete remission (CR) compared with allogeneic HSCT (allo-HSCT). Thus, combining CAR T cells with auto-HSCT may represent a promising treatment strategy.Methods: This phase 2 trial evaluated the safety and efficacy of sequential CD22/CD19 CAR T cells combined with an auto-HSCT "sandwich" strategy in patients with Philadelphia chromosome–negative (Ph-negative) B-cell acute lymphoblastic leukemia (B-ALL), including adolescents and young adults (AYA) as well as adults who were unable or declined to allo-HSCT. The primary and secondary end points were OS and LFS, respectively.Results: At a median follow-up of 28 months, the median OS and LFS were not reached. The 2-year OS and LFS rates were 97% (95% confidence interval [CI], 90%–100%) and 72% (95% CI, 58%–90%), respectively. All 35 patients who completed the sandwich strategy survived. Continuous MRD-negative CR rates after the second CAR T-cell infusion were 80% by multiparameter flow cytometry and 70% by next-generation sequencing of immunoglobulin H rearrangements. OS and LFS did not differ between poor and standard genetic risk groups. Compared with the allo-HSCT external control group, the sandwich strategy showed improved OS and comparable LFS. No cases of immune effector cell–associated neurotoxicity syndrome or severe cytokine release syndrome were observed.Conclusion: The CD22/CD19 CAR T-cell and auto-HSCT sandwich strategy represents a promising approach for the treatment of Ph-negative B-ALL in AYA and adult patients, offering high efficacy and a favorable safety profile.

25COASNOV93

Title: Mechanisms of tumor aggressiveness driven by ablation-induced niche remodeling

Shuyue Gao, Ting Luo, Fangying Fan et.al.

(BBA) - Reviews on Cancer, Volume 1880, Issue 6, November 2025
https://doi.org/10.1016/j.bbcan.2025.189449

Abstract: Tumor niche represents a dynamic, functionally specialized microenvironment defined by reciprocal interactions between tumor cells and their surrounding stroma. However, emerging evidence suggests that ablation-induced niche remodeling may promote tumor aggressiveness, counteracting therapeutic benefits. This review summarizes current insights into the role of ablation-induced niche remodeling in tumor progression. We begin with a bibliometric analysis to illustrate research trends and identify the hotspots. We then explore the underlying biological mechanisms of niche remodeling post-ablation, with a focus on three key aspects: resistance to cell death, immune cell reprogramming toward immunosuppression, and enhanced tumor invasiveness and migration. These insights may inform future research directions and support the development of more effective clinical strategies.

25COASNOV94

Title: Unraveling the role of mitochondrial dynamics in cancer stem cells: Molecular basis and therapeutic implications

Gaia Giannitti, Sara Marchesi, Riccardo Garavaglia et.al.

(BBA) - Reviews on Cancer, Volume 1880, Issue 6, November 2025
https://doi.org/10.1016/j.bbcan.2025.189450

Abstract: Many tumors consist of heterogeneous cell populations derived from a minority of cancer stem cells (CSCs), which possess distinct metabolic profiles that contribute to resistance against conventional anticancer therapy and increase the risk of tumor relapse. These unique CSC phenotypes are largely supported by altered mitochondrial function and turnover, regulated through continuous cycles of mitochondrial biogenesis, fission, fusion, and mitophagy. Consequently, understanding mitochondrial regulatory mechanisms in CSCs could reveal novel targets for cancer therapy. This article explores how mitochondrial dynamics contribute to CSC metabolic adaptation and drug resistance, alongside recent advances in the development of mitochondria-targeted drugs and their therapeutic usage.

25COASNOV95

Title: The evolving landscape of antibody-drug conjugates in small cell lung cancer: From research progress to clinical application

Haoyu Wang, Chenyue Zhang, Haiyong Wang et.al.

(BBA) - Reviews on Cancer, Volume 1880, Issue 6, November 2025
https://doi.org/10.1016/j.bbcan.2025.189445

Abstract: Antibody-drug conjugates (ADCs), one of the emerging developing classes of antitumor drugs, have transformed the therapeutic paradigm in oncology. It stands out due to its properties of boasting the strength of both chemotherapy and targeted therapy. In small cell lung cancer (SCLC), ADC has also demonstrated its potential and appealing effect. Clinical trials of ADCs in SCLC are currently in full swing. While ADC has brought some

encouraging results so far, several obstacles have been encountered, such as drug resistance, drug toxicities and the difficulty in the selection of patients benefiting from ADCs. Thus, a deepened and comprehensive understanding of the fundamental researches, as well as summarization of ADC development in SCLC might offer us some enlightenment and solutions to these tricky issues. Therefore, in the present review, we elaborate on the structure and mechanism of ADC, clinical trials conducted in SCLC. Additionally, we also outline the obstacles and propose future directions of ADC in SCLC, highlighting its in-depth research and prospective application in SCLC.

25COASNOV96

Title: Functional dichotomy of autophagy signaling in tumor microenvironment driving hallmarks in oral cancer

Sushmita Patra , Bishnu Prasad Behera, Birija Sankar Patro et.al.

(BBA) - Reviews on Cancer, Volume 1880, Issue 6, November 2025
https://doi.org/10.1016/j.bbcan.2025.189451

Abstract: As a cytoprotective mechanism, autophagy recycles damaged proteins and organelles via the lysosomal degradation pathway in response to diverse stress conditions. However, its role in tumor microenvironment, including oral cancer, is still a point of contention. Although excessive autophagy is associated with cell death, many studies have revealed elevated autophagy levels in advanced stages of oral cancer, providing a suitable niche for growth and proliferation. On the contrary, disruption of basal level autophagy also contributes to oral cancer development at the early stage due to increased oxidative stress and accumulation of genetic mutations. This atypical dependence of oral cancer cells on autophagy is associated with cellular features, stage, and requirements. The present study highlights the involvement of key autophagy-related proteins in oral cancer progression and explores their interaction with oncogenic signaling pathways that drive proliferation, chemoresistance, metabolic reprogramming, and metastasis. Furthermore, increased autophagy in cancer-associated fibroblasts, immune cells, and macrophages within the tumor microenvironment contributes to fibroblast activation, cytokine secretion, and immune suppression, enhancing tumor plasticity. Notably, crosstalk between autophagy and the NLRP3 inflammasome has emerged as a significant factor in promoting oral cancer progression and metastasis. Finally, accumulating evidence supports the therapeutic potential of autophagy modulators, which enhance apoptosis and suppress tumor growth, suggesting that targeting autophagy could offer promising treatment strategies for resistant oral cancers.

25COASNOV97

Title: Animal models in preclinical evaluation of CAR-T cell therapy: Advantages and limitations

Lasse von Bornemann Fløe, Maya Graham Pedersen, Bjarne K. Møller et.al.

(BBA) - Reviews on Cancer, Volume 1880, Issue 6, November 2025
https://doi.org/10.1016/j.bbcan.2025.189455

Abstract: Chimeric Antigen Receptor T (CAR-T) cell therapy is a promising new treatment category. Animal models have played a pivotal role in advancing CAR-T cell therapy. However, no animal model fully replicates human physiology, leading to unsuccessful translation from preclinical models to clinical trials. Understanding the advantages and

limitations of various animal model choices requires insight into CAR-T cell mechanisms and their interactions across experimental contexts. CAR-T cell immunobiology differs between animal models and humans. This disparity is reflected in the limited translational capacity of pharmacological parameters and the absence of key immunological interactions in animal models compared to those seen in human trials. Additionally, the antigen specificity of the CAR introduces translational limitations. Differences in antigen density and expression among different cellular populations across species are critical factors to consider when interpreting preclinical results. Xenoreactivity, stemming from the original T-cell receptor repertoire, also limits experimental duration and timing in mouse models. Modeling human cancer in animal models requires many considerations. Cancer heterogeneity varies significantly between patient-derived xenografts and cell-line-based xenografts. Syngeneic models more accurately mimic interactions between CAR-T cells and other immune components, while xenograft models better reflect human tumor antigen expression. Beyond CAR-T-specific challenges, issues with standardization and replication in animal studies affect the reliability of the results. Furthermore, ethical guidelines should guide experimental planning to minimize animal use and prioritize humane treatment. This review explores the strengths and limitations of animal models preclinical CAR-T cell therapy research, while offering critical considerations for interpreting results and designing experiments.

25COASNOV98

Title: Intricate role of DRP1 and associated mitochondrial fission signaling in carcinogenesis and cancer progression

Soumya Ranjan Mishra, Priyadarshini Mishra, Prakash Kumar Senapati et.al.

(BBA) - Reviews on Cancer, Volume 1880, Issue 6, November 2025
https://doi.org/10.1016/j.bbcan.2025.189453

Abstract: The process of mitochondrial fission is a major determinant of mitochondrial homeostasis. DRP1 is the chief architect of the mitochondrial fission process, and the DRP1 recruitment to the mitochondrial outer membrane is necessary for the mitochondrial division. DRP1 contributes to cancer progression by promoting cell proliferation, enhancing resistance to therapy, inhibiting apoptosis, suppressing immune responses, and sustaining cancer stem cell heterogeneity and self-renewal. Moreover, DRP1 drives metabolic reprogramming to support enhanced energy production and biosynthesis required for tumor growth and survival. In addition, DRP1-mediated mitochondrial fission also favours NLRP3 inflammasome activation within the tumor microenvironment, which regulates cancer progression. Interestingly, elevated levels of DRP1 expression have been identified as a significant prognostic marker, correlating with poor survival outcomes across multiple cancer types. Many DRP1 inhibitors have been developed for cancer treatment, but more specific and selective agents are needed to improve efficacy and reduce off-target effects. A comprehensive understanding of DRP1's role in cancer cells is essential for developing DRP1 inhibitors, which hold promise as novel anticancer therapies and may enhance the effectiveness of conventional treatments.

25COASNOV99

Title: Advances in artificial intelligence for spatial transcriptomics in cancer: Special focus on Yin Yang 1 (YY1) and Raf kinase inhibitor protein (RKIP)☆

Lekhya Dommalapati, Rachael Guenter, Yuvasri Golivi et.al.
(BBA) - Reviews on Cancer, Volume 1880, Issue 6, November 2025
https://doi.org/10.1016/j.bbcan.2025.189456
Abstract: Spatial transcriptomics (ST) plays a pivotal role in cancer research, offering a unique perspective on gene expression within the cancer microenvironment, further revolutionizing our current understanding of the subject. From addressing the limitations of traditional bulk RNA sequencing by preserving spatial context, this review discusses the importance of integrating machine learning (ML), artificial intelligence (AI), and statistical methods for interpreting ST data within oncology. Herein, we use examples from studies involving Raf kinase inhibitor protein (RKIP) and Ying Yang 1 (YY1) to illustrate applications for some of the ST techniques discussed. We explore how applying supervised learning techniques, such as Support Vector Machines (SVMs) and Random Forests (RFs), can significantly help further cancer classification and prediction of clinical outcomes and advance personalized medicine. Additionally, exploring unsupervised learning approaches like clustering and dimensionality reduction methods (PCA, t-SNE, UMAP) allows us to see hidden structures in ST data that may be overlooked. This review discusses recent tools and techniques that have been introduced within the last few years, underlining the transformation brought into ST by ML, AI, and statistical methods that provide new insight into oncogenic drivers such as YY1 and RKIP, cancer heterogeneity, and avenues for personalized medicine approaches in cancer treatment.

25COASNOV100

Title: Cancer-associated thrombosis in cholangiocarcinoma: Exploring a phenotype of tumor aggressiveness

Luca Fabris, Yahima Frión-Herrera, Massimiliano Cadamuro et.al.
(BBA) - Reviews on Cancer, Volume 1880, Issue 6, November 2025
https://doi.org/10.1016/j.bbcan.2025.189457
Abstract: Cholangiocarcinoma (CCA) is the liver malignancy with the most rapid increase in incidence and lethality in recent years. Venous thromboembolism (VTE) is a common complication of the cancer-associated hypercoagulable state, which may incite tumor progression and dissemination, thereby increasing cancer-related morbidity and mortality. Compared to other cancer types, occurrence of VTE in CCA has been underestimated, though recent evidence indicates it may behave as prognostic factor of worst outcome. Given the need for novel predictive scores and treatment approaches when VTE occurs, identifying subgroups of patients with CCA who would benefit from thromboprophylaxis without increasing the risk of bleeding is a crucial but still neglected aspect of the management. The aim of this review is to summarize current observations on the clinical significance, prediction, risk assessment and the underlying mechanisms of cancer-induced thrombogenesis in CCA, as well as to identify research areas ripe for prioritization in the near future.

25COASNOV101

Title: Oncogenic mutation-driven metabolism-immunity regulatory axis: Potential prospects for thyroid cancer precision therapy

Tingting Zhan, Hengtong Han, Tianying Zhang et.al.

(BBA) - Reviews on Cancer, Volume 1880, Issue 6, November 2025
https://doi.org/10.1016/j.bbcan.2025.189459

Abstract: Oncogenes enhance cancer development, and their specific activating mutations exemplify the mechanisms that initiate and mediate thyroid cancer (TC) progression. Research has predominantly focused on how oncogenes promote the development of different TC subtypes by influencing the downstream signaling pathways. Targeted therapies show significant efficacy; however, they often induce drug resistance through feedback activation or compensatory signaling bypasses. Recent evidence indicates that thyroid oncogenes initiate and mediate TC progression, and contribute to drug resistance in distinct TC subtypes through induced metabolic reprogramming and immune microenvironment remodeling. Hence, we propose the concept "Oncogene-Metabolism-Immunity axis." We discussed the molecular mechanisms by which oncogene-driven metabolic reprogramming and tumor immune microenvironment Remodeling (TIME), and their mutual interactions, induce TC progression, drug resistance, and immune evasion. Finally, we systematically evaluated and summarized potential strategies targeting key oncogenes, metabolic catalysts, immune checkpoints (ICs), and combination therapies to enhance the efficacy of targeted treatments for TC and overcome drug resistance.

25COASNOV102

Title: Revolutionizing bladder cancer research: Harnessing 3D organoid technology to decode tumor heterogeneity and propel personalized therapeutics

Helin Kang , Xi Liu, Dan Ge et.al.

(BBA) - Reviews on Cancer, Volume 1880, Issue 6, November 2025
https://doi.org/10.1016/j.bbcan.2025.189454

Abstract: Bladder cancer (BC), characterized by remarkable tumor heterogeneity, remains a challenging malignancy with limited therapeutic options. Emerging three-dimensional (3D) organoid models are transforming our understanding of BC biology by closely mimicking the complex tumor microenvironment (TME) and cellular interactions, far surpassing traditional two-dimensional (2D) cell culture systems. This review underscores the innovative advances in bladder cancer organoid technology, emphasizing their unique strengths in capturing intratumoral heterogeneity, enhancing drug sensitivity assessments, and facilitating personalized treatment approaches. We discuss diverse organoid systems, including spheroids, assembloids, and patient-derived organoid xenografts (PDOX), highlighting their exceptional ability to replicate individual patient tumor profiles. Furthermore, we explore integrated organoid-on-chip cultivation techniques incorporating 3D bioprinting and microfluidics, which notably improve precision, reproducibility, and scalability in organoid-based drug screening platforms. We advocate for optimized organoid cultivation protocols and synergistic integration with high-throughput analytical technologies, aiming ultimately to accelerate regimen breakthroughs in personalized medicine for bladder cancer patients.

25COASNOV103

Title: Sensory neuro-tumor crosstalk: Therapeutic opportunities and emerging frontiers in cancer neuroscience

Ying Wang, Zhixin Ye, Ye Yuan et.al.

(BBA) - Reviews on Cancer, Volume 1880, Issue 6, November 2025

https://doi.org/10.1016/j.bbcan.2025.189464

Abstract: Emerging evidence in cancer neuroscience highlights the crucial role of sensory nerves in tumor progression, an aspect of cancer pathobiology previously overlooked. Mechanistically, tumor-associated sensory neurons establish a self-reinforcing oncogenic loop via secreted neurotrophic factors (e.g., NGF/BDNF), which directly promote cancer cell growth, spread, and treatment resistance through Trk activation. Concurrently, tumors rewire their local environment through dysregulated expression of axon guidance molecules, facilitating invasive growth. Importantly, nociceptive signaling activated during perineural invasion not only mediates cancer-related pain but also shapes an immunosuppressive microenvironment through neuropeptide-mediated changes in immune cell function. Current therapeutic strategies targeting tumor-associated nerves focus on: (1) Pharmacological blockade of nerve-tumor communication using small-molecule inhibitors (e.g., Trk inhibitor larotrectinib); (2) Bioelectronic modulation of neural activity via modalities such as transcutaneous electrical nerve stimulation. Notably, preclinical models reveal enhanced efficacy when combining neural modulation with immune checkpoint inhibitors. Technological breakthroughs, including single-cell analysis for precise nerve targeting and advanced drug delivery systems, are improving therapeutic precision. Consequently, understanding the complex interactions between nerves and tumors requires integrated approaches combining cancer biology, neuroimmunology, and systems neuroscience. This conceptual shift not only reshapes our understanding of cancer pathophysiology but also opens new avenues for precision therapies aligned with modern oncology.

25COASNOV104

Title: Targetable axes of tumor-associated macrophages: An MSF framework for precision immunotherapy

Zhenting Lu, Midie Xu, Junzhe Tang et.al.

(BBA) - Reviews on Cancer, Volume 1880, Issue 6, November 2025
https://doi.org/10.1016/j.bbcan.2025.189458

Abstract: Tumor-associated macrophages (TAMs) are a central component of the tumor microenvironment and exert dual, context-dependent effects on cancer progression. This review synthesizes the mechanisms that govern TAM polarization, their bidirectional crosstalk with tumor and stromal cells, and the consequences of metabolic reprogramming. Molecular and metabolic circuits that shape TAM phenotypes and sustain immune suppression are highlighted, and therapeutic strategies targeting TAM checkpoints, metabolism, and lineage pathways are summarized. To integrate immunometabolism with single-cell and spatial profiling, we introduce a Metabolic-Spatial-Functional Axis that links dominant metabolic programs, anatomic niches, and measurable effector functions. This framework organizes TAM heterogeneity and prioritizes biomarker-guided therapeutic combinations with clear translational readouts. Collectively, these advances support precision approaches that reprogram or constrain TAMs to enhance antitumor immunity and overcome therapeutic resistance.

25COASNOV105

Title: The bridging role of neutrophils in the progression of inflammation-induced colorectal cancer

Jian Wang , Huihui Xiao , Siqian Cui et.al.
(BBA) - Reviews on Cancer, Volume 1880, Issue 6, November 2025
https://doi.org/10.1016/j.bbcan.2025.189460
Abstract: Neutrophils play a multifaceted and dynamically evolving role in the progression of inflammation-driven colorectal cancer (CRC). This review summarizes the functional reprogramming and phenotypic polarization of neutrophils under chronic inflammatory conditions, with a particular focus on their contribution to tumor immune microenvironment remodeling. Specifically, we highlight the role of neutrophil extracellular traps (NETs), released through NETosis, in establishing immunosuppressive networks and reshaping the pro-metastatic stromal niche. The review further discusses the reciprocal interactions between neutrophils and the tumor microenvironment, as well as the impact of metabolic reprogramming and gut microbiota crosstalk on inflammation-to-cancer transition. By systematically outlining the mechanisms through which neutrophils influence inflammation-associated CRC, this review aims to provide conceptual insights and a framework for future research and therapeutic intervention strategies.

25COASNOV106
Title: Rewiring amino acids in cancer
Yiqing Zhang, Jianxin Lyu, Hezhi Fang
(BBA) - Reviews on Cancer, Volume 1880, Issue 6, November 2025
https://doi.org/10.1016/j.bbcan.2025.189465
Abstract: Cancer cells often survive in harsh microenvironments. To sustain rapid growth and proliferation, they reprogram metabolic pathways through multiple mechanisms to meet the demands of biosynthesis and energy production. Both essential and non-essential amino acids support cancer cell synthesis of macromolecules such as proteins and nucleotides. They also participate in diverse biological processes, including oxidative stress defense, epigenetic regulation, and signaling pathway modulation. In this review, we summarize the role of amino acid metabolism in cancer initiation and progression, and highlight recent advances in therapies targeting amino acid metabolism. The aim of this review is to stimulate both basic research and translational studies on cancer therapy through targeting amino acid metabolism.

25COASNOV107
Title: The role of fatty acid oxidation in metabolic crosstalk between tumor cells and associated factors in the microenvironment
Suman Pakhira, Subhadip Kundu, Sib Sankar Roy
(BBA) - Reviews on Cancer, Volume 1880, Issue 6, November 2025
https://doi.org/10.1016/j.bbcan.2025.189447
Abstract: Metabolic reprogramming is a defining characteristic of cancer cells as they undergo multistage development. Cancer cells dynamically adjust their metabolism to aid their survival and to retain their malignant traits within the adverse tumour microenvironment (TME). Fatty acid oxidation (FAO) is a major source of cellular bioenergy, making it a key player in driving cancer cell growth. Over the past few years, an accumulating body of literature has shed light on the role of dysregulated FAO in cancer progression. Besides energy production, FAO also plays a protective role by mitigating lipotoxicity-induced cell death and preventing oxidative stress through NADPH production. Moreover, FAO is

intricately linked with numerous critical signaling pathways, substantiating its importance as a pivotal metabolic adaptation in cancer cells. In the TME, various intrinsic and extrinsic factors continuously modulate the behaviour of cancer cells, including their metabolic attributes, such as the activation of FAO. Additionally, alterations in FAO within non-cancerous stromal cells also play a critical role in orchestrating the tumor progression. Despite the emerging recognition of FAO's significance in cancer biology, the precise molecular mechanisms underlying its dysregulation within the TME remain poorly understood. Given the pivotal role of FAO in bioenergetically priming the tumor progression, its aberrant regulation has become a focal point of cancer research, offering potential avenues for novel therapeutic strategies. This review provides an overview of recent advances in understanding how different microenvironmental factors modulate FAO to influence tumor progression.

25COASNOV108

Title: The mechanical landscape of cancer: Exploring mechanical characteristics-based therapeutic approaches

Hongdan Chen, Yinde Huang, Supeng Yin

(BBA) - Reviews on Cancer, Volume 1880, Issue 6, November 2025

https://doi.org/10.1016/j.bbcan.2025.189463

Abstract: Tumor mechanical alterations have emerged as a critical but underexplored marker of cancer. Cells within the tumor microenvironment (TME) are constantly exposed to matrix remodeling, aberrant shear stress, cytoskeletal tension, and tumor thrombi, all of which modulate tumor progression, therapy resistance, and stromal remodeling. This review summarizes recent advances in understanding how mechanical cues regulate tumor behavior through mechanotransduction pathways, and evaluates therapeutic strategies targeting extracellular matrix (ECM) stiffness, cytoskeletal contractility, ion channels, and physical interventions. While these approaches demonstrate translational promise, most studies remain descriptive, and major challenges, including off-target effects, limited drug penetration, and biomarker validation, continue to impede clinical application. We highlight the emerging concept of “tumor mechanomics”, which integrates biomechanical fingerprints with molecular and clinical data, offering a framework for developing predictive biomarkers and guiding precision oncology.

25COASNOV109

Title: Steroidal derivatives in pancreatic cancer: Paving the way to new anticancer drugs

Ana R. Gomes, Elisiário J. Tavares-da-Silva, Fernanda M.F. Roleira et.al.

(BBA) - Reviews on Cancer, Volume 1880, Issue 6, November 2025

https://doi.org/10.1016/j.bbcan.2025.189468

Abstract: Pancreatic cancer remains one of the most life-threatening cancers worldwide with limited therapeutic options and a poor prognosis. Despite the advances in treatment regimens, the death rate of pancreatic cancer patients continues to rise, justifying the need for novel therapeutic agents. Steroidal derivatives, with their unique modifiable framework, have emerged as a promising class of compounds in drug discovery, namely for the search for novel anticancer drugs. A comprehensive review of studies on the anticancer activity of

synthetic and natural steroidal derivatives for potential pancreatic cancer treatment was conducted, highlighting their structural versatility, mechanisms of action, and recent advances in their development. For this, an extensive literature search was conducted in two main databases – PubMed and Web of Science. In the preclinical setting, the steroidal derivatives described throughout this review display their cytotoxicity by different mechanisms, which culminate in cell death mostly by apoptosis. Remarkably, many of the pathways affected by this class of compounds are considered key players in many of the hallmarks of cancer, which reinforces the importance of studying steroidal derivatives for the treatment of pancreatic cancer.
This review summarises the current state of research and underscores the potential of steroidal derivatives as a groundwork for novel therapeutic approaches in pancreatic cancer management, outlining future directions for their development as effective anticancer agents.

25COASNOV110

Title: E-cadherin: A potential biomarker in cancer and a therapeutic target

Puja Kumari, Sagarika Dash, Dibyendu Samanta

(BBA) - Reviews on Cancer, Volume 1880, Issue 6, November 2025
https://doi.org/10.1016/j.bbcan.2025.189466

Abstract: Tumorigenesis is a complex, multifaceted process that deregulates normal cellular functions, including cell growth, proliferation, and apoptosis. The primary factors driving tumorigenesis include the activation of oncogenes, inhibition of tumor suppressor genes, and the disruption of cell-cell contact. E-cadherin, a critical component of adherens junctions, plays an integral role in cell adhesion, maintaining tissue integrity, and contributing to developmental processes. E-cadherin facilitates the regulation of proliferation through contact inhibition under physiological conditions, acting as a tumor suppressor, and the alterations in E-cadherin expression are a major driving force in the development of various cancers. However, ongoing research has revealed the significance of E-cadherin in cancer progression, emphasizing its functional duality in tumorigenesis. This review summarizes E-cadherin's diverse and complex functions in various cancers, the underlying molecular mechanisms, and its role as a potential cancer biomarker across different cancer types. Further, we highlight numerous therapeutic strategies designed to target E-cadherin expression to treat various cancers.

25COASNOV111

Title: STAT3 axis in cancer and cancer stem cells: From oncogenesis to targeted therapies

Deepika Godugu, Rameswari Chilamakuri, Saurabh Agarwal

(BBA) - Reviews on Cancer, Volume 1880, Issue 6, November 2025
https://doi.org/10.1016/j.bbcan.2025.189461

Abstract: The signal transducer and activator of transcription 3 (STAT3) is a cytoplasmic transcription factor that is essential in regulating cellular homeostasis. Aberrant and persistent activation of STAT3 triggers the oncogenic progression of multiple cancers. STAT3 can be activated by both canonical and non-canonical pathways, leading to its nuclear translocation and regulation of the transcription of multiple target genes to promote tumor cell proliferation, drug resistance, differentiation, inflammation, immune evasion, and

angiogenesis. Persistent activation of STAT3 correlates with the poor prognosis of cancer patients. Notably, STAT3 plays a crucial role in the maintenance of cancer stem cells (CSCs), contributing to disease relapse, metastasis, and poor clinical outcomes. Given its multifaceted role in tumor biology, STAT3 is an attractive target for therapeutic intervention. Various small molecules, peptides, and natural compounds targeting STAT3 are currently under different stages of preclinical and clinical evaluation. Despite promising advances, challenges such as drug resistance, selectivity, and toxicity remain obstacles in the development of effective STAT3-targeted therapies. This review provides a comprehensive overview of STAT3 structure, activation mechanisms, and its functional role in tumor biology and CSC maintenance. We also highlight current progress in STAT3-targeted therapeutic strategies, including agents in clinical trials, and discuss the future potential of STAT3 inhibition in precision oncology.

25COASNOV112

Title: The roles and perspectives of YY1 in immune central tolerance establishment

Gustavo Ulises Martínez-Ruiz, Ricardo Valle-Rios, Marco Velasco-Velazquez et.al.

(BBA) - Reviews on Cancer, Volume 1880, Issue 6, November 2025
https://doi.org/10.1016/j.bbcan.2025.189469

Abstract: Thymic epithelial cells (TEC) drive the proper differentiation of thymocytes for generating self-tolerant naïve T cells. TEC are functionally heterogeneous, as revealed by advancements in single-cell technologies, the development of new mouse models, and the examination of mouse, human, and zebrafish samples. While multiple cell-intrinsic regulators of TEC have been identified, many remain to be discovered. A comprehensive molecular characterization of each TEC subset and, ultimately, of all TECs, will help to develop strategies for their therapeutic modulation. Here, we review the potential role of the multifunctional transcription factor YY1 in thymus development and function, with a focus on TEC.

25COASNOV113

Title: The multifaceted roles of ISG15 in cancer: Conjugated and free forms

Xinran Liu, Qiujin Ma, Zhao Jia et.al.

(BBA) - Reviews on Cancer, Volume 1880, Issue 6, November 2025
https://doi.org/10.1016/j.bbcan.2025.189473

Abstract: Interferon-stimulated gene product 15 (ISG15) is a ubiquitin-like protein. It functions as a conjugated form by covalently modifying target proteins (ISGylation), or in a free form, both are involved in a broad variety of cellular processes. Increasing studies report the critical and complex roles of ISG15 in cancer progression and development. Herein, based on its conjugated or free form, we summarize ISG15-related oncogenic characteristics, such as cancer stemness, invasion and metastasis, anti-apoptosis and cancer drug resistance, and review ISG15-regulated oncogenic pathways, highlighting the molecular regulations of ISG15 in different cancers. This review aims to provide new insights into how ISG15 affects tumor pathogenesis, and propose potential cancer interventions targeting ISG15.

25COASNOV114

Title: The role of fatty acid oxidation in the tumor microenvironment: Implications for

cancer progression and therapeutic strategies
Nasot Rashed, Wenbin Liu, Xiangjian Luo
(BBA) - Reviews on Cancer, Volume 1880, Issue 6, November 2025
https://doi.org/10.1016/j.bbcan.2025.189474
Abstract: Fatty acid oxidation (FAO), or β-oxidation, is a catabolic process that breaks down fatty acids into acetyl-CoA. FAO plays a pivotal role in the metabolic reprogramming of cancer cells and the tumor microenvironment (TME), serving as a crucial energy source that sustains cellular functions under conditions of nutrient deprivation and metabolic stress. This process significantly influences cancer cell survival, proliferation, metastasis, and therapeutic resistance. In this review, we discuss the biological functions of FAO in cancer cells, immune cells, and stromal cells, with a particular focus on its regulatory role in tumor progression and therapy resistance. Furthermore, we explore FAO inhibitors and emerging therapeutic strategies targeting FAO as a potential approach to disrupting tumor metabolism and enhancing cancer treatment efficacy.

25COASNOV115
Title: Advancing oncology drug development: Innovative approaches to enhance success rates while reducing animal testing
Hans Hendriks
(BBA) - Reviews on Cancer, Volume 1880, Issue 6, November 2025
https://doi.org/10.1016/j.bbcan.2025.189467
Abstract: Drug development remains a high-risk endeavour, particularly in oncology, where failure rates exceed 90 %. This review examines emerging tools and strategies designed to enhance preclinical success rates, aligning with the 3Rs principle: Reduction, Refinement, and Replacement of animal testing.Traditional 2D in vitro screening remains fundamental in early anticancer drug development due to its cost-effectiveness and reproducibility. However, 3D in vitro culture systems, including patient-derived organoids, better recapitulate tumour structure, providing more accurate predictions of clinical response. Additionally, Organ-on-a-chip platforms further enhance physiological relevance and complement conventional animal toxicology models. Despite their promise, these technologies facechallenges in standardisation, validation, and regulatory acceptance.Artificial intelligence is also emerging as a transformative tool in oncology drug discovery and development. However, its widespread adoption is currently constrained by limited access to high-quality datasets, concerns around data security, privacy, and underdeveloped computational infrastructure.For in vivo studies, patient-derived xenograft (PDX) models remain the gold standard, offering robust and translationally relevant platforms for efficacy testing. Hybrid models, such as PDX-derived organoids and PDX-derived cell cultures, provide complementary systems that integrate in vitro and in vivo insights.While these innovations offer long-term potential to reduce animal use, more innovative experimental designs and methods, such as the Single Mouse Trial and the Hollow Fibre Assay, may reduce animal numbers in the short term without compromising data quality.Together, these advances contribute to a more ethical, efficient, and predictive framework for the development of preclinical anticancer drugs.

25COASNOV116
Title: Decoding the role of zinc finger proteins in urological malignancies

Lei Yang, Ying Gan, Yu Fan et.al.
(BBA) - Reviews on Cancer, Volume 1880, Issue 6, November 2025
https://doi.org/10.1016/j.bbcan.2025.189470
Abstract: Zinc finger proteins (ZNFs), among the most expansive families of transcription factors in eukaryotes, are distinguished by their distinctive zinc-coordinated motifs, which facilitate intricate interactions with DNA, RNA, and other proteins. These multifaceted interactions are central to their roles in regulating gene expression and modulating key signaling pathways, thus governing a spectrum of cellular processes such as differentiation, proliferation, and apoptosis. Recent studies have elucidated the crucial involvement of ZNFs in the pathogenesis of urological malignancies, including kidney, bladder, and prostate cancers. The inherent complexity and heterogeneity of these cancers necessitate an in-depth exploration of the molecular mechanisms underpinning tumor progression, with ZNFs emerging as central regulators in both oncogenic and tumor-suppressive capacities. This review provides a comprehensive examination of the diverse roles of ZNFs in urological cancers, highlighting their mechanistic actions, interactions with pivotal signaling networks, and contributions to the tumorigenic landscape. Furthermore, it delves into the translational potential of ZNFs, contemplating their utility as diagnostic biomarkers, prognostic tools, and promising therapeutic targets in clinical oncology.

25COASNOV117

Title: Mitochondrial dynamics and metabolic attributes regulate function of natural killer cell and infiltration in tumor microenvironment modulating disease progression

Sayak Ghosh,Rittick Dutta, Devyani Goswami et.al.
(BBA) - Reviews on Cancer, Volume 1880, Issue 6, November 2025
https://doi.org/10.1016/j.bbcan.2025.189471
Abstract: Mitochondria in natural killer (NK) cells orchestrate a dynamic interplay between energy production and immune regulation, placing them at the forefront of oncogenesis and tumor microenvironment (TME) infiltration. This review unravels the intricate disruptions in mitochondrial dynamics—fission, fusion, and biogenesis—that hypoxia imposes within the TME, culminating in impaired NK cell functionality. Hypoxia-driven mitochondrial fragmentation, mediated by HIF-1α and mTOR-Drp1 signaling, cripples NK cell cytotoxicity, proliferation, and maturation, while elevated ROS levels and metabolic reprogramming bolster tumor immune evasion. The metabolic landscape of the TME adds another layer of complexity, with amino acid depletion significantly hindering NK cell performance. Arginine and leucine deficiencies suppress proliferation and mTOR activation, whereas disrupted glutamine metabolism impairs cMyc-driven metabolic adaptation. Additionally, immunosuppressive catabolites like nitric oxide and L-kynurenine exacerbate NK cell dysfunction by curbing cytokine production and receptor expression. Targeting these metabolic vulnerabilities offers a promising strategy; specifically, interventions aimed at amino acid pathways could simultaneously restrict nutrient availability within the tumor microenvironment and preserve NK cell functionalities. Emerging strategies spotlight the potential of NK cells to induce autophagic death in hypoxic cancer cells, a mechanism that could restore their cytotoxic potential. Furthermore, immune checkpoint pathways, such as PD-1 and CTLA-4, amplify mitochondrial dysfunction, underscoring their therapeutic significance. By addressing hypoxia, metabolic dysregulation, and mitochondrial

reprogramming, this review illuminates actionable strategies to reinvigorate NK cell-mediated antitumor responses and pave the way for transformative cancer therapies.

25COASNOV118

Title: Detection methods for mitochondrial DNA heteroplasmy and their potential single-cell applications in cancer

Tianguang Cheng, Min Pan, Yi Qiao et.al.

(BBA) - Reviews on Cancer, Volume 1880, Issue 6, November 2025
https://doi.org/10.1016/j.bbcan.2025.189472

Abstract: Mitochondrial DNA (mtDNA) is crucial for cellular metabolism, oxidative stress responses, and genomic stability, with mutations linked to cancer progression and therapeutic resistance. Mitochondrial heteroplasmy, the coexistence of wild-type and mutant mtDNA within a cell or across populations, plays a key role in mitochondrial dysfunction, tumor heterogeneity, and disease pathogenesis. Advances in single-cell technologies like quantitative PCR (qPCR), digital droplet PCR (ddPCR), next-generation sequencing (NGS), and long-read sequencing (TGS) have enabled precise mapping of heteroplasmic variants, providing insights into their role in cancer. This review evaluates current detection methods, discussing their strengths, limitations, and relevance to cancer research. We also explore the biological implications of heteroplasmy in cellular dynamics, nuclear mitochondrial DNA segments (NUMTs), and cancer pathogenesis, highlighting emerging technologies and future directions for studying mtDNA mutations at single-cell resolution in cancer. Ultimately, this review provides a critical synthesis of how single-cell mtDNA heteroplasmy analysis is reshaping our understanding of tumorigenesis and identifies key methodological and challenges that must be addressed to realize its full potential in precision oncology.

25COASNOV119

Title: Unstructured but critical: The role of YY1 and YY2 disorder in promoter recognition networks, transcriptional control, and oncogenesis

Małgorzata Figiel, Katarzyna Pustelny, Marta Dziedzicka-Wasylewska et.al.

(BBA) - Reviews on Cancer, Volume 1880, Issue 6, November 2025
https://doi.org/10.1016/j.bbcan.2025.189475

Abstract: The transcription factors Yin Yang 1 and Yin Yang 2 are key regulators of gene expression and play complex roles in cancer development. Although closely related in sequence and structure, YY1 and YY2 differ in their degree of intrinsic disorder, interaction profiles, and regulatory potential. Both proteins are subject to cancer-associated alterations, including changes in expression levels and somatic mutations, many of which correlate with clinical outcomes.This review synthesizes a comparative analysis of YY1 and YY2, with a focus on their disordered regions, interaction networks, and promoter targeting mechanisms. YY1 exhibits a higher degree of intrinsic disorder and a greater number of predicted Molecular Recognition Features (MoRFs), enabling a broader and more competitive range of interactions. YY2, in contrast, is more structurally ordered and engages a more limited set of partners. While both proteins recognize specific and highly similar DNA motifs, their binding is relatively weak, and functional specificity is conferred primarily through distinct protein–protein interactions and regulatory complex assembly.We integrate these findings within the framework of Brodsky's model of promoter recognition, which emphasizes the role of

dynamic, cooperative interactions in guiding transcription factor specificity. By mapping cancer-associated mutations and post-translational modifications onto functional regions, we highlight how such alterations may disrupt interaction networks and promoter selection. Finally, we explore the therapeutic potential of selectively targeting YY1/YY2 interactions, despite the challenges posed by their intrinsically disordered domains.

25COASNOV120

Title: Role of macrophage PKM2 in inflammation and tumor progression and its targeted therapy

Yafei Li, Lingao Zhu, Lu Liu et.al.

(BBA) - Reviews on Cancer, Volume 1880, Issue 6, November 2025

https://doi.org/10.1016/j.bbcan.2025.189478

Abstract: Macrophages play a dual role of promoting or inhibiting in inflammation and tumor progression, highly dependent on the dynamic changes of M1/M2 polarization. In inflammation, M1/M2 polarization balance determines the outbreak of inflammation or tissue repair. In the tumor microenvironment, M1 tumor-associated macrophages (TAMs) exert both anti-tumor and pro-tumor effects, while M2 TAMs promote tumor progression. PKM2 regulates the M1/M2 polarization and cytokine secretion of macrophages through the pyruvate kinase activity of tetramers as well as the protein kinase activity and transcriptional co-activator function of dimers. This review summarizes the role and molecular mechanism of macrophage PKM2 in inflammation and tumor progression, highlighting its potential as a therapeutic target in inflammatory diseases and cancers. Macrophage PKM2 plays a promoting role in inflammation and tumor progression due to its dual regulatory characteristics of metabolism and immunity. It can not only meet the energy demands of macrophages through glycolytic metabolism, but also affect the immune response through enzyme activity-dependent and non-dependent mechanisms. The non-enzyme activity-dependent mechanism by which PKM2 regulates immune responses serves as a bridge connecting cellular metabolism and immune responses. The unresolved issues include the functional heterogeneity of macrophage PKM2 across different macrophage subtypes, its specific roles in lipid and amino acid metabolism, its contribution to tumor microenvironmental metabolic reprogramming, and PKM2-mediated interactions of macrophages with other cells.

25COASNOV121

Title: Dissecting the dual roles of lysosomal membrane proteins: Mediators of autophagy–apoptosis crosstalk in tumor progression

Jiahao Xu, Yujie Jin, Shiqiang Liu et.al.

(BBA) - Reviews on Cancer, Volume 1880, Issue 6, November 2025

https://doi.org/10.1016/j.bbcan.2025.189477

Abstract: Tumor progression is closely related to the complex interactive regulation between autophagy and apoptosis signaling pathways, particularly the molecular mechanisms mediated by lysosomal membrane proteins (LMPs), and their dynamic regulatory processes have become an important direction of current research. However, there is a lack of in-depth and systematic reviews on this topic. This review focuses on the multi-dimensional mechanisms by which LMPs mediate the regulation of the autophagy–apoptosis crosstalk via

key molecules like Beclin1, Autophagy-related (ATG), Caspase, PARP, and Bax/Bcl-2 in tumor progression. In addition, it highlights their roles in signaling pathways, drug-mediated cell cycle and combination therapy mechanisms, autophagic and apoptotic crosstalk underlying synergistic and antagonistic effects, and other key biological processes. Overall, as the core hub of the autophagy–apoptosis crosstalk network, the multifactorial synergistic effect mediated by LMPs is crucial in tumor progression. In-depth analysis of this mechanism not only elucidates the molecular pathological basis of tumorigenesis but also provides a theoretical basis for the development of novel anti-tumor intervention strategies targeting LMPs.

25COASNOV122

Title: Research progress on gut microbiota in colorectal cancer immunotherapy

Jing Li, Yingkun Yue, Jiaxin Pan et.al.

(BBA) - Reviews on Cancer, Volume 1880, Issue 6, November 2025
https://doi.org/10.1016/j.bbcan.2025.189476

Abstract: Immune checkpoint inhibitors (ICIs) have demonstrated significant clinical benefits in treating various malignancies. However, their therapeutic efficacy exhibits considerable interindividual variability in patients with colorectal cancer (CRC). In recent years, growing attention has been focused on the regulatory role of the gut microbiota and its metabolic microenvironment in modulating ICIs responses. This article systematically reviews key advances in understanding how the gut microbiota and its metabolites influence ICIs efficacy. For example: Specific bacterial species (e.g., Lactobacillus paracasei and Fusobacterium nucleatum) may regulate ICIs efficacy by modulating antigen presentation or the tumor immune microenvironment. Microbial metabolites, such as short-chain fatty acids (SCFAs), can enhance immune function and thereby improve ICIs outcomes. Potential microbiome-targeted interventions—including probiotic/prebiotic combinations, optimized antibiotic administration timing, refined fecal microbiota transplantation (FMT) protocols, and engineered synthetic biology-based bacterial therapies—are also discussed. By synthesizing current evidence, this review provides a theoretical foundation for developing novel personalized immunotherapy strategies for CRC, with a focus on microbiome modulation to optimize ICIs treatment efficacy.

25COASNOV123

Title: Revisiting CHK1 and WEE1 kinases as therapeutic targets in cancer

Nehal Arvind Kumar, P. Manasa, Jaikanth Chandrasekaran

(BBA) - Reviews on Cancer, Volume 1880, Issue 6, November 2025
https://doi.org/10.1016/j.bbcan.2025.189482

Abstract: Uncontrolled cell division is a defining characteristic of cancer, driven by genomic instability. This instability disrupts the DNA damage response network, exacerbates replication stress, and impairs cell cycle checkpoints. Although conventional DNA-damaging therapies like chemotherapy and radiotherapy exploit this vulnerability, they often cause substantial damage to healthy tissues, leading to adverse effects that may inadvertently promote tumour resilience. Targeted DDR inhibition, exemplified by Poly [ADP-ribose] polymerase inhibitors, has achieved major clinical success, functioning through a synthetic lethality approach in tumours with a defective homologous recombination repair pathway.

Extending this strategy to the ATR-CHK1-WEE1 axis, a central responder to replication stress and regulator of intra-S and G2/M checkpoints, offers a promising therapeutic window, particularly in cancers with G1/S checkpoint defects. However, realising this potential requires a deeper understanding of tumour-specific DNA damage response defects, identification of robust biomarkers, and improved patient stratification needs. Currently, the clinical development of CHK1 and WEE1 inhibitors demonstrates their potential, especially in combination with standard-of-care therapies, where they capitalise on elevated replication stress to induce selective tumour cell death. This review outlines recent advances, challenges, and future directions in targeting CHK1 and WEE1 kinases, highlighting their potential to advance precision oncology in the future.

25COASNOV124

Title: Snake venom-derived peptides as anticancer candidates: Pioneering next-generation therapies

José R. Almeida, Edgar A. Pinos-Tamayo, Bruno Mendes et.al.

(BBA) - Reviews on Cancer, Volume 1880, Issue 6, November 2025
https://doi.org/10.1016/j.bbcan.2025.189479

Abstract: Cancer treatment has come a long way, but not all cancers can be completely cured. The current therapeutic landscape has significantly reduced mortality rates; however, it remains associated with side effects, limited accessibility, financial burden, drug shortages, and emotional as well as mental health consequences for patients. Hence, despite significant advances, the development of novel therapies remains a focal point of research. In this review, we explore the current state of snake venom-inspired peptides as templates for the design of much-needed innovative anticancer agents. Initially, we examine conventional cancer treatments, their main challenges, and the niche filled by newly approved peptide-based therapies. Then, we present a high-level overview of the potential of snake venoms as broad-spectrum libraries of bioactive components and discuss a roadmap for mining these rich and complex mixtures to pioneer the next generation of cancer drugs, leading to the emergence of “oncovenomics”. Harnessing the potential of modern in silico approaches, we delve into the structure, biochemical parameters, and bioactivity of venom-inspired peptides. Our research identified more than 30 snake venom-derived peptides with micromolar lytic action against different cancer cells, including solid and liquid tumours. Transitioning from in vitro monolayer analyses to clinical settings remains an unfulfilled goal, with the majority of studies failing to progress to more advanced stages, including the preclinical phase involving in vivo experiments. Here, we also describe how artificial intelligence, and the integration of other cutting-edge technologies can provide an expandable framework for translating the high in vitro potential of venom-derived peptides into clinically useful therapies. Lastly, we examined the translational challenges and the strategies proposed to overcome them. In summary, snake venom-derived peptides are attractive scaffolds for drug discovery programs, demonstrating historical benefits. However, overcoming the existing barriers in their development requires further multidisciplinary efforts. On the horizon, advances in high-throughput research tools and peptide engineering strategies offer opportunities for introducing next-generation venom peptide-based therapeutics to address cancer in clinical practice.

25COASNOV125

Title: RKIP and tumor immune evasion: Remodeling the immunosuppressive tumor microenvironment

Evagelia Skouradaki, Giasemi C. Eptaminitaki, Evagelia Kirio et.al.

(BBA) - Reviews on Cancer, Volume 1880, Issue 6, November 2025
https://doi.org/10.1016/j.bbcan.2025.189481

Abstract: Raf-1 Kinase Inhibitor Protein (RKIP) is a well-known metastasis suppressor that regulates key oncogenic signaling pathways. Emerging evidence also points to a dual role for RKIP as an immunomodulatory molecule, influencing the tumor immune microenvironment, a complex niche that promotes immune evasion and overall tumor progression. This review explores RKIP's impact on immune surveillance via its interactions with signaling pathways and cellular components of the tumor microenvironment, as well as its role in recruiting and polarizing immune cells with different dynamics in reshaping an immunocompetent milieu. We further discuss how RKIP downregulation promotes immune evasion, alters cytokine profiles, and reduces effector immune cell infiltration. Current studies suggest that RKIP supports type I interferon signaling and antigen presentation, while its loss contributes to an immunosuppressive, pro-metastatic environment. Therefore, by regulating the expression of RKIP in the pathways that control TME architecture, the TME can be reprogramed towards an immunoprotected milieu. Altogether, this review underscores RKIP's role in tumor immunity, offering new perspectives for therapeutic strategies aimed at overcoming cancer immune evasion and improving immunotherapy efficacy.

25COASNOV126

Title: Targeting sex hormone signaling: A promising therapeutic alternative for glioblastoma

Juan Carlos Quintero, Omar Rafael Alemán, Ignacio Camacho-Arroyo

(BBA) - Reviews on Cancer, Volume 1880, Issue 6, November 2025
https://doi.org/10.1016/j.bbcan.2025.189486

Abstract: Glioblastoma is the most common and malignant primary brain tumor of the central nervous system, with conventional therapy yielding very poor results in overall patient survival and quality of life. The low life expectancy at diagnosis of just 15 months, highlights the need for novel therapeutic alternatives. Glioblastoma has a higher incidence in men than in women, suggesting a critical role of sex hormone signaling in tumor maintenance and progression. There is now ample evidence that sex hormones impact glioblastoma malignancy. Testosterone, through the androgen receptor, promotes proliferation, migration, and invasion of tumor cells. Interestingly, estradiol and progesterone show both pro- and anti-tumor effects, depending on the dose and the specific receptors expressed in the cells. Sex hormones regulate gene activity by binding to intracellular receptors, which act as ligand-activated transcription factors. Additionally, the presence of membrane receptors for estrogens and progesterone can promote rapid cellular responses, activating signaling pathways such as PI3K/AKT and MAPK in tumor cells. Thus, the regulation of sex hormone activity and receptor function can directly affect tumor progression and survival. This article analyzes the impact of sex hormone signaling on the malignancy of glioblastomas.

25COASNOV127

Title: Employing bacteriophages to combat cancer

Alicja Węgrzyn, Sylwia Bloch, Grzegorz Węgrzyn

(BBA) - Reviews on Cancer, Volume 1880, Issue 6, November 2025
https://doi.org/10.1016/j.bbcan.2025.189485

Abstract: Bacteriophages are viruses infecting bacterial cells; therefore, their application in cancer research may initially appear counterintuitive. Nevertheless, bacteriophages have been employed in the development of numerous advanced biotechnological tools, which has led to the emergence of multiple approaches utilizing them for improved cancer diagnostics and novel therapeutic strategies. Unlike other recently published reviews in this field, this paper does not emphasize technological principles or focus on specific cancer type. Instead, we provide a broad overview of innovative concepts and highlight recent advances in the use of bacteriophages in anti-cancer research. In particular, we discuss their roles in: (i) early cancer diagnosis and detection of tumorigenic mutations, (ii) elimination of bacteria that promote carcinogenesis and modulation of the microbiome influencing tumor growth, (iii) development of anti-cancer vaccines, (iv) modulation of cancer-related immune responses, (v) targeted delivery of anti-cancer drugs, and (vi) genetic modification of cancer cells through therapeutic DNA delivery.

25COASNOV128

Title: Immune archetypes TIME classification system for nasopharyngeal carcinoma: A new direction for precision immunotherapy

Fei Lu, Xueqi Bai, Zihan Lv et.al.

(BBA) - Reviews on Cancer, Volume 1880, Issue 6, November 2025
https://doi.org/10.1016/j.bbcan.2025.189487

Abstract: In the complex tumor immune microenvironment (TIME), tumor cells are typically surrounded by host immune components that can either suppress or promote tumor progression. The stromal compartment usually responds to tumor cells through inflammatory processes, often reflecting a single immune state or class. This pattern is also observed in the tumor microenvironment (TME) of nasopharyngeal carcinoma (NPC). However, recent advances in single-cell profiling have revealed that multiple distinct immune states can coexist around NPC tissues. In this review, we delineate and classify the immune “archetypes” of TMEs in NPC—defined as cellular assemblages and gene expression profiles that are characteristic and recurrent at the bulk tumor level. We further summarize studies suggesting that NPC TMEs can be broadly categorized into 11 major immune archetypes. Considering their potential evolutionary origins and functional roles, these archetypes appear to be associated with specific vulnerabilities within the TME, which may be exploited as therapeutic targets. Such insights may provide novel strategies for NPC treatment, thereby enhancing patient outcomes and improving prognosis.

25COASNOV129

Title: Advances in tumor micro-environment and immunotherapy of squamous cell carcinoma of the tongue

Shaopeng Chang , Longhui Li , Yumiao Liu et.al.

(BBA) - Reviews on Cancer, Volume 1880, Issue 6, November 2025

https://doi.org/10.1016/j.bbcan.2025.189483
Abstract: Tongue squamous cell carcinoma (TSCC), the most prevalent oral malignancy, demonstrates rising global incidence and mortality rates, while current therapies exhibit limited efficacy in advanced-stage disease. The tumor microenvironment (TME) constitutes an intricate ecosystem of immune cells, fibroblasts, and extracellular matrix (ECM), which collectively regulate TSCC progression, immune evasion, and therapeutic resistance. Tumor immunotherapies targeting TME have been increasingly validated in clinical trials, and despite the ability to capture relevant immune features in TME, challenges such as low individual response rates and immunotherapy resistance still exist in the clinic. In this review, we address the mechanisms of TSCC-associated immune cells as well as extracellular-related components in TME, summarize the effects of each component of TME on tumor immune response, and look forward to the application of tumor immunotherapy and immune-combination therapies to improve the efficacy of individualized precision medicine for TSCC.

25COASNOV130

Title: Nanoparticulate delivery and targeting of RNA to the brain

Aditya Gupta, Raghu Ramanathan, Chittalsinh M. Raulji et.al.

(BBA) - Reviews on Cancer, Volume 1880, Issue 6, November 2025
https://doi.org/10.1016/j.bbcan.2025.189480

Abstract: The blood-brain barrier (BBB) presents a critical challenge in treating central nervous system (CNS) disorders, particularly aggressive brain cancers such as glioblastoma (GBM) and medulloblastoma (MB). RNA therapies exploit endogenous cellular machinery to modulate gene expression, targeting previously undruggable pathways. RNA and CRISPR gene therapies hold transformative potential for brain cancer but demand breakthroughs for enhanced drug transport across the BBB. While clinical achievements in non-CNS diseases validate their efficacy, interdisciplinary collaboration is essential to advance nanoparticles (NPs) engineering, immune evasion, and non-invasive delivery for CNS applications. NPs are indispensable for advancing RNA therapies in brain cancer, with lipid nanoparticles (LNPs) and viral vectors leading clinical translation. Innovations in targeting (e.g., GLUT1, RVG peptide, ApoE mimetic peptide) and non-invasive delivery (e.g., focused ultrasound) are critical to overcome the BBB limitations. This review highlights the different strategies that can be utilized to deliver RNA-based therapies to the brain and summarizes the recent clinical efforts to deliver the RNA.

25COASNOV131

Title: M6A methylation in tumor immune microenvironment: Multidimensional mechanism and targeted therapy strategies

Senxu Lu, Junxiu Liu, Shixin Chen et.al.

(BBA) - Reviews on Cancer, Volume 1880, Issue 6, November 2025
https://doi.org/10.1016/j.bbcan.2025.189489

Abstract: N6-methyladenosine (m6A) modification, a dynamic and reversible post-transcriptional RNA alteration, plays a critical role in the precise regulation of gene expression and is fundamentally implicated in the interplay between tumor cells and the immune system. This review focuses on the regulatory mechanisms of m6A methylation in

tumor immunology. We examine how m6A modifications within tumor cells reprogram the tumor immune microenvironment by modulating immune checkpoints, canonical signaling pathways, and cytokine secretion, as well as directly regulating immune-related genes. Crucially, we also dissect how m6A modification within immune cells shapes the immune microenvironment. Furthermore, we propose novel therapeutic strategies combining m6A targeting with immunotherapy. Collectively, this review provides novel insights into the role of m6A methylation in tumor immunology and paves the way for future research directions.

25COASNOV132

Title: Hyperthermia-induced apoptosis: The role of magnetic nanoparticles in targeted delivery for breast cancer treatment

Pankaj Garg, Madhu Krishna, David Horne et.al.

(BBA) - Reviews on Cancer, Volume 1880, Issue 6, November 2025
https://doi.org/10.1016/j.bbcan.2025.189490

Abstract: Magnetochemistry is opening new frontiers in the targeted treatment of breast cancer (BC), offering a precise and innovative way to deliver therapies exactly where they're needed. Beyond drug delivery, magnetic nanoparticles (MNPs) can generate localized heat under alternating magnetic fields, initiating controlled hyperthermia that induces apoptotic cell death in tumor tissues. MNPs, particularly iron-oxide-based magnetite (Fe_3O_4) and maghemite (γ-Fe_2O_3), can be magnetically guided toward tumor sites and subsequently activated under alternating magnetic field (AMFs) (typically 100–500 kHz and 10–40 kA m−1) to generate therapeutic heat through Néel and Brownian relaxation losses. At the tumor, drugs can be released in a controlled manner in response to environmental cues such as pH changes, enzymes, or magnetic stimuli. By harnessing this dual role of MNPs, as targeted carriers and thermal effectors, researchers achieve spatially selective, minimally invasive treatment. Mechanistically, magnetically induced hyperthermia elevates local temperature to 42–46 °C, which triggers reactive oxygen species (ROS) generation, mitochondrial membrane depolarization, and caspase-3/9 activation—hallmarks of apoptosis in BC cells. This integrated approach not only concentrates drugs at the tumor but also sensitizes cancer cells to chemo- and radiotherapy, while minimizing systemic toxicity. Static or dynamic magnetic fields can be used to steer these particles, while their surfaces can be engineered through chemical bonding, physical encapsulation, or adsorption techniques. Moreover, combining magnetic targeting with antibody-based recognition improves specificity and therapeutic impact. While the promise of magnetochemistry in BC treatment is clear, ongoing research is essential to optimize these technologies and bring them fully into clinical practice.

25COASNOV133

Title: AI-powered vaccine breakthroughs: Targeting pancreatic cancer with neoantigens and combination therapies

Jiaxin Zhang, Lin Xiao, Yueshui Zhang et.al.

(BBA) - Reviews on Cancer, Volume 1880, Issue 6, November 2025
https://doi.org/10.1016/j.bbcan.2025.189484

Abstract: The five-year survival rate for Pancreatic Ductal Adenocarcinoma (PDAC) remains below 10 %, primarily due to the limited efficacy of conventional chemotherapy and immune checkpoint inhibitors against its triple-immune-sequestered, low-TMB tumor

microenvironment(TME). This situation has been furter exacerbated by the stagnation of traditional vaccine development, driven by inefficient antigen screening and high tumor heterogeneity.Artificial intelligence (AI) exhibits remarkable advantages in the design of pancreatic ductal adenocarcinoma (PDAC) vaccines. It can integrate multi – omics data to efficiently unearth cryptic neoantigens from low - tumor mutation burden (TMB) samples, significantly enhancing the screening efficiency. Through dynamic modeling, AI can rationally plan the timing of combined vaccine therapies, effectively reducing the degree of T - cell exhaustion. By leveraging the digital twin model, AI can remarkably improve the matching accuracy between antigens and human leukocyte antigen (HLA). Additionally, it can construct a monitoring system to provide early warnings of antigen loss risks, thus gaining adjustment time for clinical treatments.This review aims to accomplish three primary objectives: demonstrate AI's potential in breaking the therapeutic impasse to overcome manufacturing-related treatment delays for 25–30 % of patients; further delineates the logical progression of AI from concept to clinical application; thereby provides a translational framework to bridge the gap between research and patient benefit.

25COASNOV134

Title: The mitochondrial nexus: Targeting metabolic vulnerabilities, oxidative stress, and immunomodulation to induce cancer cell death

Woo Hyun Park

(BBA) - Reviews on Cancer, Volume 1880, Issue 6, November 2025
https://doi.org/10.1016/j.bbcan.2025.189491

Abstract: Mitochondria, far from being mere cellular powerhouses, act as central command hubs dictating cell fate by integrating metabolic cues with life-or-death decisions. In cancer, these organelles undergo profound functional and structural reprogramming to support relentless proliferation, survival, and adaptation to stress. This metabolic plasticity, however, creates unique vulnerabilities exploitable for therapeutic gain. This comprehensive review synthesizes recent insights into the multifaceted roles of mitochondria in cancer, focusing on how inhibiting their core functions can trigger diverse cell death pathways and modulate the tumor microenvironment. This paper delves into the central role of mitochondria in orchestrating various forms of regulated cell death (RCD), including apoptosis, ferroptosis, necroptosis, and the newly defined cuproptosis. A primary focus is placed on the dual nature of mitochondrial reactive oxygen species (ROS), which can promote tumorigenesis but can also be pharmacologically elevated to catastrophic levels, triggering oxidative stress-induced demise. This review systematically categorizes and discusses a burgeoning pharmacopeia of mitochondrial inhibitors—targeting the electron transport chain (ETC), metabolic enzymes like glutaminase, protein homeostasis, and ion channels—and analyzes their mechanisms of action, preclinical evidence, and clinical translation status. Furthermore, this paper examines how these agents can overcome chemoresistance and synergize with existing treatments, including the exciting interface with immunotherapy, where mitochondrial fitness is paramount for robust anti-tumor T-cell responses and the induction of immunogenic cell death (ICD). By dissecting the complex interplay between mitochondrial inhibition, metabolic disruption, oxidative stress, and cell death, this review highlights the immense promise of mitochondria-targeted therapies and charts the course for future innovations in oncology.

25COASNOV135

Title: Opposing roles of YY1 and RKIP in cancer progression and therapy resistance

Christos Rigopoulos, Stavroula Baritaki, Ilias Georgakopoulos-Soares

(BBA) - Reviews on Cancer, Volume 1880, Issue 6, November 2025
https://doi.org/10.1016/j.bbcan.2025.189488

Abstract: Yin Yang 1 (YY1) and Raf kinase inhibitory protein (RKIP, encoded by PEBP1) are multifunctional regulators with antagonistic roles in tumor biology. YY1 functions as a context-dependent transcription factor and chromatin organizer, integrating enhancer–promoter looping and super-enhancer activity to drive oncogenic transcriptional programs, immune evasion, and therapy resistance. By contrast, RKIP restrains the NF-κB, MAPK and STAT3 pathways, suppressing epithelial–mesenchymal transition, metastasis, and chemoresistance. Recent pan-cancer transcriptomic analyses highlight a recurrent pattern of YY1 upregulation and RKIP downregulation, with inverse correlations in several tumor types (e.g., lung, colorectal and kidney). Clinically, high YY1 expression is associated with poor survival and diminished responses to chemotherapy, TRAIL, and immune checkpoint blockade, whereas high RKIP predicts improved outcomes and restored therapeutic sensitivity. YY1 and RKIP also modulate key immune compartments: YY1 promotes Treg expansion, myeloid-derived suppressor cell (MDSC) accumulation, tumor-associated macrophage (TAM) polarization, and impaired antigen presentation, while RKIP counteracts these processes and enhances cytotoxic T and NK cell activity. Therapeutically, YY1 can be targeted through BET/p300 inhibitors, emerging PROTAC degraders, and RNA- or CRISPR-based approaches; RKIP restoration is under investigation via kinase and pathway modulators. Together, YY1 and RKIP constitute a regulatory axis with prognostic and predictive value, offering potential for biomarker-driven patient stratification and novel therapeutic strategies in precision oncology.

25COASNOV136

Title: Posttranslational modifications in Helicobacter pylori-associated gastric pathogenesis: Bridging inflammation and carcinogenesis

Wei Li, Tong Liu, Tianhua Wu et.al.

(BBA) - Reviews on Cancer, Volume 1880, Issue 6, November 2025
https://doi.org/10.1016/j.bbcan.2025.189492

Abstract: Helicobacter pylori (H. pylori), a Group I carcinogen that affects approximately half of the global population, is the primary aetiological agent of chronic gastritis, peptic ulcers, gastric adenocarcinoma, and gastric mucosa-associated lymphoid tissue lymphoma. Its pathogenesis involves intricate interactions among bacterial virulence factors, host genetics, and environmental factors. We detail the critical role of diverse protein posttranslational modifications (PTMs) in mediating H. pylori-induced gastric mucosal damage and carcinogenesis. We describe how H. pylori exploits and dysregulates a broad spectrum of host and bacterial PTMs (encompassing acetylation, ubiquitination, S-nitrosylation, disulfide bond formation, citrullination, methylation, glycosylation, phosphorylation, SUMOylation, and ADP-ribosylation) to establish infection, evade immune responses, drive chronic inflammation, and promote malignant transformation. Collectively, these findings reveal a complex, multilayered PTM network that is central to H. pylori pathogenesis. Understanding these mechanisms provides crucial insights for the development of novel diagnostic

biomarkers; methylation profiles; anti-citrullinate keratin 1 (Cit-K1) antibodies, maps of PTM dynamics; targeted therapeutic strategies, including PTM enzyme inhibitors, antivirulence agents such as H. pylori disulfide bond-forming protein A inhibitors, epigenetic modulators, glycoconjugate vaccines/adhesion blockers, and optimized drug delivery systems such as N-acetylcysteine liposomes. Furthermore, this knowledge supports improved risk stratification for managing persistent cancer risk even after eradication.

25COASNOV137

Title: Strong Electric Fields on Water Microdroplets Enable Near-Unity Selectivity in H2O2 Photosynthesis

Kejian Li, Wenbo You, Yucheng Zhu et.al.

J. Am. Chem. Soc. 2025, 147, 40, 2025

https://doi.org/10.1021/jacs.5c06077

Abstract: Selective conversion of solar energy to chemical bonds remains a grand challenge in artificial photosynthesis. Though H2O2 production via photocatalytic two-electron oxygen reduction (2e–-ORR) offers a sustainable alternative to the energy-intensive anthraquinone process, competing hydrogen evolution reaction (HER) severely limits both efficiency and selectivity. Here, we reveal that the strong electric fields on water microdroplet surfaces serve as powerful selectivity switches, directing photogenerated electrons exclusively toward H2O2 synthesis while completely suppressing hydrogen evolution. This interfacial electric field control mechanism transforms ZnIn2S4-based photocatalysts─commonly dominated by HER─into H2O2 producers with near-unity selectivity and production rates 2 orders of magnitude higher than bulk reactions. Through spatially resolved spectroscopy characterizations and theoretical calculations, we elucidate that the high electric fields on water microdroplets simultaneously enhance charge carrier separation, lower energy barriers for 2e–-ORR, and erect kinetic barriers against HER. Beyond providing an energy-efficient route to selective H2O2 photosynthesis, this study offers valuable insights into selectivity control in other solar-to-chemical transformations without the need for catalyst modification or system engineering.

25COASNOV138

Title: Anomeric Selectivity of Glycosylations through a Machine Learning Lens

Natasha Videcrantz Faurschou, Victor Friis, Priyanka Raghavan et.al.

J. Am. Chem. Soc. 2025, 147, 40, 2025

https://doi.org/10.1021/jacs.5c07561

Abstract: Predicting the stereoselectivity of glycosylations is a major challenge in carbohydrate chemistry. Herein we show that it is possible to build machine learning models that can predict the major anomer of a glycosylation, whether the other anomer is observed as the minor product, and the anomeric ratio of the two anomers. The three models are integrated into a publicly available tool, GlycoPredictor. From a statistical analysis of literature data, we analyze glycosylation trends and compare them to known trends in the field of carbohydrate chemistry, making it possible to elucidate a hierarchy of rules governing the stereoselectivity of glycosylations and discover promising new trends that complement expert intuition, which are tested in novel glycosylation methods.

25COASNOV139

Title: Mechanically Adaptive Cathode–Electrolyte Interphase via Dynamic Covalent Chemistry for Long-Life Ni-Rich Lithium Batteries

Yi-Shun Li, Yao-Lu Ye, Zi-Xin Xie et.al.

J. Am. Chem. Soc. 2025, 147, 40, 2025
https://doi.org/10.1021/jacs.5c09355

Abstract: High-nickel LiNi0.83Co0.12Mn0.05O2 (NCM83) cathodes suffer from interfacial instability resulting from cathode–electrolyte reactions and anisotropic mechanical strain within secondary particles. Herein, we present a mechanically adaptive cathode–electrolyte interphase (CEI) engineered via a dynamic covalent network that features a supramolecular ion-conducting polyurethane ureido-pyrimidinone (SPU-UPy) elastomer. The dynamic network integrates cooperative hydrogen bonds and disulfide bonds and imparts exceptional mechanical resilience and autonomous self-healing capabilities that allow it to accommodate volume fluctuations without compromising structural integrity. The SPU-UPy layer is also designed with strong transition metal ion–O/N coordination bonds that greatly enhance adhesion to the NCM83 surface and mitigate transition metal dissolution in the electrolyte. The polyether backbone facilitates efficient Li-ion transport across the interface and ensures a homogeneous interfacial Li concentration during intercalation/deintercalation. Consequently, the dynamic CEI-coated NCM83 cathodes achieve exceptional long-term cycling stability with a high-capacity retention of 82.2% after 400 cycles at 1 C. This work elucidates the critical role of dynamic covalent chemistry in stabilizing Ni-rich cathode interfaces and establishes a new paradigm for the design of high-energy-density batteries through mechano-adaptive interfacial engineering.

25COASNOV140

Title: On-Demand Nonalternating Copolymerization Enables Upcycling of Mixed Polyethylene and Nylon Plastics

Wen-Li Zhang, Shi-Yu Chen, Xiao-Bing Lu et.al.

J. Am. Chem. Soc. 2025, 147, 40, 2025
https://doi.org/10.1021/jacs.5c09549

Abstract: The increasing accumulation of plastic waste in the environment brings about a potential danger for ecosystems and human society; mechanical recycling remains one of the most economical strategies to deal with the growing crisis of plastic pollution; however, it suffers from substantial performance deterioration when processing immiscible blends of polyethylene and nylon plastics. Here, we report on-demand nonalternating copolymerization of ethylene with carbon monoxide (CO) via a facile tandem gas compensation strategy, which achieves a precision control over carbonyl incorporation with uniform distribution across a broad range (0–50%). Such a synthetic advance offers a unique multiblock structure having short polar segments ((CH2–CH2)n–CO−) (n < 4) and extended nonpolar methylene sequences (n > 4). Remarkably, the resulting quasi-multiblock copolymer (q-MBCP) delivers a robust compatibilization for polyethylene and nylon blends, thus transforming brittle materials into mechanically tough composites. This work elucidates the mechanistic evolution between nonpolar polyethylene and polar alternating polyketone phases, while offering a practical and sustainable solution to advance closed-loop recycling of mixed plastic waste.

25COASNOV141

Title: Biomimetic Dual Asymmetric MXene-Based Nanofluidics for Advancing Osmotic Power Generation

Jingyi Guo, Tianhao Liu, Weiwen Xin et.al.

J. Am. Chem. Soc. 2025, 147, 40, 2025
https://doi.org/10.1021/jacs.5c10164

Abstract: Nanofluidics-based reverse electrodialysis offers a promising approach for harnessing the osmotic energy that exists between saline and fresh water, thereby providing a sustainable source of power. Nevertheless, the key obstacle to realizing a commercially viable power output stems from inadequate ion permselectivity in nanofluidics. Here, we engineer dual asymmetric MXene-based composite nanofluidics (DA-MXCNs) composed of a negatively charged, porous MXene layer and a positively charged, confined MXene layer, which strategically incorporates asymmetric channel dimensions and opposing charge distributions. This design simultaneously reduces ion diffusion paths and amplifies ion potential differences, thereby optimizing the ion permeability and selectivity. The DA-MXCNs exhibit a 3.4-fold increase in ion flux (7.71 mmol m–2 h–1) over the unmodified nanofluidics, and thus a high Na+ selectivity coefficient of 0.985 and a Na+/Cl– selectivity ratio of approximately 65.7, indicative of superior preferential cation transport. Experimental and theoretical evidence supports that the dual asymmetric manipulations not only enable unidirectional and rapid cation transport but also create a high energy barrier for anions and a low one for cations, thereby achieving ultrahigh ion selectivity. Utilizing the DA-MXCNs, the osmotic energy conversion system achieves an impressive power density of up to 126.0 W m–2, which surpasses the performance of existing MXene-based nanofluidics and shows the capacity for powering a variety of electrical devices. This strategy, grounded in optimized permselective nanofluidics, lays the foundation for advancements in ion batteries and ion separation technologies.

25COASNOV142

Title: DNA-Templated Assembly of Metalloprotein Mimics with Hydrolytic Activity

Fangzhou Zhao, Ziyi Sun, Hanadi F. Sleiman

J. Am. Chem. Soc. 2025, 147, 40, 2025
https://doi.org/10.1021/jacs.5c10056

Abstract: Metalloproteins perform a wide range of biological and chemical functions, but elucidating their sequence–function relationships is difficult due to their complex folding pathways and various interactions involved. In this study, we use a covalently branched DNA trimer to scaffold the assembly of diverse peptide secondary structures into higher-order metalloprotein mimics. These structures exhibit zinc ion binding and hydrolytic activity, resembling the natural enzyme carbonic anhydrase (CA). By independently addressing each peptide fragment, we constructed a diverse library of protein mimics, enabling a systematic, high-throughput exploration of peptide structure–function relationships. This strategy expands the design potential beyond conventional coiled-coil motifs, offering a powerful methodology for constructing functional protein-based architectures.

25COASNOV143

Title: Engineering Cu/Ru Heterointerface-Shelled Nanocavities by the Kirkendall

Effect for Highly Efficient Nitrate Electroreduction to Ammonia

Shuangqun Chen, Zhouhao Zhu, Kepeng Song et.al.

J. Am. Chem. Soc. 2025, 147, 40, 2025
https://doi.org/10.1021/jacs.5c11097

Abstract: Electrochemical nitrate (NO3–) reduction to ammonia (NH3) offers a sustainable approach for NH3 synthesis while concurrently addressing NO3– pollution. However, achieving efficient NO3–-to-NH3 conversion remains challenging due to sluggish multistep proton-coupled electron transfer processes and poor intermediate converison. Here, we present a nanocatalyst featuring a hollow nanocavity encased within a shell rich in Cu/Ru heterointerfaces, which synergistically leverages both interfacial and structural advantages to effectively lower energy barriers and accelerate intermediate conversion kinetics, thereby enhancing the overall catalytic performance for NH3 production. Density functional theory (DFT) computations, supported by operando and control experiments, reveal that CuRu heterointerfaces with their optimized electronic structure act as the primary active sites, establishing a favorable NO3–-to-NH3 reaction pathway. Simultaneously, the catalytic synergy between Cu and CuRu sites enables tandem catalysis, which is further amplified by nanocavity-induced spatial confinement of the key intermediate NO2–. This nanocatalyst is realized via a Kirkendall effect–driven strategy, with its structural features systematically optimized. The resulting catalyst demonstrates outstanding NH3 production performance in a 0.1 M KNO3 + 0.1 M KOH electrolyte, delivering a Faradaic efficiency of 97.4%, a yield of 152.6 mg h–1 mgmetal–1, and an energy efficiency of 40% at a low potential of −0.1 VRHE─positioning it as a top contender among state-of-the-art NO3–-to-NH3 electrocatalysts. By elucidating mechanistic insights into interfacial effects, tandem catalysis, and nanoconfinement, this work highlights the synergistic impact of compositional and structural engineering and offers a generalizable design strategy for advancing NO3–-to-NH3 electroconversion and broader sustainable catalytic transformations.

25COASNOV144

Title: Impact of Carbene Ligands on the Properties and Reactivity of Diazoboranes

Chonghe Zhang, Agustin Valles, Junyi Wang et.al.

J. Am. Chem. Soc. 2025, 147, 40, 2025
https://doi.org/10.1021/jacs.5c11090

Abstract: While diazo compounds and organic azides have been extensively studied over the past two centuries, their boron analogs, diazoboranes, were only successfully isolated last year, and their properties remain largely unexplored. This study presents a systematic investigation of the synthesis, properties, and reactivity of diazoboranes. In this work, the diazoborane library is expanded to eight species by varying the carbene ligands coordinated to boron, allowing the identification of key correlations between ligand electronic properties and diazoborane behavior. The results demonstrate that increasing carbene π-acidity weakens the B–N bond while strengthening the N–N bond, significantly decreasing thermal stability. Kinetic studies reveal that less π-acidic carbenes promote a second-order decay mechanism, leading to dibora-azine formation, whereas more π-acidic carbenes favor first-order dinitrogen dissociation, facilitating borylene generation. Electrochemical studies indicate that redox potentials also correlate with carbene π-acidity. Three representative reactivity studies are presented in which the same substrate reacts with different diazoboranes to yield either

different products or the same product via different reaction mechanisms. These insights provide a generalizable framework for tuning diazoborane properties, facilitating their use in cycloaddition chemistry and small-molecule activation.

25COASNOV145

Title: Bio-inspired Deconjugative Isomerization of Borylated Dienoates

Amélia Messara, Byeongseok Kweon, Ferdinand Woge et.al.

J. Am. Chem. Soc. 2025, 147, 40, 2025
https://doi.org/10.1021/jacs.5c11995

Abstract: The evolutionary success of (poly)ene isomerization paradigms in generating molecular diversity is manifest throughout biosynthesis. Algorithms to relocate short π-systems, often against a thermochemical bias, with simultaneous regio- and stereocontrol, are a feat of precision that remains challenging to translate to a laboratory setting. The divergent biosynthesis of vitamin D and tachysterol from previtamin D, leveraging positional or geometric isomerization, is a powerful exemplar. Inspired by this venerable blueprint, a deconjugative isomerization of borylated dienoates has been developed under the auspices of photochemical activation. Alleviating ground-state thermochemical restrictions through light-induced reactivity enables facile bifurcation of the diene and carbonyl chromophores: this occurs by a geometric isomerization/[1,5]-hydrogen shift sequence that emulates previtamin D photobiology. Broad functional group tolerance is observed, allowing the process to be leveraged in complex settings that would otherwise require multistep approaches. It is envisaged that the operationally simple, enabling nature of this strategy, coupled with the traceless nature of the boron handle, will stimulate interest in poly(ene) relocation strategies and begin to reconcile the paucity of synthetic methods with their ubiquity in biosynthesis.

25COASNOV146

Title: Germanium-Mediated Catalysis via Ge(II)/Ge(III)/Ge(IV) or Ge(II)/Ge(IV) Redox Cycling

Yihan Zhou, Zhuchunguang Liu, Huan Mu et.al.

J. Am. Chem. Soc. 2025, 147, 40, 2025
https://doi.org/10.1021/jacs.5c12407

Abstract: Main group elements have recently emerged as promising candidates for redox catalysis, challenging the traditional reliance on transition metals. Despite heavy group 14 elements, such as germanium, possessing variable oxidation states that suggest their redox catalytic potential, their practical applications have been limited. In this study, we present the synthesis of a carbodiphosphoranyl germanium(II) compound and investigate its redox catalytic application. This organogermanium(II) species exhibits excellent catalytic performance in promoting the transfer hydrogenation of azoarenes and imines under mild conditions. Mechanistic studies revealed two distinct catalytic platforms based on GeII/GeIII/GeIV and GeII/GeIV redox cycles at a single germanium center. These results enable us to achieve the catalytic hydrogenation of azoarenes mediated by frustrated radical pairs (FRPs), as well as the catalytic chemoselective dearomatization of N-heteroarenes undergoing a GeII/GeIV redox process. Our work demonstrates the capacity of main group catalysts to facilitate diverse challenging chemical transformations through regulating the catalytic modes.

25COASNOV147

Title: Potential Pulsing-Induced Fe Undercoordination in NiFe (Oxy)Hydroxide Enhances Electrochemical Oxygen Evolution

Zhi-Peng Wu, Shouwei Zuo, Ruitao Wu et.al.

J. Am. Chem. Soc. 2025, 147, 40, 2025

https://doi.org/10.1021/jacs.5c12507

Abstract: Undercoordinated metal centers serve as key catalytic sites for the oxygen evolution reaction (OER) in water electrolysis. However, their inherent instability under oxidative conditions leads to rapid deactivation, limiting practical applications. Here, we demonstrate that reductive potential pulsing (RPP) is an effective strategy for generating and sustaining highly active undercoordinated Fe species in NiFe (oxy)hydroxide (NiFeOOH) during prolonged OER operation. Implementing this approach in an anion exchange membrane water electrolyzer enables a remarkable 40% enhancement in current density, achieving stable operation at 0.7 A/cm2 for 180 h. A key insight from operando X-ray absorption characterization reveals that the OER activity of NiFeOOH is directly correlated with dynamically modulated Fe coordination, while the chemical state of Ni remains largely unchanged during OER and RPP processes. Beyond providing new insights into the long-standing debate over NiFeOOH active sites, this study introduces a practical approach to enhancing both activity and stability, with potential applicability to other electrochemical systems.

25COASNOV148

Title: Methylation and Alkylation of Pyridines at the meta Position Using Aldehydes or Aldehyde Surrogates

Zhi-Hao Chen, Lu Liu, Yun-Bo Wang et.al.

J. Am. Chem. Soc. 2025, 147, 40, 2025

https://doi.org/10.1021/jacs.5c13428

Abstract: The installation of methyl groups can significantly enhance the drug potency, motivating the development of diverse methylation strategies. C–H methylation is particularly attractive, yet a broadly applicable method for meta-C–H methylation of pyridines─the most common N-heterocyclic pharmacophore─remains elusive. Herein, we report a method for meta-methylation of pyridines that utilizes dihydropyridines, generated in situ, in conjunction with benzotriazolylmethanol or paraformaldehyde as the methylating agent, enabling the construction of a diverse array of meta-methyl-substituted pyridines with excellent selectivity for monomethylation. Moreover, the method can be readily extended to meta-alkylation using aldehydes as alkyl sources. Density functional theory calculations, control experiments, and kinetic studies were performed to elucidate the reaction mechanisms, in which the cooperation of the borane catalyst with the base was crucial for the deoxygenation step. Given the impact of methyl groups on molecular potency and the prevalence of pyridine pharmacophores, we anticipate that this method may offer a powerful handle for accessing new drug candidates.

25COASNOV149

Title: Overriding Norrish Type II to Access Cyclopropanols

James W. Pearson, Samantha L. Dudra, Anthony F. Palermo et.al.

J. Am. Chem. Soc. 2025, 147, 40, 2025
https://doi.org/10.1021/jacs.5c13001
Abstract: The propensity for photoexcited aryl ketones to undergo 1,5-hydrogen atom transfer (HAT) reactions is a fundamental process in organic synthesis and polymer degradation. Since its discovery in 1958, Norrish–Yang photocyclization has become a prominent method to access cyclobutanols under mild photoirradiative conditions. Despite its successful extension to larger ring systems, access to medicinally relevant 3-membered rings remains limited due to the strong kinetic preference for 1,5-HAT over 1,4-HAT. In this work, we demonstrate the first photocyclization of β-boryl aryl ketones to cyclopropanols. Our strategy relies on solvent-controlled selective population of the π,π* triplet state over the n,π* triplet state, with the former preferentially undergoing 1,4-boryl group transfer over 1,5-HAT. This protocol proceeds under mild irradiative conditions with excellent functional group tolerance, providing access to a broad range of highly valuable cyclopropanol scaffolds.

25COASNOV150

Title: Gelatinase-Responsive Short Peptide Conjugate as a Precision Therapy Against Methicillin-Resistant Staphylococcus aureus

Snehanka Bose, Samya Sen, Taniya Mariyam et.al.
J. Am. Chem. Soc., 147, 41, 2025
https://doi.org/10.1021/jacs.5c11249
Abstract: Methicillin-resistant Staphylococcus aureus (MRSA) is resistant to most antibiotics, posing a major challenge to effective treatment. To address this, a gelatinase-responsive short peptide has been synthesized, selectively targeting pathogenic MRSA while sparing beneficial bacteria in the microflora. The therapeutic peptide, Py-FFRPLGVRGKKQK (Py-FGGK; Py: Pyrene), comprises a fiber-forming Py-FFR sequence, a gelatinase-cleavable linker (PLGVRG), and a heparan sulfate (HS)-binding motif (KKQK). HS is found ubiquitously on the MRSA-infected site. Py was used as a fluorescent marker apart from favoring self-aggregation through π-stacking interactions. Reverse-phase HPLC studies showed a serum half-life of ∼4.5 h, and isothermal calorimetry confirmed moderate binding with heparin sulfate (HPS) (3.08 ± 0.2 × 104 M–1), a pharmaceutical analogue of HS. Cationic lysine-derivatives in Py-FGGK, helped in specific binding to HS at the MRSA-infected site, followed by gelatinase-mediated cleavage at the G–V site, releasing the active component Py-FFRPLG (Py-FG), which self-assembled into amyloid fibrils via aggregation of the bis-phenylalanine moieties on the MRSA surfaces causing remarkable antibacterial activity. Py-FGGK is highly effective in biofilm disruption, leakages of cellular constituents, in situ ROS generation, killing biofilm-embedded cells, and favoring cellular migration in NIH/3T3 Cells that help wound healing. The significance of each synthon in Py-FGGK is demonstrated by control studies using various model peptides with appropriate structural variations. Biocompatibility of Py-FGGK as a potential therapeutic agent is ensured through hemolysis assay and insignificant mortality toward live HEK293 and WI38 cells. Its efficacy in wound healing and recovery of MRSA-infected female albino Wistar rats is also demonstrated.

25COASNOV151

Title: Deactivation of Interfacial Recombination Center for Thermally Stable Perovskite Solar Cells

Xin Liang, Sanwan Liu, Tiankai Zhang et.al.

J. Am. Chem. Soc., 147, 41, 2025
https://doi.org/10.1021/jacs.5c11581

Abstract: We report here on deactivation of the recombination center at the perovskite/Spiro-MeOTAD interface for thermally stable perovskite solar cells (PSCs). Investigation into the chemical reactivity of oxidized Spiro-MeOTAD (Spiro-MeOTAD•+) reveals that the Spiro-MeOTAD•+-induced interfacial recombination center is a key factor contributing to lowering open-circuit voltage (VOC) and thereby power conversion efficiency (PCE) of PSCs under thermal stress. To deactivate the recombination center via suppressing chemical reactivity, a functional molecule of 3-aminopropyltriethoxysilane (APTES) is inserted between the perovskite film and the Spiro-MeOTAD-based hole transporting layer (HTL). The alkoxy head in APTES is found to coordinate with the perovskite, and the amino tail reacts with the triphenylamine moiety of Spiro-MeOTAD•+, which effectively captures the excess oxidized Spiro-MeOTAD. As a result, the nonradiative recombination of perovskite is deactivated and the oxidation level of HTL is modulated, leading to a significant increase in VOC from 1.032 to 1.19 V after introducing APTES, along with a certified PCE of 25.6%. Thermal stability tests at 85 °C for 1000 h following the ISOS-D2I protocol show that 82% of the initial PCE is retained by the deactivation approach.

25COASNOV152

Title: Photoredox Fe-Catalyzed Aminoalkylation toward Sterically Hindered Chiral β-Amino Acids

Tianze Zhang, Pengwei Gu, Hanmin Huang

J. Am. Chem. Soc., 147, 41, 2025
https://doi.org/10.1021/jacs.5c12328

Abstract: β-Amino acids represent a vital class of structural motifs in natural products and pharmaceuticals, motivating sustained research efforts in organic synthesis and peptidomimetics. Despite the development of numerous methods for the preparation of β-amino acids, sterically hindered variants continue to pose challenges for their synthesis. In this context, an alternative approach via carboxyalkylation of prevalent tertiary amine scaffolds offers a promising yet underexplored strategy for the streamlined synthesis of β-amino acid derivatives. Herein, we report the development of an iron-porphyrin/photoredox dual catalytic system for the C(sp3)–C(sp3) cross-coupling of tertiary amines and α-halo acyl compounds, enabling the efficient assembly of sterically hindered β-amino acid frameworks. Mechanistic studies disclosed that the iron catalyst participates in the single-electron oxidation with α-carbonyl radical to generate a ferric enolate intermediate, thereby facilitating Mannich-type addition to afford the desired β-amino acid derivatives. Furthermore, the utilization of chiral auxiliaries enabled efficient stereocontrol over the aminoalkylation process, providing a platform for synthesizing a broad array of chiral β-amino acid derivatives.

25COASNOV153

Title: Direct Deaminative Halogenation at Hindered Tertiary Centers

Zhangkai Cui, Panpan Ma, Qi Sun et.al.

J. Am. Chem. Soc., 147, 41, 2025
https://doi.org/10.1021/jacs.5c13592

Abstract: General strategies for direct deaminative halogenation of α-tertiary amines─including those relevant to three-dimensional scaffolds─have remained an unsolved challenge in synthetic chemistry, primarily due to the difficulty of direct cleavage of C–N bonds at congested tertiary carbon centers. We report a radical-mediated deaminative halogenation platform that overcomes these limitations using commercially available O-diphenylphosphinyl hydroxylamine. By modulating reaction conditions, we redirect the inherent hydrogenation pathway toward halogen-atom transfer, enabling the efficient halogenation of sterically hindered substrates. This practical, one-pot transformation enables efficient chlorination, bromination, and iodination of structurally diverse amines while maintaining excellent functional group compatibility. The power of this methodology is also showcased by the straightforward preparation of valuable aryl-halide isosteres, including halogenated derivatives of bicyclo[1.1.1]pentane, bicyclo[2.2.1]heptane, bicyclo[2.2.2]octane, 2-azabicyclo[2.1.1]hexane, and cubane. Combining a broad substrate scope with operational simplicity and scalability, this advance provides a robust platform for late-stage molecular diversification and opens new avenues for the development of next-generation chlorine-containing drug candidates.

25COASNOV154

Title: Biosynthesis of the 5-Isoxazolidinone-Containing Hexacyclic Structure of Parnafungin

Zuodong Sun, Karl M. Yost, Gerald F. Bills et.al.

J. Am. Chem. Soc., 147, 41, 2025
https://doi.org/10.1021/jacs.5c14217

Abstract: Parnafungins A–D (1–4) are fungal natural products that inhibit eukaryotic poly(A)-polymerase and were first discovered by Merck & Co., Inc., through a Candida albicans Fitness Test (CaFT) screening program. The biological activity of parnafungins is a result of the unique fused hexacyclic structure highlighted by a 5-isoxazolidinone (5ILD) N-heterocycle. In this work, we characterize the complete biosynthetic pathway of parnafungins through heterologous reconstitution and enzymatic assays. Nearly half of the 26-gene biosynthetic gene cluster of parnafungin is responsible for the production of a known polyketide natural product, blennolide C. Starting from the blennolide C fragment, a three-enzyme cascade involving CoA-ligase ParJ, P450 ParO, and DUF829 ParD catalyzes the formal biaryl cross-coupling between blennolide C and anthranilate. Subsequent oxidative cyclization generates a phenanthridine product that is then reduced by atypical short-chain reductase ParT. N-Hydroxylation by flavin-dependent monooxygenase ParB and subsequent lactonization catalyzed by a homologue of dienenolactone hydrolase ParF form the 5ILD ring and complete the biosynthesis of 1 and 2. Methylation of 1 forms parnafungin C (3), and lastly epoxidation forms parnafungin D (4). Together, our work revealed the chemical logic and enzymology in extending the biosynthetic pathway of a well-characterized natural product, blennolide C, to introduce considerable additional structural diversity that affords

parnafungins with unique biological activity.

25COASNOV155

Title: Mechanistic Insights into the Light-Driven Difunctionalization of Alkenes with a Sulfonyl-Based Reagent: A Catalyst-Free Approach

Rakesh Maiti, Aritra Nath, Ana B. R. Guimarães et.al.

J. Am. Chem. Soc., 147, 42, 2025
https://doi.org/10.1021/jacs.5c08562

Abstract: Visible-light-mediated difunctionalization of nonactivated alkenes offers a sustainable and efficient strategy for constructing diverse molecular frameworks relevant to medicinal chemistry, polymer science, and synthesis of fine chemicals. While established approaches─such as photoredox catalysis, energy transfer (EnT), and ligand-to-metal charge transfer (LMCT)─have demonstrated success, they typically require external photocatalysts to achieve high reactivity. Alternatively, electron donor–acceptor (EDA) complexes have been explored, but these methods often rely on specially designed substrates, limiting the scope of this reaction. To overcome these limitations, we present a DFT-guided approach for identifying suitable radicals for light-mediated difunctionalization of nonactivated alkenes, eliminating the requirement of auxiliary catalysts or reagents. Our DFT calculations elucidate general reaction mechanisms and provide insights into regioselectivity. Additionally, time-dependent DFT (TD-DFT) calculations are employed to simulate UV–vis spectra and analyze the orbitals involved in key photoinduced transitions, guiding the selection of appropriate light sources. We further investigated the electrophilic and nucleophilic properties of the generated radicals to predict the regioselectivity of their additions. This study provides a framework for designing atom-economical difunctionalization reactions without relying on photocatalysts or substrate-specific EDA complexes and opens new avenues for further development in this area.

25COASNOV156

Title: Construction of Kondo Chains by Engineering Porphyrin π-Radicals on Au(111)

Yan Zhao, Kaiyue Jiang, Peng-Yi Liu et.al.

J. Am. Chem. Soc., 147, 42, 2025
https://doi.org/10.1021/jacs.5c09846

Abstract: Quantum manipulation of molecular radical spins provides a crucial platform for exploring emergent phenomena in many-body systems. Here, we combine surface-confined synthesis with scanning tunneling microscopy (STM) tip-induced dehydrogenation to achieve atom-precise engineering of quasi-one-dimensional porphyrin-based Kondo chains (1–7 units) on Au(111). High-resolution STS measurements and low-energy effective modeling collectively demonstrate that π-radicals at each fused-porphyrin unit form Kondo singlets screened by conduction electrons. Adjacent singlets develop direct coherent coupling via quantum-state-overlap-enabled electron tunneling. Crucially, chiral symmetry in the effective model governs zero-mode distribution─present in odd-length chains yet absent in even-length chains─which dictates pronounced odd–even quantum effects in STS spectra of finite chains. Furthermore, the number of parallel porphyrin chains nonmonotonically tunes the competition between the Kondo effect and spin exchange, showing opposing trends in strength and demonstrating that both wave function overlap and the SOMO–LUMO gap

collectively govern these interactions. This work simultaneously resolves the dimensional dependence of many-body correlations in confined quantum systems and pioneers approaches for quantum-critical manipulation in molecular spin architectures.

25COASNOV157

Title: Enhancing C2+ Product Faradaic Efficiency in CO2 Reduction Using Fluorine-Stabilized Superhydrophobic Copper (δ+)

Geetansh Chawla, Nilutpal Dutta, Siddhi Kediya et.al.

J. Am. Chem. Soc., 147, 42, 2025

https://doi.org/10.1021/jacs.5c10233

Abstract: Oxide-derived (OD) Cu catalysts are recognized for their effectiveness in producing C2+ products, but often revert to their metallic state, reducing selectivity due to the loss of their positive oxidation state. Here, we report a novel strategy to incorporate fluorine (F) into Cu2O nanospheres using hydrofluoric acid (HF). While halogen acids have traditionally been employed to etch metals and create cavities for confinement effects, this work goes a step further by inserting F ions into the lattice. Among all halogens, F provided the best lattice stability and was thus selected for catalyst testing. F incorporation was found to stabilize the Cu (δ+) oxidation state, achieving an impressive Faradaic efficiency (FE) of 91.9 ± 2.03% for C2+ products, predominantly ethylene (67%), at a current density of 250 mA cm–2. High-field 1D and 2D 19F magic-angle spinning (MAS) solid-state nuclear magnetic resonance (ssNMR) spectroscopy provided definitive evidence of F substitution at oxygen vacancies and the formation of a surface layer of HF. Water contact angle (WCA) measurements revealed enhanced hydrophobicity, with the 3 M HF-treated Cu2O exhibiting superhydrophobicity (WCA = 161°), which effectively suppressed hydrogen evolution (HER). In situ Raman spectroscopy confirmed prolonged stability of the Cu2O phase in the F-incorporated catalyst, while in situ ATR-FTIR spectroscopy with isotopic labeling elucidated the mechanistic pathway for ethylene production. Additionally, density functional theory (DFT) calculations offered mechanistic insights into ethylene formation, while Bader charge analysis revealed the electronic role of F incorporation in Cu2O, thereby providing insight into its enhanced selectivity.

25COASNOV158

Title: Asymmetric Total Syntheses of Hetidine-Type C20-Diterpenoid Alkaloids: Spirasines V and VI, Spiradine D, and the Proposed Structures of Spirafines II and III

Fengjie Yao, Yufei Wu, Yidian Sheng et.al.

J. Am. Chem. Soc., 147, 43, 2025

https://doi.org/10.1021/jacs.5c13564

Abstract: Herein we describe a divergent strategy toward the asymmetric total syntheses of five hetidine-type C20-diterpenoid alkaloids, namely, spirasines V and VI, spiradine D, and the proposed structures of spirafines II and III. Crucial transformations include an Enders asymmetric addition, an oxidative dearomatization induced Diels–Alder cycloaddition, and a MHAT-initiated transannular radical cyclization. The heterocyclic rings were assembled by an efficient reductive cyclization sequence at a late stage. Our approach has enabled the total syntheses of these natural products in 17–20 steps from commercially available starting materials with high enantio- and diastereocontrol.

25COASNOV159

Title: Chiral Lithium Amides as Key Reagents in Enantioselective Synthesis of 2-Alkylpyridines with Multiple Stereocenters

Dyllan P. Ly, Leroy Lu, Priya Kandiyal et.al.

J. Am. Chem. Soc., 147, 43, 2025
https://doi.org/10.1021/jacs.5c13977

Abstract: A direct enantioselective conjugate addition of 2-alkylpyridines enables efficient construction of complex functionalized pyridinyl scaffolds with contiguous stereocenters. This method leverages chiral lithium amides as traceless stereodirecting auxiliaries, operating through defined aggregation of organolithium intermediates to achieve excellent enantio- and diastereocontrol.

25COASNOV160

Title: Topological Derivative Strategy for Large-Pore Three-Dimensional Covalent Organic Frameworks

Haorui Zheng, Hui Li, Jie Ji et.al.

J. Am. Chem. Soc., 147, 43, 2025
https://doi.org/10.1021/jacs.5c10534

Abstract: The pursuit of three-dimensional covalent organic frameworks (3D COFs) with ultralarge pores faces fundamental challenges from structural interpenetration. We address this limitation through a topology-driven design strategy that transforms edge-transitive scu nets into two distinct derivative frameworks─mmm and jcg─via symmetry-controlled monomer selection. This approach yields contrasting pore evolution behaviors: while mmm series COFs (JUC-693 to JUC-695) show unpredictable pore size fluctuations (2.6 → 3.9 → 1.2 nm) due to complex interpenetration patterns, jcg series frameworks (JUC-696 to JUC-698) exhibit controlled expansion up to a record of 5.1 nm pore diameter in JUC-698. Comprehensive characterization, including macromolecular encapsulation studies with vitamin B12 and myoglobin, confirms the structural integrity and accessibility of these engineered pores. Our findings establish topology-directed design as a powerful tool for overcoming interpenetration barriers in porous materials development.

25COASNOV161

Title: Insights into the Dynamical Sodium Occupancy Evolution and Rate-Limiting Steps in Hard Carbon

Ying Ge, Yanling Qiu, Jianxin Han et.al.

J. Am. Chem. Soc., 147, 43, 2025
https://doi.org/10.1021/jacs.5c12673

Abstract: Accurate understanding of the sodium-storage mechanisms and behaviors is essential for advancing hard carbon (HC) anodes, yet significant controversies persist regarding the sloping and low-voltage-plateau sodiation processes. This work leverages quantitative in situ NMR with Raman spectroscopy and electrochemical analysis to achieve a critical quantified understanding. The approach definitely identifies a transition of Na+ from intercalation/adsorption sites to quasi-metallic sodium clusters within closed pores in the early stage of the plateau and subsequently cluster-grow alongside adsorption/intercalation-reoccupy during the late plateau. Notably, our results demonstrate that adsorbed Na+

maintains a significantly higher mobility than intercalated Na+ during the transition. This transition exhibits strong correlation with decreasing diffusion coefficient during the process, critically governing the rate performance of HC. This understanding clearly explains the enhanced plateau kinetics of HC by introducing abundant defects and closed pores and enlarging carbon layers, which provide a fast transition pathway into quasi-metallic sodium. As a result, our strategically designed HC material achieves a high reversible capacity of 413.2 mAh g–1 at 30 mA g–1 and an exceptional rate capability of 253.0 mAh g–1 at 1500 mA g–1. These fundamental insights into Na+ release and the transition-storage mechanism provide a critical foundation for the rational design of high-performance HC materials.

25COASNOV162

Title: Dual-Site Cobalt-Doped RuO2/TiO2 Electrocatalyst Enables Stable and Cost-Efficient Acidic Oxygen Evolution for PEM Water Electrolysis

Jing Liang, Yuanyuan Zhao, Chenyu Yang et.al.

J. Am. Chem. Soc., 147, 43, 2025

https://doi.org/10.1021/jacs.5c14137

Abstract: Developing efficient, cost-effective, and durable electrocatalysts for proton exchange membrane water electrolysis (PEMWE) remains a significant challenge, requiring the stabilization and enhancement of catalyst activity under harsh conditions. Here, we present cobalt-doped ruthenium dioxide (Co0.3Ru0.7O2) on TiO2 as an electrocatalyst toward an acidic oxygen evolution reaction. The Co0.3Ru0.7O2–TiO2 achieves an impressive overpotential of 322 mV at 1 A cm–2 and demonstrates stable operation for over 1000 h at 500 mA cm–2 in a PEMWE device. Comprehensive experimental and theoretical calculation results demonstrate that the doping of Co atoms into the rutile RuO2 lattice optimizes the geometric configuration. Moreover, the lattice-matched interface between Co0.3Ru0.7O2 and TiO2 promotes interfacial electron redistribution and stabilizes active centers under oxidative conditions. This facilitates a dual-site fully parallel oxidation (DFO) pathway in which intermediates are synchronously adsorbed and desorbed at Ru and Co sites, enabling direct O–O coupling. This work highlights the synergistic effect of the Ru–Co dual sites and TiO2 support in establishing a stable, self-regulating electronic environment that drives efficient intermediate transformation via the DFO mechanism.

25COASNOV163

Title: Alternating Current-Driven Diol Epimerization via a Deplete–Regenerate Strategy

Shaolong Qi, Duren Yin, Changqin Huang et.al.

J. Am. Chem. Soc., 147, 43, 2025

https://doi.org/10.1021/jacs.5c13881

Abstract: Epimerization is a powerful strategy for stereochemical editing, granting access to under-represented isomers without altering molecular connectivity. Although photocatalytic methods have recently expanded the epimerization toolkit, electrocatalytic alternatives have remained limited by redox incompatibilities that preclude simultaneous oxidation and reduction under direct current (DC) electrolysis. Here we report a general electrocatalytic epimerization enabled by alternating-current (AC) electrolysis. A deplete–regenerate strategy enables temporal separation of redox events: the thiol mediator is exhaustively oxidized

during the anodic half-cycle (depletion prior to substrate activation), and subsequent polarity reversal regenerates the thiol in situ to quench the radical intermediate. This time-domain control allows the oxidative and reductive steps to occur in distinct phases. The method accommodates a broad range of functional groups and is compatible with complex bioactive molecules. Mechanistic investigations (kinetic analysis, cyclic voltammetry, and deuterium labeling) support a model wherein the AC waveform sustains catalytic turnover by resolving the redox incompatibility through this time-separated deplete–regenerate sequence.

25COASNOV164

Title: Achieving Record-Breaking Urea Synthesis on Crystalline–Amorphous Hybrid via Electrochemical-Chemical Looping

Zhong Cheng, Xiaodeng Wang, Dafeng Yan et.al.

J. Am. Chem. Soc., 147, 43, 2025

https://doi.org/10.1021/jacs.5c13721

Abstract: Electrocatalytic C–N coupling of nitrate and CO2 represents a paradigm shift in sustainable urea synthesis. We demonstrate that amorphous CuOx-coated crystalline Cu nanowires achieve a record-breaking urea yield rate of 0.89 mol h–1 g–1 via novel electrochemical-chemical looping. Mechanistic investigations reveal a three-step catalytic cycle: (i) electro-reductive generation of Cu0 and oxygen vacancies (Ov); (ii) Ov-mediated nitrate activation via oxygen atom insertion, spontaneously yielding nitrogen-bonded nitrite (*NO2) while oxidizing Cu0 to catalytically active Cu+; and (iii) Cu+-catalyzing C–N coupling between *NO2 and CO2 to form urea. This pathway circumvents conventional rate-limiting nitrate reduction step, reducing the electron transfer requirement from 16e– to 12e– for urea synthesis. Notably, direct nitrite utilization fails to generate Cu+ or nitrogen-bonded intermediates, instead forming oxygen-bonded species with markedly reduced C–N coupling activity–a finding that overturns conventional understanding. Our work establishes new fundamental principles for efficient urea synthesis and provides insights into catalyst design and green chemistry.

25COASNOV165

Title: Boosting Electrochemical CO2 Reduction to Formate over La-Doped SnO2 via Pinning Effect and Water Activation

Yanlin Wang, Guilin Li, Jiaqi Feng et.al.

J. Am. Chem. Soc., 147, 44, 2025

https://doi.org/10.1021/jacs.5c03978

Abstract: Electrochemical reduction of CO2 to formate over Sn-based catalysts offers an effective carbon-neutral approach for chemical production and renewable energy storage. However, poor selectivity under high current densities persists, primarily due to the instability of Sn–O active sites and slow water dissociation. In this work, a La-doped SnO2 catalyst is synthesized for efficient CO2 conversion to formate. Detailed in situ experimental and theoretical studies reveal that La doping induces a pinning effect that effectively stabilizes the Sn–O structure, decreasing the energy barrier for *OCHO conversion. Meanwhile, La species accelerate water activation to provide *H species, and then the moderate *H coverage promotes formate production. As a result, the La-doped SnO2 exhibits high formate selectivity over a broad potential window from −0.8 to −1.2 V vs reversible

hydrogen electrode (RHE), achieving a formate Faradaic efficiency of up to 93.2% with a partial current density of −315.4 mA cm–2 at −1.0 V vs RHE. This work may provide insights into the pinning effect and encourage more design strategies to explore lanthanide element doping for efficient CO2 electroreduction catalysts.

25COASNOV166

Title: Equivalent Atrop- and Positional Isomerism in Styrene Derivatives Prepared by Enantioselective 1,3-DiarylationC

Amit Kumar Simlandy, Yiyao Hu, Turki M. Alturaifi et.al.

J. Am. Chem. Soc., 147, 44, 2025
https://doi.org/10.1021/jacs.5c10118

Abstract: Isomerism, the ability of a single set of atoms within a molecule to exist in different three-dimensional spatial arrangements connecting through distinct bonding networks, gives rise to distinct physical, chemical, and biological properties from a common set of atomic building blocks. While different forms of isomerism are now well appreciated, a rare phenomenon is the coexistence of multiple equivalent forms of isomerism within a given pair of molecules. Here, we report that a simple combination of palladium and amino acid cocatalysts converts ortho-alkenyl benzaldehydes into substituted styrenes possessing equivalent atrop- and positional isomerism. Mechanistically, the reaction proceeds through successive Mizoroki–Heck arylation promoted by the amino acid cocatalyst. DFT calculations show that the atroposelectivity arises from stereoselective β-H elimination in the second arylation cycle, whereas the formation of Z products with constrained rotation about the chiral axis is driven by the thermodynamic stability of the Z isomer.

25COASNOV167

Title: Ultrafast Nonradiative Relaxation Limits the Efficiency of Photoinduced Bond Homolysis in Molecular LMCT Photocatalysts

Rachel Weiss, Bryan Kudisch

J. Am. Chem. Soc., 147, 44, 2025
https://doi.org/10.1021/jacs.5c10766

Abstract: Ligand-to-metal charge transfer photocatalysts (LMCT PCs) are being increasingly implemented toward construction and functionalization of organic molecules. Leveraging photoinduced metal–ligand bond homolysis, these PCs generate reactive intermediates ranging from halogen radicals to radical cross-coupling partners. Despite their growing synthetic utility, key mechanistic questions remain surrounding both the surprising inefficiency of this photodissociation chemistry and the puzzling success of nonprecious metal photocatalysts despite low energy ligand field states. Herein, femtosecond transient absorption (TA) spectroscopy is implemented to address these mysteries using FeCl4– and CeCl62–, which photogenerate Cl• under mild conditions, as model systems. Ultrafast dynamics and complementary TA actinometry indicate that the homolysis efficiency is limited by relaxation to a lower energy excited state within the LMCT excited state manifold at a faster rate than relaxation to ligand field states. These results provide a mechanistic explanation for the low photochemical efficiencies observed in benchtop reactions that have encumbered otherwise proficient PCs.

25COASNOV168

Title: Azaanthraquinone PCET Catalysis Enables Chemoselective Decarboxylative Functionalization of Diverse Carboxylic Acids

Takeshi Inoue, Daiki Tomiya, Masaaki Fuki et.al.

J. Am. Chem. Soc., 147, 44, 2025
https://doi.org/10.1021/jacs.5c10807

Abstract: The advancement of a proton-coupled electron transfer (PCET) strategy holds significance to expand the synthetic applicability and energy efficiency of photoredox chemistry. However, the current implementation of this strategy is typically narrow in terms of the redox potential and reaction efficiency. In this study, a novel PCET catalyst containing an azaanthraquinone skeleton has been developed for the decarboxylative functionalization of a wide range of carboxylic acids, including aromatic and perfluoroalkyl carboxylic acids. By integrating the aza-arene and benzoquinone moieties into a single molecule, this catalyst suppresses the previously problematic back electron transfer (BET) through rapid intersystem crossing from singlet to triplet states and the facilitated electron transfer from the substrate to the excited triplet catalyst via PCET. This catalyst enables a variety of decarboxylative functionalization reactions from challenging substrates, such as benzoic acids and fluoroalkanoic acids, to proceed under mild conditions with high chemoselectivity.

25COASNOV169

Title: Seawater to Sustainable Fuel: Sunlight-Driven Green Hydrogen Generation with an Atomically Dispersed Photocatalyst

Satyadeep Waiba, Manami Banerjee, Lindsey Frederiksen et.al.

J. Am. Chem. Soc., 147, 44, 2025
https://doi.org/10.1021/jacs.5c11004

Abstract: Green hydrogen is widely regarded as a key to a sustainable future, offering a clean and flexible fuel option for decarbonizing the energy, transport, and industrial sectors. While photocatalytic approaches are known for generating hydrogen directly from water, most existing methods require (over)stoichiometric amounts of sacrificial reagents, which is far from ideal for the production of green hydrogen. To address this challenge, we have developed an atomically dispersed Ni-based photocatalyst that achieves hydrogen evolution rates of up to 270 μmol/g/h (168 mmol/gNi/h). Remarkably, this photocatalyst also exhibits high photoreactivity under direct sunlight, producing up to 17 μmol/g/h (10.6 mmol/gNi/h) of hydrogen. Impressively, the catalyst can even generate green hydrogen directly from seawater, up to 144 μmol/g/h, demonstrating significant potential for real-world applications. The photocatalyst is exceptionally stable, remaining active even after 720 h (140 h of irradiation and 580 h resting time) of operation and retaining high performance over more than 15 cycles. Furthermore, comprehensive spectroscopic and structural analyses─including HRTEM, PXRD, ssNMR, XPS, and XAS─provide detailed structural insights and confirm the atomically dispersed nature of the Ni species. In-depth mechanistic studies have elucidated the critical role of atomic dispersion in enabling robust photocatalytic efficiency.

25COASNOV170

Title: Fast and Reliable NMR-Based Fragment Scoring for Drug Discovery

Ridvan Nepravishta, Juan C. Munoz-Garcia, Kenneth Cameron et.al.

J. Am. Chem. Soc., 147, 44, 2025
https://doi.org/10.1021/jacs.5c11092

Abstract: Fragment-Based Drug Discovery (FBDD) is a powerful strategy used in the development of new therapeutics. Molecular fragments are screened against a target protein, where interactions are typically characterized by a low affinity. Nuclear Magnetic Resonance (NMR) spectroscopy is well-suited to detect weak protein–ligand interactions and is therefore often used in FBDD. However, while NMR is very effective in initial screening, follow-up NMR experiments to measure binding affinities (i.e., KD values) are labor-intensive and time-consuming. To address this challenge, we have developed an innovative SHARPER NMR fragment scoring technique. The high sensitivity of SHARPER NMR dramatically reduces the data acquisition times, allowing faster and more accurate quantification of fragment KD values from ligand titration curves. To further accelerate fragment scoring, a machine learning model was developed that accurately ranks fragment affinities from only two SHARPER titration points. The resulting integrated method, termed "ML-boosted 1H LB SHARPER NMR", produced significant time savings; using a 600 MHz QCI cryoprobe, KD values of up to 144 ligands in a day could be determined under our conditions, compared with only a handful achievable by traditional approaches. The proposed methodology will shorten the transition from hits to lead compounds, accelerating the drug discovery process by rapidly and reliably evaluating fragment binding, providing informed decision-making in the early stages of FBDD.

25COASNOV171

Title: Modulating Hydrogen Exchange Capabilities by Heterogenizing Pd Nanoclusters onto Ni3C Multipods for Efficiently Driving the "Formaldehyde-Nitrate" Tandem Electrochemical System

Zulakha Zafar, Bin Zhao, Rida Javed et.al.

J. Am. Chem. Soc., 147, 44, 2025
https://doi.org/10.1021/jacs.5c11608

Abstract: Nitrate and formaldehyde, common industrial byproducts and waterborne pollutants, pose serious environmental and health hazards, yet their efficient conversion remains challenging due to sluggish hydrogen (H*) transfer and limited recycling strategies. While recent studies have explored nitrate reduction (NO3RR) and formaldehyde oxidation (FOR) coupling, they faced critical limitations such as no H2 generation, a lack of electricity output, and reliance on Cu-based catalysts prone to deactivation. This work presents Pd nanoclusters on nickel carbide (Pdnc-Ni3C) that serve as a noncopper bifunctional catalyst that possesses superior H* exchange capabilities enabling dual-directional catalysis of NO3RR and FOR. At the cathode, Pdnc-Ni3C achieves an onset potential of +0.27 V vs RHE, and 98% Faradaic efficiency for NH3 at −0.3 V. At the anode, Pdnc-Ni3C achieves an efficient FOR at a low onset potential of 0.04 V and enables a broad oxidation window (0–1.2 V) with high current density (up to 910 mA cm–2), outperforming previously reported Cu- and Ni-based systems. Differential electrochemical mass spectra reveal a previously unexplored intermolecular coupling pathway for H2 evolution, advancing mechanistic insight into the 1-electron formaldehyde oxidation process. By coupling the NO3RR and FOR, a high-performance "Formaldehyde–Nitrate" galvanic cell is achieved with an OCV of 0.88 V and peak power density of 7.4 mW cm–2. Distinctively, this Ni based system simultaneously

converts industrial waste into green energy carriers (H2, NH3) and value-added chemicals (formate) while producing electricity, offering both environmental and economic benefits.

25COASNOV172

Title: Self-Organization of Microcompartments Powered by Enzyme-Driven Solutal Flows at the Water–Oil Interface

Pankaj S. Patwal, B. V. V. S. Pavan Kumar

J. Am. Chem. Soc., 147, 44, 2025

https://doi.org/10.1021/jacs.5c11877

Abstract: Design of microcompartments capable of self-organization via consumption of energy or fuel to power opposable short-range forces is a step toward realization of adaptive cellular materials capable of intelligent behaviors. Here, we report active microgel compartments (a-MC) containing urease capable of self-organization at the water–oil interface via the regulation of short-range interparticle interactions consisting of urease-powered repulsive solutal flows and attractive capillary forces. The conversion of urea into denser products of ammonia and bicarbonate by urease within the a-MC causes density-driven outward flows leading to repulsive interactions with neighboring a-MCs at the water–oil interface. The modulation of repulsive solutal flows allowed the a-MCs to self-organize into nonclose-packed 2D lattices at high urease activity and 1D chains at low urease activity and high population density. These repulsive solutal flows are fueled by urea, so by limiting the supply of urea, we could achieve disassembly of 2D clusters at high urea concentration and reassembly upon a drop in urea levels. In binary mixtures of active and passive (no urease) microgel compartments, the passive microgel compartments showed increasing orthogonal assembly with a rise in their population density. Immobilization of 2D clusters of a-MCs allowed us to set up long-range collective solutal flows to execute microcompartment cargo logistics and to form fluidic traps for controlling assembly and position of binary/ternary microcompartment clusters for enhanced chemical signaling. Our work presents opportunities for the development of autonomous soft microbots, precision microscale cargo logistics, and intelligent matter.

25COASNOV173

Title: Direct Electrosynthesis of C3+ Hydrocarbons from CO2 via Size-Controlled Nickel Nanoislands on a Carbon Support

Maral Vafaie, Roham Dorakhan, Amin Morteza Najarian et.al.

J. Am. Chem. Soc., 147, 44, 2025

https://doi.org/10.1021/jacs.5c12052

Abstract: Direct synthesis of C3+ hydrocarbons via the electrochemical CO2 reduction reaction is highly desirable for producing sustainable chemicals. However, this approach remains challenging due to the limited ability of current electrocatalysts to adsorb and couple key reaction intermediates effectively, with promising systems, such as Ni oxyhydroxide-derived catalysts, still exhibiting partial current densities toward C3+ hydrocarbons <0.9 mA cm–2. Motivated by the limited activity and control over the active site environment of these systems, we hypothesize that reducing the size of metallic Ni modifies its electronic states and introduces interfacial metal–support sites that promote more balanced *CO adsorption, critical for facilitating C–C coupling beyond C2 intermediates. Here, we report a plasma-

assisted deposition method to synthesize size-controlled metallic Ni nanoislands on a carbon support. Characterization revealed that reducing the nanoisland size (<12 nm) forms undercoordinated, electron-deficient, and strained surfaces with a downshifted d-band center─features associated with weakened *CO binding, favoring intermediate coupling and C3+ hydrocarbon formation. Nanoislands as small as ∼3.5 nm delivered a 120-fold increase in C3+ hydrocarbon specific activity relative to large particles (bulk-like Ni). CO stripping voltammetry shows weaker *CO adsorption on isolated nanoislands. While C3+ partial current densities remain low (∼0.1 mA cm–2), these findings identify nanoparticle size and metal–support interactions as key design parameters for advancing CO2 conversion to long-chain hydrocarbons, offering a foundation for further improvement, as demonstrated by a >20-fold enhancement in the Ni-mass-based activity versus state-of-the-art catalysts.

25COASNOV174

Title: Stereoselective Photoenzymatic Hydroarylation for the Construction of Quaternary Stereocenters

Felix C. Raps, Chufan A. Jin, Alexandra C. Brown et.al.

J. Am. Chem. Soc., 147, 44, 2025

https://doi.org/10.1021/jacs.5c12440

Abstract: Quaternary carbon stereocenters are a crucial component of many bioactive molecules, but they can be challenging to prepare stereoselectively. Olefin hydroarylations are an attractive means for preparing this motif; however, existing methods struggle to set stereocenters on substrates lacking traditional catalyst binding handles. Here, we report a stereoselective photoenzymatic olefin hydroarylation using a repurposed Baeyer–Villiger monooxygenase. Three rounds of iterative site-saturation mutagenesis yielded a photoenzyme capable of preparing valuable tetrahydroquinolines in high yields with excellent enantioselectivity. The engineered variant accepts various arene substituents, highlighting the synthetic utility of this methodology. DFT calculations and control experiments suggest that the protein templates a through-space interaction between the tertiary radical and aromatic group, which attenuates the oxidation potential of the radical, enabling C–C bond formation.

25COASNOV175

Title: Engineering an Imine Reductase for Enantioselective Synthesis of Atropisomeric Amides

Zhouchang Yao, Runze Meng, Zitian Zhou et.al.

J. Am. Chem. Soc., 147, 44, 2025

https://doi.org/10.1021/jacs.5c12724

Abstract: Atropisomeric amides possess unique axial chirality arising from the rotation-restricted Caryl–Camide bond and find broad application in bioactive molecules and asymmetric catalysis. However, catalytic asymmetric methods for their synthesis remain underdeveloped, with no biocatalytic approaches reported. Herein, we report the first efficient biocatalytic strategy for the atroposelective synthesis of atropisomeric amides via dynamic kinetic resolution using engineered imine reductases (IREDs). Structure-guided engineering of an IRED from Kutzneria albida provided a quadruple mutant (IRED-68-M4) capable of catalyzing the stereoconvergent synthesis of diverse napthamides and benzamides in high yields and excellent enantioselectivities (up to 98% yield, >99:1 er). Gram-scale synthesis of

an axially chiral napthamide was also demonstrated. Moreover, protein X-ray crystallography and molecular modeling studies revealed the structural basis of the enhanced catalytic performance of the IRED-68-M4 variant.

25COASNOV176

Title: Dinickela-bicyclo[4,4,0]-decadiene Complex with a Linear Heterometallic Mg–Ni–Ni–Mg Chain

Yanping Cai, Stella Christodoulou, Laurent Maron et.al.

J. Am. Chem. Soc., 147, 44, 2025

https://doi.org/10.1021/jacs.5c13473

Abstract: Transition metal–diene complexes constitute a fundamental class of organometallic compounds, in which conjugated dienes typically behave as neutral π-donor ligands. While doubly reduced enediyl derivatives have been occasionally documented in the literatures, dinuclear transition metal complexes featuring such bonding motifs have not been explored. Herein, we report a heterometallic complex [(LMg)2Ni2(C4H6)2] (L = [(DIPPNCMe)2CH]−, DIPP = 2,6-iPr2C6H3) featuring a linear Mg–Ni–Ni–Mg bonded chain, which was formed by the reaction of LMgBu·Et2O with Ni(cod)2 (cod: 1,5-cyclooctadiene). Experimental and computational studies reveal two s-trans-butadiene ligands bridging the Ni–Ni bond in a doubly reduced enediyl configuration. This unique bonding arrangement results in a dinickela-bicyclo[4,4,0]-decadiene framework containing a heterocyclic trans-cycloalkene moiety. Treatment of [(LMg)2Ni2(C4H6)2] with the additional butadiene afforded [(LMg)2Ni2(C4H6)3], involving three C4H6 ligands bound to nickel centers, in which they behave as two doubly reduced enediyl ligands and one neutral butadiene ligand. In contrast, upon exposure to carbon monoxide (CO), a ligand exchange reaction occurred, yielding [(LMg)2Ni2(C4H6)(CO)4] with one C4H6 ligand, which is considered as a dinickelacyclo-4-hexene supported by Mg-metalloligands.

25COASNOV177

Title: Development of Dual-Receptor Lysosome-Targeting Chimeras for Protein Degradation

Kun Wang, Ke Wang, Cong Wang et.al.

J. Am. Chem. Soc., 147, 44, 2025

https://doi.org/10.1021/jacs.5c13695

Abstract: A growing array of lysosome-targeting chimeras (LYTACs) have recently emerged as therapeutic candidates to treat malignancies and other diseases via targeted protein degradation. We established a novel dual lysosome-targeting receptor-dependent protein degradation strategy that leverages the synergistic actions of the C-X-C chemokine receptor 4 (CXCR4) and folate receptor 1 (FOLR1) to degrade extracellular and membrane proteins. Using this strategy, we developed dual-receptor lysosome-targeting chimeras to achieve efficient lysosomal degradation of programmed cell death ligand 1 (PD-L1) and epidermal growth factor receptor (EGFR). The EGFR chimera inhibited the growth of transplanted T790M-mutated drug-resistant EGFR-driven lung cancer tumors by degrading EGFR. This dual-targeting strategy exhibits significantly better protein degradation capabilities compared with single lysosome-targeting chimeras, providing a novel platform for developing drugs targeting cancer.

25COASNOV178

Title: Atropisomeric Indene (AtroInd) Libraries: Design, Catalytic Synthesis, and Applications

Yuan Zheng, Jingran Zhang, Jingyi Bai et.al.

J. Am. Chem. Soc., 147, 44, 2025
https://doi.org/10.1021/jacs.5c13866

Abstract: The development of chiral indenyl metal complexes has been hindered by inefficient synthetic methods, significantly lagging behind the well-established Cp metal complexes. In this study, we present a streamlined and highly efficient synthesis of novel atropisomeric indenes (AtroInds) via asymmetric palladium-catalyzed Suzuki–Miyaura cross-coupling reactions. Leveraging this method, AtroInd libraries, encompassing varying steric and electronic properties, were readily constructed. The resulting AtroInd–Rh(III) complexes were prepared with ease and subjected to comprehensive characterization, revealing exceptional catalytic efficiency in asymmetric catalysis. Computational studies provided profound insights into the reaction pathway and the critical factors governing enantioselectivity, thereby enhancing our mechanistic understanding. This integrated approach not only addresses the prevailing synthetic challenges in the preparation of chiral indenes but also establishes a new paradigm for the design and synthesis of novel ligand libraries through advanced synthetic methodologies.

25COASNOV179

Title: Nickel-Catalyzed Asymmetric α-Alkenylations of Acyclic Amides that Provide Tertiary Stereocenters

Asik Hossain, Gregory C. Fu et.al.

J. Am. Chem. Soc., 147, 44, 2025
https://doi.org/10.1021/jacs.5c14143

Abstract: Carbonyl groups and alkenes are ubiquitous in organic chemistry─present in target molecules as well as versatile handles for conversion into other functional groups. Whereas the coupling of the α position of a carbonyl compound with an alkenyl electrophile represents an attractive approach to uniting these useful functionalities, to date there have been few reports of catalytic asymmetric variants of this bond construction. Most of the progress to date has involved cyclic carbonyl compounds (obviates the issue of controlling the E/Z geometry of the nucleophile) and the generation of quaternary stereocenters (obviates undesired side reactions of the β,γ-unsaturated carbonyl product, such as racemization or isomerization to the more stable α,β-unsaturated carbonyl compound). Herein, we establish that a chiral nickel catalyst can couple acyclic racemic Reformatsky-type reagents (α-zincated amides) with alkenyl halides to generate β,γ-unsaturated amides that bear a tertiary α stereocenter with good enantioselectivity and good yield. The products can be transformed into other useful families of enantioenriched compounds, including intermediates in total synthesis. Mechanistic studies are consistent with a nickel(0)/nickel(II) pathway for asymmetric carbon–carbon bond formation.

25COASNOV180

Title: Bioinspired Total Syntheses of Skeletally Diverse Lycopodium Alkaloids

Yu-Fei Ou, Yuan Jin, Zai-Feng Yuan et.al.

J. Am. Chem. Soc., 147, 44, 2025
https://doi.org/10.1021/jacs.5c15169
Abstract: The phlegmarine skeleton is widely recognized as a key biogenetic intermediate in Lycopodium alkaloids. On this basis, we designed a phlegmarine-derived common intermediate that enables the collective, asymmetric total syntheses of 12 Lycopodium alkaloids with five distinct carbon skeletons. This intermediate was prepared on a decagram scale using commercially available (R)-pulegone in an eight-step sequence, with a stereoselective Michael addition as a key transformation. Subsequent selective carbon–carbon bond formation of this pivotal intermediate─(C4–C10, C4–C12, C1–C14, and C4–C13)─along with a skeletal rearrangement, delivered five frameworks: the huperzimine, lycodine, lycopodine, and phlegmarine classes, which were represented by (−)-hupserrine A, (−)-β-obscurine, (−)-lycopodine, (−)-cermizine B, and the lyconadin C diastereomer, respectively. Furthermore, we developed the first asymmetric total synthesis of (−)-hupserrine A, which bears a complex [6/6/5/6/7] pentacyclic cage structure and inhibits the 5-HT3A receptor (IC50 = 10.6 μM).

25COASNOV181

Title: Hydrogen-Mediated Reductive Cross-Coupling of Aryl Iodides with Activated Aryl and Heteroaryl Bromides

Weijia Shen, Yu-Hsiang Chang, Brandon I. Gonzalez et.al.
J. Am. Chem. Soc., 147, 44, 2025
https://doi.org/10.1021/jacs.5c15725
Abstract: Hydrogen-mediated reductive cross-couplings of aryl iodides with activated aryl and heteroaryl bromides are described, along with related homocouplings (Ullmann reactions) and vinylic reductive couplings that occur with cine-substitution. To corroborate key events in the catalytic cycle, Pd-to-Pd transmetalation and cross-selective reductive elimination, dianionic diarylpalladate complexes [Pd(Aryl)(μ-Br)Br]2[NPr4]2 bearing p-fluorophenyl, p-methoxyphenyl and p-nitrophenyl moieties were prepared. Stoichiometric reactions of these complexes in the presence of iodide demonstrate that Pd-to-Pd transmetalation by way of monomeric arylpalladates occurs at a greater rate than reductive elimination and that cross-selective C–C reductive elimination is favored for electronically distinct aryl partners. Hydrogen-mediated reductive cross-coupling of aryl iodides with α-bromostyrene occurs with cine-substitution (as observed in related formate-mediated processes), consistent with carbopalladation of α-bromostyrene by monomeric arylpalladates Pd(Aryl)I2[NBu4] that arise upon dissociation of [Pd(Aryl)(μ-I)I]2[NBu4]2.

25COASNOV182

Title: Deep-Red to Near-Infrared Light-Driven Radical Generation from Organoboron Compounds via Ligand-Induced Direct Excitation Catalysis

Yusuke Miyamoto, Kanji Muraoka, Sho Murakami et.al.
J. Am. Chem. Soc., 147, 44, 2025
https://doi.org/10.1021/jacs.5c17266
Abstract: We report a catalytic strategy for generating carbon-centered radicals from organoboron compounds under deep-red to near-infrared (DR to NIR) light irradiation via direct excitation of substrate–catalyst complexes. Aza-dipyrromethene (ADP) catalysts form

photoactive borate intermediates that enable C–B bond cleavage through ligand-induced photochemical activation. Mechanistic studies support the role of direct excitation. This method allows diverse transformations, including Giese addition, C-heteroatom bond formation, radical–radical coupling, and nickel-catalyzed cross-coupling reactions.

25COASNOV183

Title: Single-Cell Fluorescence Analysis of Lipid Droplet Compositional Dynamics during Triacylglycerol Catabolism

Junwei Wang, Keiji Kajiwara, Manish Kesherwani et.al.

J. Am. Chem. Soc., 147, 45,2025

https://doi.org/10.1021/jacs.5c11742

Abstract: Lipid droplets (LDs) are dynamic organelles essential to lipid metabolism and energy homeostasis, yet their compositional heterogeneity in living cells remains poorly understood. Here, we present LipiPB Red, a red-emissive fluorescent probe with exceptional photostability, high polarity sensitivity, and long-term retention within LDs, even under serum-containing conditions. When applied to fluorescence lifetime imaging microscopy (FLIM), LipiPB Red enables discrimination between triacylglycerol (TAG) and diacylglycerol (DAG) content within individual LDs. FLIM analysis revealed pronounced compositional heterogeneity among LDs in hepatoma cells. This heterogeneity was abolished, with a concomitant increase in average fluorescence lifetimes, upon genetic knockdown or pharmacological inhibition of adipose triglyceride lipase (ATGL), implicating ATGL-mediated lipolysis as a key regulator of LD diversity. Moreover, coimaging with autophagy markers revealed reduced fluorescence lifetimes in LDs localized within both autophagosomes and autolysosomes. These findings indicate a sequential lipid degradation cascade during lipophagy, where lipid hydrolysis is initiated prior to lysosomal fusion.

25COASNOV184

Title: Cell Membrane-Anchored Click Reaction Enhances Porphyrin Uptake for Highly Efficient Photodynamic Therapy of Breast Tumors

Yu Ma, Xiaoyang Liu, Qiaochu Jiang et.al.

J. Am. Chem. Soc., 147, 45,2025

https://doi.org/10.1021/jacs.5c13182

Abstract: Enhancing cell uptake of drugs for better therapy is a fundamental scientific problem in pharmaceutics. The “hydrophobic–hydrophilic–hydrophobic” structure has shown the potential of enhancing cell uptake of drugs. Thus, cell membrane-anchored formation of this structure should additionally enhance cell uptake of drugs but has not been reported. In this work, we rationally designed acid-deshielding cysteine-PEG-DSPE (DA-Cys-PD) and PE-porphyrin-PEG-CBT (Por-CBT). After DA-Cys-PD anchors on the tumor cell membrane, the weak acidic environment of the cell deshields the anchor to yield Cys-PD, which subsequently click-reacts with Por-CBT to yield Por-Luc-PD with a “hydrophobic–hydrophilic–hydrophobic” structure. This in situ formed structure significantly enhances the cellular uptake of porphyrin and its consequent photodynamic therapeutic effect on breast tumors. Particularly, with the assistance of the cell membrane-anchored click reaction, porphyrin uptake in cancer cells or breast tumors is increased roughly to be 7.8-fold or 3.9-fold of that of the negative control group whose Cys is acid-inactive, respectively. The

enhanced porphyrin uptake leads to highly efficient photodynamic therapy of breast tumors with a remarkable tumor growth inhibition rate of 64.1% compared with that of 5.5% of the negative control group. This approach of cell membrane-anchored click reaction provides people with a simple and feasible avenue for enhancing cell uptake of drugs/probes, as well as their therapeutic/diagnostic effects.

25COASNOV185

Title: Copper-Catalyzed Enantioselective Synthesis of N-Heterocycle-Substituted Quaternary Carbon Stereogenic Centers

Minjeong Seo, Hyunwoo Kim

J. Am. Chem. Soc., 147, 45,2025

https://doi.org/10.1021/jacs.5c13377

Abstract: The enantioselective construction of all-carbon quaternary stereogenic centers adjacent to N-heterocycles remains a long-standing challenge in asymmetric catalysis. Herein we report a copper-catalyzed enantioselective hydropyridylation of 1,1-disubstituted allenes with 2-halopyridines that proceeds via a nucleophilic aromatic substitution (SNAr) pathway. This transformation enables the efficient synthesis of α-quaternary N-heterocyclic compounds with a broad substrate scope in high yields (up to 96%) with excellent enantioselectivities (up to 99% ee). The methodology is compatible with various functional groups and N-heterocycles and can be extended to copper-catalyzed boropyridylation, affording versatile alkenylboronates. Mechanistic studies, including deuterium labeling, kinetic isotope effect analysis, and DFT calculations, support a 2,3-hydrocupration followed by a stereodetermining SNAr step. This strategy provides a practical and general approach for constructing structurally diverse azaarene-containing quaternary centers, which are potentially valuable for drug discovery and development.

25COASNOV186

Title: Capturing the Hybrid Palladium(I)-Radical Pair Relevant to Photoexcited Palladium Catalysis

Sagnik Chakrabarti, Siddhartha Banerjee, Liviu M. Mirica et.al.

J. Am. Chem. Soc., 147, 45,2025

https://doi.org/10.1021/jacs.5c14709

Abstract: Understanding and controlling one-electron chemistry in palladium coordination compounds can unlock reactivity that is inaccessible to ground-state Pd chemistry. One burgeoning area involves the photochemical excitation of a Pd0 catalyst to activate alkyl halides, substrates that are traditionally challenging to activate thermally, and Pd compounds supported by wide bite-angle diphosphines such as Xantphos are privileged catalysts in this realm. Mononuclear PdI halide compounds supported by such ligands are proposed as key intermediates formed during the photoexcitation of Pd0 species; however, no examples of isolated mononuclear PdI halide compounds have been reported to date. Herein, we report that a Xantphos ligand (tBuXantphos) with tert-butyl substituents on the phosphorus atoms enables the isolation and full spectroscopic characterization of neutral, three-coordinate PdI-chloride and -bromide compounds as crystalline solids. Furthermore, the corresponding Pd0 complex is capable of cleaving C–X bonds in alkyl halides upon photoexcitation with visible light, forming the respective PdI halide species. This provides definitive experimental

evidence for this elementary step nearly 30 years after the original proposal by Suzuki and Miyaura. In addition, a PdII monomethyl compound supported by the same ligand framework undergoes Pd–C bond homolysis under visible light irradiation to form the same PdI halide species. Finally, the reactivity difference between the bulky tBuXantphos and less sterically hindered diarylether-based diphosphines was examined in model stoichiometric and catalytic reactions. Overall, these findings provide unambiguous experimental evidence for the role of PdI compounds as critical intermediates in photochemical palladium chemistry.

25COASNOV187

Title: Kinetic, Spectroscopic, and Computational Investigation of Oxidative Aminative Alkene Cleavage Reveals an N-Iodonium-Iminoiodinane Pathway

Florian Ruepp, Vasily Grebennikov, Mykola Avramenko et.al.

J. Am. Chem. Soc., 147, 45,2025

https://doi.org/10.1021/jacs.5c14977

Abstract: The combination of hypervalent iodine(III) oxidants and ammonia sources has been applied in various oxidative aminative transformations of high synthetic value. Central to these reactions is the proposed in situ generation of a four-electron oxidizing intermediate, commonly referred to as iodonitrene. However, this species' mechanism of formation, nature, and relevance to N-atom transfer remains uncertain. Furthermore, evidence for its direct implication as the key reactive intermediate remains elusive. Herein, we present an extensive mechanistic study of a recently published oxidative aminative cleavage of alkenes, which allowed us to obtain key insights into these understudied aspects of hypervalent iodine-mediated nitrogen atom insertion. Through in situ 19F nuclear magnetic resonance (NMR), initial rate kinetics, linear free energy relationships (LFER), H/D and 12C/13C kinetic isotope effect (KIE) determination, electrospray ionization mass spectrometry (ESI-MS) and density functional theory (DFT) studies, we show that the formation of an N-iodonium-iminoiodinane is rate-determining in this reaction. This species is highly electrophilic and capable of concerted, asynchronous transfer of a [PhI–N]+ unit to double bonds. These findings point toward the N-iodonium-iminoiodinane, not an iodonitrene, being the active N-atom transfer agent generated from the combination of hypervalent iodine(III) oxidants and ammonia. This ultimately deepens our understanding of this commonly used reagent combination and will help to inform the development of methods and reagents for oxidative amination reactions using this reactive manifold.

25COASNOV188

Title: Catalytic Enantioselective C(sp3)–C(sp3) Cross-Coupling of Tertiary Nitriles with Allyl Halides to Quaternary Stereocenters

Gui-Feng Ding, Zi-Hao Chen, Jiang-Lian Deng et.al.

J. Am. Chem. Soc., 147, 45,2025

https://doi.org/10.1021/jacs.5c15414

Abstract: Quaternary stereocenters are prevalent in natural products and bioactive molecules, where they influence the molecular structure, conformation, and function by enhancing the fraction of sp3 character. The enantioselective construction of such structures via cross-coupling remains a long-standing challenge, owing to the steric demands of forging C(sp3)–C(sp3) bonds and the limited accessibility of suitable tertiary carbon coupling

partners. Here, we report a palladium-catalyzed asymmetric decyanative allylation (ADCNA) platform of C(sp3)–C(sp3) cross-coupling that transforms stable and readily available tertiary nitriles into enantioenriched acyclic and cyclic compounds bearing quaternary centers. This process proceeds via the selective addition of in situ-formed allyl zinc reagent to the cyano group, followed by retro-Thorpe-type C–CN bond cleavage and asymmetric allylation, guided by newly developed chiral ligands. The method exhibits a broad substrate scope across three classes of tertiary nitriles─malononitriles, α-cyano indolinones, and α-cyano lactones─offering high yields and excellent enantioselectivities under mild conditions. This research establishes a conceptually distinct retrosynthetic paradigm, from prochiral or racemic quaternary carbons to enantioenriched quaternary centers, enabled by chemoselective C–C bond cleavage and stereoselective C–C bond formation. The synthetic utility of this strategy is demonstrated by the downstream synthesis of a monoamine reuptake inhibitor and a CNGA2 channel blocker as well as synthetic intermediates of natural products physovenine and physostigmine.

25COASNOV189

Title: Precise Synthesis of Pyrene-Based Molecular Nanocarbons Driven by Dehydro-Diels–Alder Reactions

Jian Li, Haohua Chen, Ya Wang et.al.

J. Am. Chem. Soc., 147, 45,2025

https://doi.org/10.1021/jacs.5c15627

Abstract: Molecular nanocarbons are critical bridges between small polycyclic aromatic hydrocarbons and extended graphene lattices, driving advances across materials science, optoelectronics, and quantum technologies. However, the atomically precise synthesis of such systems, particularly those featuring K-region and cove-type topologies, remains an enduring challenge. Here, we present a de novo modular strategy that overcomes this constraint by directing K-region growth via annulation of preorganized aryl acetylnaphthalene precursors with acetylenedicarboxylate. The strategy mirrors the hierarchical construction of pyrene by formally inserting naphthalene fragments into spatially defined molecular scaffolds. This method integrates Suzuki–Miyaura coupling with a Zn(OTf)2-catalyzed cascade comprising Friedel–Crafts alkylation, dehydro-Diels–Alder cycloaddition, and dehydrogenative aromatization. The platform affords structurally diverse pyrene-based molecular nanocarbons with programmable control over topology and dimensionality, spanning linear, contorted, and three-dimensional π-architectures. These results establish a generalizable blueprint for bottom-up synthesis of complex carbon-rich architectures with atomic precision.

25COASNOV190

Title: Pyridine-to-Pyridazine Skeletal Editing

Wonjun Choi, Ahyoung Jang, Sungwoo Hong

J. Am. Chem. Soc., 147, 45,2025

https://doi.org/10.1021/jacs.5c15601

Abstract: Nitrogen-containing heterocycles underpin many pharmaceuticals, where subtle atomic rearrangements can markedly alter efficacy and safety. Pyridines are ubiquitous scaffolds in pharmaceuticals, yet their close analogues, pyridazines with two adjacent ring

nitrogens, remain underexplored owing to limited synthetic access. Here, we report a skeletal editing strategy that converts pyridines into pyridazines by replacing one ring carbon with nitrogen while preserving aromaticity. The sequence comprises N-amine assembly, followed by an m-chloroperoxybenzoic acid (mCPBA)-mediated ring-remodeling sequence proceeding via a 1,2-diazatriene intermediate to effect carbon-to-nitrogen substitution. The two-step process is operationally simple, runs at ambient temperature in air, and requires no UV irradiation or preinstalled groups. The method shows broad functional-group tolerance, including complex, drug-derived molecules, providing rapid, scalable access to pyridazines. This platform expands heterocyclic chemical space and enables late-stage diversification for drug discovery.

25COASNOV191

Title: Upgrading Sodium-Mediated Deprotonative Borylation to Catalytic Regimes: Regioselective Control and Mechanistic Implications

Clarence Tan, Andreu Tortajada, Ana McGinley et.al.

J. Am. Chem. Soc., 147, 45,2025
https://doi.org/10.1021/jacs.5c15994

Abstract: Organoboron compounds are essential to pharmaceutical synthesis, yet current catalytic C–H borylation methods remain largely limited to transition-metal and borenium catalysts. Deprotonative borylation presents a complementary approach for functionalizing acidic C–H bonds, but has traditionally required stoichiometric amounts of organometallic bases. Herein, we report the prototypal example of catalytic deprotonative borylation mediated by sodium. The use of an iminoborane as a trapping agent is key to the catalytic system, where unstable metalated intermediates are rapidly trapped to form a sodium borylamide, which can deprotonate the substrate to achieve catalytic turnover. Optimization of reaction conditions allows the borylation of base-sensitive substrates, such as fluoroarenes and pyridines, under noncryogenic conditions, affording good to excellent yields. Furthermore, selective stepwise borylation of multiple acidic C–H bonds can be achieved through stoichiometric control of the iminoborane reagent. A comprehensive mechanistic understanding of this transformative reaction has been established through density functional theory calculations, kinetic studies, and the isolation of key catalytic intermediates characterized by X-ray diffraction and NMR spectroscopy.

Diagnostic Services
(Pathology**, C**ancer Screening **& R**adio-diagnosis**)**

25COASNOV1:
Title: The Dublin International Society of Urological Pathology (ISUP) Consensus Conference on Best Practice Recommendations on the Pathology of Urachal Neoplasms.
Reis, Henning MD*; Al-Ahmadie, Hikmat MD
The American Journal of Surgical Pathology 49(11):p e18-e26, November 2025
https://doi.org/10.1097/PAS.0000000000002416
Abstract: This manuscript summarizes the first part of the proceedings of the 2023 Dublin ISUP Consensus Conference encompassing the best practice recommendations on the pathology of neoplasms of urachal origin. The rationale for convening this consensus conference was the lack of structured and consented histopathologic recommendations in these rare tumors. Consensus among the meeting participants (n=80) was reached on the following statements: (1) combination of gross, histologic, clinical and imaging findings with exclusion of secondary tumor metastasis are to be used in the diagnosis of urachal carcinoma; (2) the 2022 World Health Organization (WHO) separate criteria for the diagnosis of urachal adenocarcinoma and for nonglandular carcinoma should be applied; (3) specific elements are to be evaluated and recorded in the gross examination of resection specimens containing urachal tumors; (4) sampling considerations for resection specimens containing urachal tumors are advised; (5) participants are against using 5% or 10% cutoff for the extent of intraepithelial carcinoma in urachal mucinous cystic tumor of low malignant potential; (6) use of immunohistochemical markers for the differential diagnosis of urachal adenocarcinomas in transurethral resection (TUR) specimen is considered optional; (7) similar tumor classificatory (nosology) rules for carcinomas arising from bladder mucosa (eg, urothelial carcinoma, squamous cell carcinoma, and neuroendocrine carcinoma) should be applied for nonglandular urachal carcinomas; (8) a new staging approach other than the previously proposed systems should be designed for urachal carcinoma; (9) a system modifying the current Tumor-Node-Metastasis (TNM)/American Joint Committee on Cancer (AJCC) staging system for urinary bladder cancer is considered appropriate for a study in urachal carcinoma; and (10) several histologic elements are to be reported when diagnosing urachal carcinoma in TUR and resection specimens. This report from the Dublin ISUP consensus conference will serve as a practice recommendation for pathologists and as a guide for future standardized reporting protocols and research regarding urachal tumors. In addition, an international database for urachal cancers under the guidance of ISUP is being planned to be established to address pertinent issues in the pathology of urachal cancers.

25COASNOV2
Title: Establishing the Diagnosis of Germ Cell Tumors in Patients Presenting With Metastatic Disease: A Series of 55 Cases Emphasizing Challenges Commonly Encountered in Core Biopsies.
Bhardwaj, Swati MBBS et.al.
The American Journal of Surgical Pathology 49(11):p 1097-1104, November 2025.
https://doi.org/10.1097/PAS.0000000000002438

Abstract: Germ cell tumors (GCTs) are the most common nonhematopoietic malignancies in young men and typically present as primary testicular masses. However, in ~12% of cases, GCTs manifest as metastatic disease without a known testicular primary, leading to significant diagnostic challenges. We retrospectively reviewed 55 cases of GCTs presenting as metastases, focusing on the morphologic and immunohistochemical pitfalls encountered in core biopsy specimens. Among a total of 55 cases, seminoma was the most common histologic subtype (61%), followed by embryonal carcinoma (14%) and mixed GCTs (13%), with a median age of 44 years (range: 21 to 87 y). The most frequently biopsied metastatic sites were the retroperitoneum (55%) and left neck (22%). Notably, only 7% of cases had an identified testicular mass at diagnosis. Only a third (32%) of cases were submitted with an initial diagnosis of GCT, while 10% were misclassified as non-GCT malignancies. Histologic features such as crush artifact (83%) and necrosis (54%) frequently obscured morphology, leading to extensive IHC panels. Cytokeratin expression (particularly CAM 5.2 and AE1/3) was identified in 51% of cases, often confounding the diagnosis. A greater number of IHC stains were performed at outside institutions compared with intramurally (9 vs. 4, *P*=0.0001). The use of OCT3/4 and CD30 proved crucial in diagnosing seminomas and embryonal carcinomas, respectively. In rare cases (n=4) with atypical histology, fluorescence in situ hybridization (FISH) for isochromosome 12p provided additional diagnostic support. Diagnosing metastatic germ cell tumors in needle biopsies remains a significant challenge, often compounded by lack of a known testicular mass, cytokeratin expression, and confounding histologic features such as crush artifact and necrosis that could be used as clues rather than impediments to diagnosis. Awareness of these findings, along with careful integration of clinical context, histology, and immunohistochemistry, is critical to avoid misdiagnosis, particularly in light of the exquisite chemosensitivity of GCTs. The use of reliable markers like OCT3/4 and CD30, coupled with a high index of suspicion in men with retroperitoneal or left neck masses, can aid in improving diagnostic accuracy.

25COASNOV3

Title: DNA Methylation Profiling Separates SDH-Deficient GISTs From KIT-PDGFRA-Driven GISTs and Identifies Predictive Biomarkers for Targeted Therapy.

Chłopek, Małgorzata PhD

The American Journal of Surgical Pathology 49(11):p 1105-1113, November 2025.
https://doi.org/10.1097/PAS.0000000000002444

Abstract: Succinate dehydrogenase (SDH), a critical enzyme in the citric acid cycle and respiratory electron transport chain, consists of 4 subunits: SDHA, SDHB, SDHC, and SDHD. Deficiency of a single subunit leads to the loss of SDH activity which is implicated in the development of a subset of gastrointestinal stromal tumors (GISTs): SDH-deficient GISTs. These GISTs arise almost exclusively in the stomach, have a female predilection, and primarily affect children and young adults. Their characteristic morphologic features include multinodular architecture, lymphovascular invasion, and lymph node metastasis. At the molecular level, these tumors lack *KIT*, *PDGFRA, BRAF*, or *NF1* mutations, which are alternative oncogenic drivers typically observed in GIST. Recently, a sarcoma DNA methylation classifier was developed and was shown to be a valuable diagnostic tool. This study evaluated the DNA methylation classifier results for 30 SDH-deficient GISTs and discovered that methylation profiles clustered in a unique region separate from GISTs and

leiomyosarcomas. Moreover, *MGMT* promoter methylation, a predictive biomarker of tumor cell sensitivity to alkylating agent chemotherapy, was identified in 6 primary and 5 metastatic tumors. In addition, 3 primary and 4 metastatic tumors showed gain/low-level amplification of *MDM4*, which pathologically activates MDM4-p53 axis, a target of inhibitors. In summary, these findings expand the sarcoma DNA methylation classifier to include SDH-deficient GIST as a new sarcoma DNA methylation entity and identified 2 predictive biomarkers for targeted therapy: methylation of *MGMT* promoter and gain/low-level amplification of *MDM4*.

25COASNOV4

Title: Genomics of T-Cell Lymphomas With CD30/CD15 Co-Expression: Comparison With Anaplastic Large-Cell Lymphoma, ALK-Negative.

de Castro, Joao V. Alves MD et.al.

The American Journal of Surgical Pathology 49(11):p 1114-1124, November 2025.

https://doi.org/10.1097/PAS.0000000000002447

Abstract: The proper categorization of mature T-cell neoplasms with coexpression of CD30/CD15 is unresolved. Prior studies suggested an overlap with ALK-negative anaplastic large cell lymphoma (ALCL). We evaluated the morphologic, immunophenotypic, and molecular features of 28 T-cell lymphomas coexpressing CD30/CD15, and performed a comparison with 8 ALK/CD15-negative ALCL and published data. Clinical information was retrieved from the submitting physician. Immunohistochemistry, TRG and IG gene rearrangement, DNA and RNA targeted next-generation sequencing, and fluorescence *in situ* hybridization for *DUSP22* rearrangement were performed. Cases were classified as conforming to 3 histologic variants: ALCL-like, Hodgkin-like, and PTCL-NOS-like. Median age was 62 years (range: 33 to 87). Male:female ratio was 3:1. Twenty-four cases presented with lymphadenopathy (24/28, 85.7%). Six cases had skin involvement (6/28, 21.4%), including 4 primary cutaneous cases (4/28, 14.3%). Ten cases were designated as ALCL-like, 12 as Hodgkin-like, and 2 as PTCL-NOS-like. There was frequent loss of T-cell markers, with expression of CD3 in 7/27 cases (25.9%), CD2 in 15/23 (65.2%), and expression of at least one cytotoxic marker in 13/24 (54.2%). *DUSP22* was rearranged in 4 cases (4/16, 25%). The JAK-STAT pathway was frequently altered due to mutations in *JAK1* (6/28, 21.4%), *STAT3* (5/28, 17.8%), and *JAK2* fusions (2/28, 7.1%). PI3K-AKT-mTOR pathway alterations due to *PIK3R1* mutations (5/28, 17.8%) were also frequent and mutually exclusive with JAK-STAT pathway activation. In summary, most T-cell neoplasms with CD30/CD15 coexpression share clinical, morphologic, immunophenotypic, and molecular features with *ALK*-negative ALCL but do not segregate as a homogeneous entity as defined by histologic or genetic features.

25COASNOV5

Title: MUC4-positive Fibroblastoma: A Distinctive Hyalinized Spindle Cell Neoplasm With Aberrant Nuclear Beta-catenin Expression and Frequent Biallelic Inactivation of APC.

Repetto, Federico MD

The American Journal of Surgical Pathology 49(11):p 1125-1132, November 2025.

https://doi.org/10.1097/PAS.0000000000002441

Abstract: Among soft tissue tumors, MUC4 is expressed in low-grade fibromyxoid sarcoma and sclerosing epithelioid fibrosarcoma, and is regarded as a specific and sensitive marker for these malignant entities. These tumors are driven by oncogenic fusions involving *FUS* or *EWSR1* as a 5' partner and *CREB3L1* or *CREB3L2* as a 3' partner. In this study, we describe the clinicopathologic and molecular features of a distinctive fibroblastic soft tissue neoplasm characterized by consistent co-expression of MUC4 and beta-catenin, and frequent underlying *APC* inactivation without evidence of *EWSR 1* or *FUS* rearrangements. Fifteen hyalinized spindle cell neoplasms with MUC4 and aberrant nuclear beta-catenin co-expression were identified from our institutional archives. The cohort comprised 15 adult patients (6 female, 9 male) with a median age of 40 years (range: 20 to 61). Tumors arose in the extremities (n=9), trunk (n=5), and retroperitoneum (n=1), with a median size of 8.5 cm (range: 2.8 to 18.0 cm). The tumors consisted of a hypocellular proliferation of spindled-to-stellate fibroblastic cells in a variably hyalinized collagenous stroma. No atypia, fascicular growth, or myxoid stroma was present. Targeted DNA sequencing was successfully performed on 8 tumors. In addition, 8 tumors underwent FISH testing to assess for *FUS* and/or *EWSR1* rearrangement. In the majority of tumors, DNA sequencing demonstrated *APC* inactivation (7/8; 88%). In 6 of these cases, 2 concurrent deleterious *APC* alterations were present, indicative of biallelic inactivation. No rearrangements involving *FUS* or *EWSR1* were identified by NGS and/or FISH. Clinical follow-up data were available for 4 patients, with no local recurrences or metastases reported, including 1 patient followed for 8 years. No patients had a known history of familial adenomatous polyposis. We describe a novel fibroblastic soft tissue neoplasm characterized by co-expression of MUC4 and beta-catenin and frequent underlying *APC* inactivation, for which we propose the name "MUC4-positive fibroblastoma."

25COASNOV6

Title: Risk of disease progression in first-line metastatic colorectal cancer therapy to guide disease reassessments—analysis of 11 trials by AIO and GONO

M.M. Germani

Annals of Oncology, Volume 36, Issue 11p1307-1318
https://doi.org/10.1016/j.annonc.2025.08.001

Abstract: We evaluated the distribution and risk of disease progression (PD) in first-line therapy of unresected metastatic colorectal cancer (mCRC) patients receiving chemotherapy + biologics. The aim of the analysis is to provide guidance for the timing of disease reassessments during first-line therapy. Patients and methods- Individual data of 2939 unresected patients from TRIBE, MOMA, TRIBE2, VALENTINO, ATEZOTRIBE, TRIPLETE, FIRE-3, XELAVIRI, PANAMA, FIRE-4 and FIRE-4.5 were analyzed. The frequency and risk of PD events were calculated for individual timepoints during therapy. *RAS/BRAF* profiling, tumor sidedness, type of therapy and early tumor shrinkage (ETS) were used to identify subgroups for risk assessment. A Cox regression model to predict first-line progression-free survival (PFS) was built. Results- In the overall population, the maximum frequency of PD events was observed at 7.6 months, with an absolute PD risk of 19%. Then, the PD risk flattened, achieving a maximum of 23% at 14 months in *RAS/BRAF*-wild-type patients (n = 1786), 25% at 10 months in *RAS*-mutant patients (n = 973) and 35% at 8 months in *BRAF*-mutant patients (n = 180). Eastern Cooperative Oncology

Group performance status >0, right-sidedness, initially unresected primary tumor, higher number of organs involved by metastases and *BRAF* mutation were independently associated with a higher risk of PD in first line. The impact of baseline characteristics on PFS was mitigated after incorporation of ETS in the model. Conclusions- The distribution of PD events does not follow a Gaussian pattern, with the highest density observed between the third and fourth reassessment of a bimonthly surveillance schedule. In clearly unresectable patients, restaging should focus on the interval between 6 and 10 months and not on the initiation of systemic therapy. Our model might be helpful to schedule radiological reassessments according to baseline characteristics, early response and the expected duration of each treatment efficacy.

25COASNOV7

Title: Final overall survival and safety analyses of the phase III PSMAfore trial of [^{177}Lu]Lu-PSMA-617 versus change of androgen receptor pathway inhibitor in taxane-naive patients with metastatic castration-resistant prostate cancer

K. Fizazi et.al.

Annals of Oncology, Volume 36, Issue 11p1319-1330

https://doi.org/10.1016/j.annonc.2025.07.003 External Link

Abstract: In PSMAfore, [^{177}Lu]Lu-PSMA-617 (^{177}Lu-PSMA-617) prolonged radiographic progression-free survival (rPFS) in taxane-naive patients with metastatic castration-resistant prostate cancer (mCRPC), with a favourable safety profile, versus a change in androgen receptor pathway inhibitor (ARPI). We report the final overall survival (OS) analysis and updated safety data. Patients and methods-PSMAfore (NCT04689828) was an open-label, international, phase III trial. Patients with prostate-specific membrane antigen (PSMA)-positive mCRPC who had experienced disease progression once on a previous ARPI and were candidates for ARPI change were randomized 1 : 1 to ^{177}Lu-PSMA-617 or ARPI change to abiraterone or enzalutamide. Crossover from ARPI change to ^{177}Lu-PSMA-617 was allowed after centrally confirmed radiographic progression. Endpoints included rPFS (primary), OS (key secondary), and safety (secondary). Results-Patients were randomized to ^{177}Lu-PSMA-617 or ARPI change (n = 234 each): 141/234 participants (60.3%) randomized to ARPI change crossed over (75.4% of those with centrally confirmed radiographic progression). The median OS was 24.48 months [95% confidence interval (CI) 19.55-28.94 months] with ^{177}Lu-PSMA-617 versus 23.13 months (95% CI 19.61-25.53 months) with ARPI change [hazard ratio (HR) 0.91, 95% CI 0.72-1.14, P = 0.20] based on the intention-to-treat (ITT) principle; the crossover-adjusted OS HR by inverse probability of censoring weighting modelling was 0.59 (95% CI 0.38-0.91). For ^{177}Lu-PSMA-617 versus ARPI change, exposure-adjusted incidences of grade ≥3 and serious treatment-emergent adverse events were 60.8 versus 85.1 and 32.5 versus 49.9 per 100 patient-treatment years, respectively. Dry mouth occurred in 135/227 participants (59.5%; 2/227 grade ≥3) and anaemia in 62/227 (27.3%; 14/227 grade ≥3) in the ^{177}Lu-PSMA-617 arm. Conclusions- OS analyses did not show a statistically significant difference between the ^{177}Lu-PSMA-617 and ARPI arms based on the ITT principle; results were likely confounded by the high rate of crossover. The safety profile of ^{177}Lu-PSMA-617 was favourable with no new safety signals identified.

25COASNOV8

Title: Fracture-related hospitalisations in newly diagnosed high-risk localised or metastatic hormone-sensitive prostate cancer: secondary analysis of the STAMPEDE phase III trials of docetaxel and zoledronic acid using healthcare systems data

C. Jones et.al.

Annals of oncology, Volume 36, Issue 11p1331-1341
https://doi.org/10.1016/j.annonc.2025.07.005

Abstract: Androgen deprivation therapy (ADT), the mainstay systemic treatment for high risk non-metastatic (M0) and metastatic (M1) prostate cancer is associated with bone loss and increased fracture risk. The STAMPEDE trial tested the addition of zoledronic acid (ZA) ± docetaxel (with prednisolone) to ADT. Both regimens may impact bone health. However, long-term fracture incidence remains uncertain. Patients and methods-Health systems data were obtained for patients recruited from England and randomised to standard-of-care (SOC) ADT compared with SOC plus ZA or docetaxel or both docetaxel and ZA. ICD10 diagnosis and OPCS procedure codes from inpatient hospital admissions were used to identify fracture-related hospitalisations. Flexible parametric competing risks models were used to estimate 5- and 10-year cumulative incidence and sub-distribution hazard ratios (SDHR). Results-2140 of 2705 (79%) patients recruited from trial sites in England were eligible for this secondary analysis. Linked data were available for 2042/2140 (96%) pts (734 M0, 1308 M1). 5-year cumulative incidence of fracture for M0 and M1 patients treated with SOC only was 11% [95% confidence interval (CI), 8% to 15%] and 23% (95% CI, 19% to 28%), respectively. 10-year cumulative incidence in M0 patients was 26% (95% CI, 20% to 33%). Allocation to ZA significantly reduced the risk of fracture in M1 patients (SDHR 0.73, 95% CI 0.55-0.97; $P = 0.015$) but not M0 patients (SDHR 0.88, 95% CI 0.59-1.32; $P = 0.549$). Docetaxel had no clear effect on the risk of fracture in M0 ($P = 0.570$) or M1 ($P = 0.264$) patients. Conclusions- High cumulative incidence of fracture was observed in both M0 and M1 prostate cancer patients receiving ADT. The addition of ZA to ADT ± docetaxel significantly reduced long-term fracture risk in M1 participants but had no clear effect in M0 disease. These data support the use of bone protective agents to reduce fracture risk in men with M1 prostate cancer undergoing ADT.

25COASNOV9

Title: Prognostic significance of early on-treatment evolution of circulating tumor DNA in advanced ER-positive/HER2-negative breast cancer

A. Mamann et.al

Annals of oncology, Volume 36, Issue 11p1342-1355
https://doi.org/10.1016/j.annonc.2025.06.015

Abstract: Patients with advanced estrogen receptor-positive, HER2-negative breast cancer commonly develop resistance to treatment with hormone therapy and cyclin-dependent kinase 4/6 (CDK4/6) inhibitors. Responders cannot be distinguished from nonresponders after the first cycle of treatment under current practice. We assessed circulating tumor DNA (ctDNA) measures at early timepoints as prognostic markers. Patients and methods Paired plasma samples were collected at baseline and early on-treatment (median 28 days) from 369 patients with advanced ER-positive/HER2-negative breast cancer treated in the PADA-1 trial with hormone therapy and a CDK4/6 inhibitor. Cell-free DNA was profiled with a 497-gene

panel (Guardant360 LDT). Results- Baseline ctDNA levels, including the mean variant allele frequency (VAF) [progression-free survival (PFS) hazard ratio (HR) 1.07, 95% confidence interval (CI) 1.05-1.09), $P < 0.001$; overall survival (OS) HR 1.08, 95% CI 1.05-1.11, $P < 0.001$] and the number of driver somatic mutations (PFS HR 1.13, 95% CI 1.07-1.19, $P < 0.001$; OS HR 1.16, 95% CI 1.07-1.24, $P < 0.001$) were prognostic. Early on-treatment ctDNA dynamics were also associated with outcomes, including the number of driver somatic mutations with VAF > 0.5% at both timepoints (PFS HR 1.39, 95% CI 1.27-1.53, $P < 0.001$; OS HR 1.51, 95% CI 1.35-1.68, $P < 0.001$) and the number of driver somatic mutations with a VAF increase (PFS HR 1.31, 95% CI 1.19-1.44, $P < 0.001$; OS HR 1.10, 95% CI 1.02-1.18, $P = 0.02$). A ctDNA-based risk model incorporating baseline and dynamic ctDNA features was independently prognostic from RECIST in multivariable models (test set: OS HR 4.10, 95% CI 1.93-8.72, $P < 0.001$; PFS HR 1.86, 95% CI 1.16-2.97, $P = 0.009$). The integration of ctDNA features into a clinical model improved survival discrimination for PFS [C-index 64.7% (± 2.5%) for a ctDNA and clinical model versus 59.3% (± 2.2%) for a clinical-only model, $P = 0.027$] and for OS [C-index 70.0% (± 3.4%) versus 60.3% (± 4.2%), $P = 0.035$]. Conclusions- Early on-treatment evolution of ctDNA is prognostic for both PFS and OS in advanced ER-positive/HER2-negative breast cancer. A ctDNA-based risk model improves upon traditional RECIST and clinical parameters, advocating for ctDNA as a prognostic biomarker in clinical practice.

25COASNOV10

Title: Impact of anthracyclines in genomic high-risk, node-negative, HR-positive/HER2-negative breast cancer

N. Chen et.al.

Annals of oncology, Volume 36, Issue 11, p1356-1365

https://doi.org/10.1016/j.annonc.2025.08.002

Abstract: The benefit of anthracyclines for patients with high 21-gene recurrence score (RS) is unclear, despite the widespread use of RS to guide adjuvant chemotherapy treatment for hormone receptor (HR)-positive /human epidermal growth factor receptor 2 (HER2)-negative breast cancer. This study aimed to assess whether patients with RS ≥ 31 would have improved outcomes with the addition of anthracyclines to taxane-based chemotherapy. Patients and methods-We included patients from TAILORx with RS ≥ 11 who received treatment with either taxanes with cyclophosphamide (TC) or taxane with anthracyclines/cyclophosphamide (T-AC). Distant recurrence-free interval (DRFI), distant recurrence-free survival (DRFS), and overall survival (OS) were compared, controlling for age, tumor size and grade, receptor status, and RS. Spline regression was used to estimate adjusted hazard ratio (aHR) for receipt of T-AC (versus TC) for these endpoints as a function of RS. Results-A total of 2549 patients who received either T-AC or TC were included in the primary analysis. In patients with RS ≥ 31, receipt of T-AC was associated with improved DRFI (5-year rate of 96.1% with T-AC versus 91.0% with TC, aHR 0.31, $P = 0.006$), DRFS (95.4% versus 89.8%, aHR 0.49, $P = 0.032$), and a trend toward improved OS (adjusted 5-year rate 97.3% versus 93.6%, aHR 0.67, $P = 0.31$). Spline regression demonstrated increasing anthracycline benefit with increasing RS. Conclusion-Patients with early-stage, HR-positive/HER2-negative breast cancer with the highest genomic risk disease (RS ≥ 31) may benefit from the addition of an anthracycline to taxane-based adjuvant chemotherapy.

Genomic RS testing may predict anthracycline benefit more accurately than clinicopathological factors such as nodal status.

25COASNOV11

Title: Prediction of survival after de-escalated neoadjuvant therapy in HER2-positive early breast cancer: a pooled analysis of three WSG trials

M. Graeser et.al.

Annals of oncology, Volume 36, Issue 11

https://doi.org/10.1016/j.annonc.2025.07.016

Abstract: We analyzed outcomes and survival predictors in three West German Study Group (WSG) randomized de-escalation trials (ADAPT-HR−/HER2+, ADAPT-TP, TP-II) in human epidermal growth factor receptor 2 (HER2)-positive early breast cancer (eBC) investigating short (12-week) neoadjuvant treatments with or without chemotherapy. Patients and methods- A total of 713 patients were analyzed; neoadjuvant chemotherapy (paclitaxel plus pertuzumab plus trastuzumab): n = 149, neoadjuvant chemotherapy-free (pertuzumab plus trastuzumab, trastuzumab-only)/antibody–drug conjugate (ADC, trastuzumab emtansine) treatment: n = 564. Patients with pathological complete response (pCR, ypT0/is ypN0) were allowed to omit further chemotherapy; chemotherapy was mandatory after non-pCR. The primary endpoint of each trial was pCR; survival was the secondary endpoint. Survival was analyzed using the Kaplan–Meier method and Cox regression. Results-Median follow-up was 60.7 months. In total, 10 (7%) and 74 (13%) invasive disease-free survival (iDFS) events, 8 (5%) and 51 (9%) distant DFS (dDFS) events, and 6 (4%) and 34 (6%) deaths occurred in the neoadjuvant chemotherapy and chemotherapy-free/ADC groups, respectively; the respective 5-year survival rates were 96% [95% confidence interval (CI) 92% to 99%] and 88% (95% CI 85% to 91%) for iDFS (hazard ratio 0.56, 95% CI 0.29-1.08, P = 0.083) and 98% (95% CI 93% to 99%) and 97% (95% CI 95% to 98%) for overall survival (hazard ratio 0.88, 95% CI 0.36-2.11, P = 0.775). The 5-year iDFS rates in patients with pCR were 98% (95% CI 91% to 99%) after chemotherapy and 94% (95% CI 89% to 97%) after chemotherapy-free/ADC treatment (hazard ratio 0.76, 95% CI 0.27-2.12, P = 0.609). iDFS was comparable between patients with and without adjuvant chemotherapy after pCR to chemotherapy-free/ADC treatment (hazard ratio 1.25, 95% CI 0.39-4.00, P = 0.712). In multivariable analysis, node-negative status and pCR were favorably associated with iDFS in the chemotherapy-free/ADC group. Conclusions- This pooled analysis demonstrates that neoadjuvant de-escalation trials with further pCR-adapted treatment (de-)escalation are feasible and appear safe for HER2-positive eBC patients. Twelve-weekly neoadjuvant paclitaxel plus HER2 blockade is effective and well tolerated. Neoadjuvant chemotherapy-free/ADC treatments can be viable alternatives for stage I-II eBC. Excellent survival after pCR to neoadjuvant chemotherapy-free/ADC treatment lays the groundwork for further de-escalation strategies.

25COASNOV12

Title: Re-examining post-operative chemoradiotherapy in head and neck cancer: an updated long-term combined analysis of RTOG 9501/EORTC 22931

Z.S. Zumsteg et.al.

Annals of oncology, Volume 36, Issue 11

https://doi.org/10.1016/j.annonc.2025.07.004

Abstract : Post-operative chemoradiation (CRT) is generally recommended for head and neck cancer patients with extranodal extension (ENE) and/or positive margins, but not for patients without these features, based on a *post hoc* analysis of Radiation Therapy Oncology Group (RTOG) 9501 and European Organisation for Research and Treatment of Cancer (EORTC) 22931. However, this analysis lacked tests of interaction necessary to identify a predictive biomarker. In addition, updated data are now available. Patients and methods- This study assessed 744 patients enrolled on RTOG 9501 and EORTC 22931, randomized trials that compared CRT with radiation (RT) following surgery. Overall survival (OS) was analyzed with Cox regression. Cancer-specific mortality (CSM), other-cause mortality (OCM), and recurrence outcomes were analyzed with competing risks methodology. Tests of interaction assessed for differential benefits of CRT in various subgroups. Results- Median follow-up was 6.9 years. Among all patients, CRT improved OS [hazard ratio (HR) 0.81, 95% confidence interval (CI) 0.68-0.97, $P = 0.026$]. Although CRT improved OS in the subgroup with ENE and/or positive margins (HR 0.71, 95% CI 0.57-0.89, $P = 0.003$) and not in those without these features (HR 0.94, 95% CI 0.68-1.30, $P = 0.7$), tests of interaction showed no evidence of a differential effect of CRT in these subgroups (P-interaction = 0.17). There was also no evidence of interaction when analyzing other outcomes, or when assessing ENE and margin status individually. While CRT significantly reduced CSM (HR 0.68, 95% CI 0.55-0.83, $P < 0.001$), it also significantly increased OCM (HR 1.51, 95% CI 1.07-2.12, $P = 0.018$). Post-operative CRT improved locoregional recurrence (HR 0.64, 95% CI 0.48-0.85, $P = 0.002$), but not distant metastasis (HR 0.83, 95% CI 0.64-1.08, $P = 0.17$). Conclusions- Concurrent chemotherapy improved OS in head and neck cancer patients undergoing post-operative radiotherapy in the combined populations of EORTC 22931 and RTOG 9501. ENE and/or positive margins are not predictive biomarkers, and patients without these features may still benefit from CRT. CRT improved CSM, but this was partly offset by higher OCM. Refining the population most likely to benefit from post-operative CRT, taking into consideration both oncologic and patient-related factors, needs further exploration.

25COASNOV13

Title: Incidence trends and long-term survival in early-onset colorectal cancer: a nationwide Swedish study

S. Barot et.al.

Annals of oncology, Volume 36, Issue 11
https://doi.org/10.1016/j.annonc.2025.07.019

Abstract: Early-onset colorectal cancer (EOCRC, diagnosis before age 50) is increasing globally. Survival comparisons with late-onset colorectal cancer (CRC) are inconsistent, however, and long-term excess mortality remains poorly understood. This Swedish population-based study aimed to evaluate trends in incidence, survival, and long-term excess mortality in early- versus late-onset CRC. Materials and methods-We identified all incident colorectal adenocarcinomas recorded in the Swedish National Cancer Register from 1993 to 2019. Incidence trends were quantified using annual percentage changes and relative survival differences were assessed using excess mortality rate ratios, both from Poisson regression models with 95% confidence intervals (CIs). Results-A total of 47 864 right-sided colon, 40 664 left-sided colon, and 47 082 rectal cancer cases were included. EOCRC patients were

more frequently diagnosed with metastatic disease, compared with late-onset CRC. EOCRC incidence increased across all subsites, with annual percentage changes ranging from 2.04 (95% CI 1.51-2.56) for rectal to 2.64 (95% CI 2.02-2.37) for right-sided colon cancer, while an increase among late-onset cases was observed only for right-sided colon cancer. Crude 5-year relative survival was similar across age groups, but after full adjustment (including metastatic stage), EOCRC was associated with better survival, with excess mortality rate ratios ranging from 0.76 (95% CI 0.68-0.84) for rectal cancer to 0.83 (95% CI 0.74-0.92) for right-sided colon cancer. Notably, excess mortality remained elevated 5-10 years after diagnosis in both age groups. Conclusions- EOCRC incidence is increasing in Sweden, aligning with global trends. Although younger patients were more often diagnosed at an advanced stage of disease, they had similar crude survival and better stage-adjusted survival, compared with older patients. The persistent long-term excess mortality in both groups, even during periods when CRC patients are typically considered statistically cured, highlights the need for extended follow-up and tailored survivorship care.

25COASNOV14

Title: Efficacy and safety of biweekly single-dose actinomycin D versus multiday methotrexate in low-risk gestational trophoblastic neoplasia: a prospective multicenter randomized trial

F. Jiang et.al.

Annals of oncology, Volume 36, Issue 11

https://doi.org/10.1016/j.annonc.2025.06.006

Abstract: Cure rates for low-risk gestational trophoblastic neoplasia (GTN) are high, but there is no consensus on optimal first-line chemotherapy. Here we evaluated the efficacy and safety of biweekly single-dose actinomycin D (Act-D) versus an 8-day methotrexate (MTX)-folinic acid regimen as first-line single-agent chemotherapy for low-risk GTN. Patients and methods-This multicenter, randomized, controlled trial enrolled patients with International Federation of Gynecology and Obstetrics (FIGO) stage I-III, low-risk GTN (FIGO 2000 prognostic scores 0-4) across eight centers in China (ClinicalTrials.gov identifier: NCT04562558). Patients were randomized (1 : 1) to Act-D (1.25 mg/m^2, maximum 2 mg, every 14 days) or MTX-folinic acid (50 mg i.m. days 1, 3, 5, and 7; leucovorin rescue, days 2, 4, 6, and 8). Treatment continued until β-human chorionic gonadotropin normalization, followed by 2-3 consolidation cycles. Primary outcomes were complete remission (CR) rates for single-agent chemotherapy and overall CR rates. Secondary outcomes were time to CR, chemotherapy cycles, toxicity, and anti-Müllerian hormone changes. Results-Between 27 September 2020, and 18 June 2024, 228 patients were randomized to MTX or Act-D. Act-D achieved significantly higher single-agent CR rates than MTX (72.8% versus 54.4%, P = 0.0038) with shorter median remission time (7.86 versus 9.43 weeks, P = 0.0296). Overall CR rates were 100% in both groups following combination chemotherapy for resistant cases. Most adverse events were grade 1-2, but grade ≥2 nausea and vomiting and hair loss were more frequent with Act-D, and alanine aminotransferase was more frequently elevated in the MTX group. Anti-Müllerian hormone reductions were transient in both groups. After a 28.5-month median follow-up, recurrence rates remained low and comparable (MTX 0.88% versus Act-D 0.88%; P > 0.05). Fertility outcomes were favorable in both groups. Conclusions-Biweekly Act-D demonstrated superior efficacy and faster remission than the 8-day MTX

regimen as first-line single-agent chemotherapy for low-risk GTN, offering a well-tolerated option despite a higher incidence of nausea, vomiting, and hair loss.

25COASNOV15

Title:. Efficacy and safety of biweekly single-dose actinomycin D versus multiday methotrexate in low-risk gestational trophoblastic neoplasia: a prospective multicenter randomized trial

F. Jiang et.al

Annals of oncology, Volume 36, Issue 10 p1123-1131

https://doi.org/10.1016/j.annonc.2025.06.006

Abstract: Cure rates for low-risk gestational trophoblastic neoplasia (GTN) are high, but there is no consensus on optimal first-line chemotherapy. Here we evaluated the efficacy and safety of biweekly single-dose actinomycin D (Act-D) versus an 8-day methotrexate (MTX)-folinic acid regimen as first-line single-agent chemotherapy for low-risk GTN. Patients and methods-This multicenter, randomized, controlled trial enrolled patients with International Federation of Gynecology and Obstetrics (FIGO) stage I-III, low-risk GTN (FIGO 2000 prognostic scores 0-4) across eight centers in China (ClinicalTrials.gov identifier: NCT04562558). Patients were randomized (1 : 1) to Act-D (1.25 mg/m^2, maximum 2 mg, every 14 days) or MTX-folinic acid (50 mg i.m. days 1, 3, 5, and 7; leucovorin rescue, days 2, 4, 6, and 8). Treatment continued until β-human chorionic gonadotropin normalization, followed by 2-3 consolidation cycles. Primary outcomes were complete remission (CR) rates for single-agent chemotherapy and overall CR rates. Secondary outcomes were time to CR, chemotherapy cycles, toxicity, and anti-Müllerian hormone changes. Results-Between 27 September 2020, and 18 June 2024, 228 patients were randomized to MTX or Act-D. Act-D achieved significantly higher single-agent CR rates than MTX (72.8% versus 54.4%, P = 0.0038) with shorter median remission time (7.86 versus 9.43 weeks, P = 0.0296). Overall CR rates were 100% in both groups following combination chemotherapy for resistant cases. Most adverse events were grade 1-2, but grade ≥2 nausea and vomiting and hair loss were more frequent with Act-D, and alanine aminotransferase was more frequently elevated in the MTX group. Anti-Müllerian hormone reductions were transient in both groups. After a 28.5-month median follow-up, recurrence rates remained low and comparable (MTX 0.88% versus Act-D 0.88%; P > 0.05). Fertility outcomes were favorable in both groups. Conclusions-Biweekly Act-D demonstrated superior efficacy and faster remission than the 8-day MTX regimen as first-line single-agent chemotherapy for low-risk GTN, offering a well-tolerated option despite a higher incidence of nausea, vomiting, and hair loss.

25COASNOV16

Title: *DNA methyltransferase 3A (DNMT3A)* mutations and PD-(L)1 blockade efficacy in non-small-cell lung cancer

B. Ricciuti et.al.

Annals of oncology, Volume 36, Issue 10 p1123-1131

https://doi.org/10.1016/j.annonc.2025.06.003

Abstract: Despite significant improvements in overall survival with programmed cell death protein (ligand) 1 [PD-(L)1] inhibition, most patients with metastatic non-small-cell lung cancer (NSCLC) do not respond to immune checkpoint inhibition (ICI). Growing evidence

suggests the importance of genomic alterations in modulating anticancer immune response and predicting ICI efficacy. However, the genomic correlates of response to ICI in NSCLC are largely unknown. Design-Patients with advanced NSCLC treated with ICI and comprehensive genomic profiling from multiple independent cohorts were included. Beta-binomial modelling of sequencing read counts was used to infer mutation clonality. NSCLC samples from Cancer Genome Atlas Program (TCGA) and NSCLC cell lines from Cancer Cell Lines Encyclopedia (CCLE) were used for transcriptomic analyses. Results-Among 1539 NSCLCs, we identified deleterious *DNA methyltransferase 3A* (*DNMT3A*) mutations in 4.7% of cases. Patients with *DNMT3A*-mutant NSCLC had improved response rate (41.7% versus 21.5%, $P < 0.001$), progression-free survival [hazard ratio (HR) 0.61, $P < 0.001$], and overall survival (HR 0.66, $P < 0.01$) with PD-(L)1 blockade, compared with *DNMT3A* wild-type cases. *DNMT3A* mutations had no impact on OS among patients with advanced NSCLC who did not receive ICI (HR 0.88, $P = 0.41$). In examining the impact of *DNMT3A* clonality on immunotherapy outcomes to account for potential clonal hematopoiesis of indeterminate potential contamination, we confirmed that clonal *DNMT3A* mutations were associated with improved outcomes compared with *DNMT3A* wild-type cases. In NSCLC cell lines with pathogenic *DNMT3A* mutations, DNMT3A RNA and protein expression were decreased. In the TCGA, NSCLCs with high versus low DNMT3A expression exhibited lowered expression of pathways involved in innate and adaptive immune response, including interferon-γ (INFγ), major histocompatibility complex (MHC)-II antigen presentation, tumor necrosis factor-α (TNF-α), and PD-1 signaling. Conclusion-Somatic *DNMT3A* mutations can be detected in a fraction of NSCLCs and are associated with a decreased DNMT3A expression and a favorable immunophenotype, and predict improved ICI efficacy.

25COASNOV17

Title: Identifying the genomic landscape of *EGFR*-mutant lung cancers with central nervous system metastases

J.A. Wilcox et.al.

Annals of oncology, Volume 36, Issue 11

https://doi.org/10.1016/j.annonc.2025.06.001

Abstract: Despite the intracranial efficacy of osimertinib, central nervous system (CNS) metastases remain a major cause of morbidity and mortality in *EGFR*-mutant non-small-cell lung cancer (NSCLC). The genomic drivers of CNS dissemination are poorly understood. Patients and methods-We analyzed the clinicogenomic features of patients with *EGFR*-mutant NSCLC receiving first-line osimertinib with extracranial next generation sequencing (NGS) ($n = 262$) and individuals with intracranial NGS ($n = 81$). Paired extra- and intracranial NGS was available for 14 patients. Time-to-event analyses were conducted from time of metastatic diagnosis, except for time-to-treatment discontinuation (TTD), which began at treatment initiation. Results-Among 262 patients receiving first-line osimertinib, 53% developed CNS metastases (36% *de novo*, 16% acquired on treatment). The cumulative incidence of brain (BrM) and leptomeningeal metastases (LM) was 39% and 2% at 1 year, 49% and 6% at 3 years, and 54% and 12% at 5 years, respectively. CNS metastases correlated with a higher frequency of *CARD11* amplifications (14% versus 3%, $P = 0.031$) and a lower frequency of *MDM2* amplifications (1% versus 13%, $P = 0.008$) in extracranial NGS specimens, with otherwise similar genomic profiles. Patients who developed CNS

metastases on treatment had worse overall survival (OS) [hazard ratio (HR) = 3.67, 95% confidence interval (CI) 2.41 to 5.59], followed by those with *de novo* (HR = 1.61, 95% CI 1.15 to 2.26), compared with those who never developed CNS metastases ($P < 0.001$). In multivariable Cox regression, atypical *EGFR* mutations were associated with shorter OS. Cell cycle pathway alterations were more frequent in BrM than LM samples (93% versus 47%, $P = 0.003$, q = 0.03). No other significant genomic differences were found between BrM and LM, or between paired CNS and systemic samples. Conclusions- Patients with atypical *EGFR* mutations or acquired CNS metastases on osimertinib have worse outcomes. Comparative NGS profiling of intra- and extracranial tumors suggest that CNS dissemination is driven by mechanisms beyond single-gene alterations.

25COASNOV18

Title: Neoadjuvant intralesional targeted immunocytokines (daromun) in stage III melanoma

K.C. Kähler et.al.

Annals of oncology, Volume 36, Issue 11

https://doi.org/10.1016/j.annonc.2025.06.014

Abstract: This phase III trial assessed daromun, a combination of two fibronectin-targeting immunocytokines (L19IL2 and L19TNF), as a neoadjuvant treatment for patients with clinically detectable stage IIIB/C melanoma [American Joint Committee on Cancer (AJCC) version 7]. Patients and methods- Patients were randomized to weekly intralesional daromun administrations (13 million IU of L19IL2 and 400 µg of L19TNF) for 4 weeks followed by surgery, or upfront surgery. Pretreatment with approved adjuvant agents was allowed. The primary endpoint was recurrence-free survival (RFS): events were disease recurrence or death from any cause after complete surgical tumor resection (ClinicalTrials.gov NCT02938299). Results- A total of 246 patients were randomized and included in the intention-to-treat analysis: 74% had undergone two or more prior surgical resections and 35% had received prior systemic therapy. At a median follow-up of 21 months, the neoadjuvant group ($n = 122$) had a significantly longer RFS than the upfront surgery group ($n = 124$), with a median RFS of 16.7 months and 6.8 months, respectively [hazard ratio (HR) 0.59, 95% confidence interval (CI 0.41-0.86), $P = 0.005$, log-rank test]. The risk of distant recurrence was reduced by 40% in the neoadjuvant arm (HR 0.60, 95% CI 0.37-0.95, $P = 0.029$). Grade ≥3 treatment-related adverse events (TRAEs) were 6.7% in the surgery-alone arm and 27.1% in the daromun arm, mostly injection site reactions. Conclusions- Neoadjuvant daromun resulted in a significantly longer RFS than upfront surgery in patients with locally advanced melanoma. TRAEs were transient and manageable. Neoadjuvant daromun is a new therapeutic option for patients with stage III melanoma, including those with locoregional recurrence after surgery and previous adjuvant therapy.

25COASNOV19

Title: *BRCA1/2* and homologous recombination repair alterations in high- and low-volume metastatic hormone-sensitive prostate cancer: prevalence and impact on outcomes

D. Olmos et.al.

Annals of oncology, Volume 36, Issue 10

https://doi.org/10.1016/j.annonc.2025.05.534

Abstract: Alterations in *BRCA1/2* (BRCA) and other homologous recombination repair (HRR) genes have a negative impact on outcomes in patients with metastatic castration-resistant prostate cancer (mCRPC). Poly(adenosine diphosphate-ribose) polymerase inhibitors, the only treatment demonstrated to improve the prognosis of patients with mCRPC, are also being developed for the treatment of patients with metastatic hormone-sensitive prostate cancer (mHSPC). To fully assess their potential benefit in this setting, it is essential to understand how BRCA and HRR defects may influence the prognosis of conventionally treated patients with low and high disease volume. Patients and methods-Eligible mHSPC patients diagnosed between January 2018 and December 2023 underwent paired somatic/germline DNA sequencing. Cases with alterations in one or more HRR genes were classified as BRCA, HRR non-BRCA, non-BRCA or non-HRR. Radiographic progression-free survival, time to castration resistance and overall survival were reported for all subgroups; associations between mutations and outcomes were assessed after controlling for treatment modality and baseline characteristics using inverse probability of treatment weighting models. Results-Of 556 patients, 159 (28.6%) had HRR gene alterations: 69 (12.4%) with BRCA and 90 (16.2%) with HRR non-BRCA mutations. mHSPC was synchronous in 451 patients (81.1%) and was classified as high-volume (CHAARTED criteria) in 306 (55%) patients. Within the HRR subgroup, patients with BRCA mutations had significantly worse outcomes across all endpoints ($P < 0.005$ for all comparisons). Differences in prognosis by BRCA and HRR status were observed in both low- and high-volume subgroups and were independent of treatment with androgen receptor pathway inhibitors or taxanes. Conclusion-Presence of HRR mutations, particularly BRCA alterations, significantly worsened prognosis, regardless of disease volume or treatment regimen. These findings underscore the importance of integrating tumour biology for accurate risk stratification in mHSPC and the design of new treatment strategies and follow-up.

25COASNOV20

Title: Predicting the 10-year risk of cardiomyopathy in long-term survivors of childhood cancer

K. Petrykey et.al.

Annals of oncology, Volume 36, Issue 10
https://doi.org/10.1016/j.annonc.2025.05.539

Abstract: Considering the heightened risk of cancer treatment-related cardiomyopathy and cardiac death in long-term survivors of childhood cancer, we aimed to develop and validate a clinically applicable risk prediction model for cardiomyopathy. Patients and methods-Childhood cancer survivors from the St. Jude Lifetime Cohort, [SJLIFE, model-development; $n = 3479$; median age 32.3 years, interquartile range (IQR) 24.4-40.9 years] and the Childhood Cancer Survivor Study (CCSS, model-validation; $n = 6875$; median age 33.2 years, IQR 27.9-38.9 years) were assessed for demographic and cardiovascular risk factors, treatment exposures, and polygenic risk scores (PRSs) for cardiomyopathy, heart failure, cardiac structure and function, and anthracycline-related cardiomyopathy risk. Multivariable Poisson regression predicted the 10-year risk of cardiomyopathy (Common Terminology Criteria for Adverse Events grade ≥3: requiring heart failure medications or heart transplantation or leading to death) following baseline visit/survey. Model

performance was assessed by area under the receiver operating characteristic curve (AUC). Results-Cardiomyopathy was clinically identified in 75 (2.2%, SJLIFE) and self-reported in 87 (1.3%, CCSS) survivors within 10 years of the baseline assessment. AUC of the clinical model with sex, age at cancer diagnosis, cumulative anthracycline, and mean heart radiation doses was 0.833 (SJLIFE) and 0.812 (CCSS). Age at baseline, hypertension, and genetic ancestry showed associations with higher cardiomyopathy rates in SJLIFE but did not increase AUC in CCSS (0.812). Adding PRSs for hypertrophic cardiomyopathy and left ventricular end-systolic volume improved AUC in CCSS (0.822; $P = 0.016$). Compared with existing survivorship-care guidelines, the PRS model classified fewer survivors as high-risk or moderate-risk, while identifying survivors in those categories as having 1.5-times greater risk. Conclusions-We developed and validated models with highest-to-date performance for estimating the 10-year risk of cardiomyopathy in survivors of childhood cancer. Results could enhance identification of at-risk survivors beyond current guidelines.

25COASNOV21

Title: Enfortumab vedotin plus pembrolizumab in untreated locally advanced or metastatic urothelial carcinoma: 2.5-year median follow-up of the phase III EV-302/KEYNOTE-A39 trial

T.B. Powles et.al.

Annals of oncology, Volume 36, Issue 10

https://doi.org/10.1016/j.annonc.2025.05.536

Abstract: At the primary analysis of the EV-302 trial, enfortumab vedotin plus pembrolizumab (EV+P) demonstrated a statistically significant and clinically meaningful improvement in progression-free survival (PFS) and overall survival (OS) compared with chemotherapy in patients with previously untreated locally advanced or metastatic urothelial carcinoma (la/mUC). Patients and methods-We present an updated analysis of efficacy and safety in the overall population, with a median follow-up of 2.5 years, providing an additional year of follow-up since the primary analysis. Results-The median PFS by blinded independent central review was 12.5 months [95% confidence interval (CI) 10.4-16.6 months] for the EV+P arm and 6.3 months (95% CI 6.2-6.5 months) for the chemotherapy arm [hazard ratio (HR) 0.48, 95% CI 0.41-0.57]. The median OS was 33.8 months (95% CI 26.1-39.3 months) for the EV+P arm and 15.9 months (95% CI 13.6-18.3 months) for the chemotherapy arm (HR 0.51, 95% CI 0.43-0.61). Safety data with an additional year of follow-up were consistent with those of the primary analysis. Conclusion-The continued survival benefit with EV+P compared with chemotherapy in this updated analysis reinforces EV+P as the standard of care for the first-line treatment of patients with la/mUC.

25COASNOV22

Title: Utility of the Singapore recurrence nomogram in a US cohort with a higher proportion of borderline and malignant phyllodes tumours

Ellery H Reason et.al.

Journal of clinical pathology, Volume 78, Issue 11

https://doi.org/10.1136/jcp-2025-210252

Abstract: Aims For phyllodes tumours (PT), local and distant recurrence rates increase with higher grades and are difficult to predict. The Singapore nomogram has been used to predict recurrence events for PT. We aimed to test this nomogram for accuracy in a US cohort and to compare with a histological score. Methods Patients with PT were selected from a prospective institutional database. Histological parameters and margin status were used to estimate the nomogram score and the histological score, as previously defined. Multivariable analyses were used to estimate the association of recurrence-free survival (RFS) with individual factors, nomogram score and histological score. Harrel's C-index was estimated. Results Of 81 PT cases, 25.9% were benign, 40.7% borderline and 33.3% malignant. Recurrences occurred in 33.3% (n=27). The adjusted RFS analysis including the four factors used in the Singapore nomogram performed well (C-index of 0.78). However, despite a higher nomogram score being associated with increased risk of recurrence (HR 1.03, 1.01–1.05, p=0.007), the individual numeric scale defined in the nomogram only moderately fit our data (C-index of 0.66). Patients with higher histological scores also had an increased risk of recurrence (HR 1.25, 1.07–1.47, p=0.005; C-index of 0.70). Conclusion Histological score more accurately predicted PT recurrence in our cohort, which includes a higher proportion of higher-grade PT. Refining the nomogram to include factors specific to malignant PT and factors with more variance, as well as refining the assigned weights, may result in improved performance. This study identifies an opportunity for international collaboration to refine the predictive model.

25COASNOV23

Title: High upgrade rate to invasive carcinoma makes subclassification of papillary carcinoma of the breast in core needle biopsy unnecessary

Di Ai et.al.

Annals of oncology, Volume 36, Issue 10
DOI-https://doi.org/10.1136/jcp-2025-210259

Abstract: Aims Papillary carcinoma diagnosed in core needle biopsy (CNB) refers to carcinoma with papillary features but no definitive invasion, including papillary ductal carcinoma in situ (DCIS), papilloma with DCIS, encapsulated papillary carcinoma (EPC) and solid papillary carcinoma (SPC). This study assesses the upgrade rate of papillary carcinoma in CNB and supports the use of 'papillary carcinoma' as an umbrella term. Methods A retrospective review identified 41 CNB cases of non-invasive papillary carcinoma with subsequent excision (2011–2018). H&E and immunohistochemistry slides from CNBs were reviewed, and excisional diagnoses were retrieved. Results All 41 CNB cases were either DCIS or upgraded to invasive carcinoma upon excision, with an overall upgrade rate to invasive carcinoma of 39% (16/41). Subtypes showed varying upgrade rates: 16.7% (1/6) for papillary DCIS, 25% (1/4) for papilloma with DCIS, 83.3% (5/6) for SPC, 100% (1/1) for EPC and 33.3% (8/24) for unclassifiable papillary carcinoma. No lymph node metastases, recurrences or breast cancer-related mortality were observed during the follow-up period. Conclusions Given the high upgrade rate, subclassification of papillary carcinoma in CNB lacks clinical significance. The term 'papillary carcinoma' should be used in CNB, and lymph node removal warrants further investigation.

25COASNOV24

Title: Rethinking alcoholic foamy degeneration of the liver: a study of nine cases highlighting complex pathological findings

Dhaarica Jeyanesan et.al.

Annals of oncology, Volume 36, Issue 10
DOI-https://doi.org/10.1136/jcp-2024-209939

Abstract: Aims To reveal clinicopathological characteristics of alcoholic foamy degeneration (AFD)—an uncommon form of alcoholic liver injury. Methods Clinicopathological features of AFD (n=9) were examined in comparison to those of severe alcoholic hepatitis (SAH; n=12). Results Patients with AFD presented with either biochemical liver dysfunction (n=1) or clinical jaundice (n=8). One case had undergone liver transplantation for alcohol-related cirrhosis and hepatocellular carcinoma 2 years and 3 months before presentation. AFD cases were histologically classified into three groups. The non-jaundiced case had mixed macro- and microvesicular bland steatosis. Seven jaundiced cases showed more complex microscopic features with lobular inflammation, acidophilic bodies, cholestasis and lobular distortion. Hepatocytes were pleomorphic, some extensively enlarged with clear cytoplasm, somewhat resembling ballooning degeneration; however, it was mainly due to accumulated lipid droplets ('pseudoballooning'). The remaining case also had predominant changes of AFD, but a few foci showed classical ballooning hepatocytes and Mallory–Denk bodies, in keeping with mixed AFD and steatohepatitis. When compared with patients with SAH, those with AFD had lower white blood cell and neutrophil counts and higher cholesterol levels (all $p<0.001$). On imaging, ascites and varices were less common in AFD than in SAH (11% vs 75%, $p=0.014$; 0% vs 67%, $p=0.008$, respectively). All seven patients with AFD who successfully abstained from alcohol experienced rapid improvement in liver function. Conclusions- Microscopic findings of AFD are more complex than currently thought, and some cases may be mistaken for steatohepatitis. AFD may also develop in conjunction with steatohepatitis or following liver transplantation.

25COASNOV25

Title: Gone but not forgotten: expanding the spectrum of ORISE (submucosal lifting agent) associated diagnostic pitfalls and complications

Pooja Dhorajiya et.al.

Annals of oncology, Volume 36, Issue 10
https://doi.org/10.1136/jcp-2024-209419

Abstract: Aims A synthetic lifting agent, ORISE, used for endoscopic mucosal resections, has been recalled from the market since November 2022 due to clinical complications. Despite this, the impact of ORISE-associated complications is expected to persist in the foreseeable future. We present a large single institutional series of therapeutic resections from patients for whom ORISE was used for initial endoscopic procedures, highlighting the pitfalls and complications associated with its use. Methods All specimens showing lifting agent granulomata (LAGs) associated with the use of ORISE were identified. The H&E slides were reviewed to define the morphological characteristics and extent of LAG in the intestinal wall and other organs. The clinical impression and gross findings were compared with the final pathological diagnosis. Results 34 cases (28 resections and 6 repeat endoscopic mucosal resection specimens) showed LAG. On microscopy, 20.5% showed no residual disease,

64.7% also showed residual precursor lesion and 14.7% also showed malignancy. In 64.2% of cases, a mass lesion was seen grossly but no malignancy was identified microscopically. ORISE was present in vascular spaces (n=9), lymph nodes (n=2), other organs such as appendix (n=1) and omentum/peritoneum (n=1). The major discordance between clinical impression (mass/neoplasm) and final pathology (no residual malignancy) was seen in 4/34 (11.8%) cases. LAGs were seen up to 10 months after the use of ORISE in the prior endoscopic procedure. Conclusion ORISE deposits may mimic residual/disseminated neoplasm and prompt inadvertent changes in surgical decisions. Awareness of this pitfall is essential to prevent unwarranted surgical resections in patients undergoing follow-up for endoscopically resected lesions.

25COASNOV26

Title: Invasion risk of cutaneous squamous cell carcinoma in situ by histological subtype: a retrospective cohort study

Danielle K Stamer et.al.

Annals of oncology, Volume 36, Issue 10

https://doi.org/10.1136/jcp-2024-209608

Abstract: Aims Cutaneous squamous cell carcinoma in situ (SCCis) can be classified histopathologically into four subtypes: full-thickness (FT), hypertrophic actinic keratosis (HAK), Bowenoid, and acantholytic types. 3%–5% of SCCis lesions progress to invasive squamous cell carcinoma (iSCC), however progression risk by subtype has not been assessed. Aim one of this study is to quantitatively assess the risk of iSCC associated with each histological subtype of SCCis. Aim two is to evaluate if the histological grade of iSCC differs among subtypes of the associated SCCis. Methods The pathology information system at our institution was queried for cutaneous SCCis cases with and without associated iSCC from 2020 to 2022. The study group consisted of 65 cases of SCCis with associated iSCC and control group 65 randomly selected cases of SCCis without invasion. For each case SCCis subtype was classified as FT, HAK, Bowenoid or acantholytic type. iSCCs were classified as low grade if well to moderately differentiated (LG) and high grade (HG) if moderately to poorly differentiated. Results iSCC was most often associated with HAK-type SCCis, followed by acantholytic and FT-type SCCis, with Bowenoid type rarely associated with iSCC. 41% (14/34) of iSCCs associated with HAK-type SCCis were HG compared with 84% (21/25) for FT-type SCCis. Conclusions iSCC is most often associated with HAK-type SCCis, followed by acantholytic and FT-types, and rarely with Bowenoid type. HG invasive SCC is most often associated with FT-type, and LG with HAK-type SCCis. Stratifying SCCis by subtype can inform clinical management.

25COASNOV27

Title: Immunohistochemical evaluation of ERG expression in soft tissue tumours: a tissue microarray study of 489 cases

David I Suster et.al.

Annals of oncology, Volume 36, Issue 10

https://doi.org/10.1136/jcp-2025-210045

Abstract: Aims To investigate immunohistochemical expression of the E26 transformation-specific factors (ETS)-related gene (*ERG*) in a large number of soft tissue neoplasms using a

tissue microarray technique. Methods 489 cases of soft tissue neoplasms, including benign and malignant entities, were collected from the files of the respective institutions and constructed into tissue microarrays. Tissue microarrays were stained for ERG immunohistochemistry using two antibodies, EP111 and EPR3864. Results A total of 25 cases (5.1%) were identified that were positive for ERG using the monoclonal antibody EP111 and 15 cases (3%) using the monoclonal antibody EPR3864, including rhabdomyosarcoma, peripheral nerve sheath tumours, synovial sarcoma, myxofibrosarcoma, epithelioid sarcoma, dermatofibrosarcoma protuberans, low-grade fibromyxoid sarcoma, nodular fasciitis and dedifferentiated liposarcoma. The most consistently stained tumours included synovial sarcoma, rhabdomyosarcoma and benign and malignant peripheral nerve sheath tumours. Various other fibroblastic proliferations, including dermatofibrosarcoma protuberans, myxofibrosarcoma, low-grade fibromyxoid sarcoma and nodular fasciitis, also showed positive staining in a small fraction of cases. One case of dedifferentiated liposarcoma showed nuclear positivity for ERG, and one case of epithelioid sarcoma was also positive. Conclusions This study supports the value of ERG as a highly sensitive and specific marker for the diagnosis of vascular neoplasms but also demonstrates rare cases of aberrant staining and underscores the need to assess soft tissue tumours using a panel of stains and interpret the results of immunohistochemistry in the appropriate histological and clinical context.

25COASNOV28

Title: FNA biopsy of breast specimens effectively harvests cells for patient-derived organoids modeling ductal carcinoma in situ

Julia Ye MD et.al.

Cancer cytopathology, Volume133, Issue11

https://doi.org/10.1002/cncy.70052

Abstract: Patient-derived organoids (PDOs) generated from benign breast tissue and breast carcinomas have successfully recapitulated their in vivo counterparts. PDOs model tumorigenesis and allow for screening novel therapeutics personalized to individual patients. However, acquiring cells to generate PDOs is cumbersome. This study demonstrates the feasibility of fine-needle aspiration biopsy (FNAB) for harvesting cells for PDOs modeling ductal carcinoma in situ (DCIS) and compares the efficacy with core needle biopsy (CNB). Methods-Surgical specimens from patients with biopsy-proven DCIS were used for this study. CNB was performed on fresh specimens in the operating room, and tissue was mechanically dissociated before culture in basement membrane extract (BME) and organoid medium to generate PDOs. FNAB was performed in the pathology gross room on fresh specimens, and the aspirate was similarly submitted for culture. Results-PDOs were successfully generated in 15 of 18 specimens obtained by CNB and seven of 11 specimens obtained by FNAB. The average time to initial organoid growth was 4 days for FNAB specimens compared to 19.3 days for CNB specimens. Tumor cells were seen on seven of 11 FNAB smears and 16 of 18 CNB touch preps. Immunofluorescence staining confirmed the presence of both luminal and myoepithelial cells in derived PDOs. Conclusions-FNAB effectively obtains cells for PDOs modeling DCIS. CNB yielded PDOs with a high success rate, but they were slow to establish. The time to organoid growth was significantly shorter

for FNAB specimens. Thus, FNAB offers an efficient alternative for breast PDO culture and can reduce the time and resources spent on generating PDO cultures.

25COASNOV29

Title: Diagnostic utility of p53, SMAD4, and the novel biomarker PON2 in FNA of pancreatic ductal adenocarcinoma

Ruimeng Yang et.al.

Cancer cytopathology, Volume133, Issue11

https://doi.org/10.1002/cncy.70058

Abstract: Accurate cytologic diagnosis of pancreatic ductal adenocarcinoma (PDAC) remains challenging. In this retrospective study, the authors assessed the utility of p53, SMAD4, and paraoxonase-2 (PON2) expression in fine-needle aspiration (FNA) diagnosis of PDAC. Methods-Cytologic cases with sufficient cell block material were retrieved from pathology archives. p53 and SMAD4 immunostains were performed in two separate cohorts, primary cohort (10 benign and 23 PDAC cases) and indeterminate cohort (3 atypical and 17 suspicious cases). PON2 immunostain was performed in the primary cohort (10 benign and 23 PDAC cases). p53 and SMAD4 immunostains were qualitatively assessed and PON2 test was evaluated by semiquantitative H-score. Results-In the primary cohort, p53 aberrant expression and SMAD4 loss were identified in 74% and 48% of PDAC cases compared to none in benign lesions. The combination of p53 and SMAD4 achieved a superior performance with an area under the curve (AUC) value of 0.96, compared to either marker alone (AUC = 0.87 and 0.74, respectively). In the indeterminate cohort, p53 aberrant expression or SMAD4 loss was seen in 13 of 17 (76%) malignant follow-up cases. PON2 was variably expressed in PDAC cases with H-scores ranging from 110 to 290, significantly higher in PDACs compared to benign cases ($p < .001$). Furthermore, strong PON2 expression was seen in two PDAC cases with wild-type p53 and intact SMAD4 expression. Conclusions-Combined p53 and SMAD4 immunostaining could help improve FNA diagnosis of PDACs, particularly in challenging cases. PON2 is differentially expressed in PDAC cases and may serve as a potential biomarker, warranting further investigation.

25COASNOV30

Title: Neutrophil-calibrated atypical squamous cells in ThinPrep urine cytology for detecting squamous differentiation in urothelial carcinoma

Ayako Furuhata CT, IAC, PhD et.al.

Cancer cytopathology, Volume133, Issue11

https://doi.org/10.1002/cncy.70055

Abstract: Urothelial carcinoma with squamous differentiation (UCSD) carries adverse outcomes, yet cytological recognition is challenging because keratinized atypical squamous cells (ASCs) often show deceptively low nuclear-to-cytoplasmic ratios. A size-based ASC classification anchored to neutrophils was evaluated as a biological internal reference. Methods-All cytology specimens were prepared with the ThinPrep liquid-based cytology system. Seventeen urine cytology specimens from histologically confirmed UCSD and 79 cytologically benign (BE) specimens with squamous cells were retrospectively reviewed. ASCs with orangeophilic cytoplasm were subclassified by nuclear size relative to the adjacent neutrophils: ASC-S (small nuclei; >1× neutrophil) and ASC-L (large nuclei; >2×

neutrophil). Counts were obtained from five high-power fields. UCSD was stratified by the extent of squamous differentiation (<50% vs. ≥50%). Results-No ASC-S/L was identified in BE specimens, whereas either subtype was present in 15 of the 17 UCSD cases, which yielded a cohort-level sensitivity of 88% and specificity of 100% for UCSD detection (95% CI, 65.7%–96.7% and 95.4%–100%, respectively). ASC-S was more prevalent than ASC-L, and was observed across Paris System categories—including atypical urothelial cells (AUCs)—whereas ASC-L appeared mainly in suspicious for high-grade urothelial carcinoma/high-grade urothelial carcinoma. ASC-S counts tended to increase with greater histological squamous differentiation, and were detectable even when tissue involvement was <50%. Conclusions-Neutrophil-calibrated ASC classification provides an objective, biologically grounded framework that aligns cytology with histology in UCSD. Reporting ASC-S/L—particularly ASC-S in equivocal (AUC) specimens—may facilitate earlier recognition of squamous differentiation and inform subsequent tissue evaluation. Prospective, multi-institutional validation with interobserver agreement and receiver operating characteristic–based thresholds is warranted.

25COASNOV31

Title: Assessment of the efficiency and accuracy of an artificial intelligence assistive system in the diagnosis of Pap cervical atypical glandular cell cytology

Xin Zhang MD et.al.

Cancer cytopathology, Volume133, Issue11

https://doi.org/10.1002/cncy.70056

Abstract: A diagnosis of atypical glandular cells (AGC) on Papanicolaou (Pap) slides is rare but has clinically significant findings associated with high-risk cervical and endometrial lesions. The authors evaluated the efficiency and diagnostic performance of an artificial intelligence (AI)-assisted platform (Riuqian WSI-2400; with the registered trademark AICyte) in identifying AGCs on Pap slides. Methods- A retrospective analysis of 485 Pap cases was conducted, including 185 cases with AGCs, 50 cases with high-grade squamous intraepithelial lesions, 50 cases with low-grade squamous intraepithelial lesions, and 200 negative cases; of these, 264 cases had histologic correlations. An experienced cytopathologist reviewed all slides using conventional microscopy and AICyte. Then, the same cases were evaluated by two other pathologists using the AICyte system. Results- The initial study demonstrated a kappa value of 0.744, which indicated strong agreement of the Pap interpretation from the same pathologist between using microscopy and AICyte methods, whereas the average interpretation time was significantly reduced with AICyte (137 vs. 44 seconds). Diagnostic consensus among three pathologists using the AICyte system was strong, with a Kendall W coefficient of 0.802. The AICyte-pathologist consensus reached an exact match with original interpretations in 95.1% of cases. AICyte-assisted interpretations demonstrated improved specificity and diagnostic accuracy for glandular lesions compared with original interpretations while maintaining 100% sensitivity and negative predictive value. Conclusions- To the authors' knowledge, this is the first study focusing on assessment of AGCs on an artificial intelligence system. The findings demonstrated that the AICyte system offers substantial improvements in efficiency and diagnostic consistency for the interpretation of AGCs and significantly reduces slide reading time. These results support the

potential of AI to augment performance, especially in resource-limited settings or high-volume screening environments.

25COASNOV32

Title: Prognostic significance of pelvic washing cytology in early stage endometrial cancer: A 10-year matched cohort analysis from a large single institute

Minhua Wang MD, PhD et.al.

Cancer cytopathology, Volume133, Issue11
https://doi.org/10.1002/cncy.70057

Abstract: Pelvic washing (PW) cytology has been excluded from endometrial cancer staging by the 2009 International Federation of Gynecology and Obstetrics (FIGO) criteria, and its prognostic significance in earlystage disease remains controversial. In this study, the authors evaluated the clinicopathologic correlates and prognostic impact of positive PW cytology in a large institutional cohort using a matched case–control design. Methods-A retrospective case–control cohort was created by reviewing PWs for endometrial cancer from 2013 to 2023 in the authors' pathology database. Cases with positive PW were retrieved from consecutive patients who had FIGO 2009 stage I or II endometrial cancer. The control group was comprised of randomly selected patients with negative PWs who were matched to patients in the positive PW group on patient age, tumor histologic subtype, FIGO grade, and disease stage. Cox proportional hazards models and multivariable logistic regression analyses were used to correlate survival outcomes and to identify predictors of cytologic positivity. Results- The cohort included 88 patients who had positive PW cytology and 223 matched controls. Positive PW cytology was independently associated with significantly worse disease-free survival (hazard ratio, 4.33; $p < .001$) and demonstrated borderline significance for overall survival (hazard ratio, 1.67; $p = .05$). The presence of free-floating tumor cells in the fallopian tubes was an independent predictor of positive PW cytology ($p < .001$). Conclusions- The current study demonstrates that positive PW cytology is an independent adverse prognostic factor in patients with stage I/II endometrial cancer and suggests that PW cytology status should be considered for accurate risk stratification of patients who have early stage endometrial cancer although it is not part of the current FIGO staging criteria.

25COASNOV33

Title: Analyzing the impact of molecular testing on the cytological diagnosis of thyroid nodules: Insights from our institution's experience

Dokpe Y. Emechebe MD et.al.

Cancer cytopathology, Volume133, Issue11
https://doi.org/10.1002/cncy.70051

Abstract: Fine-needle aspiration cytology (FNAC) is a preferred method for evaluation of thyroid nodules. Under The Bethesda System for Reporting Thyroid Cytopathology, approximately 15%–30% of FNAC results fall into an indeterminate category: atypia of undetermined significance (AUS), follicular neoplasm (FN), and suspicious for malignancy (SFM), Bethesda classes III, IV, and V respectively. Molecular testing of indeterminate nodules helps evaluate the risk of malignancy and guide management decisions. This retrospective study assesses the impact of molecular testing on thyroid nodule classification in our institution, with an emphasis on indeterminate results. Methods- A 9-year retrospective

analysis (January 2015–December 2023) was conducted at the University of North Carolina Health System. FNAC cases were classified per The Bethesda System. Molecular testing results and, when available, surgical pathology outcomes were reviewed. The study compared pre- and post-implementation data of routine reflex molecular testing of thyroid nodule diagnosis. Results- A total of 3992 thyroid aspirates were evaluated: 490 (12.3%) nondiagnostic (class I), 2096 (52.5%) benign (class II), 1041 (26.1%) AUS (class III), 136 (3.4%) FN (class IV), 89 (2.2%) SFM (class V), and 140 (3.5%) malignant (class VI). Indeterminate cytology (classes III–V) accounted for 32% of all aspirates ($n = 1266$). Before molecular testing, the AUS rate was 19.8% with an AUS:malignant ratio of 5.4. Post-implementation, the AUS rate rose to 30.1%, with a ratio of 8.9. This increase was statistically significant ($p = .029$). Conclusion- Implementation of molecular testing was associated with a significant rise in indeterminate cytologic diagnoses, particularly AUS.

25COASNOV34

Title: Neural or Neural-Related Colorectal Lesion Incidence Varies by Site, and Multifocal Cases Are Often Syndromic: Insights From a Series of 593 Patients

Irene Y. Chen, MD

Arch Pathol Lab Med (2025) 149 (10): 904–912.

https://doi.org/10.5858/arpa.2024-0435-OA

Abstract: Colorectal lesions with neural differentiation encompass various entities, often presenting with overlapping histologic or immunohistochemical profiles. Most research has focused on single entities, lacking a comprehensive comparative analysis of these lesions. Objective- To characterize and compare colorectal lesions with neural differentiation. Design-This study retrospectively examined cases of neural or neural-related colorectal lesions diagnosed between 2004 and 2020 across 2 institutions, analyzing clinical, histologic, and endoscopic features. Results-The cohort included 634 lesions from 593 patients (269 males and 324 females; mean age, 57 years; range, 13–85 years). Most patients were asymptomatic (83%, 490 of 593) and had solitary lesions (92%, 545 of 593), predominantly polypoid or nodular (96%, 610 of 634). Common types included benign fibroblastic polyp/perineurioma (n = 231 of 634, 36%), mucosal Schwann cell hamartoma (n = 203, 32%), and ganglioneuroma (n = 146, 23%), mostly centered in the mucosa (99%, $P < .001$) of the left colon (n = 318, $P < .001$). In contrast, granular cell tumors (n = 31, 5%) often involved the submucosa (n = 26, 84%; $P < .001$) of the cecum and ascending colon (n = 23, 74%; $P < .001$). Rare lesions like schwannoma (n = 13 of 634, 2%) and neurofibroma (n = 5 of 634, 1%) were found in various sites. A subset of patients (n = 48, 8%) had synchronous and/or metachronous lesions. Of these, 23 (48%) had genetic evidence of a syndromic manifestation ($P < .001$), with multiple ganglioneuromas in Cowden syndrome (n = 16) being the most common scenario. Conclusions-This is the largest comparative study of neural colorectal lesions, highlighting lesion types' association with colon segments and histologic layers. Multifocal presentations, though rare, are usually linked to genetic syndromes.

25COASNOV35

Title: Comparison of Molecular Testing Methodologies for *CIC*-Rearranged Sarcomas Open Access

Selene C. Koo, MD, PhD

Arch Pathol Lab Med (2025) 149 (10): 913–921.
https://doi.org/10.5858/arpa.2024-0407-OA

Abstract: Context- Molecular detection of a capicua transcriptional repressor (*CIC*) rearrangement is critical for diagnosing *CIC*-rearranged sarcoma (*CIC*-RS) but is analytically challenging. Objective- To compare the technical performance of fluorescence in situ hybridization (FISH), whole-transcriptome sequencing (RNA-seq), and DNA methylation profiling for *CIC*-rearrangement detection in a large, mainly pediatric cohort. Design-The study cohort consisted of 44 distinct patient tumors that were positive, equivocal, or suggestive for *CIC* rearrangement, including 18 central nervous system and 26 extra–central nervous system solid tumors. Forty tumors underwent FISH to detect *CIC* rearrangement, 31 underwent transcriptome sequencing, and 34 underwent methylation array analysis. Results for tumors tested by multiple testing modalities were compared. Results-Fusions were detected in 27 cases: *CIC*::double homeobox 4 (*DUX4*) (n = 15), *CIC*::NUT midline carcinoma family member 1 (*NUTM1*) (n = 4), *CIC*::leucine twenty homeobox (*LEUTX*) (n = 3), *CIC*::NUT family member 2B (*NUTM2B*) (n = 1), ataxin 1 (*ATXN1*)::*NUTM1* (n = 1), *ATXN1*::NUT family member 2A/B (*NUTM2A/B*) (n = 1), *CIC*::*DUX4* proximity effect (n = 1), and dedicator of cytokinesis 1 (*DOCK1*)::*DUX4* (n = 1). Twenty-five tumors were tested by all 3 testing modalities. Apparent false-negative rates were 20% (3 of 15) for *CIC* FISH, 14% (2 of 14) for transcriptome sequencing, and 14% (2 of 14) for methylation array analysis. Both false-negative methylation array results had *CIC*::*LEUTX* fusion. Conclusions-Awareness of molecular testing pitfalls in the appropriate detection of *CIC* rearrangement is critical. Any *CIC* FISH result may need to be further confirmed, either with unequivocal immunohistochemical support or by another molecular method. A positive RNA-seq or methylation array analysis result may be sufficient evidence for a diagnosis of *CIC*-RS in the appropriate histologic context. A negative or inconclusive/unclassified RNA-seq or methylation array analysis result in a tumor with high initial suspicion for CIC-RS likely requires careful reevaluation.

25COASNOV36

Title: Artificial Intelligence–Based Classification of Renal Oncocytic Neoplasms: Advancing From a 2-Class Model of Renal Oncocytoma and Low-Grade Oncocytic Tumor to a 3-Class Model Including Chromophobe Renal Cell Carcinoma

Katrina Collins, MD

Arch Pathol Lab Med (2025) 149 (10): 922–929.
https://doi.org/10.5858/arpa.2024-0374-OA

Abstarct: Context- Distinguishing between renal oncocytic tumors, such as renal oncocytoma (RO), and a subset of tumors with overlapping characteristics, including the recently identified low-grade oncocytic tumor (LOT), can present a diagnostic challenge for pathologists owing to shared histopathologic features. Objective- To develop an automatic computational classifier for stratifying whole slide images of biopsy and resection specimens into 2 distinct groups: RO and LOT. Design- A total of 269 whole slide images from 125 cases across 6 institutions were collected. A weakly supervised attention-based multiple-instance–learning deep learning (DL) model was trained and initially evaluated through 5-fold cross validation with case-level stratification, followed by validation using an independent holdout data set. Quantitative performance evaluation was based on accuracy

and the area under the receiver operating characteristic curve (AUC). Results-The developed model data set yielded generalizable performance, with a 5-fold average testing accuracy of 84% (AUC = 0.78), and a closely aligning accuracy of 83% (AUC = 0.92) on the independent holdout data set. Conclusions- The proposed artificial intelligence approach contributes toward a comprehensive solution for addressing commonly encountered renal oncocytic neoplasms, encompassing well-established entities like RO along with the challenging "gray zone" LOT, thereby proving applicable in clinical practice.

25COASNOV37

Title: Evaluation of Laboratory-Derived Immunohistochemical Assays for Folate Receptor α Expression in Epithelial Ovarian Cancer and Comparison With a Companion Diagnostic

Arch Pathol Lab Med (2025) 149 (10): 930–937.
https://doi.org/10.5858/arpa.2024-0210-OA

Abstract: Context-The VENTANA FOLR1 (FOLR1-2.1) RxDx (FOLR1 CDx) assay, developed by Roche Tissue Diagnostics, is a Food and Drug Administration–approved immunohistochemical assay intended for use in the assessment of folate receptor α (FRα) expression in formalin-fixed, paraffin-embedded epithelial ovarian, fallopian tube, and primary peritoneal tumor specimens. No published reports have compared the performance of other available FRα antibodies with the approved FOLR1 CDx. Objective-To assess the performance of research FRα laboratory-developed tests compared with the FOLR1 CDx. Design-The performance of 6 FRα-targeting antibodies was compared with the approved FOLR1 CDx in normal fallopian tube specimens. Two antibodies were selected for further assessment and compared with the FOLR1 CDx in ovarian tumor specimens. Results-Of the 6 antibodies tested, 4 displayed a lack of specific membrane staining and/or high , whereas 2 antibodies, produced by Leica Biosystems and Biocare Medical, respectively, exhibited specific and sensitive FRα staining. When assessed for their ability to correctly identify FRα-positive samples (per the FOLR1 CDx label, ≥75% of viable tumor cells with moderate and/or strong membranous staining intensity), both assays overpredicted FRα positivity compared with the FOLR1 CDx in archival ovarian tumor samples. Conclusions-These data highlight the need for caution in antibody selection when developing immunohistochemistry-based assays, as some antibodies failed to cleanly and specifically identify FRα expression. We identified 2 antibodies appropriate for further investigation; however, as developed, these antibodies may overselect patients for treatment with FRα-targeted therapies.

25COASNOV38

Title: Clinical Evaluation of the Heparin Therapeutic Window Using Activated Clotting Time in Neurological Interventional Radiology at an Academic Medical Center

Melody B. Nelson, DCLS

Arch Pathol Lab Med (2025) 149 (10): 938–943.
https://doi.org/10.5858/arpa.2024-0399-OA

Abstract: Context-Activated clotting time (ACT) is useful for monitoring heparin therapy in neurointerventional radiology (NIR). We previously used the Hemochron Signature Elite instrument for measuring ACT in NIR. Objective-To evaluate the suitability of measuring ACT using i-STAT in NIR by comparing its performance with Hemochron and a laboratory-

based anti-Xa (anti–factor Xa) assay. Design-All ACT measurements were performed in duplicate, using 2 Hemochron and 2 i-STAT devices in 53 samples from 15 unique multidose heparin administrations in NIR procedures and 110 samples in cardiovascular procedures. Samples were tested simultaneously within 1 minute of each other. Results-For 12 of the 15 procedures in NIR, anti-Xa was assessed at the beginning of the procedure and at the end of all procedural dosing. We also reviewed the patient's charts anonymously for any indication of postprocedural neurological bleeding. Interinstrument variability was much higher with Hemochron than with i-STAT. We also observed lower ACT values with i-STAT than with Hemochron. Therefore, the historical ACT range of 250 to 300 seconds for Hemochron was revised to 200 to 250 seconds for i-STAT devices. In the therapeutic window for anti-Xa, ACT results from both instruments exhibited a linear correlation. However, at supratherapeutic range for anti-Xa, ACT results from Hemochron exhibited more linear correlation, while i-STAT ACT demonstrated a plateau effect. No patient had any evidence of severe postprocedural neurological bleeding. Conclusions- The i-STAT analyzers produce more reproducible ACT results, but the target range should be lowered to 200 to 250 seconds. This range appears to provide adequate and safe heparin therapy, confirmed by anti-Xa assay results and clinical outcome.

25COASNOV39

Title: Loss of H3K27me3 Is Not Specific to Malignant Triton Tumor: Immunohistochemical Analysis of 23 Cases of Embryonal Rhabdomyosarcoma Open Access

Laura M. Warmke, MD

Arch Pathol Lab Med (2025) 149 (10): 944–949.
https://doi.org/10.5858/arpa.2024-0199-OA

Abstract: Context-Malignant peripheral nerve sheath tumor (MPNST) is a rare, often high-grade sarcoma. A small subset of MPNST shows evidence of heterologous rhabdomyoblastic differentiation, also known as malignant triton tumor (MTT). Immunohistochemical loss of histone 3 lysine 27 trimethylation (H3K27me3) has previously been described as a reliable marker for both MPNST and MTT. Objective- To assess the loss of H3K27me3 as a potential tool for discriminating MTT from embryonal rhabdomyosarcoma (ERMS). Design- We studied the immunohistochemical expression of H3K27me3 in 23 pediatric cases of confirmed ERMS. Of the 23 patients, 21 were male and 2 were female, with an age range of 2 months to 18 years (median, 5 years). Most of the tumors arose in the paratesticular soft tissue (n = 14), with other locations including the pelvis (n = 3), thigh (n = 2), abdomen (n = 1), orbit (n = 1), prostate gland (n = 1), and parotid gland (n = 1). All cases had characteristic morphologic features of ERMS. Results- By immunohistochemistry, all tested cases expressed desmin (18 of 18), myogenin (20 of 20), and MyoD1 (5 of 5). More than half of the cases (12 of 23; 52%) showed loss (nuclear absence) of H3K27me3, defined as staining in less than 5% of the tumor cells. The remaining cases demonstrated some degree of partial staining with H3K27me3, ranging from 5% to 40% of the tumor cells. No significant correlation between H3K27me3 expression and clinicopathologic features was identified. Conclusions- Loss of H3K27me3 frequently occurs in ERMS (52%) and is not reliable in distinguishing ERMS from MTT.

25COASNOV40

Title: The State of Pathology Student Interest Groups in Allopathic and Osteopathic Medical Schools in the United States: Current Practices and Opportunities for Improvement Open Access

Cullen M. Lilley, MD

Arch Pathol Lab Med (2025) 149 (10): 950–959.
https://doi.org/10.5858/arpa.2024-0279-OA

Abstract: Context-With the gradual decline in pathology residency applicants during the past few decades, the successful recruitment of quality medical students into the field will rely on a multidimensional approach. One of the means by which medical students are exposed to and recruited into the field of pathology is through student interest groups (SIGs). Though SIGs have been cited as a successful method for recruitment, the strategies for running a successful SIG have not been fully explored. Objective-To assess the functioning of pathology SIGs and provide a cross-sectional analysis of the challenges pathology SIGs face, what resources are needed, and how national organizations can most effectively support their functioning. Design- A multi-institutional survey was developed and deployed in December 2023 via email to College of American Pathologists medical student members and Future Pathologist Champions. Results-Of the 125 responses elicited from medical student members and Future Pathologist Champions, 78% (n = 97) indicated their institution had a pathology SIG. Faculty members were noted to be an important aspect to the SIG's success, especially by providing guidance and mentorship. Respondents also touted the regular hosting of events as another key component to success. Importantly, when asked about funding, most of the 78 respondents reported that their pathology SIGs relied on funding from their institution (58%; n = 45), but a large minority also received funding through grants/scholarships (36%; n = 28) or sponsorships from external organizations (28%; n = 22). Conclusions-This study provides a first-of-its-kind quantitative and qualitative account of the establishment and maintenance of pathology SIGs from the personnel participating in their daily functioning.

25COASNOV41

Title: Lung MRI: Indications, Capabilities, and Techniques—*AJR* Expert Panel Narrative Review

Lea Azour, MD

American journal of Roentgenology, Volume 225, Issue 4
https://doi.org/10.2214/AJR.25.32637

Abstract: Lung MRI provides both structural and functional information across a spectrum of parenchymal and airway pathologies. MRI, using current widely available conventional sequences, provides high-quality diagnostic images that allow tissue characterization and delineation of lung lesions; dynamic evaluation of expiratory central airway collapse, diaphragmatic or chest wall motion, and the relation of lung masses to the chest wall; oncologic staging; surveillance of chronic lung pathologies; and differentiation of inflammation and fibrosis in interstitial lung disease. Ongoing technologic advances, including deep learning acceleration methods, may enable future applications in longitudinal lung cancer screening without ionizing radiation exposure and in the regional quantification of ventilation and perfusion without hyperpolarized gas or IV contrast media. Although society statements highlight appropriate indications for lung MRI and the modality has

performed favorably relative to CT or FDG PET/CT in various indications, the examination's clinical utilization remains extremely low. Ongoing barriers to adoption include limited awareness by referring physicians, as well as insufficient proficiency and experience by radiologists and technologists. In this *AJR* Expert Panel Narrative Review, we review the clinical indications for lung MRI, describe the examination's current capabilities, provide guidance on protocols comprising widely available pulse sequences, introduce emerging techniques, and issue consensus recommendations.

25COASNOV42

Title: Contrast-Enhanced Voiding Urosonography and Radionuclide Cystography for Diagnosing Vesicoureteral Reflux Using VCUG as the Reference Standard: Systematic Review and Meta-Analysis

Shireen E. Hayatghaibi, PhD et.al.

American journal of Roentgenology, Volume 225, Issue 4

https://doi.org/10.2214/AJR.25.32739

Abstract: Fluoroscopic voiding cystourethrography (VCUG) is the most commonly used imaging test for the detection of vesicoureteral reflux (VUR) in children, although contrast-enhanced voiding urosonography (ceVUS) and radionuclide cystography (RNC) are also used for this purpose. Objective- The purpose of this study was to perform a systematic review and meta-analysis to determine the sensitivity and specificity of ceVUS and RNC for the detection of pediatric VUR using VCUG as the reference standard. Evidence acquisition- The Embase, MEDLINE, BIOSIS, Scopus, Cochrane, and Web of Science databases were searched from their date of inception through June 9, 2024, for studies performed in children that reported the sensitivity and specificity of ceVUS or RNC for the detection of VUR using VCUG as the reference standard. Studies' risk of bias was assessed using the QUADAS-2 tool. Diagnostic performance data were extracted from each study on a kidney-ureter level if available and on a patient level otherwise. Pooled sensitivity and specificity were estimated using bivariate random-effects models. Metaregression analysis was performed. Evidence synthesis- Of 2757 unique studies screened, 42 studies with 3124 total children were included in the final analysis. Twenty-six and 16 studies were at overall high and low risk of bias, respectively. Using VCUG as the reference standard, ceVUS (37 studies) had pooled sensitivity of 86% (95% CI: 82–90%) and pooled specificity of 92% (95% CI: 90–94%). Using VCUG as the reference standard, RNC (five studies) had pooled sensitivity of 81% (95% CI: 62–92%) and pooled specificity of 89% (95% CI: 75–95%). In metaregression analysis, publication year, sample size, patient age, and overall risk of bias had no significant association with sensitivity or specificity for either ceVUS or RNC (all $p > .05$). Conclusion- Pooled diagnostic performance estimates were derived for the available imaging tests for detecting VUR. However, most studies had an overall high risk of bias, highlighting a need for higher quality comparative studies.

25COASNOV43

Title: Contrast-Enhanced Mammography–Guided Biopsy: A Step-by-Step Guide

Olena O. Weaver, MD et.al.

American journal of Roentgenology, Volume 225, Issue 4

https://doi.org/10.2214/AJR.25.33038

Abstract: Although contrast-enhanced mammography (CEM) is not yet approved by the U.S. FDA for screening, diagnostic use of CEM as an alternative to breast MRI is becoming more widely accepted. CEM-guided biopsy has emerged as a modified stereotactic biopsy approach for sampling suspicious enhancing lesions that are visible only on recombined CEM images, and direct CEM-guided biopsy is becoming increasingly recognized as an essential component of efficient CEM workflows. Implementation of CEM-guided biopsy remains in its early stages, and further efforts from breast imagers and vendors will be required to optimize the technical quality of imaging and targeting during CEM-guided biopsy, to maximize the usefulness of the procedure and thereby the usefulness of CEM itself. In this Clinical Perspective, we explore the current status of CEM-guided biopsy based on relevant literature and the authors' clinical experience. We summarize indications and techniques and provide practical tips for performing these procedures, including step-by-step guidance, troubleshooting suggestions, and alternative approaches.

25COASNOV44

Title: Utility of CAD-RADS 2.0 Plaque Burden Grades and Stenosis Categories on Coronary CTA for Predicting Cardiac Events in Patients With Acute Chest Pain: A Multicenter Study

Ji Won Lee, MD, PhD et.al.

American journal of Roentgenology, Volume 225, Issue 4
https://doi.org/10.2214/AJR.25.33005

Abstract: Coronary Artery Disease Reporting and Data System (CAD-RADS) 2.0 incorporated reporting of plaque burden grades in addition to stenosis categories. OBJECTIVE. The purpose of this study was to assess the usefulness of plaque burden grades and CAD-RADS categories, determined on coronary CTA by use of CAD-RADS 2.0, in predicting cardiac events in patients presenting to the emergency department (ED) with acute chest pain. METHODS. This retrospective study included patients who underwent coronary CTA after presenting to the ED with acute chest pain at one of four centers from January 2018 to December 2021. A single radiologist reviewed examinations at each center to assign a plaque burden grade by calculating a coronary artery calcium score on noncontrast images and to assign a CAD-RADS category by assessing vessel stenosis on contrast-enhanced CTA images, with both assignments made using CAD-RADS 2.0. The reviewing radiologist at each center also assessed examinations for the presence of high-risk plaque. The EMR was reviewed for cardiac events, reflecting a composite outcome of cardiac-related death, myocardial infarction, or hospitalization for unstable angina. Prognostic models were compared. RESULTS. The study included 2032 patients (1085 men and 947 women; mean age, 58.4 years). During a median follow-up of 15.2 months, 63 patients (3.1%) had cardiac events. In a multivariable Cox model adjusting for clinical variables, cardiac events showed significant independent associations with CAD-RADS 3 (HR = 7.1), CAD-RADS 4 (HR = 13.6), CAD-RADS 5 (HR = 17.6), and high-risk plaque (HR = 2.5) but not with plaque burden grades. For predicting cardiac events, the C statistic was 0.67 for a model including clinical variables; 0.74 for a model including clinical variables and plaque burden grades; 0.86 for a model including clinical variables, CAD-RADS categories, and high-risk plaque; and 0.87 for a model including clinical variables, plaque burden grades, CAD-RADS categories, and high-risk plaque. The model with clinical variables, CAD-RADS categories,

and high-risk plaque but without plaque burden grades showed the highest net clinical benefit across threshold probabilities from 20% to 100%.
CONCLUSION. Addition of plaque burden grades did not provide further prognostic benefit in models using CAD-RADS categories.

25COASNOV45
Title: Photon-Counting Detector CTA in Standard- and Ultrahigh-Resolution Modes for Diagnosing Coronary Artery Stenosis Using Invasive Angiography as the Reference: A Prospective Study
Mengzhen Wang, MD et.al**.**
American journal of Roentgenology, Volume 225, Issue 4
https://doi.org/10.2214/AJR.25.33021
Abstract: The literature reports excellent diagnostic performance of coronary CTA using photon-counting detector (PCD) CT, albeit obtained using various acquisition and reconstruction protocols. OBJECTIVE. The purpose of this study was to assess the diagnostic performance for detecting significant stenosis of coronary CTA performed by PCD CT with various standard-resolution (SR) and ultrahigh-resolution (UHR) protocols, using invasive coronary angiography (ICA) as the reference standard. METHODS. This prospective study enrolled inpatients undergoing coronary CTA between October 2023 and October 2024. Participants underwent coronary CTA by PCD CT, sequentially alternating between SR (collimation: 144 × 0.4 mm) and UHR (collimation: 120 × 0.2 mm) modes across participants. SR examinations were reconstructed into normal (SR_{normal}) and virtual noncalcium (SR_{VNCa}) image sets, both using 0.6-mm slice thickness and Bv40 kernel. UHR examinations were reconstructed into normal (UHR_{normal} [0.6-mm slice thickness, Bv40 kernel]) and thin (UHR_{thin} [0.2-mm slice thickness, Bv64 kernel]) image sets. Two radiologists independently measured the diameter of stenoses. The final analysis included patients who underwent ICA after CTA; a cardiologist reviewed the ICA images to determine the reference standard. Stenoses were considered significant at a threshold of 50% or greater. RESULTS. The SR group included 61 patients (mean age, 67 ± 9 [SD] years; 46 men, 15 women; 788 segments analyzed). The UHR group included 61 patients (67 ± 11 years; 43 men, 18 women; 825 segments analyzed). Per-segment sensitivity, specificity, and accuracy for reader 1 were 92.9%, 89.9%, and 90.5% for SR_{normal}, respectively; 92.9%, 91.6%, and 91.8% for SR_{VNCa}; 96.0%, 92.4%, and 93.0% for UHR_{normal}; and 100.0%, 98.6%, and 98.8% for UHR_{thin}; and for reader 2 were 92.9%, 88.8%, and 89.6% for SR_{normal}; 93.5%, 92.3%, and 92.5% for SR_{VNCa}; 96.0%, 91.6%, and 92.2% for UHR_{normal}; and 100.0%, 98.9%, and 99.0% for UHR_{thin}. Significant ($p < .05$) differences included SR_{VNCa} versus SR_{normal} for specificity for both readers and accuracy for reader 2; UHR_{thin} versus UHR_{normal} for sensitivity, specificity, and accuracy for both readers; and UHR_{thin} versus SR_{VNCa} for sensitivity, specificity, and accuracy for both readers. CONCLUSION. Coronary CTA performed by PCD CT achieved high diagnostic performance in the SR or UHR mode. Performance was higher for SR_{VNCa} than SR_{normal} and for UHR_{thin} than either UHR_{normal} or SR_{VNCa}.

25COASNOV46
Title: Multimodal Generative Artificial Intelligence Model for Creating Radiology Reports for Chest Radiographs in Patients Undergoing Tuberculosis Screening

Eun Kyoung Hong, et.al.
American journal of Roentgenology, Volume 225, Issue 4
https://doi.org/10.2214/AJR.25.33059
Abstract: . Chest radiographs play a crucial role in tuberculosis screening in high-prevalence regions, although widespread radiographic screening requires expertise that may be unavailable in settings with limited medical resources. OBJECTIVE. The purpose of this study was to evaluate a multimodal generative artificial intelligence (AI) model for detecting tuberculosis-associated abnormalities on chest radiography in patients undergoing tuberculosis screening. METHODS. This retrospective study evaluated 800 chest radiographs obtained from two public datasets originating from tuberculosis screening programs. A generative AI model was used to create free-text reports for the radiographs. AI-generated reports were classified in terms of presence versus absence and laterality of tuberculosis-related abnormalities. Two radiologists independently reviewed the radiographs for tuberculosis presence and laterality in separate sessions, without and with use of AI-generated reports, and recorded if they would accept the report without modification. Two additional radiologists reviewed radiographs and clinical readings from the datasets to determine the reference standard. RESULTS. By the reference standard, 378 of 800 radiographs were positive for tuberculosis-related abnormalities. For detection of tuberculosis-related abnormalities, sensitivity, specificity, and accuracy were 95.2%, 86.7%, and 90.8% for AI-generated reports; 93.1%, 93.6%, and 93.4% for reader 1 without AI-generated reports; 93.1%, 95.0%, and 94.1% for reader 1 with AI-generated reports; 95.8%, 87.2%, and 91.3% for reader 2 without AI-generated reports; and 95.8%, 91.5%, and 93.5% for reader 2 with AI-generated reports. Accuracy was significantly lower for AI-generated reports than for both readers alone ($p < .001$), but significantly higher with than without AI-generated reports for one reader (reader 1: $p = .47$; reader 2: $p = .03$). Localization performance was significantly lower ($p < .001$) for AI-generated reports (63.3%) than for reader 1 (79.8%) and reader 2 (77.9%) without AI-generated reports and did not significantly change for either reader with AI-generated reports (reader 1: 78.7%, $p = .71$; reader 2: 81.5%, $p = .23$). Among normal and abnormal radiographs, reader 1 accepted 91.7% and 52.4%, whereas reader 2 accepted 83.2% and 37.0%, respectively, of AI-generated reports. CONCLUSION. Although AI-generated reports may augment radiologists' diagnostic assessments, the current model requires human oversight, given inferior standalone performance.

25COASNOV47

Title: Use of a Template-Matching Clavicle Fracture Atlas for Surrogate Dating of Humeral and Femoral Fractures in Young Infants: A Six-Reader Study

Jade Iwasaka-Neder, MD, MPH
American journal of Roentgenology, Volume 225, Issue 4
https://doi.org/10.2214/AJR.25.33184
Abstract: Fracture dating is important in suspected infant abuse. Birth-related clavicle fractures are common and may provide surrogates to aid long bone fracture dating in infants. OBJECTIVE. The purpose of this study was to assess the impact of a template-matching clavicle fracture timeline atlas on radiologists' performance in dating birth-related fractures of the clavicle, humerus, and femur in young infants. Methods. This retrospective study

included infants 90 days old or younger who underwent radiography of a birth-related clavicle fracture from April 1, 2021, to July 31, 2024 or a birth-related fracture of the humerus or femur from December 1, 2011, to July 31, 2024. All eligible radiographs of each fracture were identified, representing distinct observations for the purposes of analysis. Patient age (expressed as days) at the time of radiograph acquisition served as the reference standard for fracture ages. A nonrigid image registration technique was applied to a nonoverlapping preassembled database of radiographs of birth-related clavicle fracture, to create a fracture dating atlas. Six readers (three trainees and three pediatric radiologists) independently reviewed the radiographs in separate sessions without and with use of the atlas to estimate fracture ages. Interreader agreement was assessed using intraclass correlation coefficients (ICCs). Fracture aging performance was assessed using mean absolute errors (MAEs). RESULTS. The analysis included 145 infants (87 male and 58 female infants) with 269 fracture radiographs (104 of the clavicle, 128 of the humerus, and 37 of the femur). The mean fracture age was 26 ± 19 [SD], 22 ± 14, and 21 ± 13 days for clavicle, humerus, and femur fractures, respectively. Interreader agreement for estimating fracture ages improved from moderate (ICC = 0.69) without use of the atlas to excellent (ICC = 0.91) with use of the atlas. The MAE in fracture dating was significantly lower ($p < .05$) with than without use of the atlas for all six readers for clavicle fractures (range, 4.8–5.5 vs 5.8–10.1 days), for all six readers for humeral fractures (range, 6.0–12.1 vs 3.0–3.8 days), and for five of six readers for femur fractures (range, 7.4–17.2 vs 3.3–4.8 days). MAE without and with use of the atlas was 8.8 versus 4.3 days, respectively, across trainee readers and 8.4 versus 4.0 days, respectively, across attending physician readers. CONCLUSION. The fracture dating atlas yielded significant improvements in radiologists' performance for dating infant clavicle, humerus, and femur fractures.

Medical Oncology
(Chemotherapy**, H**ematology **& R**adiotherapy**)**

25COASNOV01:
Title: Low-Dose Aspirin for PI3K-Altered Localized Colorectal Cancer
Anna Martling, M.D., Ph.D.
N Engl J Med 2025;393:1051-1064, VOL. 393 NO. 11
https://doi.org/10.1056/NEJMoa2504650
Abstract: Aspirin reduces the incidence of colorectal adenoma and colorectal cancer among high-risk persons. Observational studies suggest that aspirin may also improve disease-free survival after diagnosis, particularly among patients with tumors harboring somatic *PIK3CA* mutations. However, data from randomized trials are lacking. Methods-We conducted a double-blind, randomized, placebo-controlled trial involving patients with stage I, II, or III rectal cancer or stage II or III colon cancer with somatic alterations in PI3K pathway genes. The patients were assigned in a 1:1 ratio to receive 160 mg of aspirin or matched placebo once daily for 3 years. Patients with prespecified *PIK3CA* hotspot mutations in exon 9 or 20 (group A alterations) and those with other moderate- or high-impact somatic variants in *PIK3CA*, *PIK3R1*, or *PTEN* (group B alterations) were eligible for randomization. The primary end point was colorectal cancer recurrence, assessed in a time-to-event analysis, in patients with group A alterations. Secondary end points included colorectal cancer recurrence in patients with group B alterations, disease-free survival, and safety. Results-Alterations in PI3K pathway genes were detected in 1103 of 2980 patients (37.0%) with complete genomic data. Of 515 patients with group A alterations and 588 patients with group B alterations, 314 and 312, respectively, were assigned to receive aspirin or placebo. The estimated 3-year cumulative incidence of recurrence was 7.7% with aspirin and 14.1% with placebo (hazard ratio, 0.49; 95% confidence interval [CI], 0.24 to 0.98; P=0.04) among patients with group A alterations and 7.7% and 16.8%, respectively (hazard ratio, 0.42; 95% CI, 0.21 to 0.83), among those with group B alterations. The estimated 3-year disease-free survival was 88.5% with aspirin and 81.4% with placebo (hazard ratio, 0.61; 95% CI, 0.34 to 1.08) among patients with group A alterations and 89.1% and 78.7%, respectively (hazard ratio, 0.51; 95% CI, 0.29 to 0.88), among those with group B alterations. Severe adverse events occurred in 16.8% of aspirin recipients and 11.6% of placebo recipients. Conclusions - Aspirin led to a significantly lower incidence of colorectal cancer recurrence than placebo among patients with *PIK3CA* hotspot mutations in exon 9 or 20 and appeared to have a similar benefit among those with other somatic alterations in PI3K pathway genes. (Funded by the Swedish Research Council and others; ALASCCA ClinicalTrials.gov number, NCT02647099; EudraCT number, 2015-004240-19.)

25COASNOV2
Title: Orforglipron, an Oral Small-Molecule GLP-1 Receptor Agonist, in Early Type 2 Diabetes
Julio Rosenstock, M.D.
N Engl J Med 2025;393:1065-1076, VOL. 393 NO. 11
https://doi.org/10.1056/NEJMoa2505669

Abstract: Orforglipron is a small-molecule, nonpeptide glucagon-like peptide-1 (GLP-1) receptor agonist in clinical development for type 2 diabetes and weight management. Additional data on the efficacy and safety of orforglipron are needed. Methods In this phase 3, double-blind, placebo-controlled trial, we randomly assigned participants in a 1:1:1:1 ratio to receive orforglipron at one of three doses (3 mg, 12 mg, or 36 mg) or placebo once daily for 40 weeks. Participants had type 2 diabetes treated only with diet and exercise, a glycated hemoglobin level of at least 7.0% but no more than 9.5%, and a body-mass index (the weight in kilograms divided by the square of the height in meters) of at least 23.0. The primary end point was the change from baseline to week 40 in the glycated hemoglobin level. A key secondary end point was the percent change in body weight from baseline to week 40. Results A total of 559 participants underwent randomization. The mean glycated hemoglobin level at baseline was 8.0%. At week 40, the estimated mean change from baseline in the glycated hemoglobin level was −1.24 percentage points with the 3-mg dose, −1.47 percentage points with the 12-mg dose, −1.48 percentage points with the 36-mg dose, and −0.41 percentage points with placebo. All three doses of orforglipron were superior to placebo with respect to the primary end point; the estimated mean difference from placebo was −0.83 percentage points (95% confidence interval [CI], −1.10 to −0.56) with the 3-mg dose, −1.06 percentage points (95% CI, −1.33 to −0.79) with the 12-mg dose, and −1.07 percentage points (95% CI, −1.33 to −0.81) with the 36-mg dose (P<0.001 for all comparisons). The mean glycated hemoglobin level at week 40 was 6.5 to 6.7% with orforglipron. The percent change in body weight from baseline to week 40 was −4.5% with the 3-mg dose, −5.8% with the 12-mg dose, −7.6% with the 36-mg dose, and −1.7% with placebo. The most common adverse events were mild-to-moderate gastrointestinal events, most of which occurred during dose escalation. No episodes of severe hypoglycemia were reported. Permanent discontinuation of orforglipron or placebo due to adverse events occurred in 4.4 to 7.8% of participants receiving orforglipron and 1.4% of participants receiving placebo. Conclusions-In adults with early type 2 diabetes, orforglipron significantly reduced the glycated hemoglobin level over a period of 40 weeks. (Supported by Eli Lilly; ACHIEVE-1 ClinicalTrials.gov number, NCT05971940.)

25COASNOV3

Title: Apixaban for Extended Treatment of Provoked Venous Thromboembolism

Gregory Piazza, M.D. et.al.

N Engl J Med 2025;393:1166-1176, VOL. 393 NO. 12
https://www.nejm.org/doi/full/10.1056/NEJMe2510701

Abstract: The appropriate duration of anticoagulation for venous thromboembolism (VTE) in patients who have a transient provoking factor (e.g., surgery, trauma, or immobility) and concomitant enduring risk factors is uncertain. Methods-In this single-center, double-blind, randomized trial, adults with VTE after the occurrence of a transient provoking factor who had at least one enduring risk factor and had completed at least 3 months of anticoagulation were assigned to receive oral apixaban (at a dose of 2.5 mg twice daily) or placebo for 12 months. The primary efficacy outcome was the first symptomatic recurrent VTE. The primary safety outcome was the first episode of major bleeding according to the criteria of the International Society on Thrombosis and Hemostasis. Results-A total of 600 patients underwent randomization (mean age, 59.5 years; female sex, 57.0%; non-White race, 19.2%).

The trial population had a broad range of provoking factors and enduring risk factors. Symptomatic recurrent VTE occurred in 4 of the 300 patients (1.3%) in the apixaban group and in 30 of the 300 patients (10.0%) in the placebo group (hazard ratio, 0.13; 95% confidence interval [CI], 0.04 to 0.36; P<0.001). Major bleeding occurred in 1 patient in the apixaban group and none in the placebo group. Clinically relevant nonmajor bleeding was observed in 14 of 294 patients (4.8%) in the apixaban group and in 5 of 294 patients (1.7%) in the placebo group (hazard ratio, 2.68; 95% CI, 0.96 to 7.43; P=0.06). One patient in the apixaban group and 3 patients in the placebo group died, with no deaths attributed to cardiovascular or hemorrhagic causes. Nonhemorrhagic, nonfatal adverse events occurred in 6 patients (2.0%) in each group. Conclusions-Among patients with provoked VTE and enduring risk factors, low-intensity therapy with apixaban for 12 months resulted in a lower risk of symptomatic recurrent VTE than placebo, with a low risk of major bleeding. (Funded by Bristol-Myers Squibb–Pfizer Alliance; HI-PRO ClinicalTrials.gov number, NCT04168203.)

25COASNOV4

Title: Measurable Residual Disease–Guided Therapy for Chronic Lymphocytic Leukemia

Authors: Talha Munir, Ph.D., Sean Girvan, M.Sc., David A. Cairns, et.al.

N Engl J Med 2025;393:1166-1176, VOL. 393 NO. 12

https://doi.org/10.1182/blood.2025030421

Abstract: An interim analysis of progression-free survival in this trial showed that ibrutinib–venetoclax was superior to fludarabine–cyclophosphamide–rituximab (FCR) among patients with chronic lymphocytic leukemia (CLL). Whether ibrutinib–venetoclax is more effective than ibrutinib alone is unclear.Methods: In this phase 3, multicenter, open-label trial, we randomly assigned patients with CLL to receive ibrutinib–venetoclax, ibrutinib alone, or FCR. The primary end points were undetectable measurable residual disease (MRD) in bone marrow within 2 years in the ibrutinib–venetoclax group as compared with the ibrutinib-alone group and progression-free survival in the ibrutinib–venetoclax group as compared with the FCR group. A powered secondary end point was progression-free survival in the ibrutinib–venetoclax group as compared with the ibrutinib-alone group. Other secondary end points included overall survival.Research Summary: Measurable Residual Disease–Guided Therapy for CLLResults: A total of 172 of the 260 participants (66.2%) in the ibrutinib–venetoclax group had undetectable MRD in bone marrow within 2 years, as compared with none of the 263 participants in the ibrutinib-alone group (P<0.001) and 127 of the 263 participants (48.3%) in the FCR group. With a median follow-up of 62.2 months, disease progression or death occurred in 18 participants (6.9%) in the ibrutinib–venetoclax group, as compared with 59 (22.4%) in the ibrutinib-alone group (hazard ratio, 0.29; 95% confidence interval [CI], 0.17 to 0.49; P<0.001) and 112 (42.6%) in the FCR group (hazard ratio, 0.13; 95% CI, 0.08 to 0.21; P<0.001). Progression-free survival at 5 years was 93.9% with ibrutinib–venetoclax, 79.0% with ibrutinib alone, and 58.1% with FCR. Death occurred in 11 participants (4.2%) in the ibrutinib–venetoclax group, as compared with 26 (9.9%) in the ibrutinib-alone group (hazard ratio, 0.41; 95% CI, 0.20 to 0.83) and 39 (14.8%) in the FCR group (hazard ratio, 0.26; 95% CI, 0.13 to 0.50). Sudden death occurred in 3, 8, and 4 participants in the ibrutinib–venetoclax, ibrutinib-alone, and FCR groups, respectively.Conclusions: With

extended follow-up and increased enrollment, our trial showed that undetectable MRD and extended progression-free survival were more common with ibrutinib–venetoclax than with ibrutinib alone or FCR. The results for overall survival were also consistent with a benefit of ibrutinib–venetoclax. (Funded by Cancer Research UK and others; FLAIR ISRCTN Registry number, ISRCTN01844152; EudraCT number, 2013-001944-76.)

25COASNOV5

Title: Early Tirofiban Infusion after Intravenous Thrombolysis for Stroke

Chunrong Tao, M.D., Ph.D

N Engl J Med 2025;393:1191-1201, VOL. 393 NO. 12

https://doi.org/10.1056/NEJMoa2503678

Abstract: Intravenous thrombolysis remains a standard treatment for acute ischemic stroke within 4.5 hours after onset. Vascular reocclusion may occur after intravenous thrombolysis and may be preventable with an antiplatelet agent within the first 24 hours after thrombolysis. Tirofiban, a platelet glycoprotein IIb–IIIa receptor antagonist, has reduced macrovascular reocclusion in experimental models. Methods-In this phase 3, multicenter, double-blind, randomized, placebo-controlled trial conducted at 38 centers in China, we assigned patients with acute ischemic noncardioembolic stroke who presented within 4.5 hours after stroke onset and who were not eligible for thrombectomy to receive a 24-hour intravenous infusion of tirofiban or placebo within 60 minutes after intravenous thrombolysis. The primary efficacy outcome was an excellent functional outcome, defined as a score of 0 to 1 on the modified Rankin scale, at 90 days. The safety outcomes were symptomatic intracranial hemorrhage within 36 hours and death at 90 days.Results A total of 414 patients were assigned to receive tirofiban and 418 to receive placebo. Thrombolytic agents included alteplase (in 75% of the patients) and tenecteplase (in 25%). At 90 days, a score of 0 to 1 on the modified Rankin scale was reported in a higher percentage of patients in the tirofiban group than in the placebo group (65.9% vs. 54.9%; risk ratio, 1.20; 95% confidence interval, 1.07 to 1.34; P=0.001). Symptomatic intracranial hemorrhage occurred in 1.7% of the patients in the tirofiban group and none in the placebo group. Mortality at 90 days was 4.1% in the tirofiban group and 3.8% in the placebo group. Conclusions-In patients with acute ischemic noncardioembolic stroke who underwent thrombolysis within 4.5 hours after onset, early tirofiban increased the likelihood of an excellent functional outcome. The incidence of intracranial hemorrhage was low but higher with tirofiban than placebo.

25COASNOV6

Title: Tezepelumab in Adults with Severe Chronic Rhinosinusitis with Nasal Polyps

Brian J. Lipworth, M.D. et.al.

N Engl J Med 2025;392:1178-1188, VOL. 392 NO. 12

https://doi.org/10.1056/NEJMoa2414482

Abstract: Treatment with tezepelumab has been effective for sinonasal symptoms in patients with severe, uncontrolled asthma and a history of chronic rhinosinusitis with nasal polyps, but its efficacy and safety in adults with severe, uncontrolled chronic rhinosinusitis with nasal polyps is unknown. Methods-We randomly assigned adults with physician-diagnosed, symptomatic, severe chronic rhinosinusitis with nasal polyps to receive standard care and either tezepelumab (at a dose of 210 mg) or placebo subcutaneously every 4 weeks for 52

weeks. The coprimary end points were the changes from baseline in the total nasal-polyp score (range, 0 to 4 [for each nostril]; higher scores indicate greater severity) and the mean nasal-congestion score (range, 0 to 3; higher scores indicate greater severity) at week 52. Key secondary end points assessed in the overall population were the loss-of-smell score, the total score on the Sinonasal Outcome Test (SNOT-22; range, 0 to 110; higher scores indicate greater severity), the Lund–Mackay score (range, 0 to 24; higher scores indicate greater severity), the total symptom score (range, 0 to 24; higher scores indicate greater severity), and the first decision to treat with nasal-polyp surgery or use of systemic glucocorticoid therapy, or both, assessed in time-to-event analyses (individual and composite). Results-In total, 203 patients were assigned to receive tezepelumab and 205 to receive placebo. At week 52, the patients who received tezepelumab had significant improvements in the total nasal-polyp score (mean difference vs. placebo, −2.08; 95% confidence interval [CI], −2.40 to −1.76) and the mean nasal-congestion score (−1.04; 95% CI, −1.21 to −0.87) (P<0.001 for both scores). Tezepelumab significantly improved the loss-of-smell score (mean difference vs. placebo, −1.01; 95% CI, −1.18 to −0.83), SNOT-22 total score (−27.44; 95% CI, −32.51 to −22.37), Lund–Mackay score (−5.70; 95% CI, −6.37 to −5.03), and total symptom score (−6.96; 95% CI, −8.09 to −5.83) (P<0.001 for all scores). Surgery for nasal polyps was indicated in significantly fewer patients in the tezepelumab group (0.5%) than in the placebo group (22.0%) (hazard ratio, 0.02; 95% CI, 0.00 to 0.09); there was significantly less use of systemic glucocorticoids with tezepelumab (5.2%) than with placebo (19.3%) (hazard ratio, 0.11; 95% CI, 0.04 to 0.25) (P<0.001 for both time-to-event analyses). Conclusions-Tezepelumab therapy led to significantly greater reductions in the size of nasal polyps, the severity of nasal congestion and sinonasal symptoms, and the use of nasal-polyp surgery and systemic glucocorticoids than placebo in adults with severe, uncontrolled chronic rhinosinusitis with nasal polyps.

25COASNOV7

Title: NPY-functionalized niosomes for targeted delivery of margatoxin in breast cancer therapy.

Eftekhari, Z., Chiani, M. & Kazemi-Lomedasht, F.

Med Oncol 42, 465 (2025).
https://doi.org/10.1007/s12032-025-03026-3

Abstract: Neuropeptide Y (NPY) and the voltage-gated potassium channel Kv1.3 are closely associated with breast cancer progression and apoptosis regulation, respectively. NPY receptors (NPYRs), which are overexpressed in breast tumors, contribute to tumor growth, migration, and angiogenesis. In parallel, Kv1.3 plays a pivotal role in mitochondrial-mediated apoptosis, and its inhibition can induce cancer cell death. To exploit these mechanisms, we developed and characterized a novel niosomal drug delivery system encapsulating margatoxin (MgTx), a potent Kv1.3 inhibitor, and functionalized with NPY for targeted breast cancer therapy. Niosomes were synthesized via a modified thin-film hydration method and decorated with NPY peptides to enable selective binding to NPYR-overexpressing cancer cells. Physicochemical analyses using dynamic light scattering (DLS), atomic force microscopy (AFM), and field emission scanning electron microscopy (FESEM) confirmed a nanoscale size range (134–161 nm), spherical morphology, and successful surface modification. The system demonstrated high encapsulation efficiency, prolonged stability at

4°C, and sustained MgTx release over 72 h. In vitro cytotoxicity studies revealed that NPY-decorated MgTx-loaded niosomes significantly reduced the viability of MCF-7 and MDA-MB-231 breast cancer cells while exerting minimal toxicity on non-tumorigenic MCF-10A cells. qRT-PCR analysis indicated upregulation of pro-apoptotic genes (*Bax, Caspase-3*) and downregulation of anti-apoptotic *Bcl2*, confirming induction of apoptosis in treated cancer cells. These findings highlight the potential of NPY-functionalized niosomes as an effective and selective nanoplatform for targeted breast cancer therapy.

25COASNOV8

Title: Exploring the anticancer potential of *R. tridentata* extracts: a cytotoxicity study against human prostate cancer cell lines (LNCaP and DU145).

Kudamba, A., Bbosa, G.S., Lugaajju, A. *et al.*

Med Oncol 42, 463 (2025).

https://doi.org/10.1007/s12032-025-02953-5

Abstract: This study investigates the cytotoxic effects of *R. tridentat*a extracts on prostate cancer cells, providing insight into its potential therapeutic benefits and scientific validation for its traditional use in cancer treatment. The cytotoxicity of *R. tridentata* extracts was evaluated on prostate cancer cell lines (LNCaP and DU 145) using the MTT assay, with doxorubicin as a reference standard. Our findings demonstrated significant concentration- and time-dependent cytotoxic effects of the extracts on both cell lines ($p < 0.0024$ to $p < 0.0002$). Notably, the methanol extract exhibited potent cytotoxicity, with IC_{50} values ranging from 124.07 to 211 µg/mL (DU145) and 100 to 180 µg/ml (LNCaP) over 24–72 h ($p < 0.0024$ to $p < 0.0001$), highlighting its therapeutic potential. This study unveils the promising cytotoxic activity of *R. tridentata* extracts, particularly methanol extracts, against prostate cancer cells, showcasing their concentration- and time-dependent effects. These findings underscore the potential of plant-derived extracts as therapeutic agents for cancer treatment, warranting further research.

25COASNOV9

Title: Diosgenin enhances the effect of radiation on head and neck cancer cells through apoptosis induction, G2/M cell cycle arrest, and ROS generation.

Mohammadi, M., Koosha, F., Amini, S.M. *et al.*

Med Oncol 42, 461 (2025).

https://doi.org/10.1007/s12032-025-03019-2

Abstract: Radiotherapy is a cornerstone in treating head and neck cancers, yet its effectiveness is often limited by factors such as hypoxia and cancer stem cells. This study evaluated the radiosensitizing potential of diosgenin in KB cancer cells and normal HDF cells exposed to 4 Gy X-rays, with or without diosgenin. Cell viability, apoptosis, cell cycle distribution, ROS production, and expression of intrinsic apoptosis-related genes were assessed using MTT assays, flow cytometry, and RT-qPCR, respectively. Diosgenin alone reduced KB cell viability and, when combined with radiation (63 µM + 4 Gy), further decreased viability to 27.93 ± 1.8%, which was significantly lower than with either treatment alone ($p < 0.05$), while exhibiting lower toxicity in HDF cells. Diosgenin also induced G2/M arrest and amplified radiation-induced apoptosis, sub-G1 accumulation, and ROS production. These effects correlated with a marked increase in the Bax/Bcl-2 mRNA ratio in the

combination group compared to either treatment alone ($p < 0.0001$), indicating activation of the intrinsic apoptotic pathway. Overall, the results suggest that diosgenin enhances the effect of radiation on head and neck cancer cells and may serve as a promising adjunct to radiotherapy.

25COASNOV10

Title: The effect of *U2AF1* mutation on erythroid differentiation and sensitivity to demethylation drug treatment.

Liu, Y., Li, X., Wang, H. *et al.*

Med Oncol 42, 459 (2025).
https://doi.org/10.1007/s12032-025-02956-2

Abstract: Myelodysplastic syndrome (MDS) is a group of blood disorders characterized by impaired maturation of erythroid cells. Mutations in the U2 small nuclear RNA auxiliary factor 1 (*U2AF1*) gene, particularly S34 (S34F/Y) and Q157 (Q157P/R), have been identified in 5–10% of MDS patients. By analyzing *U2AF1* expression in hematopoietic stem progenitor cells and different blood cells in the GEO database, we have found the expression pattern of *U2AF1* showed a significant stage specificity during normal erythropoiesis. To explore the specific impact of *U2AF1* alterations on cellular function, we transduced K562 cells with lentivirus carrying four different types of *U2AF1* mutants. Our results showed that these mutations significantly inhibited the growth of K562 cells. Mutations at the S34 sites (S34F and S34Y) reduced the mRNA expression levels of erythroid-related transcription factors *GATA1*, *NF-E2*, *EKLF,* and *GFI-1B.* The proportion of cells with $CD71^{low}CD235a^{hig}$ decreased, as well as the content of hemoglobin in K562 cells. In contrast, mutations at the Q157 site had opposite effects on these expression levels in K562 cells. Furthermore, we classified patients' risk ratings into three categories based on IPSS-R: moderate high-risk MDS, high-risk MDS, and very high-risk MDS. A total of 12 patients were analyzed, including 5 at moderate high-risk and 3 patients carrying mutations. Among 3 high-risk individuals, only one carried a mutation. 4 individuals at very high-risk, with 0 patients carrying the mutation. MDS patients with *U2AF1* mutations (S34F, S34Y, Q157P, R156H) had significantly lower white blood cell, hemoglobin, and platelet counts than the MDS patients without these alterations. We hypothesize that treatment with Azacitidine (AZA) may lead to better recovery levels of hemoglobin and platelets for patients with *U2AF1* mutations. Meanwhile, we found that *U2AF1*-mutated MDS patients have better responsiveness to demethylating drugs. We isolated and cultured peripheral blood mononuclear cells (PBMCs) carrying the *U2AF1* S34F mutation from a high-risk MDS patient with a 7q chromosome deletion. The demethylating drug AZA could significantly inhibit their proliferation and induce apoptosis in the MDS PBMCs. In summary, our research demonstrated the following: (1) The effect of *U2AF1* mutation on erythrocyte differentiation that S34 mutation inhibits the differentiation process, but the Q157 mutation promotes the differentiation process. (2) The level of erythrocyte changes in *U2AF1*-mutated MDS patients should receive more attention. (3) It also showed that demethylating drugs have promising therapeutic effects in treating MDS patients carrying *U2AF1* mutations.

25COASNOV11

Title: Machine learning integration of bulk and single-cell RNA-seq data reveals glycolytic heterogeneity in colorectal cancer.

Du, Y., Miao, Z., Li, P. *et al.*

Med Oncol 42, 458 (2025).
https://doi.org/10.1007/s12032-025-03007-6

Abstract: As one of the most prevalent malignancies worldwide, colorectal cancer (CRC) exhibits a strong metabolic dependency on glycolysis, which fuels tumor expansion and shapes an immunosuppressive microenvironment. Despite its clinical significance, the regulatory landscape and cellular diversity of glycolytic metabolism in CRC require systematic exploration. Multi-omics datasets (bulk/scRNA-seq and spatial transcriptomics) were analyzed to quantify glycolytic signatures. Core regulatory genes were selected via integrated pathway mapping and a machine learning framework incorporating five-feature selection algorithms. Cellular subpopulations were delineated by metabolic profiles, with niche interactions modeled through ligand–receptor network analysis. Findings were validated across multicenter cohorts. Our analyses identified a tumor subpopulation characterized by a High Glycolytic State (*HGS*), displaying elevated glycolytic signature alongside stem-like properties. Spatial profiling demonstrated relative enrichment of *HGS cells* in central tumor regions, potentially reflecting adaptation to nutrient-limited conditions. Among the molecular features associated with *HGS* maintenance, five candidate regulators (*PFKP, ERO1A, FKBP4, HDLBP, HSPA5*) showed correlation with unfavorable clinical outcomes. Our study characterizes the metabolic heterogeneity of CRC and suggests a potential role for *HGS cells* in shaping the tumor microenvironment. The molecular features identified here may offer insights into metabolic dependencies that could be explored for future therapeutic targeting.

25COASNOV12

Title: Effect of pyrogallol nanocomposite on miRNA and its associated pathways during radiation-induced toxicity in small intestine of irradiated Balb/C mice.

Parvathikandhan, S., Anbarasu, S.V., Narayanan, K. *et al.*

Med Oncol 42, 457 (2025).
https://doi.org/10.1007/s12032-025-02989-7

Abstract: Cancer is the abnormal and uncontrolled growth of cells that changes the structure of nearby cells or tissues. Cancer treatment strategies include surgery, chemotherapy, immunotherapy, and radiotherapy. Radiation therapy is one of the most frequently used cancer treatment modalities. Ionizing radiation not only kills cancer cells but also affects surrounding normal cells, causing extensive damage to all organs including the liver, kidneys, and intestines. Thus, identifying radioprotective agents is crucial to reduce the side effects of radiotherapy. Recently, nanocomposites have played a crucial role in cancer diagnosis and treatment as well as in reducing radiation-induced side effects. In this study, we tested pyrogallol nanocomposites for radiation-induced toxicity. Pyrogallol is a catechin molecule found in oak, eucalyptus, and other hardwood plants and is an amino polysaccharide produced by the deacetylation of chitin found in crustaceans and insects. In this study, pyrogallol and chitosan nanoparticles were blended to form a pyrogallol nanocomposite (PyNC). We investigated changes in miRNA expression in the small intestine of irradiated

BALB/c mice. BALB/c mice were divided into four groups: control, irradiated (10 Gy), irradiated (10 Gy) + PyNC (40 μg/kg body weight), and PyNC alone (40 μg/kg body weight). We analyzed miRNA expression, apoptotic genes, inflammatory genes, and fibrotic genes using real-time PCR, and apoptotic proteins were analyzed by Western blotting and immunohistochemistry. Our results revealed that radiation modulated miRNA expression patterns regulated by PyNC. Analysis of the miRNA online database revealed that the miRNA targets were casp9, IL7, IL7R, JUN, MMP9, Bcl2, and SMAD4. Furthermore, real-time PCR, Western blotting, and immunohistochemistry analyses revealed that radiation increased apoptotic proteins, inflammatory markers, and TGF-β and its associated molecules, which effectively decreased upon PyNC treatment in irradiated BALB/c mice. Additionally, PyNC treatment inhibited DNA fragmentation and oxidative stress in the small intestine of irradiated BALB/c mice. Overall, we suggest that PyNC effectively protects the small intestine from radiation-induced toxicity by altering miRNAs and their associated molecular targets, including apoptosis, inflammation, and fibrosis. However, overexpression or knockout studies of miRNAs during radiation-induced toxicity are warranted**.**

25COASNOV13

Title: Wedelolactone induces pyroptosis to suppress retinoblastoma by inhibiting the Nrf2/Keap1 signaling pathway.

Jiang, Y., Jiang, H., Wu, G. *et al.*

Med Oncol 42, 456 (2025).

https://doi.org/10.1007/s12032-025-02916-w

Abstract: Retinoblastoma is an intraocular malignancy with limited therapeutic options, imposing a severe health burden on young patients. Wedelolactone (WDL), a natural product from *E. prostrata*, possesses an anti-retinoblastoma activity, with the underlying regulatory mechanism remaining unknown. Methods- Retinoblastoma cell lines and xenograft nude mouse models were treated with WDL and RTA-408, an agonist for nuclear factor-erythroid 2-related factor 2 (Nrf2). Western blotting was conducted to determine the protein expression levels of kelch-like ECH-associated protein 1 (Keap1) and Nrf2. We performed the cell counting kit-8 assay, the 5-ethynyl-2-deoxyuridine staining, and flow cytometry to detect cell viability, proliferation, and apoptosis, respectively. The tumor progression in vivo was evaluated via the measurement of volume, weight, and proliferation levels of solid tumors. Monosodium urate crystal was applied to activate pyroptosis which was assessed by the expression detection of pyroptosis-related indicators. Results-WDL treatment elevated the expression of Keap1 and reduced the level of Nrf2. RTA-408 suppressed WDL-induced pyroptosis of retinoblastoma cells and reversed the effect of WDL on inhibiting retinoblastoma cell proliferation, promoting tumor cell apoptosis, and repressing the growth of solid tumors of the xenograft models. In addition, monosodium urate-induced pyroptosis partially restored the anti-retinoblastoma effect of WDL impaired by RTA-408. Conclusion-WDL triggers pyroptosis by inhibiting the Nrf2/Keap1 signaling pathway to exert anti-retinoblastoma effects.

25COASNOV14

Title: Water-based propolis enhances 5-fluorouracil drug efficiency in gastric and colorectal cancer cells through cell stress response, anti-migratory, and apoptotic effects regardless of p53 status.

Göksoy, M.A., Aksüt, Y., Şengelen, A. *et al.*

Med Oncol 42, 449 (2025).
https://doi.org/10.1007/s12032-025-03023-6

Abstract: Digestive system tumors, including gastric and colorectal cancers, have notable global incidence and mortality rates. While 5-Fluorouracil (5-FU) is widely used in treating gastrointestinal (GI) cancers, resistance often limits its effectiveness. Recent research has focused on the potential of natural products, such as propolis, a resin produced by honeybees, as adjuncts in cancer therapy. This study examined whether water-based propolis (WBP) could enhance the therapeutic effects of 5-FU on AGS (p53-wild-type) and Caco-2 (p53-null) cancer cell lines, aiming to propose a new combined treatment strategy. The findings demonstrated that WBP and 5-FU exhibited dose- and time-dependent cytotoxicity, with WBP increasing the therapeutic efficiency of 5-FU by reducing its half-maximal inhibitory concentration in both cancer cell lines, and reducing 5-FU toxicity in non-cancerous cells. Notably, cancer cells expressing p53 showed greater sensitivity to 5-FU; however, WBP demonstrated similar effects in both cell lines. The combined therapy of WBP (100 µg/mL for 48-h) and 5-FU (10 µg/mL for 48-h) with synergistic effects significantly reduced cell proliferation and motility. Moreover, combined treatments caused increased reactive oxygen species production, collapse of mitochondrial membrane potential, endoplasmic reticulum stress, and autophagy, thus leading to cell cycle arrest and apoptosis compared to individual treatments and controls, regardless of p53 expression in both cancer cells. These findings suggest that WBP, a natural product, could supplement 5-FU chemotherapy by enhancing its antitumor effectiveness, warranting further investigation for treating GI cancers.

25COASNOV15

Title: A novel long non-coding RNA, PICSAR, promotes thyroid cancer progression through the hsa-miR-320A/hsa-miR-485/RAPGEFL1 axis.

Hejazi, M., Jafari, T., Yari, A. *et al.*

Med Oncol 42, 448 (2025).
https://doi.org/10.1007/s12032-025-02987-9

Abstract: Among endocrine cancers, thyroid carcinoma (TC) is the most prevalent and ranks sixth in global mortality rates. Aberrant expression of long non-coding RNA (lncRNAs) is associated with the progression of various human cancers, including TC. The role of PICSAR lncRNA (LINC00162) has been validated in different human cancers. Therefore, this study aimed to assess the expression levels and functions of lncRNA PICSAR in thyroid cancer tumorigenesis. This comprehensive approach combined in silico and in vitro methods to explore the molecular mechanisms and clinical significance of PICSAR in thyroid cancer. This work assessed the expression of the long non-coding RNA LINC00162 and identified differentially expressed genes (DEGs) using the Cancer Genome Atlas (TCGA) database. Interactions among LINC00162, hsa-miR-320A, hsa-miR-485, and RAPGEFL1 were investigated using the LncACT and miRDB databases. Bioinformatics techniques were employed to conduct functional enrichment analysis to clarify the relevant molecular

pathways. For the investigation of LINC00162 expression in TC samples, 50 matched samples of thyroid carcinoma and adjacent normal tissue were gathered. Real time PCR was used to objectively evaluate the expression levels of the targeted genes. Every tissue sample was examined pathologically. A specific siRNA was transfected into a thyroid cancer cell line to examine the functional role of LINC00162. The impact of LINC00162 silencing was then assessed by measuring the level of target genes expression following the transfection. Based on TCGA-THCA analysis and qRT-PCR on tissue samples, LINC00162 (PICSAR) was markedly overexpressed in thyroid cancer tissues compared to normal samples. However, no discernible correlation was found between LINC00162 expression and the pathological characteristics of thyroid cancer. Our bioinformatics predictions based on lncRNA-microRNA interactions demonstrate that LINC00162 acts as a molecular sponge for the downregulated microRNAs hsa-miR-320A and hsa-miR-485 in thyroid cancer. RAPGEFL1, a gene associated with the development of thyroid cancer, is upregulated in conjunction with this downregulation. The LINC00162-miRNA-RAPGEFL1 axis is involved in critical carcinogenic processes, including thiamine metabolism, cell cycle control, and folate biosynthesis, according to functional enrichment analysis. Additionally, a bioinformatics study revealed a negative association between PICSAR and the NUDT3 gene, while a positive correlation was found with the SNX18P14 gene. Thyroid cancer cells transfected with LINC00162-specific siRNA showed significant downregulation of LINC00162 and RAPGEFL1, alongside an increase in hsa-miR-320A and hsa-miR-485, ultimately inhibiting the growth of thyroid cancer. These findings suggest that targeting PICSAR may offer a treatment strategy for thyroid cancer by altering important biological processes. In conclusion, LINC00162, which is overexpressed in thyroid cancer, acts as a molecular sponge for hsa-miR-320A and hsa-miR-485, regulating key oncogenic pathways and leading to the upregulation of RAPGEFL1. These effects are reversed upon siRNA-mediated silencing of LINC00162, indicating its potential as a promising therapeutic target for thyroid cancer. RAPGEFL1 regulates the Rap signaling pathway, controlling adhesion, migration, polarity, and metabolism to maintain cellular and tissue homeostasis. Its dysregulation is linked to various diseases, highlighting its potential as a therapeutic target.

25COASNOV16

Title: Chrysin mitigates therapy-induced senescence in breast cancer via cGAS–STING pathway inhibition.

Billimoria, R., Bhatt, P.

Med Oncol 42, 445 (2025).
https://doi.org/10.1007/s12032-025-02993-x

Abstract: Breast cancer continues to be a leading cause of cancer-related deaths among women globally, with cellular senescence having a complex role in its progression. Senescence is linked to chronic inflammation via the senescence-associated secretory phenotype (SASP). The cyclic guanosine monophosphate–adenosine monophosphate (cGMP-AMP) synthase (cGAS)–stimulator of interferon genes (STING) pathway, activated by cytoplasmic chromatin fragments (CCFs) marked by histone modifications (H3K27me3 and H3K9me3), is crucial for SASP production. This study investigates the potential of a natural flavonoid, Chrysin, as a senomorphic agent that targets these CCF markers to reduce inflammation in senescent breast cancer cells. We induced senescence in MDA-MB-231 and

MCF-7 cells using doxorubicin and analyzed the expression levels of inflammatory cytokines IL-6 and IL-8 after treatment with various concentrations of Chrysin through qRT-PCR. Western blotting and immunofluorescence revealed significantly reduced CCF markers H3K9me3 and H3K27me3, along with decreased STING phosphorylation. Notably, Chrysin did not change the expression of senescent markers p16 or p21. Additionally, Chrysin effectively inhibited SASP-driven breast cancer cell invasion and colony formation, highlighting its potential as both an anti-inflammatory agent and a senomorphic drug. Chrysin notably decreases H3K9me3 and H3K27me3-marked CCF levels, suppressing cGAS–STING pathway activation and reducing IL-6 and IL-8 levels. Our findings indicate that Chrysin represents a promising therapeutic strategy, targeting the epigenetic landscape of CCFs and modulating the SASP to mitigate the harmful effects of senescent cells in the tumor microenvironment.

25COASNOV17

Title: Gold nanoparticles capped with inclusion complex for the delivery of Chrysin in triple-negative breast cancer.

Velhal, K., Sah, P., Raut, R. *et al.*

Med Oncol 42, 441 (2025).

https://doi.org/10.1007/s12032-025-03011-w

Abstract: Chrysin (CHR), a naturally occurring flavonoid with promising anticancer potential, suffers from poor water solubility, limiting its therapeutic applications. To address this, β-Cyclodextrin (β-CD) inclusion complexes (ICs) of CHR were synthesized via the freeze-drying method at varying molar ratios (1:1, 1:2, 1:3, 1:4), with the 1:4 ratio exhibiting the highest entrapment efficiency (95.23%) and selected for further study. These ICs were then functionalized onto gold nanoparticles (AuNPs) to develop CHR-β-CD-AuNPs, enhancing drug delivery and stability. Characterization by UV–Vis, FTIR, NMR, NTA, and TEM confirmed successful encapsulation, hydrogen bonding, and spherical morphology with an average particle size of ~ 43 nm. Molecular docking supported strong interactions between CHR and β-CD. In vitro studies against human triple-negative breast cancer (MDA-MB-231) cells demonstrated that CHR-β-CD-AuNPs exhibited potent cytotoxicity with an IC_{50} of 22.17 ± 1.24 mg/L, significantly lower than CHR/β-CD ICs (IC_{50}: 22.84 ± 1.00 mg/L) and free CHR (IC_{50} > 100 mg/L, $p < 0.001$). Hoechst and phalloidin staining revealed clear apoptotic features such as nuclear fragmentation and cytoskeletal disruption. Gene expression analysis showed upregulation of Bax and Caspase-3 and downregulation of Bcl-2, confirming apoptosis induction. Furthermore, scratch wound assays demonstrated significant inhibition of cancer cell migration, with wound closure reduced to 8.38 ± 0.74% (IC) and 15.27 ± 1.05% (IC-AuNPs) compared to 74.41 ± 1.22% in untreated controls ($p < 0.001$). These findings establish that β-CD-based CHR-AuNP nanocarriers substantially improve the solubility, stability, and therapeutic efficacy of CHR, offering a promising nanoformulations strategy for enhanced targeted breast cancer therapy.

25COASNOV18

Title: Circ_0000847 promotes the migration, invasion, and EMT process in colorectal cancer through binding to IGF2BP2 to enhance IGF2 mRNA stability.

Zhang, A., Zheng, Y.

Med Oncol 42, 436 (2025).
https://doi.org/10.1007/s12032-025-02877-0

Abstract: Colorectal cancer (CRC) stands as one of the most prevalent forms of malignant gastrointestinal tumors. Circular RNAs (circRNAs) could serve as promising targets for therapeutic intervention in CRC. This study aims to uncover the significance and influence of circRNAs within the landscape of CRC. CircRNA microarray, RNase R assay, and fluorescence in situ hybridization were conducted to verify the expression and characteristics of circRNA. The biological behaviors of CRC cells were evaluated by cell counting kit-8, transwell assay, and wound-healing assay. The underlying mechanism was revealed using quantitative real-time PCR, Western bot, silver staining assay, biotin-labeled RNA pulldown, and RNA immunoprecipitation. The results indicated that circ_0000847, a CRC-associated circRNA, was over-expressed in CRC. Inhibition of circ_0000847 effectively restrained the migratory and invasive behaviors of CRC cells, alongside suppressing their epithelial-mesenchymal transition (EMT). Circ_0000847 bound to IGF2BP2, thereby enhancing the IGF2 mRNA stability. Importantly, overexpression of IGF2 abrogated the inhibitory effect of circ_0000847 depletion on CRC cellular processes. In addition, circ_0000847 promoted tumor growth in vivo. In summary, by engaging with IGF2BP2, circ_0000847 plays a role in stabilizing IGF2 mRNA, which in turn curtails the advancement of CRC. Hence, circ_0000847 could serve as an innovative and potentially pivotal target for the development of CRC therapies.

25COASNOV19

Title: Genistein enhances TLR3-mediated apoptosis and immune signaling in breast cancer cells.

Kaleli, S., Ozkan, A.D., Eskiler, G.G. *et al.*

Med Oncol 42, 435 (2025).
https://doi.org/10.1007/s12032-025-02856-5

Abstract: Breast cancer is one of the most common malignant tumors globally and the second leading cause of cancer-related death in women. Toll-like receptors (TLR) constitute a family of transmembrane receptors playing a crucial role in innate immunity. TLR3 is a type of TLR that is activated following Poly (I:C) double-stranded RNA binding. TLR3 activation leads to tumor suppression, and TLR3 directly causes apoptotic effects in cancer cells. Genistein (GEN), a phytoestrogen found in soy, inhibits cellular proliferation, induces apoptosis, and arrests the cell cycle. Therefore, it is important to determine the roles of immunotherapeutic agents targeting TLR3 in cancer treatment. The study aimed to determine the anti-inflammatory effect of GEN on breast cancer cells for the first time. The anti-inflammatory effects of GEN on the TLR3 signaling pathway were evaluated using Annexin V and cell cycle analysis, immunofluorescence assay, acridine orange staining, Western blotting, and ELISA cytokine release level in MCF-7 (hormone-dependent) and MDA-MB-231 (triple negative) breast cancer cells. The GEN alone treatment increased apoptosis, cell cycle arrest, apoptotic cell morphology, and the expression of TLR3, IRF3, AP-1, and p-NF-kB proteins. Additionally, higher levels of INF-β and TNF-α in both cells compared to treatment with Poly I:C alone were detected. These effects were more pronounced in MCF-7 cells than in MDA-MB-231 cells. Stimulation of the TLR3 signaling pathway was enhanced in the presence of GEN, leading to increased apoptosis.

25COASNOV20

Title: Anticancer efficacy of nerolidol, cyclophosphamide, and their combination against breast cancer cell line MCF-7.

Tousif, M., Nadeem, M., Tabassum, M. *et al.*

Med Oncol 42, 430 (2025).
https://doi.org/10.1007/s12032-025-02997-7

Abstract: In cancer, chemotherapeutic agents like cyclophosphamide (CP), is the most frequently used drug but the side effects caused by it, limits it's application. Therefore, creation of anticancer medicines with high efficacy and no or minimum side effects is a priority. In recent times, research on natural bioactive has been increased since they are efficient, safe, and economical. We earlier proved that Nerolidol (NER), a naturally derived sesquiterpene alcohol is a natural bioactive compound that could significantly reduce the CP-induced organ toxicities in Swiss albino mice. Thus, in this study, we intended to evaluate the anti-cancer property of NER alone and its potentiating effect in combination with CP in Michigan Cancer Foundation-7 (MCF-7) breast cancer cell line. MCF-7 is one of the most extensively used human breast cancer cell line, primarily because it closely resembles estrogen receptor-positive (ER^+), luminal-type breast cancer, which accounts for a significant proportion (~ 70%) of clinical breast cancer cases. MCF-7 cells are also non-invasive and less aggressive, which makes them suitable for early-stage tumor modelling and cytotoxicity screening. It provides a well-characterized and clinically relevant model for evaluating the efficacy of anticancer agents. MTT assay, clonogenic assay, cytotoxicity, wound healing assay, and cell cycle arrest was assessed to determine the anticancer properties of NER, CP, and their combination against MCF-7 cells. The change in nuclear morphology was determined by 4′, 6-diamidino-2- phenylindole (DAPI) to assess apoptosis. The NER, CP, and their combination at IC_{50} concentration was found to be cytotoxic against MCF-7 cells, inhibited colony formation, migration of MCF-7 cells and arrested the cell cycle at G0/G1, G2/M, and S phase, respectively. Thus, NER, CP, and their combination showed anticancer property against MCF-7 cells, when administered alone or in combination, but the combination treatment proved to be the best.

25COASNOV21

Title: Modeling Population-Level Impacts of Cell-Free DNA Screening for Colorectal Cancer in Canada.

Hutchinson JM, Ruan Y, Chia BJ, et al.

JAMA Oncol. 2025;11(7):694–699.
https://doi.org/10.1001/jamaoncol.2025.0908

Abstract: Importance - Cell-free DNA (cfDNA) testing is an emerging approach for colorectal cancer screening that has been approved in the US. The impact of cfDNA testing in the Canadian setting, assuming adherence mirroring prior real-world cfDNA work and assay performance from a Guardant Health study, is unknown. Objective - To estimate how cfDNA screening impacts clinical and economic outcomes in Canada compared with existing screening approaches (fecal immunochemical testing [FIT] or colonoscopies). Design, Setting, and Participants- The OncoSim-Colorectal model (version 3.6.5.7) was used to simulate participation, relative effectiveness, and cost of introduction of cfDNA tests every 3 years. A population of 32 million Canadians were simulated and examined for outcomes and

costs between 2024 and 2092. Exposures -Screening with colonoscopy, FIT, or cfDNA. Main Outcomes and Measures- Screen-detected colorectal cancer cases, deaths, health-adjusted person-years, potential years of life lost, and cost of cancer screening and management were examined. Results- Under higher participation, cfDNA detected 393 087 cases of colorectal cancer between 2024 and 2092 compared with 156 009 cases in the FIT scenario, and cfDNA reduced overall mortality by 121 383 deaths compared with current predictions with FIT. Linear regression models indicated that approximately 78% participation with 80% adherence or 69% participation with 100% adherence to cfDNA screening would be required to reduce deaths below the levels achieved by colonoscopy testing. Higher costs were associated with cfDNA testing, where each health-adjusted person-year had a cost of CAD $234.80 (US $164.06), and 0.025 deaths were averted per CAD $100 000 (US $69 874) additional dollars spent compared with FIT testing. When cfDNA testing was modeled with the same participation as FIT testing (43%), there was worse overall population impact (eg, greater number of deaths), emphasizing the importance of high participation for cfDNA testing to improve outcomes. Conclusions and Relevance - This study suggests that cfDNA testing could result in increased detection of colorectal cancer and reduced mortality if higher participation than reported in previous studies is achieved at the population level. Patient input on acceptance of blood-based vs stool-based screening may help inform real-world implementation.

25COASNOV22

Title: Trends in Surgical Overtreatment of Prostate Cancer.

Monda SM, Demus T, Jaime-Casas S, et al.

JAMA Oncol. 2025;11(7):700–706.

https://doi.org/10.1001/jamaoncol.2025.0963

Abstract: Importance- Over treatment of prostate cancer is a public health concern that undermines prostate cancer screening efforts. Objective- To assess trends in pathologic grade on prostatectomy during the past 2 decades as a surrogate for overtreatment. Design, Setting, and Participants- This retrospective cohort study examined the grade of prostate cancer on final pathology reports among patients undergoing prostatectomy between January 1, 2010, and September 1, 2024, in 2 parallel cohorts: Surveillance, Epidemiology, and End Results (SEER), a nationwide cancer registry, and Michigan Urological Surgery Improvement Collaborative (MUSIC), a statewide clinical registry. The presence of higher-risk features among patients who underwent grade group 1 prostatectomy during this period was also assessed. Exposures- The primary exposure of interest was year of radical prostatectomy. Main Outcomes and Measures- the primary outcome was the proportion of all prostatectomies that were pathologic grade group 1 (pGG1) on final pathology reports. The secondary outcome was the proportion of pGG1 prostatectomies with a higher-risk preoperative feature, assessed as a binary variable and including at least 1 of the following: more than 50% of biopsy cores positive, prostate-specific antigen of 10 ng/mL or higher, or grade group 2 on biopsy. Results- A total of 162 558 male patients in SEER (median [IQR] age, 63 [57-67] years) and 23 370 in MUSIC (median [IQR] age, 64 [59-69] years) underwent prostatectomy. The proportion of radical prostatectomies resulting in pGG1 on final pathology reports decreased from 32.4% (5852 of 18 071) to 7.8% (978 of 12 500) between 2010 and 2020 in SEER and from 20.7% (83 of 401) to 2.7% (32 of 1192) between

2012 and 2024 in MUSIC. A more recent prostatectomy was associated with a lower likelihood of a pGG1 prostatectomy while controlling for age and race within SEER (odds ratio [OR] per 5 years, 0.41; 95% CI, 0.40-0.42; $P < .001$) and MUSIC (OR per 5 years, 0.39; 95% CI, 0.36-0.43; $P < .001$). Within a subset analysis of those prostatectomies that were final pGG1, a more recent prostatectomy was associated with the presence of a higher-risk preoperative feature, including more than 50% of biopsy cores positive, prostate-specific antigen of 10 ng/mL or higher, and grade group 2 on prior biopsy within SEER (OR per 5 years, 1.60; 95% CI, 1.54-1.67; $P < .001$) and MUSIC (OR per 5 years, 1.60; 95% CI, 1.34-1.90; $P < .001$) Conclusions and Relevance- This cohort study found that since 2010, the frequency of pGG1 prostatectomies markedly decreased, and those few that were performed were more likely to have a higher-risk feature. This reduction in the proportion of prostatectomies that are pGG1 likely reflects improved diagnostic pathways, adherence to active surveillance protocols for low-risk cases, and ongoing efforts at both the state and national levels to minimize unnecessary surgical interventions in patients diagnosed with clinically insignificant prostate cancer.

25COASNOV23

Title: Harm-Benefit Balance of Immune Checkpoint Inhibitors in Non–Small Cell Lung Cancer.

Heyward J, Lesko CR, Murray JC, Mehta HB, Segal JB.

JAMA Oncol. 2025;11(7):707–716.
https://doi.org/10.1001/jamaoncol.2025.0985

Abstract: Importance- The benefits and harms of immune checkpoint inhibitor (ICI) therapy for lung cancer vary across groups, including those typically underrepresented in randomized clinical trials. Objective - To quantify the harms and benefits of ICI-containing regimens in individuals with non–small cell lung cancer and assess heterogeneity across priority subgroups. Design, Setting, and Participants- This retrospective cohort study conducted in 2024 used 2013 to 2019 Surveillance, Epidemiology, and End Results (SEER) Medicare data of individuals 66 years or older with non–small cell lung cancer who were exposed to any ICI. Exposures- ICI + chemotherapy, single ICI (reference group). Main Outcomes Severe-immune-related adverse events (irAE; harm) and mortality (when delayed mortality was the benefit). Severe irAEs were defined using validated diagnosis and medication codes. Mortality was ascertained from Medicare data. Hazard ratios (HRs) were estimated and 95% CIs were stratified by whether an ICI was used as the first or second or later systemic anticancer treatment (SACT) and in subgroups defined by preexisting autoimmune disease, sex, and age. The harm-benefit tradeoff was described as excess severe irAEs per year of life gained in which the gain in survival time was assessed using restricted mean survival time. Results- Of 17 681 Medicare beneficiaries, 8797 (49.5%) were female, and the mean (SD) age was 74 (6.0) years. Compared with a single ICI (14 249 [80.6%]), individuals treated with ICI + chemotherapy (3432 [19.4%]) had an elevated risk of severe irAE in the first SACT setting (hazard ratio [HR], 1.18; 95% CI, 1.06-1.30) but not in the second or later SACT setting (HR, 1.04; 95% CI, 0.92-1.19); there was a decreased risk of mortality in the first SACT setting (HR, 0.66; 95% CI, 0.62-0.72) but not in the second or later SACT setting (HR, 0.94; 95% CI, 0.68-1.03). In the first SACT setting, ICI + chemotherapy delayed mortality more among patients with (vs without) autoimmune disease at baseline. For each 1

year of life gained, the risk of severe irAEs was 0.31 (95% CI, 0.09-0.53) and the tradeoff was also statistically significant in men and patients without autoimmune disease. Conclusions- The results of this cohort study suggest that given both treatment-related harms and benefits, ICI + chemotherapy use in the first SACT setting requires informed decision-making; the potential benefits of ICI + chemotherapy vs single ICI in high-risk subgroups is encouraging.

25COASNOV24

Title: Overall Survival and Quality-of-Life Superiority in Modern Phase 3 Oncology Trials: A Meta-Epidemiological Analysis.

Sherry AD, Miller AM, Parlapalli JP, et al.

JAMA Oncol. 2025;11(7):718–724.

https://doi.org/10.1001/jamaoncol.2025.1002

Abstract: Importance- Alternative end points, such as progression-free survival, are increasingly used in phase 3 randomized clinical trials (RCTs). However, alternative end points are often not valid surrogates for overall survival and quality of life (QOL) and may be less relevant to patients. Objective- To determine the proportion of phase 3 RCTs with overall survival or QOL superiority. Design and Setting- Meta-epidemiological study of 2-group, superiority-design, interventional phase 3 oncology RCTs screened from ClinicalTrials.gov and published between 2002 and 2024. Main Outcomes and Measures Alternative end-point, overall survival, and QOL superiority in the experimental group vs the reference/control group according to prespecified statistical criteria for each RCT. A secondary goal was to evaluate the quality of QOL analyses, since approaches unadjusted for baseline scores may bias results. Results -A total of 791 RCTs representing 555 580 enrolled patients were included. Alternative primary end points were most common (n = 495 [63%]). The primary end point was met in 53% of the RCTs (n = 420); alternative end-point superiority was shown in 55% (n = 434). Overall survival superiority was shown in 28% (n = 221). Patient-reported outcomes were collected in 61% of the RCTs (n = 482), but global QOL results were published in only 34% (n = 271). Most between-group global QOL analyses did not adjust for baseline scores (223 [82%]). Global QOL superiority was shown in 11% (n = 84). Among all RCTs, 32% (n = 257) demonstrated either overall survival or global QOL superiority. Superiority of both overall survival and global QOL was shown in 6% (n = 48). Among 434 RCTs with a positive alternative end point, only a minority showed superiority of either overall survival (185 [43%]) or global QOL (67 [15%]). Conclusions and Relevance- Findings of superiority-design phase 3 oncology RCTs are commonly interpreted as positive. However, this is mostly based on improvements in alternative end points. Gains in either overall survival or QOL are uncommon, even when alternative end-point findings are positive. QOL appears both underevaluated and underreported; furthermore, the majority of phase 3 QOL analyses are unadjusted for baseline scores, which lose efficiency and add bias compared with adjusted analyses. To increase the meaningfulness of late-phase research, future trial designs and regulatory processes should be refocused toward overall survival and QOL improvements.

25COASNOV25

Title: Patient-Reported Outcomes With Stereotactic Intensity Modulated Radiotherapy After Radical Prostatectomy: A Nonrandomized Clinical Trial.

Nikitas J, Ballas LK, Romero T, et al.

JAMA Oncol. 2025;11(7):726–734.
https://doi.org/10.1001/jamaoncol.2025.1059

Abstract: Importance Postoperative radiotherapy remains underused for men with biochemical recurrence or adverse pathological features after radical prostatectomy (RP). Stereotactic body radiotherapy (SBRT) may improve utilization and poses potential radiobiological advantages. Objective To evaluate physician-reported late toxic effects and 2-year patient-reported outcomes (PROs) following post-RP SBRT. Design, Setting, and Participants This phase 2, single-arm trial was conducted in 2 academic centers in the US and included a comparator cohort. Men with post-RP prostate-specific antigen greater than 0.03 ng/mL or adverse pathologic features were included. Data were collected from February 2018 to March 2021, and data were analyzed from January to October 2024. Interventions SBRT delivered at 30 to 34 Gy in 5 fractions to the prostate bed. Nodal irradiation, boost to gross disease, and/or hormonal therapy were delivered per physician discretion. Main Outcomes and Measures Late toxic effects (more than 90 days after treatment) were graded according to Common Terminology Criteria for Adverse Events version 4.03. PROs were measured using Expanded Prostate Cancer Index-26. The proportion of men whose PROs had decrements greater than twice the threshold for minimal clinically important difference (MCID) at any point during the first 2 years were evaluated. The longitudinal PROs for men receiving SBRT was compared with a cohort of 200 men receiving postoperative conventionally fractionated radiotherapy (CFRT) using logistic regression, while adjusting for baseline scores, age, and receipt of nodal irradiation. Results Of 100 patients treated with post-RP SBRT, the median (IQR) age was 68.5 (63.9-71.4) years, and the median (IQR) follow-up was 43 (37-53) months. Cumulative incidence of late grade 2 and 3 genitourinary toxic effects was 25% and 4%, respectively, and of late grade 2 and 3 gastrointestinal tract toxic effects was 3% and 3%, respectively. The proportion of patients with decrements more than 2-fold the MCID in PROs was 38.9% (37 of 95) for urinary incontinence, 17.9% (17 of 95) for urinary irritation, and 34.1% (31 of 91) for bowel function. Compared with the CFRT cohort, the adjusted odds ratio for patients receiving SBRT experiencing decrements more than 2-fold the MCID was 1.55 (95% CI, 0.87-2.76; $P = .14$) for urinary incontinence, 0.94 (95% CI, 0.46-1.94; $P = .87$) for urinary irritation, and 1.03 (95% CI, 0.57-1.84; $P = .93$) for bowel function. Conclusions and Relevance In this nonrandomized clinical trial, post-RP SBRT was well-tolerated, with no measurably different decline in urinary or bowel PROs through 2 years compared with CFRT. Randomized studies and longer follow-up will better define the toxic effects and efficacy profile of post-RP SBRT.

25COASNOV26

Title: Neoadjuvant PD-1 and PD-L1 Blockade With Chemotherapy for Borderline Resectable and Unresectable Stage III Non–Small Cell Lung Cancer.

Ricciuti B, Fusco F, Cooper A, et al.

JAMA Oncol. 2025;11(7):735–741.

https://doi.org/10.1001/jamaoncol.2025.1115

Abstract: Importance- Patients with borderline resectable or unresectable stage III non–small cell lung cancer (NSCLC) with T4 and/or N2-N3 involvement face limited treatment options and poor outcomes. Neoadjuvant chemoimmunotherapy has shown promise in improving resectability and pathological responses. Objective- To evaluate the efficacy of neoadjuvant programmed cell death 1 protein (PD-1) or programmed cell death 1 ligand 1 (PD-L1) blockade combined with chemotherapy in enhancing surgical outcomes and pathological responses in patients with T4 and/or N2-N3 stage III NSCLC. Design, Setting, and Participants- This multicenter cohort study analyzed data from patients treated between February 2018 and January 2024 with neoadjuvant PD-1/PD-L1 inhibitors plus chemotherapy at academic and tertiary care centers across the US and Italy. Pathological and survival outcomes were assessed. Patients with stage III NSCLC and T4 and/or N2-N3 involvement were included. Data were collected from February 2018 to January 2024. Exposures Neoadjuvant- PD-1/PD-L1 blockade combined with platinum-based chemotherapy. Main Outcomes and Measures Pathological complete response (pCR), major pathological response, surgical resectability, and event-free survival (EFS). Results- Of 112 patients, 58 (51.8%) were female, and the median (range) age was 66 (41-84) years. A total of 84(75.0%) underwent surgical resection, achieving a pCR rate of 29.0% (24 of 83 with available final pathology) and a major pathological response rate of 42.2% (35 of 83). Patients with both PD-L1 expression of 50% or more and high tumor mutational burden achieved the highest pCR rate (4 of 9 [44.4%]; $P = .03$). Conversely, covariants in *KRAS*/*STK11* or *KRAS*/*KEAP1* were associated with lack of pCR. Patients with single-station or multistation N2/N3 disease exhibited comparable pathological outcomes. The median EFS for all resected patients was 52.6 months (95% CI, 27.8 to not reached), and this was significantly longer in patients with pCR (not reached vs 27.8 months [95% CI, 19.5 to not reached]; $P < .001$). Conclusions and Relevance- In this study, neoadjuvant PD-1/PD-L1 blockade combined with chemotherapy resulted in high pathological response rates and surgical resectability in patients with T4 and/or N2-N3 stage III NSCLC. This approach offers a viable treatment option for patients with borderline resectable or unresectable NSCLC but requires further validation through prospective studies.

25COASNOV27

Title: Tomosynthesis vs Digital Mammography Screening in Women with a Family History of Breast Cancer.

Li T, Su Y, Lee JM, et al.

JAMA Oncol. 2025;11(7):742–752.
https://doi.org/10.1001/jamaoncol.2025.1209

Abstract: Importance- Evidence on screening outcomes with digital breast tomosynthesis (DBT) vs digital mammography (DM) in women with a family history of breast cancer is limited. Objective -To compare the performance of DBT and DM screening in women with a family history of breast cancer overall and subdivided by breast cancer family history category, breast density, age group, screening interval, and screening round, and to describe characteristics of cancers detected on screening vs interval cancers. Design, Setting, and Participants In this comparative cohort study at imaging facilities affiliated with the Breast Cancer Surveillance Consortium, adult women 18 years and older with a self-reported family

history of breast cancer who underwent DBT or DM from 2011 to 2018 were included, with a 1-year follow-up for breast carcinoma. Data analysis was performed between November 2023 and August 2024. Exposures DBT or DM. Main Outcomes and Measures The main outcomes were absolute risk difference (ARD) between DBT and DM for recall rate, cancer detection rate, interval cancer rate, advanced cancer rate, biopsy rate, positive predictive values, sensitivity, and specificity, with inverse probability of treatment weighting. Results- A total of 208 945 women with a family history of breast cancer undergoing 502 357 screening examinations were included in the sample. Median (IQR) age was 58 (50-66) and 57 (49-66) years for the DBT and DM groups, respectively. Adjusted ARDs (DBT vs DM) were significant for recall rate (−1.51%; 95% CI, −2.42% to −0.59%) and specificity (1.56%; 95% CI, 0.65%-2.46%) in the overall cohort of 121 698 DBT and 380 561 DM examinations and among women with 1 first-degree relative (recall rate ARD, −1.72%; 95% CI, −2.70% to −0.74%; specificity ARD, 1.75%; 95% CI, 0.81%-2.69%). Among those with only second-degree relatives, the biopsy rate for DBT was significantly higher (ARD, 0.39%; 95% CI, 0.18%-0.61%). Significant ARDs were observed for the ductal carcinoma in situ detection rate (−0.71 per 1000 examinations; 95% CI, −1.03 to −0.38 per 1000 examinations) in women with almost entirely fatty breasts; recall rate (−1.90%; 95% CI, −2.88% to −0.92%) and specificity (1.93%; 95% CI, 0.97%-2.89%) in women with scattered fibroglandular densities. Significant ARDs were also observed for the positive predictive value for recall (1.75%; 95% CI, 0.84%-2.67%) in heterogeneously dense breasts, as well as the biopsy rate (0.48%; 95% CI, 0.16%-0.80%) and advanced cancer rate (−0.61 per 1000 examinations; 95% CI, −1.02 to −0.20 per 1000 examinations) in extremely dense breasts. DBT screening had a higher proportion than DM of screen-detected early-stage, invasive cancers with favorable prognostic characteristics. Conclusions and Relevance In this cohort study of women with a family history of breast cancer, DBT screening reduced recall rates and increased specificity compared to DM, particularly in women with 1 first-degree relative with breast cancer and those with scattered fibroglandular breast density, and reduced advanced cancer rates in women with extremely dense breasts.

25COASNOV28

Title: New Definition of Light Chain Monoclonal Gammopathy of Undetermined Significance.

Einarsson Long T, Rognvaldsson S, Thorsteinsdottir S, et al.

JAMA Oncol. 2025;11(7):753–761.
https://doi.org/10.1001/jamaoncol.2025.1285

Abstract: Importance- Recent studies suggest standard reference intervals for serum free light chains (FLC) are inaccurate and that this problem can only be partially remedied by using separate reference intervals for individuals with impaired kidney function. This decreases the utility of FLC testing in the clinical evaluation and follow-up of plasma cell disorders, particularly affecting the diagnosis of light chain (LC) monoclonal gammopathy of undetermined significance (MGUS). Objective- To evaluate the distribution of serum FLC and FLC ratios in individuals with preserved kidney function and to propose revised reference intervals and a new definition of LC-MGUS. Design, Setting, and Participants - The Iceland Screens, Treats or Prevents Multiple Myeloma (iStopMM) study is a nationwide prospective study of 75 422 participants (more than 50% of the Icelandic population) 40 years

and older who were screened for MGUS. Data were collected from September 2016 to May 2023, and data were analyzed from June 2023 to May 2024. Exposure Samples were analyzed by serum protein electrophoresis and immunofixation electrophoresis and FLC assay. Participants were actively followed up for progression. Main Outcomes and Measures The rate of abnormal FLC results using standard reference intervals was assessed, and revised age-stratified 99% reference intervals were calculated using nonparametric regression. The prevalence of LC-MGUS based on standard and revised reference intervals was evaluated along with progression to lymphoproliferative disorders. Results In total, 41 882 participants met inclusion criteria; a total of 23 786 (56.8%) were female, and the median (IQR) age was 60 (52-68) years. Using standard FLC reference intervals, 7316 κ FLC (17.5%), 1668 λ FLC (4.0%), and 1543 FLC ratios (3.7%) were abnormal. Revised reference intervals were calculated for those younger than 70 years (κ FLC, 6.3-39.0 mg/L; λ FLC, 5.9-36.7 mg/L; FLC ratio, 0.44-2.16) and 70 years or older (κ FLC, 7.0-55.8 mg/L; λ FLC, 6.4-48.0 mg/L; FLC ratio, 0.46-2.59). The prevalence of LC-MGUS was 1.54% (95% CI, 1.46-1.63) using standard intervals and 0.27% (95% CI, 0.23-0.30) using the revised intervals, yielding a decrease of 82%. None of the 1006 persons meeting LC-MGUS criteria based on standard intervals but not based on revised intervals progressed to a lymphoproliferative disorder during a median (range) follow-up of 4.6 (2.5-6.7) years. Conclusions and Relevance In this study, a new definition of LC-MGUS based on revised, more accurate FLC reference intervals decreased the false-positive rate of FLC testing by 82%.

25COASNOV29

Title: Expression of Membrane Targets for Therapeutics in RET-Positive Non–Small Cell Lung Cancer.

Marinello A, Ghigna MR, Rotow JK, et al.

JAMA Oncol. 2025;11(7):762–770.

https://doi.org/10.1001/jamaoncol.2025.1293

Abstract: Importance- Patients with advanced *RET* fusion–positive (*RET*$^+$) non–small cell lung cancer (NSCLC) who experience disease progression following treatment with *RET* inhibitors (RETis) have limited treatment options. Identifying membrane protein targets may support the assessment of novel therapies, such as antibody-drug conjugates and bispecific antibodies. Objective- To evaluate membrane target expression in *RET*$^+$ NSCLC. Design, Setting, and Participants This multicenter cohort study used centralized immunohistochemistry (IHC) on archival tissue samples and whole transcriptome sequencing (WTS) in an independent cohort. Tissue samples were collected from 12 European centers, and WTS was performed on globally sourced patient samples submitted for molecular profiling. This study included samples from patients with *RET*$^+$ NSCLC and *RET*–wild-type (*RET*-wt) adenocarcinoma controls that were analyzed by IHC and 203 *RET*$^+$ and 19 579 *RET*-wt samples analyzed by WTS. Exposures- Membrane protein expression of MET, ERBB2 (formerly HER2), epidermal growth factor receptor (EGFR), human epidermal growth factor 3 (HER3), and trophoblastic cell surface antigen 2 (TROP2) was evaluated using IHC, with samples scored on a scale of 0 to 3. Scores of 2 or greater were considered positive. Target expression as analyzed by WTS was expressed as median transcript per million scores. Main Outcomes and Measures Biomarker positivity, coexpression of biomarkers, dynamic changes in paired biopsies, and clinical correlates with survival

outcomes. Results A total of 189 patients were included in the study (among 81 patients with *RET*$^{+}$ NSCLC, the median [IQR] age was 62 [55-70] years, and there were 49 female individuals [60%]). In 93 samples from 81 patients with *RET*$^{+}$ NSCLC, positive IHC scores were observed for MET in 51 of 86 (59%), ERBB2 in 3 of 84 (3.6%), EGFR in 24 of 84 (29%), HER3 in 31 of 82 (38%), and TROP2 in 59 of 65 (91%). Compared with *RET*-wt adenocarcinoma (n = 112), *RET*$^{+}$ tumors showed higher MET (59% vs 43%; *P* = .03) and lower ERBB2 expression (3.6% vs 15%; *P* = .01). The WTS analysis from the independent cohort confirmed these results. Of 61 evaluable samples, 59 of 61 (97%) had at least 1 positive biomarker, 60 of 77 (78%) when excluding *TROP2*. *MET*/EGFR coexpression occurred in 17 of 79 evaluable samples (21.5%). Dynamic change in biomarker expression was observed in paired biopsy specimens. No significant survival differences based on target expression emerged in patients treated with RETi in the IHC and the WTS cohorts. Conclusions and Relevance -The results of this cohort study suggest that *RET*$^{+}$ NSCLC tumors frequently express MET and TROP2, with MET positivity enriched vs *RET*-wt controls. Coexpression and biomarker dynamics highlight the need for membrane target screening and novel therapeutic strategies for this population.

25COASNOV30

Title: Body Mass Index, Physical Activity, and Subsequent Neoplasm Risk Among Childhood Cancer Survivors.

Joffe L, Mirzaei S, Bhatia S, et al.

JAMA Oncol. 2025;11(8):835–845.

https://doi.org/10.1001/jamaoncol.2025.1340

Abstract: Importance High body mass index (BMI) and low physical activity levels are risk factors for adult-onset cancers. Limited data exist on their relationship with subsequent neoplasms among childhood cancer survivors. Objective- To evaluate associations between time-varying BMI/physical activity and subsequent neoplasm risk among childhood cancer survivors. Design, Setting, and Participants This retrospective cohort analysis included 5-year childhood cancer survivors diagnosed younger than 21 years of age between 1970 and 1999, enrolled in the Childhood Cancer Survivor Study (CCSS), with follow-up through September 2019 at pediatric tertiary care hospitals in the US and Canada. The data analysis was performed between March 2021 and July 2024. Exposures Self-reported time-varying BMI and maximum reported physical activity (metabolic equivalent of task h/wk [MET-h/wk]) before any subsequent neoplasm development; first assessed at cohort entry and up to 6 times thereafter. Main Outcomes and Measures Cumulative incidence by physical activity level and relative rates (RRs) by physical activity and time-varying BMI categories, adjusted for demographic and clinical variables, were estimated for any, subtype (hematologic, solid organ, central nervous system [CNS], skin), and specific (breast, thyroid, colorectal, meningioma) subsequent neoplasms using piecewise exponential models. Results Of 25 658 enrolled CCSS participants, 22 716 had BMI data before subsequent neoplasm development and met eligibility criteria for this study (46.3% female; median [range] attained age, 33.7 [5.7-67.3 years]). Among 22 716 survivors, 2554 subsequent neoplasms occurred among 2156 individuals (56.7% female; median [range] age at subsequent neoplasm diagnosis, 37.4 [13.7-63.3] years). Survivors reporting lower physical activity had higher 30-year subsequent neoplasm cumulative incidence: 18.6% (95% CI, 17.0-20.3) for 0 MET-h/wk vs 10.9% (95%

CI, 9.9-12.1) for 15-21 MET-h/wk. Obese BMI was associated with increased incidence rates of solid organ (RR, 1.22; 95% CI, 1.01-1.46), CNS (RR, 1.47; 95% CI, 1.12-1.95), and skin (RR, 1.30; 95% CI, 1.13-1.50) subsequent neoplasms. Higher physical activity (15-21 MET-h/wk) demonstrated a protective association for any (RR, 0.61; 95% CI, 0.53-0.71), solid organ (RR, 0.65; 95% CI, 0.52-0.83), CNS (RR, 0.50; 95% CI, 0.35-0.70), and skin (RR, 0.72; 95% CI, 0.60-0.86) subsequent neoplasms. BMI and physical activity were specifically associated with subsequent meningiomas and thyroid carcinomas, but not with breast or colorectal cancers, nor hematologic subsequent neoplasms. Conclusions and Relevance Among childhood cancer survivors in this cohort study, obesity was associated with an increased risk for multiple subsequent neoplasm types, while higher physical activity was associated with reduced subsequent neoplasm risk. Lifestyle interventions should be considered in future subsequent neoplasm prevention research.

25COASNOV31

Title: Long-Term Effectiveness Associated With Fecal Immunochemical Testing for Early-Age Screening.

Chiu H, Chen SL, Su C, et al.

JAMA Oncol. 2025;11(8):846–854.

https://doi.org/10.1001/jamaoncol.2025.1433

Abstract: Importance The rising incidence of young-onset colorectal cancer (CRC) has prompted health policymakers to consider lowering the recommended starting age for screening. However, population-based evidence supporting the long-term effectiveness of early-age screening remains limited.Objective To evaluate whether initiating fecal immunochemical test (FIT) screening at ages 40 to 49 years, rather than at the currently recommended age of 50 years, reduces CRC incidence and mortality. Design, Setting, and Participants This study analyzed a community-based screening cohort of Taiwanese residents aged 40 to 49 years, categorized into 4 subcohorts based on participation in early screening (age 40 to 49 years) and continuation of nationwide regular screening (50 years and older). The cohort was followed up until 2019 to compare CRC incidence and mortality across subcohorts. To mitigate self-selection bias, a delayed screening design and efficient propensity score matching was used, restricting analyses to participants attending regular screening. To validate the findings, an extended nonadherence adjustment was applied to all 4 subcohorts. Data were collected from January 2001 to December 2019, and data were analyzed from January 2021 to December 2024. Exposures Biennial FIT screening was initiated for the early screening group at ages 40 to 49 years and for the regular screening group at age 50 years, with follow-up continuing under Taiwan's national screening program. Main Outcomes and Measures Primary outcomes were CRC incidence and mortality rates, reported as cases per 100 000 person-years, with adjusted relative risks (aRRs) comparing early vs regular screening groups. Results Of 263 125 included participants, 146 796 (55.8%) were female. A total of 39 315 participated in early and regular screening, and 223 810 participated in regular screening only. The early screening group exhibited lower CRC incidence (26.1 [95% CI, 22.3-29.9] vs 42.6 [95% CI, 40.5-44.7] per 100 000 person-years) and mortality (3.2 [95% CI, 1.9-4.6] vs 7.4 [95% CI, 6.5-8.2] per 100 000 person-years). In propensity score–matched analyses, early screening significantly reduced CRC incidence (aRR, 0.79; 95% CI, 0.67-0.94) and mortality (aRR, 0.61; 95% CI, 0.38-0.98). Findings were

consistent in the extended nonadherence adjustment model, showing a 25% reduction in incidence (aRR, 0.75; 95% CI, 0.72-0.77) and a 34% reduction in mortality (aRR, 0.66; 95% CI, 0.62-0.71). Conclusions and Relevance This study found that initiating FIT screening at age 40 to 49 years was associated with further reduction in CRC mortality and incidence compared with starting screening at age 50 years. These results provide strong empirical support for lowering the CRC screening age, with substantial public health implications.

25COASNOV32

Title: Cancer Incidence and Trends in US Adults With HIV.

Haas CB, McGee-Avila JK, Luo Q, et al.

JAMA Oncol. 2025;11(8):855–863.
https://doi.org/10.1001/jamaoncol.2025.1589

Abstract: Importance People with HIV are living longer due to improvements in antiretroviral therapy over the last 2 decades. Current age-specific estimates of cancer risk among people with HIV may inform cancer prevention and clinical guidelines for this population. Objective To estimate cancer incidence rates (IRs) using a population-based linkage of HIV and cancer registries. Design, Setting, and Participants This population-based cohort study used data from 12 US states, Washington, DC, and Puerto Rico from 2001 to 2019. People with HIV and the general population in the HIV/AIDS Cancer Match Study were included in the analysis, which occurred between October 2023 and December 2024. Main Outcomes and Measures Age-standardized IRs (per 100 000 person-years) were calculated across calendar periods (2001 to 2004, 2005 to 2009, 2010 to 2014, and 2015 to 2019) and incidence rate ratios (IRRs) across calendar periods using adjusted Poisson regression. Standardized incidence ratios (SIRs) were estimated for 2010 to 2014 and 2015 to 2019, and age group–specific cancer incidence and SIRs were estimated for 2010 to 2019. Results The analysis included 7.2 million person-years among 847 107 people with HIV (5.3 million person-years among males [73%]). Comparing years 2015 to 2019 to years 2010 to 2014, incidence of diffuse large B-cell lymphoma (DLBCL) decreased 23% (IRR, 0.77; 95% CI, 0.70-0.84), Kaposi sarcoma (KS) decreased 24% (IRR, 0.76; 95% CI, 0.69-0.84), Hodgkin lymphoma decreased 25% (IRR, 0.75; 95% CI, 0.65-0.86), and cancers of the lung decreased 17% (IRR, 0.83; 95% CI, 0.77-0.90) and liver decreased 25% (IRR, 0.75; 95% CI, 0.67-0.84). Among people with HIV aged 70 to 84 years, IRs were highest for cancers of the prostate (448.01; 95% CI, 404.26-495.20), lung (269.79; 95% CI, 240.86-301.24), female breast (202.29; 95% CI, 155.79-258.32), liver (82.82; 95% CI, 67.16-101.03), and colon (107.57; 95% CI, 89.61-128.08), exceeding the IRs for DLBCL (41.83; 95% CI, 30.95-55.31) and KS (15.37; 95% CI, 9.11-24.29). From 2015 to 2019, risk remained significantly elevated in people with HIV for several cancer types, including KS (SIR, 213.87; 95% CI, 198.81-229.73), Hodgkin lymphoma (SIR, 6.29; 95% CI, 5.68-6.94), DLBCL (SIR, 5.25; 95% CI, 5.25-6.01), cancers of the anus (SIR, 17.07; 95% CI, 16.01-18.17), vulva (SIR, 11.40; 95% CI, 9.60-13.44), liver (SIR, 1.89; 95% CI, 1.74-2.05), and lung (SIR, 1.59; 95% CI, 1.51-1.68). For nearly all these cancers, SIRs significantly declined with increasing age. Conclusions and Relevance In this cohort study, significant declines in the incidence and relative risk for cancers among people with HIV demonstrate continued progress in HIV treatment and cancer prevention. These estimates may provide insight into the priorities for

prevention and early detection of cancer as the population of people with HIV enters ages with greater risk for cancer.

25COASNOV33

Title: Induction vs Adjuvant Chemoradiotherapy in Patients With High-Risk N2 to N3 Nasopharyngeal Carcinoma: A Phase 3 Randomized Clinical Trial.

Guo S, Li X, Liu L, et al.

JAMA Oncol. 2025;11(8):864–873.
https://doi.org/10.1001/jamaoncol.2025.1597

Abstract: Importance- It remains uncertain which chemotherapy sequence is more effective for locoregionally advanced nasopharyngeal carcinoma. Objective To compare the efficacy and safety of induction-concurrent with concurrent-adjuvant chemotherapy in high-risk N2 to N3 nasopharyngeal carcinoma. Design, Setting, and Participants In this open-label, randomized, phase 3 clinical trial conducted at Sun Yat-sen University Cancer Center (China) from November 20, 2017, to March 19, 2021, patients aged 18 to 65 years with stage T1-4N2-3M0 and a pretreatment Epstein–Barr virus DNA level of 1500 or more copies/mL were enrolled. The data were analyzed from December 2024 to March 2025. Intervention The patients were randomly assigned to receive 3 cycles of paclitaxel-cisplatin-fluorouracil induction chemotherapy followed by concurrent chemoradiotherapy or concurrent chemoradiotherapy followed by 3 cycles of cisplatin-fluorouracil adjuvant chemotherapy. Main Outcome and Measure -The primary end point was 3-year progression-free survival, assessed locally by the investigator and defined as the time from random assignment to documented local or regional relapse, distant metastasis, or death of any cause, whichever occurred first. Results A total of 162 patients (median [IQR] age, 44 [34-53] years; 40 female individuals [24.7%]) were assigned to the induction-concurrent group and 162 (median [IQR] age, 45 [37-52] years; 36 female individuals [22.2%]) to the concurrent-adjuvant group. Regarding the data cutoff (October 8, 2024), the median (IQR) follow-up period was 60.4 (58.2-62.6) months. The 3-year progression-free survival rates were 73.5% (95% CI, 65.9%-79.6%) in the induction-concurrent group and 70.4% (95% CI, 62.7%-76.8%) in the concurrent-adjuvant group (stratified hazard ratio, 0.86; 95% CI, 0.58-1.27; $P = .45$). The most common short-term grade 3 or worse adverse events were leukopenia (53 of 160 [33.1%] in the induction-concurrent group vs 47 of 142 [33.1%] in the concurrent-adjuvant group), neutropenia (52 [32.5%] vs 32 [22.5%], respectively), and mucositis (47 [29.4%] vs 42 [29.6%], respectively). The most common grade 3 or worse late adverse event was auditory or hearing loss (10 [6.3%] vs 12 [8.5%], respectively). Two patients in the induction-concurrent group died of treatment-related toxic effects. No treatment-related death occurred in the concurrent-adjuvant group. Conclusions and Relevance This randomized clinical trial found that induction-concurrent chemotherapy did not significantly improve progression-free survival compared with concurrent-adjuvant chemotherapy in high-risk N2 to N3 nasopharyngeal carcinoma. Both treatment strategies were effective, and clinicians should discuss with the patients about the potential risks and benefits of the induction chemotherapy or adjuvant chemotherapy to provide the most appropriate treatment for patients with high-risk features.

25COASNOV34

Title: Early ctDNA and Survival in Metastatic Colorectal Cancer Treated With Immune Checkpoint Inhibitors: A Secondary Analysis of the SAMCO-PRODIGE 54 Randomized Clinical Trial .

Taïeb J, Sullo FG, Lecanu A, et al.

JAMA Oncol. 2025;11(8):874–882.
https://doi.org/10.1001/jamaoncol.2025.1646

Abstract: Importance Immune checkpoint inhibitors (ICIs) have dramatically transformed the therapeutic landscape of deficient mismatch repair/microsatellite unstable−high (dMMR/MSI-H) metastatic colorectal cancer (mCRC); however, ICI use is challenged by primary resistance and timing of discontinuation. Whether circulating tumor DNA (ctDNA) may be predictive of progression-free survival (PFS) and overall survival (OS) in this treatment context remains unknown. Objective To assess the prognostic and predictive role of ctDNA, detected by tumor-specific methylation markers, in patients with dMMR/MSI-H mCRC treated with ICIs. Design, Setting, and Participants This prespecified secondary analysis of the SAMCO-PRODIGE 54 randomized clinical trial evaluated ctDNA in patients with dMMR/MSI-H mCRC treated with avelumab or standard chemotherapy, with or without a targeted agent in the second-line setting, to assess its prognostic role. Plasma samples were obtained prospectively for ctDNA analysis, and digital droplet polymerase chain reaction amplification of bisulfite-converted cell-free DNA (cfDNA) for *WIF1* and *NPY* genes was used to quantify ctDNA levels. These samples were collected from April 2018 to April 2021 at 49 sites in France at baseline (V1) and 1-month posttreatment initiation (V2) during. Data analyses were performed from October 1 to November 1, 2024. Intervention Avelumab or standard chemotherapy with or without targeted agents. Main Outcomes and Measures PFS and OS according to baseline ctDNA positivity or concentration, and early ctDNA variation (ΔctDNA = [V1−V2] ÷ V1). Results The predictive analysis included 99 patients (mean [SD] age, 66 [13] years; 51 female [51.5%]) with plasma samples available for ctDNA assessment at V1, of which 74 had samples available also at V2 for Change in ctDNA assessment. In the 99 patients with available V1 plasma samples, baseline ctDNA positivity or concentration were not associated with clinical outcomes. Change in ctDNA (cutoff at median value) was significantly associated with both PFS (hazard ratio [HR], 2.98; 95% CI, 1.77-5.01; $P < .001$) and OS (HR, 3.61; 95% CI, 1.81-7.17; $P < .001$). This association was evident in patients treated with avelumab (PFS HR, 4.22; 95% CI, 1.77-10.1; $P = .001$; OS HR, 17.40; 95% CI, 3.82-79.70; $P < .001$) than in those receiving chemotherapy (PFS HR, 2.09; 95% CI, 1.03-4.21; $P = .04$; OS HR, 1.51; 95% CI, 0.61-3.72; $P = .38$). Avelumab (vs chemotherapy) improved PFS in favorable ctDNA responders (HR, 0.33; 95% CI, 0.14-0.77; log-rank $P = .008$) but not in poor responders (HR, 1.32; 95% CI, 0.67-2.62; log-rank $P = .42$) Combined ctDNA response and RECIST, version 1.1, assessment accurately predicted long-term OS. In the multivariable analysis, lack of ctDNA response was associated with an increased risk of disease progression and death in the avelumab group (HR, 7.27; 95% CI, 2.23-23.7; $P = .001$) but not in the chemotherapy group (HR, 1.61; 95% CI, 0.66-3.93; $P = .30$). Conclusions The findings of this secondary analysis of an RCT found that change in ctDNA at 1-month posttreatment can predict long-term outcomes in patients with dMMR/MSI-H mCRC treated with ICIs.

25COASNOV35

Title: Utidelone Plus Bevacizumab for ERBB2-Negative Metastatic Breast Cancer and Active Brain Metastases: The U-BOMB Phase 2 Nonrandomized Clinical Trial.

Yan M, Lv H, Liu X, et al.

JAMA Oncol. 2025;11(8):883–889.
https://doi.org/10.1001/jamaoncol.2025.1694

Abstract: Importance Patients with *ERBB2* (formerly *HER2* or *HER2/neu*)-negative metastatic breast cancer (MBC) and brain metastases have poor prognosis, and effective treatment options are limited. Objective To investigate the activity and safety of utidelone plus bevacizumab in patients with *ERBB2*-negative MBC and active brain metastases. Design, Setting, and Participants This nonrandomized clinical trial was conducted at 5 hospitals in China. Adult patients with *ERBB2*-negative MBC who had untreated or progressive brain metastases were enrolled between May 5, 2022, and October 25, 2023. The data cutoff date was May 20, 2024; data were analyzed from September 15, 2022, to July 20, 2024. Interventions Patients received bevacizumab (15 mg/kg on day 1) and utidelone (30 mg/m^2 on days 1-5) every 3 weeks until disease progression or unacceptable toxic effects. Main Outcomes and Measures The primary end point was central nervous system (CNS) objective response rate (ORR) according to Response Evaluation Criteria in Solid Tumors (RECIST) version 1.1. Results A total of 47 female patients (median age, 53 years [IQR, 45-59 years]) were recruited. Of these, 35 patients had untreated brain metastases and 12 had brain metastases that had progressed after local radiotherapy. The CNS ORR was 42.6% (95% CI, 28.3%-57.8%) per RECIST version 1.1 and 40.4% (95% CI, 26.4%-55.7%) per Response Assessment in Neuro-Oncology Brain Metastases criteria. The median follow-up duration was 11.0 months (range, 2.3-23.6 months). The median progression-free survival (PFS) was 7.7 months (95% CI, 5.6-9.7), median CNS-PFS was 10.6 months (95% CI, 8.4 months to not reached), and median overall survival was 15.1 months (95% CI, 12.0 months to not reached). The most common grade 3 or higher treatment-emergent adverse events were decreased lymphocyte count in 5 patients (10.6%) and decreased white blood cell count in 3 patients (6.4%). No serious or fatal adverse events occurred. Conclusions and Relevance The findings of this nonrandomized clinical trial suggest the potential of utidelone plus bevacizumab for the treatment of patients with *ERBB2*-negative MBC and active brain metastases. This treatment approach warrants further validation in a randomized clinical trial.

25COASNOV36

Title: Therapy, Safety, and Logistics of Preoperative vs Postoperative Stereotactic Radiation Therapy: A Preliminary Analysis of a Randomized Clinical Trial.

Yeboa DN, Li J, Lin R, et al.

JAMA Oncol. 2025;11(8):890–899.
https://doi.org/10.1001/jamaoncol.2025.1770

Abstract: Therapy, Safety, and Logistics of Preoperative vs Postoperative Stereotactic Radiotherapy Visual Abstract.-Importance Preoperative stereotactic radiation therapy (SRT) vs postoperative SRT logistics and toxic effects provides clinically significant data on management outcomes. Objective To determine preoperative SRT logistics and safety profile compared with postoperative in patients with brain metastases. Design, Setting, and Participants This single-institution phase 3 randomized clinical trial included patients 18

years and older and undergoing a planned surgical resection. Patients were required to have an Eastern Cooperative Oncology Group Performance Status score of 2 or greater and be candidates for SRT within 30 days of surgical resection. Patients with radiosensitive histologies (eg, small cell lung cancer and lymphoma), brain metastasis of unknown primary, and/or radiographic evidence of leptomeningeal disease were excluded. Data were collected from December 2018 to August 2023, and data were analyzed from September 2023 to December 2024. Interventions Patients were randomized 1:1. Patients randomized to the preoperative SRT cohort underwent SRT (in 1 to 5 fractions) followed by surgical resection within 1 month of radiation therapy. Patients randomized to the postoperative SRT cohort underwent resection followed by postoperative SRT within 1 month of surgery. Main Outcomes and Measures Outcomes reported focus on nonprimary end point analysis of the trial, including comparative toxic effect outcomes of preoperative vs postoperative SRT postprocedural events, feasibility of preoperative SRT, and radiation therapy management. Results Of 103 patients, 56 (54.4%) were male, and the median (range) age was 59 (26-83) years. Of 103 patients, 83 (80.6%) completed both radiation and surgery for brain metastases while in the study. Of these, 70 patients (84%) had 1 to 4 brain metastases at enrollment, 11 (13%) had 5 to 10 lesions, and 2 (2%) had more than 10 lesions. In the preoperative stereotactic radiosurgery (SRS)/SRT cohort, 45 (88%) completed both treatments compared with 38 (73%) in the postoperative SRS/SRT arm. There were no statistically significant differences between treatment groups in 30-day postoperative morbidity or postprocedural events. The median (range) time between surgery and SRT was significantly shorter in the preoperative arm (6 [0-24] days) compared with the postoperative arm (22 [12-42] days; $P < .001$). The median (range) time from randomization to receiving both brain-directed therapies was 10 (4-31) days in the preoperative arm compared with 32.5 (19-55) days for the postoperative arm ($P < .001$). Conclusions and Relevance In this randomized clinical trial, preoperative SRT had comparable safety to postoperative SRT and resulted in shorter time to treatment completion, potentially facilitating expedited care.

25COASNOV37

Title: High-Dose Aumolertinib for Untreated EGFR-Variant Non–Small Cell Lung Cancer With Brain Metastases: The ACHIEVE Phase 2 Nonrandomized Clinical Trial.

Li H, Chen K, Gong L, et al.

JAMA Oncol. 2025;11(8):900–908.

https://doi.org/10.1001/jamaoncol.2025.1779

Abstract: Importance Central nervous system (CNS) metastases remain a significant challenge in the management of *EGFR*-variant non–small cell lung cancer (NSCLC). Objective To evaluate the activity and safety of high-dose aumolertinib in patients with untreated *EGFR*-variant NSCLC and brain metastases. Design, Setting, and Participants This was a phase 2 nonrandomized clinical trial conducted at 10 centers in China. Patients with untreated *EGFR*-variant metastatic NSCLC and brain metastases were enrolled between July 6, 2021, and August 31, 2022. The data cutoff date was October 10, 2024. Interventions Patients received aumolertinib, 165 mg, orally once daily until disease progression or unacceptable toxic effects. Main Outcomes and Measures The primary end point was 12-month progression-free survival (PFS) rate assessed by investigators according to the Response Evaluation Criteria In Solid Tumors (RECIST), version 1.1. Results A total

of 63 patients (39 female [61.9%]; median age, 60 [range, 47-76] years) were enrolled (full analysis set), and 49 had at least 1 measurable brain lesion (CNS evaluable-for-response set). Median follow-up duration was 28.8 months (95% CI, 27.0-29.8). In the full analysis set, the 12-month PFS rate was 62.1% (95% CI, 48.7-73.0), the median PFS was 20.5 months (95% CI, 12.0-26.9), the 12-month intracranial PFS rate was 76.8% (95% CI, 63.2-85.9), and the median intracranial PFS and overall survival were not reached. Systemic and intracranial objective response rates per RECIST 1.1 were 56 of 63 (88.9% [95% CI, 78.4-95.4]) and 52 of 63 (82.5% [95% CI, 70.9-90.9]) in the full analysis set and 43 of 49 (87.8% [95% CI, 75.2-95.4]) and 42 of 49 (85.7% [95% CI, 72.8-94.1]) in the CNS evaluable-for-response set, respectively. The most common grade 3 or 4 treatment-related adverse event was increased blood creatine phosphokinase (17 participants [27.0%]). No treatment-related deaths occurred. *EGFR* variant clearance in plasma circulating tumor DNA at day 1 of cycle 2 was independently associated with longer PFS (hazard ratio, 0.14 [95% CI, 0.04-0.47]; $P = .001$). Conclusions and Relevance -The findings of this nonrandomized clinical trial suggest that high-dose aumolertinib is associated with long-term survival benefit in patients with untreated *EGFR*-variant NSCLC and brain metastases, with a manageable safety profile.

25COASNOV38

Title: Global burden of cutaneous melanoma incidence attributable to ultraviolet radiation in 2022.

Langselius O, Rumgay H, de Vries E, et al

Int J Cancer. 2025; 157(6)
https://doi.org/10.1002/ijc.35463

Abstract: Cutaneous melanoma (CM) accounted for around 331,700 cancer cases globally in 2022. Ultraviolet radiation (UVR) is a major CM risk factor. In this study, we update and improve global estimates of UVR-attributable CM cases. Population attributable fractions (PAFs) were calculated by age, sex, and country using GLOBOCAN 2022 national incidence estimates comparing to a minimally exposed Nordic 1930 birth cohort reference population. Adjustments for acral lentiginous melanoma were made to exclude non-UVR-associated melanomas. In sensitivity analyses, PAFs were recalculated with a theoretical minimally exposed 1903 South Thames, England birth cohort and world region-specific reference populations. An estimated 267,353 (95% uncertainty intervals [UI]: 242,818, 278,638) CM cases were UVR attributable globally in 2022. Males contributed to a larger proportion (57%, 151,921 out of 267,353) of UVR-attributable CMs. We found significant regional variation with the highest PAF observed in Australia/ New Zealand, Northern Europe, and North America, all with more than 95% CM cases UVR-attributable. Attributable age-standardized rates were highest in regions with populations of lighter skin color such as Australia/New Zealand, Northern Europe, and North America, with 75.68 (95%UI: 74.50, 76.86), 36.82 (95%UI: 36.38, 37.26) and 33.69 (95%UI: 33.47, 33.91) attributable cases per 100,000 people. By age group, the burden increased with age, with PAF of 76.39% (95%UI: 66.24, 81.01) among people aged 30–49 versus 86.13% (95%UI: 80.04, 88.99) among 70+ years. Most of the global CM burden in 2022 was UVR-attributable. Primary prevention through increasing sun safety awareness and affordable sun protection provision options is key to reducing CM.

25COASNOV39

Title: Effects of levonorgestrel-releasing intrauterine system on recurrence and fertility outcomes during assisted reproduction after complete remission of early endometrioid endometrial cancer and precancerous lesions: A retrospective cohort study

Qujia Gama et.al.

Int J Cancer. 2025; 157(6)
https://doi.org/10.1002/ijc.35465

Abstract: To investigate the efficacy of the levonorgestrel-releasing intrauterine system (LNG-IUS) on recurrence and fertility outcomes during controlled ovarian stimulation (COS) in patients with early stage endometrioid endometrial carcinoma (EEC) and endometrial atypical hyperplasia (EAH) following successful fertility-preserving treatment. We reviewed the patients with Grade 1 presumed Stage IA EEC or EAH who underwent in vitro fertilization and embryo transfer after successful fertility-sparing treatment. A total of 176 women were enrolled in this study, undergoing 318 cycles of COS and 290 cycles of embryo transfer (ET). Twenty-one percent (37/176) patients have an LNG-IUS insertion during the initial ovarian stimulation, and the median follow-up time for this cohort was 61.3 months (interquartile range [IQR], 39.0–76.6 months), while it was 60.5 months for the other cohort (IQR, 44.9–80.3 months). Disease recurrence was experienced by 34.7% (61/176) of the patients. Compared to the non-LNG-IUS group, the LNG-IUS group had a lower recurrence rate 1 year after COS (5.4% (2/37) versus 20.9% (29/139), $p = .034$). The use of LNG-IUS was associated with a reduced recurrence rate 1 year after COS (hazard ratio = 0.203, 95% confidence interval [0.042–0.984], $p = .048$). The overall clinical pregnancy rate reached as high as 65.3% (115/176), while the cumulative live birth rates were up to 46.6% (85/176). We found that LNG-IUS during COS did not impact oocyte yield, ET, or pregnancy outcomes. The placement of LNG-IUS during COS in EEC/EAH patients is worth considering, as it is likely to reduce the recurrence of endometrial lesions without affecting fertility outcomes.

25COASNOV40

Title: Timing of surgery and 1-year postoperative outcomes in patients with breast cancer and preoperative COVID-19 history: A matched, longitudinal, ambidirectional cohort study

Yali Wang, Lijuan He, et.al.

Int J Cancer. 2025; 157(6)
https://doi.org/10.1002/ijc.35466

Abstract: Preoperative severe acute respiratory syndrome coronavirus 2 (SARS-CoV-2) infection increases the risk of postoperative complications and mortality and has long-lasting effects on multiple organ systems. The scheduling of elective surgery after SARS-CoV-2 infection depends on infection severity, vaccination status, patient factors, and surgical urgency. In the post-vaccination Omicron era of the coronavirus disease 2019 (COVID-19) pandemic, there is limited evidence regarding the medium- and long-term postoperative outcomes and optimal surgical timing for patients with breast cancer recovering from COVID-19. This ambidirectional cohort study included 392 patients who underwent breast cancer surgery either more than 2 weeks after or 12 weeks before a COVID-19 diagnosis. Patients were stratified according to the time from COVID-19 diagnosis to surgery and were

followed longitudinally for 1 year to evaluate the evolution of postoperative outcomes. Propensity score matching and stabilized inverse probability of treatment weighting methods were used to mitigate confounding factors, determine the optimal timing of surgery, and assess risk factors. No deaths or severe postoperative complications occurred within 1 year of surgery. Patients with preoperative COVID-19 history had a higher risk of medium-term adverse postoperative outcomes than those without (26.2% vs. 10.2%). Multiple analyses revealed that for patients with breast cancer and preoperative COVID-19 history, delaying surgery beyond 4 or even 8 weeks after COVID-19 diagnosis did not significantly reduce the risk of medium- or long-term adverse postoperative outcomes ($p > .05$). In the post-vaccination Omicron era, our evidence supports timely performing surgery 2 weeks after COVID-19 diagnosis in fully vaccinated patients with breast cancer.

25COASNOV41

Title: Treatment outcomes in nasopharyngeal carcinoma patients with parotid lymph node metastasis: An 11-year experience at a tertiary cancer center

Linghui Yan et.al.

Int J Cancer. 2025; 157(6)

https://doi.org/10.1002/ijc.35470

Abstract: Parotid lymph node (PLN) metastasis in nasopharyngeal carcinoma (NPC) is rare, with limited data guiding its management and prognosis. We retrospectively analyzed 6924 non-metastatic NPC patients at our tertiary cancer center, identifying 126 patients with PLN metastasis confirmed by fine-needle aspiration cytology (FNAC) and magnetic resonance imaging (MRI). Survival outcomes and prognostic factors were assessed using Kaplan–Meier estimates, log-rank tests, propensity score matching (PSM), and Cox regression. Compared to patients with N3 disease, those with PLN metastasis had worse regional relapse-free survival, distant metastasis-free survival, and progression-free survival. However, overall survival was not significantly affected. When PLN received radical-intensity radiation doses, outcomes were comparable to patients without PLN metastasis. Treatment failures with PLN involvement frequently co-occurred with regional relapse and distant metastasis. Among patients who were treated with PLN-sparing intensity-modulated radiotherapy (IMRT), compared to non-parotid relapse patients, parotid relapse patients were older, had more advanced N classification, lower baseline Epstein–barr virus DNA (EBV-DNA) level, and received fewer cycles of chemotherapy. Additionally, these recurrent PLNs were characterized by smaller size, being typically unilateral and isolated, exhibiting poor sensitivity to chemotherapy, and receiving lower doses of radiotherapy. In our study, PLN metastasis does not upstage the patient's N classification if comprehensive radiotherapy is administered at radical doses. We advise prudence when implementing parotid-sparing IMRT and strongly recommend FNAC for clinically suspicious lesions.

25COASNOV42

Title: Cachexia-induced reprogramming of visceral organ metabolism by human pancreatic cancer xenografts

Raj Kumar Sharma et.al.

Int J Cancer. 2025; 157(6)

https://doi.org/10.1002/ijc.35487

Abstract: Pancreatic cancer patients with cachexia experience functional changes in visceral organs. To further understand these functional changes, here, for the first time, we characterized metabolic changes in the spleen, liver, pancreas, lungs, heart, and kidneys induced by human pancreatic cancer xenografts. These studies identify the commonality and consequences of cachexia-induced visceral organ metabolic dysregulation. The heart, kidneys, liver, lungs, pancreas, and spleen from euthanized non-tumor-bearing control mice and from cachexia-inducing Pa04C and non-cachexia-inducing Panc1 tumor-bearing mice ($n = 8–10$ per group) were metabolically characterized with 1H magnetic resonance spectroscopy. All visceral organs, with the exception of lungs, exhibited significant weight reduction in cachectic Pa04C mice relative to normal and non-cachectic Panc1 mice. A significant reduction ($p \leq .0166$) of organ metabolites ranging from the amino acids leucine, isoleucine, valine, alanine, lysine, arginine, asparagine, glutamate, glutamine, aspartate, glycine, tyrosine, and phenylalanine, along with glucose, lactate, creatine, choline, and fumarate, depending upon the visceral organ, was observed in cachectic Pa04C mice compared to normal mice. The highest number of metabolites was reduced in the spleen, followed by the kidneys, lungs, and liver. The metabolic changes identified can lead to negative consequences in organ function by impacting pathways involved in tissue regeneration and resolving inflammation at the cellular level in cachectic mice. These results highlight the visceral organ metabolic reprogramming that can occur with cancer-induced cachexia, an understanding of which can identify noninvasive biomarkers and metabolic interventions to reduce morbidity and mortality from pancreatic cancer.

25COASNOV43

Title: Factors associated with reaching maintenance therapy in patients with advanced biliary tract cancer treated with durvalumab: Real-world results from a multicenter and multinational study

Margherita Rimini et.al.

Int J Cancer. 2025; 157(6)

https://doi.org/10.1002/ijc.35481

Abstract: Standard of care first-line systemic treatment for advanced biliary tract cancer includes chemo-immunotherapy with gemcitabine, cisplatin, and durvalumab, followed by maintenance durvalumab monotherapy. The present work aims to investigate the differences in baseline clinical and molecular characteristics between patients with early progression during chemo-immunotherapy and those who reach durvalumab maintenance therapy. The study population included patients with unresectable, locally advanced, or metastatic BTC who received treatment at 38 clinical Institutions in 12 countries from July 2021 to December 2023. The primary objective of the study was to investigate whether baseline clinical and molecular characteristics differed between patients with early progression during chemo-immunotherapy versus those reaching durvalumab maintenance therapy. Four hundred forty-eight patients were included in this study. Two hundred twenty-seven patients (50.7%) received maintenance with durvalumab monotherapy, whereas 221 (49.3%) did not receive maintenance therapy due to PD during first-line chemo-immunotherapy before completing 8 cycles. Results show that patients who received maintenance were more likely to be older (≥70 years), have an ECOG = 0, locally advanced disease, and a neutrophil-to-lymphocyte ratio (NLR) <3. A higher proportion of patients with BAP1 mutations received maintenance,

while TP53 mutations were more common in those who progressed early. According to the present analysis, a substantial proportion of patients (50.7%) with advanced BTC who were treated with chemotherapy plus durvalumab proceeded to receive maintenance therapy with durvalumab monotherapy, with a median treatment duration of 4.4 cycles. Patients ≥70 years, with ECOG PS 0, with locally advanced disease, and with NLR <3 had a higher likelihood of receiving maintenance therapy.

25COASNOV44

Title: Patient factors and modifications to intended chemotherapy for women with Stages I–IIIA breast cancer

Jenna Bhimani et.al.

Int J Cancer. 2025; 157(7)

https://doi.org/10.1002/ijc.35494

Abstract: Modifications to intended chemotherapy regimens may be due to various reasons and may impact patient outcomes. Understanding which factors are associated with chemotherapy modifications can help inform treatment planning and improve cancer care. We examined the association between patient/tumor factors and modifications to intended chemotherapy in women with Stages I–IIIA breast cancer who were treated at Kaiser Permanente Northern California and Kaiser Permanente Washington from 2005 to 2019. Modifications were defined as any dose reductions in the first cycle or throughout chemotherapy, regimen change, treatment delay (single delay >14 days) or receiving fewer cycles of any drugs than expected. We used generalized linear models of the Poisson family with a log-link function to calculate prevalence ratios (PRatios). Of 9700 women receiving adjuvant chemotherapy, 34.6% had chemotherapy modifications. Selected results are shown: positive associations were observed with age ($PRatio_{80+ \text{ vs. } 18–39}$: 1.93; 95% confidence interval [CI]: 1.50–2.50; *p*-trend <.001), body mass index (BMI) ($PRatio_{\geq 35 \text{ vs. } 18.5 \text{ to } <25}$: 1.53; 95% CI: 1.41–1.65; *p*-trend <.001), and Charlson comorbidity index ($PRatio_{3+ \text{ vs. } 0}$: 1.33; 95% CI: 1.19–1.48; *p*-trend <.001), while more recent years of diagnosis were associated with decreased prevalence of treatment modifications ($PRatio_{2015\text{-}2019 \text{ vs. } 2005–2009}$: 0.65; 95% CI: 0.61–0.69; *p*-trend <.001). Stage was also positively associated ($PRatio_{\text{Stage IIIA vs. I}}$: 1.24; 95% CI: 1.13–1.35; *p*-trend <.001), as was human epidermal growth factor-2 positive status (PRatio: 1.99; 95% CI: 1.89–2.10). In conclusion, patients with the highest likelihood of chemotherapy modifications represent those who may have more complex prescribing needs, including those of older age, higher BMI, and more comorbidity. Further understanding of how modifications could impact outcomes within these groups can inform and improve cancer care.

25COASNOV45

Title: DNA methylation biomarkers for cervical cancer risk prediction in HIV-positive Nigerian women

Yinan Zheng et.al.

Int J Cancer. 2025; 157(7)

https://doi.org/10.1002/ijc.35502

Abstract: Cervical cancer (CC) remains a significant public health issue in low- and middle-income countries (LMICs), especially in Western sub-Saharan Africa and Nigeria. While

global CC incidence and mortality have declined, these regions continue to face high rates due to inadequate screening and the high prevalence of HIV, which increases CC risk by promoting persistent HPV infections. This study aimed to identify DNA methylation (DNAm) biomarkers for cervical intraepithelial neoplasia (CIN) and CC in HIV-positive Nigerian women and to assess their potential for clinical risk prediction. From 2018 to 2020, 538 participants were recruited from Nigerian tertiary hospitals. Cervical tissue samples were analyzed for DNAm using the Infinium MethylationEPIC BeadChip array, and HPV genotyping was conducted via next-generation sequencing. An epigenome-wide association study revealed 24 significant DNAm biomarkers associated with CIN and CC. These biomarkers showed hypermethylation in tumor suppressor genes (e.g., *PRMD8*), hypomethylation in oncogenes (e.g., *MIR520H*), and aberrant methylation in genes related to HIV/HPV infection and oncogenesis (e.g., *GNB5*, *LMO4*, *FOXK2*, *NMT1*). A machine learning-based DNAm classifier achieved 92.9% sensitivity and 88.6% specificity in predicting CC risk, with higher risk observed in adjacent normal cervical samples from CIN/CC patients and HIV/HPV co-infected women. DNAm biomarkers offer a promising approach to enhancing CC screening and early detection, particularly for HIV-positive women in LMICs. The DNAm-based model developed in this study shows potential for more accurate CC risk stratification, highlighting the need for further optimization, validation, and implementation in low-resource settings.

25COASNOV46

Title: Characterization of bridging therapies in clinical trials leading to FDA approval of CAR-T cell therapies

Victoria Kaestner, **Alyson Haslam**, **Vinay Prasad**

Int J Cancer. 2025; 157(7)

https://doi.org/10.1002/ijc.35473

Abstract: During the time of chimeric antigen receptor T-cell (CAR-T) manufacturing, bridging therapy is often used to control disease. Because it often involves systemic treatment, the bridging therapies can induce responses and/or adverse events. We sought to assess bridging therapies used in CAR-T trials in a cross-sectional study. We reviewed FDA drug labels and peer-reviewed registration trial reports (including supplemental data) to evaluate the characteristics of bridging therapy used in trials testing CAR-T therapies. We looked at which bridging therapies were used, whether multiple therapies were combined, the response rates, and the reported adverse events associated with bridging therapy. Of the 11 studies testing CAR-T therapies, 10 reported the bridging therapies that were used in the study. Of those that reported the types of bridging therapies ($n = 10$), the most commonly used bridging therapy was dexamethasone (10/10, 100%), rituximab (6/10, 60%), gemcitabine (5/10, 50%), and etoposide (5/10, 50%). Of the trials, one of 11 (9%) clearly reported whether patients had responses to bridging therapy, six of 11 (55%) vaguely reported responses, and four of 11 (36%) trials did not report or mention any response information regarding bridging therapy. Although patients are often refractory to first-line therapies, which share considerable overlap with bridging therapies, these therapies may induce responses. Despite this possibility, the reporting of bridging therapy combinations and their subsequent response rates and adverse event rates are highly variable. These findings highlight the need for greater transparency in the reporting of bridging therapy to more

reliably assess the efficacy of CAR-T therapies.

25COASNOV47

Title: Long-term cardiac outcomes in breast cancer patients treated with helical tomotherapy: Evaluating the applicability of 3D-based dose constraints for intensity modulated radiation therapy

Pierre Loap et.al.

Int J Cancer. 2025; 157(7)
https://doi.org/10.1002/ijc.35474

Abstract: Adjuvant breast radiotherapy has been associated with cardiac toxicity due to older 2D and 3D techniques, with a linear relationship between mean heart dose (MHD) and ischemic cardiac events. Cardiac dose distribution differs with modern techniques like intensity-modulated radiotherapy (IMRT), potentially affecting this relationship. This study evaluates long-term cardiac toxicity in breast cancer patients treated with tomotherapy to reassess 3D-derived dose constraints. Breast cancer patients treated with tomotherapy at Institut Curie from August 2010 to December 2015 were included. Patients had undergone breast-conserving surgery or mastectomy, with some receiving chemotherapy or trastuzumab. Tomotherapy was used for anatomically challenging cases. The primary endpoint was cardiac toxicity correlated with MHD; secondary endpoints were overall and disease-specific survival. Statistical analyses included logistic regression and Cox models. Among 179 patients, the median MHD was 7.04 Gy, with 95.6% having an MHD above 5 Gy. Sixty-six patients had cardiovascular risk factors, and 28.5% were obese. Over a median follow-up of 9.1 years, eight patients (4.5%) experienced cardiovascular events—all with pre-existing risks or obesity. No significant correlation was found between MHD and major coronary events ($p = 0.607$) or heart failure ($p = 0.800$). Cardiac mortality was absent, and 10-year overall and disease-specific survival were 88.0% and 94.3%, respectively. Cardiac events in patients treated with tomotherapy were rare and driven by pre-existing risk factors. The linear MHD-toxicity relationship observed in 3D radiotherapy may not apply to IMRT, potentially leading to overestimated risks. Long-term studies are needed to refine IMRT dose constraints.

25COASNOV48

Title: Long-term risk of major cardiac events in breast cancer patients treated with intensity-modulated and 3-dimensional conformal radiotherapy: Secondary analysis of a randomized clinical trial

Nam Kyu Kang et.al.

Int J Cancer. 2025; 157(7)
https://doi.org/10.1002/ijc.35476

Abstract: We assess the relationship between radiation dose to the heart and cardiac disease within the context of modern radiotherapy techniques of 3-dimensional and intensity-modulated radiotherapy (IMRT). The KROG 15-03 study was a multicenter phase III trial involving 693 breast cancer patients who underwent breast-conserving surgery (BCS). Patients were randomly assigned to receive either IMRT or 3D-CRT following BCS. Major cardiac event (MCE), defined as the occurrence of angina pectoris or myocardial infarction requiring coronary angiography, and admission for cardiac arrhythmia related to the irradiation of the heart. The primary outcome of the study was to investigate the incidence of

MCE and factors associated with MCEs. At a median follow-up of 6.5 years, the incidence of MCEs at 6.5 years was 1.8%. The mean heart dose (MHD) for the entire cohort of 647 patients was 2.1 (±2.3) Gy. The cumulative incidence of MCEs at 6.5 years was 1.1% for the subgroup of MHD <2.9 Gy and 3.3% for the subgroup of MHD >2.9 Gy ($p = 0.010$), and 0.9% for the subgroup of age ≤55 years and 3.3% for the subgroup of age >55 years ($p = 0.006$), respectively. Multivariate analyses confirmed that MHD ($p = 0.044$; hazard ratio [HR], 1.21 per 1 Gy; 95% confidence interval [CI], 1.09–1.46) and age ($p = 0.034$; HR, 1.07 per 1 year; 95% CI, 1.03–1.14) were significant factors of MCEs. The incidence of MCE increased by 21% per 1-Gy increase in MHD within 6.5 years after radiotherapy.

25COASNOV49

Title: Comparison of outcomes between haploidentical and matched related donors for chronic myelomonocytic leukemia: A multicenter real-world study

Yu-Qian Sun

Int J Cancer. 2025; 157(7)

https://doi.org/10.1002/ijc.35485

Abstract: Allogeneic hematopoietic stem cell transplantation (HSCT) is the only curative strategy for patients with chronic myelomonocytic leukemia (CMML). However, few reports have investigated the outcomes of patients receiving haploidentical HSCT. To this end, we included 117 patients with haploidentical donors (HID) and 75 patients with matched related donors (MRD) from 28 centers across China to explore the prognostic impact of different transplantation modalities. We found no significant difference between these two groups in terms of event-free survival (EFS, $p = .211$), overall survival (OS, $p = .503$), cumulative incidence of relapse (CIR, $p = .076$) or non-relapse mortality (NRM, $p = .794$). The predominance of peripheral blood (PB) graft source over bone marrow and PB since 2020 may have contributed to the worse outcomes in the MRD group. Moreover, CMML-specific prognostic scoring system (CPSS) lower-risk patients benefited more from the HID modality with superior EFS ($p = .006$). Multivariate analysis indicated that advanced age ($p = .013$), anemia at diagnosis ($p = .010$), and donor relationship (parent-to-child, $p = .013$) were independently associated with worse EFS in the HID group. Our data suggested that HID was comparable to MRD in CMML. However, under certain conditions, such as CPSS lower-risk ones, HID was preferred.

25COASNOV50

Title: Integrin β6 expression in colorectal cancer cells promotes liver metastasis through enhanced adhesion to endothelial fibronectin

Chiara Van Passen

Int J Cancer. 2025; 157(7)

https://doi.org/10.1002/ijc.35504

Abstract: Integrin β6 is associated with poor prognosis in colorectal cancer (CRC) patients, with metastasis being a crucial determinant. Capillary endothelial cells (EC) in the liver and lung are the primary sites of contact for circulating tumour cells during metastasis. Here, we analysed the role of integrin β6 in tumour cells for their interaction with EC. Integrin β6 functions as a heterodimer with integrin αv. Interestingly, we found that liver and lung EC strongly express fibronectin, a high-affinity ligand of αvβ6. Expression of *ITGB6* in CRC

tumour cells closely correlated with their adhesion to EC. This interaction was greatly reduced by silencing *ITGB6* in the tumour cells and was integrin β6 dependent under both static and flow conditions. Binding assays with fibronectin-coated surfaces, competing RGD peptides, and integrin β6-neutralizing antibodies confirmed the crucial role of β6-fibronectin binding in the interaction between tumour cells and EC. Since metastatic tumours exhibit increased proteolytic activity, we examined integrin β6 stability under these conditions. Remarkably, β6 remained resistant to trypsin and the matrix metalloprotease 12, underscoring its role in maintaining tumour cell adhesion in proteolytic microenvironments. Furthermore, ITGB6 expression was significantly elevated in liver metastases compared to corresponding primary tumours from the same patients, suggesting an enrichment of β6-expressing cells in metastatic sites. These results suggest that tumour cell integrin β6 binding to EC-derived fibronectin may serve as a critical first step in metastasis formation. Targeting this interaction could provide a promising therapeutic strategy to repress CRC metastasis.

25COASNOV51

Title: Outcomes of Radium-223 and Stereotactic Ablative Radiotherapy Versus Stereotactic Ablative Radiotherapy for Oligometastatic Prostate Cancers: The RAVENS Phase II Randomized Trial.

Jarey H. Wang et al.

J Clin Oncol 43, 2059-2068(2025).
https://doi.org/10.1200/JCO-25-00131

Abstract: Purpose- Randomized clinical trials (RCTs) have shown progression-free survival (PFS) benefits of metastasis-directed therapy (MDT) without androgen deprivation therapy for oligometastatic castration-sensitive prostate cancer (omCSPC). Most patients with bone metastatic (BM) omCSPC recur with additional bone disease after MDT. We hypothesized the BM-targeting alpha-emitter radium-223 dichloride (Ra223) could target subclinical bone disease and delay progression. Methods-This is an investigator-initiated, multicenter, open-label phase II RCT. Eligible men with recurrent omCSPC with ≥one bone metastasis (≤three on conventional imaging and/or ≤five on molecular imaging) were randomly assigned (1:1) to stereotactic ablative radiation (SABR) MDT alone or SABR MDT with Ra223 (six cycles). Primary end point was composite PFS. Results-From August 9, 2019, to March 2, 2023, 64 patients were randomly assigned, 33 to SABR MDT and 31 to SABR MDT/Ra223 balancing for key covariates. Most SABR MDT/Ra223 patients (87%) received six cycles of Ra223. The median PFS was 11.8 months with SABR MDT and 10.5 months with SABR MDT/Ra223 (adjusted hazard ratio [aHR], 1.42 [95% CI, 0.79 to 2.56]; $P = .24$). Seven patients (11%) experienced grade 3 treatment-related adverse events (no grade 4 or 5), 2 of 33 (6%) with SABR and 5 of 30 (17%) with SABR MDT/Ra223. Patients with high-risk (HiRi) pathogenic mutations in *ATM*, *BRCA1/2*, *RB1*, or *TP53* had worse PFS (HR, 5.95 [95% CI, 1.83 to 19.3]; $P = .003$). Greater T-cell receptor (TCR) unique productive rearrangements were prognostic for improved PFS independent of the treatment arm (aHR, 0.45 [95% CI, 0.21 to 0.96]; $P = .04$). Conclusion-Adding Ra223 to SABR MDT in BM omCSPC does not delay progression of disease. We provide evidence for an HiRi mutational signature and TCR repertoire as prognostic biomarkers in omCSPC treated with SABR MDT, highlighting the importance of collecting biological correlates in RCTs for omCSPC.

25COASNOV52

Title: Characterization and Clinical Implications of p53 Dysfunction in Patients With Myelodysplastic Syndromes.

Matteo Zampini et al.

J Clin Oncol 43, 2069-2083(2025).
https://doi.org/10.1200/JCO-24-02394

Abstract: Purpose-Tumor Protein 53 (p53) expressed from gene *TP53* is a seminal tumor suppressor. We aimed to characterize mutational and nonmutational mechanisms of p53 dysfunction in myelodysplastic syndromes (MDS) and to investigate their clinical effect. Patients and Methods We analyzed a cohort of 6,204 patients with MDS and subsets of patients with available information on RNA sequencing of tumor cells (n = 109), high-dimensional phenotype of immune cells (n = 77), and multiomics analysis (RNA sequencing and proteomics) on single cells (n = 15). An independent validation was performed on 914 patients. Results-Biallelic *TP53* inactivation was a powerful driver of disease progression and identified high-risk patients, regardless of variant allele frequency. Monoallelic and biallelic inactivation represent disease stages occurring as a multihit process in MDS with *TP53* mutations, thus potentially refining the optimal timing of therapeutic interventions in these patients. We identified a subset of MDS (5%) characterized by *TP53* wild-type and hyperexpression of abnormal p53 protein in bone marrow progenitors that exhibit dismal outcome. These patients presented upstream p53 signaling aberrations in Pi3K cascade; RAS, WNT, and NF-KB pathways; and *MDM2* gene amplification, together with a downstream dysregulation of p53 targets. MDS with p53 dysfunction displayed a distinct immune dysregulation involving myeloid-derived inflammation and impaired antigen presentation, which may be a driver of their poor prognosis and provide the groundwork for innovative immunotherapies. Conclusion The identification of nonmutational p53 dysfunction in MDS may lay the foundation for a mechanistic classification of myeloid neoplasms, moving beyond a purely molecular stratification. The recognition of patients with p53 dysfunction is relevant to provide correct disease-risk assessment and interventions, as well as to refine the design of clinical trials

25COASNOV53

Title: Second-Line Endocrine Therapy With or Without Palbociclib Rechallenge in Patients With Hormone Receptor–Positive/Human Epidermal Growth Factor Receptor 2–Negative Advanced Breast Cancer: PALMIRA Trial.

Antonio Llombart-Cussac et al.

J Clin Oncol 43, 2084-2093(2025).
https://doi.org/10.1200/JCO-24-01865

Abstract: Purpose-Cyclin-dependent kinase 4 and 6 (CDK4/6) inhibitors plus endocrine therapy (ET) represents the standard first-line treatment for patients with hormone receptor–positive/human epidermal growth factor receptor 2–negative (HER2-negative) advanced breast cancer (ABC). However, there is no definitive consensus on the preferred second-line treatment option. The PALMIRA trial investigated whether palbociclib rechallenge with an alternative ET would improve the antitumor activity in patients progressing after a first-line palbociclib-containing regimen. Methods-This international, randomized, open-label, phase II study enrolled 198 patients with hormone receptor–positive/HER2-negative ABC with

disease progression after first-line palbociclib plus ET (aromatase inhibitor or fulvestrant). Patients were eligible if they showed clinical benefit to the previous regimen (response or stable disease ≥24 weeks) or had progressed on a palbociclib-based therapy in the adjuvant setting. Patients were randomly assigned (2:1 ratio) to either palbociclib rechallenge plus second-line ET (fulvestrant or letrozole) or second-line ET alone. Stratification factors were previous ET and visceral involvement. The primary end point was investigator-assessed progression-free survival (PFS). Results- Between April 2019 and October 2022, 136 and 62 patients were randomly assigned to palbociclib plus ET or ET alone, respectively. Median investigator-assessed PFS was 4.9 months (95% CI, 3.6 to 6.1) with palbociclib plus ET versus 3.6 months (95% CI, 2.5 to 4.2) with ET alone (hazard ratio, 0.84 [95% CI, 0.66 to 1.07]; *P* = .149). Grade ≥3 treatment-emergent adverse events were higher with palbociclib plus ET (47.4% *v* 10.0%), without new safety signals. Conclusion- Palbociclib rechallenge plus an alternative ET did not significantly improve PFS compared with ET alone in patients with hormone receptor–positive/HER2-negative ABC progressing on a first-line palbociclib-based ET regimen.

25COASNOV54

Title: Characteristics of Patients and Prognostic Factors Across Treatment Lines in Metastatic Colorectal Cancer: An Analysis From the Aide et Recherche en Cancérologie Digestive Database.

Jean-Baptiste Bachet et al.

J Clin Oncol 43, 2094-2106(2025).
https://doi.org/10.1200/JCO-24-01968

Abstract: Purpose- Several lines of treatment can be used sequentially in patients with metastatic colorectal cancer. We investigated the evolution of patient/tumor characteristics and their prognostic impact across treatment lines to develop an overall prognostic score (OPS). Patients and Methods - Individual patient data from 48 randomized trials were analyzed. The end point was overall survival (from random assignment to death). Missing data were imputed. The complete data set was then separated into construction (80%) and validation sets (20%). The Cox's model was used to define risk groups for survival using the OPS. The discrimination capability was assessed in each treatment-line via bootstrapping to obtain optimism-corrected calibration and discrimination C-indices. Internal validation was done in the validation set. Results- A total of 37,560 patients (26,974 in first-line [1L], 7,693 in second-line [2L], and 2,893 in third-line [3L]) were analyzed. Some clinical, biological, and molecular characteristics of patients/tumors included in therapeutic trials evolve over the lines. Seven independent prognostic variables were retained in the final multivariate model common to all lines: Eastern Cooperative Oncology Group performance status, hemoglobin, platelet count, WBC/absolute neutrophil count ratio, lactate dehydrogenase, alkaline phosphatase, and the number of metastatic sites. The OPS was used to define four patient subgroups with significantly different prognoses in 1L, 2L, and 3L, separately, with adequate C-indices: 0.65, 0.66, and 0.69 in the construction set and 0.65, 0.66, and 0.68 in the validation set, respectively. The OPS was not predictive, with 3L drugs (*v* placebo) or subsequent line (2L/1L or 3L/2L) extending survival in all prognostic groups. Conclusion- The same prognostic model using practical variables can be used before all treatment lines.

The OPS could better stratify patients in future clinical trials and help to therapeutic decision in routine practice.

25COASNOV55

Title: Randomized Phase II Study of Nab-Paclitaxel and Gemcitabine With or Without Tocilizumab as First-Line Treatment in Advanced Pancreatic Cancer: Survival and Cachexia.

Inna M. Chen et al.

J Clin Oncol 43, 2107-2118(2025).
https://doi.org/10.1200/JCO.23.01965

Abstract: Purpose-This randomized phase-II trial compared efficacy of gemcitabine/nab-paclitaxel (Gem/Nab) with or without the anti–interleukin-6 (IL-6) receptor antibody tocilizumab (Toc) for advanced pancreatic cancer (PC). Methods- A safety cohort received Gem 1,000 mg/m^2 and Nab 125 mg/m^2 on days 1, 8, and 15, and Toc 8 mg/kg on day 1 for each 28-day cycle. Participants with modified Glasgow prognostic scores of 1 or 2 were randomly assigned 1:1 to receive Gem/Nab/Toc or Gem/Nab. The primary end point was the overall survival (OS) rate at 6 months (OS6). Secondary end points were progression-free survival (PFS), overall response rate (ORR), and safety. Exploratory end points were cachexia, quality of life, and biomarkers, including the cachexia-promoting protein, growth differentiation factor 15 (GDF15). Results-Overall, 147 patients were treated, including six safety cohort participants. The median follow-up period was 8.1 months (IQR, 4.2-13.9). OS6 was 68.6% (95% CI, 56.3 to 78.1) for the Gem/Nab/Toc group and 62.0% (49.6-72.1) for the Gem/Nab group (P = .409). OS for Gem/Nab/Toc versus Gem/Nab improved at 18 months (27.1% *v* 7.0%, P = .001). No differences in median OS, PFS, or ORR were observed. Incidence of grade-3+ treatment-related adverse events (TrAEs) was 88.1% for Gem/Nab/Toc and 63.4% for Gem/Nab (P < .001). Gem/Nab/Toc decreased muscle loss versus Gem/Nab, with median change +0.1013% versus –3.430% (P = .0012) at 2 months and +0.7044 versus –3.353% (P = .036) at 4 months. Incidence of muscle loss was 43.48% on Gem/Nab/Toc versus 73.52% on Gem/Nab at 2 months (P = .0045) and 41.82% versus 68.75% (P = .0062) at 4 months. GDF15 was not changed by Gem/Nab or Gem/Nab/Toc. Conclusion- Although the primary end point was not met and TrAEs were increased by Toc, increased survival at 18 months and reduced muscle wasting support an anticachexia effect of IL-6 blockade independent of GDF15. Further studies could leverage these findings for precision anticachexia therapy.

25COASNOV56

Title: Practical Guidelines for the Treatment of Gestational Trophoblastic Disease: Collaboration of the European Organisation for the Treatment of Trophoblastic Disease (EOTTD)–European Society of Gynaecologic Oncology (ESGO)–Gynecologic Cancer InterGroup (GCIG)–International Society for the Study of Trophoblastic Diseases (ISSTD).

Christianne Lok et al.

J Clin Oncol 43, 2119-2128(2025).
https://doi.org/10.1200/JCO-24-02326

Abstract: Gestational trophoblastic diseases (GTDs) are a group of pregnancy-related premalignant and malignant diseases with generally a favorable prognosis when treated adequately. Many different treatment protocols exist worldwide. To our knowledge, this is the first set of global consensus-based guidelines for GTD. Four international organizations (European Organisation for the Treatment of Trophoblastic Diseases, European Society of Gynecologic Oncology, Gynecologic Cancer Intergroup, and International Society for the Study of Trophoblastic Diseases) delegated 53 expert GTD clinicians from 31 countries who formulated nine consensus-based definitions and the minimum criteria required to be a GTD center. Furthermore, 18 flow diagrams were developed to diagnose, treat, and follow up all forms of primary or recurrent GTD. The definitions and flow diagrams were drafted and adapted in consecutive (online) meetings until consensus was reached followed by an external review process. Here, the final guidelines are presented together with the available supporting evidence from the literature.

25COASNOV57

Title: Updated Overall Survival and Long-Term Safety With Ripretinib Versus Sunitinib in Patients With GI Stromal Tumor: Final Overall Survival Analysis From INTRIGUE.

Michael C. Heinrich et al.

J Clin Oncol 43, 2239-2244(2025).
https://doi.org/10.1200/JCO-24-02818

Abstract: In the INTRIGUE phase III trial (ClinicalTrials.gov identifier: NCT03673501), adult patients with advanced gastrointestinal stromal tumor previously treated with imatinib were randomly assigned 1:1 to ripretinib 150 mg once daily or sunitinib 50 mg once daily (4 weeks on/2 weeks off). In the primary analysis, overall survival (OS) was immature. In this study, we report the final planned analysis of OS (key secondary end point), progression-free survival (PFS) on third-line therapy (second PFS; prespecified exploratory end point), and long-term safety. Final OS analysis was prespecified to occur with approximately 200 and ≥145 events in the overall and *KIT* exon 11 intention-to-treat (ITT) populations, respectively. As of March 15, 2023, there were 211 and 151 OS events in the overall ITT and *KIT* exon 11 ITT populations, respectively. Median OS was similar between second-line ripretinib and sunitinib in both populations (overall, 35.5 *v* 31.5 months; *KIT* exon 11, 35.5 *v* 32.8 months). Median second PFS (on third-line therapy) for the overall ITT population was similar between the ripretinib and sunitinib arms (7.7 *v* 7.4 months). Safety was consistent with the primary analysis. OS from this analysis was similar between arms, and second PFS suggests that receiving ripretinib did not adversely affect the PFS of third-line therapy.

25COASNOV58

Title: Nephrotoxicity Surveillance for Childhood and Young Adult Survivors of Cancer: Recommendations From the International Late Effects of Childhood Cancer Guideline Harmonization Group.

Esmee C.M. Kooijmans et al.

J Clin Oncol 43, 2433-2448(2025).
https://doi.org/10.1200/JCO-24-02534

Abstract: Purpose- Childhood, adolescent, and young adult (CAYA) survivors of cancer are at risk of nephrotoxicity. Surveillance guidelines are important for timely diagnosis and treatment of these survivors, which could slow the progression to higher stages of kidney dysfunction. Methods-The International Late Effects of Childhood Cancer Guideline Harmonization Group established a multidisciplinary panel of 34 experts from 11 countries. The panel performed systematic literature reviews for articles published between 1990 and June 2023, graded the evidence using Grading of Recommendations Assessment, Development, and Evaluation methodology, and formulated recommendations based on evidence, clinical judgment, and consideration of benefits and harms of surveillance. Recommendations were critically appraised by two independent external experts and patient representatives. Results-Glomerular dysfunction surveillance is recommended every 2-5 years for survivors treated with ifosfamide, cisplatin, abdominal radiotherapy, total body irradiation, or nephrectomy and is reasonable after carboplatin treatment. We recommend screening for glomerular dysfunction using an estimated glomerular filtration rate (eGFR) equation that includes serum creatinine, preferably combined with serum cystatin C if available. Tubular dysfunction surveillance is recommended once at entry into long-term follow-up and with follow-up as clinically indicated for survivors treated with ifosfamide and is reasonable after cisplatin treatment. Conclusion- These recommendations inform routine, uniform long-term follow-up care for CAYA survivors of cancer at risk of nephrotoxicity.

25COASNOV59

Title: Overall Survival After Allogeneic Transplantation in Advanced Cutaneous T-Cell Lymphomas (CUTALLO): A Propensity Score–Matched Controlled Prospective Study.

J Clin Oncol 43, 2461-2466(2025).
https://doi.org/10.1200/JCO-25-00183

Abstract: Cutaneous T-cell lymphomas (CTCLs) are rare, usually refractory, and sometimes fatal diseases. Patients presenting with advanced-stage CTCL usually exhibit poor long-term survival outcomes. Only very few treatments have improved progression-free survival (PFS) in advanced CTCL, and no treatment has increased overall survival (OS). In 2023, the results of the CUTALLO trial supported the hypothesis that hematopoietic stem-cell transplantation (HSCT) was associated with significantly longer PFS as compared with standard-of-care treatment among advanced-stage patients although HSCT did not significantly affect OS. We provide herein the final OS data pertaining to the same patient population after a longer median follow-up of 38.9 months. Of the 99 patients included in the analysis, 55 (56%) were assigned to the HSCT group, whereas 44 (44%) were allocated to the non-HSCT group. The updated survival analysis reported that 16 of 55 patients (29%) in the HSCT group and 22 of 44 patients (50%) in the non-HSCT group died. The median OS was not reached in the HSCT group and 51.5 months (95% CI, 26.9 to 51.5) in the non-HSCT group (hazard ratio, 0.40 [95% CI, 0.20 to 0.80]). Compared with the standard of care for advanced CTCL, after extended follow-up, allogeneic HSCT was associated with significantly longer OS.

25COASNOV60

Title: Adoptive Cell Transfer of Tumor-Infiltrating Lymphocytes for Metastatic Acral Lentiginous Melanoma.

Paul H. McClelland et al.

J Clin Oncol 43, 2479-2489(2025).
https://doi.org/10.1200/JCO-24-02348

Abstract: Purpose-Acral lentiginous melanoma is a subtype of cutaneous melanoma arising from palmar, plantar, or subungual skin. These tumors are characterized by aggressive biology, a low tumor mutational burden (TMB), and diminished sensitivity to immune checkpoint blockade. It is unknown whether adoptive cell transfer of tumor-infiltrating lymphocytes (ACT-TIL) has efficacy in patients with acral melanoma. Methods-We analyzed prospectively collected data from 442 patients with metastatic cutaneous melanoma who were treated on clinical trials of ACT-TIL at a single institution between 1999 and 2018. Although blinded to treatment outcome and genomic data, we retrospectively identified patients who had acral subtype on the basis of clinicopathologic data available at the time of diagnosis. We then evaluated the ACT-TIL treatment outcomes of patients with acral melanoma and compared them with contemporaneously treated patients with nonacral melanoma. Results- Out of 442 included patients, 30 (7%) had acral melanoma while 412 (93%) had nonacral melanoma. Cohorts had similar clinical characteristics, protocol enrollment, and treatment-related factors. The objective response rate to ACT-TIL in patients with acral and nonacral melanomas was 43% and 40%, respectively ($P = .87$), with 3% and 16% having complete responses (CRs; $P = .07$). Median progression-free survival was 3.5 and 4.1 months ($P = .40$) and median overall survival was 13 and 17 months ($P = .79$), respectively. Acral melanomas had lower TMB and ultraviolet mutational signature scores than nonacral melanomas. Conclusion- ACT-TIL can mediate objective responses in patients with metastatic acral melanoma, and outcomes in patients with acral disease were unexpectedly comparable with those of contemporaneously treated patients with nonacral cutaneous melanoma. Further research is necessary to understand the immunologic basis of responses to ACT-TIL in acral melanoma and to increase the frequency of CRs.

25COASNOV61

Title: Phase I Study of ^{131}I-Metaiodobenzylguanidine With Dinutuximab ± Vorinostat for Patients With Relapsed or Refractory Neuroblastoma: A New Approaches to Neuroblastoma Therapy Trial.

Thomas Cash et al.

J Clin Oncol 43, 2490-2501(2025).
https://doi.org/10.1200/JCO-24-02612

Abstract: Purpose-We conducted a phase I trial to determine the safety, tolerability, and preliminary antitumor activity of ^{131}I-metaiodobenzylguanidine (MIBG) combined with the anti-GD2 antibody dinutuximab with or without the histone deacetylase inhibitor vorinostat in patients with relapsed/refractory neuroblastoma (rNBL). Methods-In part A, patients with MIBG-avid rNBL received MIBG intravenously (IV) on day 1 at 12, 15, or 18 mCi/kg per the rolling six design and dinutuximab (17.5 mg/m^2 once daily) IV on days 8-11 and 29-32 and granulocyte-macrophage colony-stimulating factor (250 mcg/m^2 once daily) subcutaneously on days 8-17 and 29-38. Autologous stem cells were infused on day 15. In part B, vorinostat at 180 mg/m^2 once daily was given orally on days 0-13 in combination with the part A recommended phase II dose (RP2D). Patients could receive two courses. Results-Forty-five eligible patients enrolled, of whom 31 were evaluable. The median age was 7.5 (range, 2.9-24.1) years. For part A (n = 19), no dose-limiting toxicities (DLTs) occurred

across all dose levels and courses, establishing the RP2D of MIBG to be 18 mCi/kg. In part B (n = 12), 1 DLT (grade 3 hypokalemia) occurred during course 1, and 3 of 11 patients who received a second course experienced DLT: grade 3 ALT increase, grade 4 hypoxia and grade 5 pneumonitis, and grade 3 fatigue. The best overall response rate (BORR; complete response [CR] + partial response [PR]) on part A was 42% with a CR/PR/minor response (MR) rate of 46%, and 19% progressive disease (PD) rate. For part B, the BORR was 42% with a CR/PR/MR rate of 75% and 0% PD rate. Conclusion-MIBG combined with dinutuximab was well tolerated with encouraging antitumor activity. Vorinostat added to this combination may augment responses in this heavily pretreated patient population.

25COASNOV62

Title: Lenvatinib Plus Pembrolizumab and Chemotherapy Versus Chemotherapy in Advanced Metastatic Gastroesophageal Adenocarcinoma: The Phase III, Randomized LEAP-015 Study.

Kohei Shitara et al.

J Clin Oncol 43, 2502-2514(2025).
https://doi.org/10.1200/JCO-25-00748

Abstract: Purpose- The phase III randomized open-label LEAP-015 study evaluated first-line lenvatinib plus pembrolizumab and chemotherapy versus chemotherapy for advanced metastatic gastroesophageal adenocarcinoma. Methods-Eligible participants 18 years and older with untreated human epidermal growth factor receptor 2–negative locally advanced unresectable or metastatic gastroesophageal adenocarcinoma were randomly assigned 1:1 to induction with oral lenvatinib 8 mg once daily plus pembrolizumab 400 mg intravenously once every 6 weeks (×2) and investigators' choice of capecitabine and oxaliplatin once every 3 weeks (×4) or fluorouracil, leucovorin, and oxaliplatin once every 2 weeks (×6) and consolidation with lenvatinib plus pembrolizumab, or chemotherapy. Dual primary end points were progression-free survival (PFS) and overall survival (OS) in participants with PD-L1 combined positive score (CPS) ≥1 and all participants. Secondary end points included objective response rate (ORR) and duration of response. Results- Of 880 participants randomly assigned, 443 received lenvatinib plus pembrolizumab and 437 received chemotherapy. The median follow-ups were 32.2 months (range, 19.0-41.7) in participants with PD-L1 CPS ≥1 and 31.8 months (19.0-41.7) in all participants. At interim analysis, PFS was statistically significant with lenvatinib plus pembrolizumab versus chemotherapy in participants with PD-L1 CPS ≥1 (median, 7.3 *v* 6.9 months; hazard ratio [HR], 0.75 [95% CI, 0.62 to 0.9]; $P = .0012$) and all participants (median, 7.2 *v* 7.0 months; HR, 0.78 [95% CI, 0.66 to 0.92]; $P = .0019$). The ORR was 59.5% versus 45.4% in participants with PD-L1 CPS ≥1 and 58.0% versus 43.9% in all participants, $P < .0001$ for both. At final analysis, OS was not statistically significant in participants with PD-L1 CPS ≥1 (median, 12.6 *v* 12.9 months; HR, 0.84 [95% CI, 0.71 to 1.00]; $P = .0244$; *P* value boundary = .0204). Grade ≥3 drug-related adverse event rates were 65% versus 49%. Conclusion-Lenvatinib plus pembrolizumab and chemotherapy versus chemotherapy provided a statistically significant improvement in PFS in advanced unresectable or metastatic gastroesophageal carcinoma at interim analysis although the clinical significance of this difference seems to be limited. No significant improvement occurred in OS in participants with PD-L1 CPS ≥1.

25COASNOV63

Title: Isatuximab Subcutaneous by On-Body Injector Versus Isatuximab Intravenous Plus Pomalidomide and Dexamethasone in Relapsed/Refractory Multiple Myeloma: Phase III IRAKLIA Study.

Sikander Ailawadhi et al.

J Clin Oncol 43, 2527-2537(2025).
https://doi.org/10.1200/JCO-25-00744

Abstract: Purpose-To report the results of the multicenter, open-label IRAKLIA trial of isatuximab subcutaneous (SC) versus intravenous (IV), plus pomalidomide and dexamethasone, in relapsed/refractory multiple myeloma (MM), to our knowledge, the first phase III MM trial using an on-body injector (OBI). Methods- Patients with ≥1 prior line of therapy were randomly assigned 1:1 to Isa OBI (1,400 mg) or IV (10 mg/kg) once weekly in cycle (C)1 and then every 2 weeks, plus pomalidomide (4 mg once daily, day [D]1-21) and dexamethasone (40 mg once weekly [age ≥75: 20 mg]) and treated until progression, unacceptable toxicity, or patient request. Coprimary end points were overall response rate (ORR; noninferiority margin, 0.839) and Isa C_{trough} (C6D1 predose; noninferiority margin, 0.8). Noninferiority of OBI versus IV was demonstrated if both coprimary end points achieved noninferiority. Results- IRAKLIA randomly assigned 531 patients (OBI, n=263; IV, n=268). After 12-month median follow-up, the ORR was 71.1% (OBI) and 70.5% (IV; relative risk, 1.008 [95% CI, 0.903 to 1.126]; lower CI exceeded noninferiority margin). The mean (standard deviation) C6D1 C_{trough} was 499 (259) μg/mL (OBI) and 340 (169) μg/mL (IV). The C_{trough} geometric mean ratio (90% CI) was 1.532 (1.316 to 1.784); lower CI exceeded noninferiority margin. Grade ≥3 treatment-emergent adverse event incidences were 81.7% (OBI) and 76.1% (IV); infusion reaction incidences were 1.5% and 25.0%. Injection site reactions occurred in 0.4% of OBI injections (all grade 1-2); 99.9% of injections completed without interruption. Conclusion-IRAKLIA demonstrated efficacy and pharmacokinetic noninferiority between Isa OBI and IV. No unexpected safety signal was observed, with excellent local tolerability of Isa OBI. Efficacy and safety were comparable with Isa IV in ICARIA-MM, except the lower OBI infusion reaction rate. These results support potential use of the OBI, designed to improve practice efficiency.

25COASNOV64

Title: Comparison of the safety profiles of CD19-targeting CAR T-cell therapy in patients with SLE and B-cell lymphoma

Fabian Müller et.al.

Blood (2025) 146 (9): 1088–1095.
https://doi.org/10.1182/blood.2025028375

Abstract: CD19-directed chimeric antigen receptor (CAR) T-cell therapy has revolutionized the treatment of relapsed/refractory B-cell non-Hodgkin lymphoma (B-NHL) and recently showed effects in autoimmune diseases, such as systemic lupus erythematosus (SLE). Despite high levels of inflammation, toxicity seemed to differ between patients with SLE and B-NHL. We therefore compared the CAR T-cell kinetics and treatment-related side effects to better define the toxicity profiles. In contrast with the similar CAR T-cell expansion, patients with SLE revealed a lower incidence and severity of cytokine-release syndrome, immune effector cell–associated neurotoxicity syndrome, and immune effector cell–associated

hematotoxicity. Although the neutrophil nadir was lower in patients with SLE after therapy, the platelet counts remained close to normal and hematotoxicity was shorter in SLE than B-NHL. The reduced hematotoxicity correlated with lower acute-phase inflammation, better hematologic reserve before CAR T-cell therapy, and distinct serum cytokine profiles. Interestingly, CAR T-cell persistence was consistently shorter, and the reconstitution of conventional T and B cells was faster in SLE. In both cohorts, B-cell reconstitution correlated with functional $CD4^+$ T-cell recovery, indicating a general biologic process of hematopoietic and immune system regeneration. In summary, similar lymphodepletion and CAR T-cell pharmacokinetics led to distinct toxicity, demonstrating that CAR T-cell therapy had a favorable side-effect profile in SLE, including faster recovery of the adaptive immune system.

25COASNOV65

Title: A phase 2 randomized study of modakafusp alfa as a single agent for patients with relapsed/refractory multiple myeloma

Sarah A. Holstein et.al.

Blood (2025) 146 (9): 1051–1064.

https://doi.org/10.1182/blood.2024027873

Abstract: Modakafusp alfa is a first-in-class immunocytokine-directing interferon alfa to $CD38^+$ cells. Our previous phase 1/2 trial identified 2 potential phase 2 doses of modakafusp alfa for patients with relapsed/refractory multiple myeloma (RRMM): 1.5 or 3 mg/kg every 4 weeks. The overall response rate (ORR) among 30 patients treated at 1.5 mg/kg was 43%. This phase 2 dose optimization study randomized 147 patients with triple-class refractory disease and ≥3 previous lines of therapy 1:1 to modakafusp alfa 120 mg (n = 71) or 240 mg (n = 75) every 4 weeks (fixed-dose equivalents of 1.5 and 3 mg/kg every 4 weeks). Patients had received a median of 6 previous lines of therapy; 66% were penta-exposed and 45% had previously been exposed to anti–B-cell maturation antigen (BCMA) therapy. Modakafusp alfa development was discontinued for strategic reasons by the sponsor and the study was terminated early. At median follow-up of 7.3 and 7.6 months in the 120- and 240-mg arms, ORRs were 32% and 41%, and median progression-free survival was 4.1 and 5.3 months, respectively. ORRs were higher in patients who had not received previous BCMA therapy (46% vs 29%). The most common treatment-related adverse events (TEAEs) in the 120- and 240-mg arms were thrombocytopenia (75% and 84%; grade ≥3, 55% and 61%; respectively) and neutropenia (68% and 73%; grade ≥3, 56% and 68%; respectively); 90% and 96% of patients, respectively, experienced grade ≥3 TEAEs; 39% and 44%, respectively, experienced serious TEAEs.

Surgical Oncology

25COASNOV01:

Title: Outcomes following exploratory surgery without subsequent resection in perihilar cholangiocarcinoma: A nationwide analysis,

Julien A. Luyten, Lydia G. van der Geest, Steven W.M. Olde Damink, Frank G. Schaap, Bas Groot Koerkamp,

European Journal of Surgical Oncology,Volume 51, Issue 11,2025,110419,
https://doi.org/10.1016/j.ejso.2025.110419.

Abstract: Definitive assessment of resectability in perihilar cholangiocarcinoma (pCCA) often requires surgical exploration. Limited data exist on whether surgical exploration without resection affects the chance of receiving subsequent systemic therapy and survival. This nationwide analysis aims to address this question. Methods Patients diagnosed with non-metastatic pCCA between 2012 and 2023 were selected from the Netherlands Cancer Registry and categorized as resected, explored (surgical exploration without resection), or non-explored (non-metastatic tumours without exploration or resection). Overall survival data was stratified by systemic therapy use. Results The cohort included 2014 patients of which 490 patients (24.3 %) underwent resection, 258 patients (12.8 %) underwent surgical exploration without resection, and 1266 patients (62.9 %) were not explored. Overall, 90-day mortality following exploration was 19.5 %. Among explored patients, 38.0 % (98/258) received systemic therapy compared to 10.6 % (134/1266) of non-explored patients ($p < 0.001$). With systemic therapy, explored patients had a median overall survival (mOS) of 14.3 months (95 % CI 12.7–18.2) from diagnosis compared to 12.8 months (95 % CI 11.6–15.8) for non-explored patients ($p = 0.350$). With best supportive care, explored patients had a mOS of 8.1 months (95 % CI 6.5–10.3) compared to 3.2 months (95 % CI 2.8–3.7) for non-explored patients ($p \leq 0.001$). Conclusion Among patients with non-metastatic pCCA receiving systemic therapy, survival outcomes are comparable between those who undergo surgical exploration and those who do not. Despite a possible impact on quality of life, these findings suggest that surgical exploration does not hinder access to systemic therapy or negatively affect survival.

Keywords: Perihilar cholangiocarcinoma; Surgical exploration; Systemic therapy; Best supportive care; Overall survival; Cancer registry

25COASNOV02:

Title: Delivering a national accelerated HPB cancer management strategy: The pancreatic and hepatocellular cancer pathway improvement project (PHCC-PIP),

Anya Adair, Christine Urquhart, Ross Carter,

European Journal of Surgical Oncology, Volume 51, Issue 11,2025,110350,
https://doi.org/10.1016/j.ejso.2025.110350.

Abstract: Diagnostic delays impact pancreatic cancer (PC) and hepatocellular carcinoma (HCC) patients. The Pathway improvement project (PIP) aimed to address this, centralizing oversight of patient's staging pathways across Scotland, thereby streamlining diagnosis to definitive treatment and improving communication. Methods A National cancer care team (CCT) received alerts from radiology departments for scans suspicious of PC or HCC. Timeline for intervention was from report of the initial investigation to commencing a

patient's definitive treatment. Baseline data were established through the existing Regional MDT Network. Timeline steps were established as Key Performance indicators. These were compared to the prospectively collected data during the intervention of the PIP. Results The retrospective audit included 387 patients with 277 patients included in the Prospective pilot. Time from image report to GP involvement (HCC $p < 0.001$: PC $p = 0.001$), CNS contact ((HCC $p < 0.05$: PC $p = 0.025$), MDT decision (HCC $p = 0.023$: PC $p = 0.003$) were all significantly improved. Median time from image report to commencing definitive treatment was reduced from 98 to 62 days for HCC patients ($p = 0.001$), and from 54 to 38 days for PC patients ($p = 0.005$). Conclusion This pilot delivered centralized ownership of patient's, reducing duration of the staging process and improving communication while using existing regional clinical pathways.

25COASNOV03:

Title: Optimal cutoff value of fine-needle aspiration thyroglobulin of metastatic lymph node in thyroid cancer patients,

Yang Yang, Xianfeng Jiang,

European Journal of Surgical Oncology, Volume 51, Issue 11, 2025, 110428,
https://doi.org/10.1016/j.ejso.2025.110428.

Abstract: Thyroglobulin in fine-needle aspiration washout fluids (FNA-Tg) has been recognized as a valuable tool for detecting lymph node metastases (LNM) in papillary thyroid carcinoma (PTC). However, the optimal cutoff value for FNA-Tg remains unclear. We analyzed interference of factors such as serum Tg, serum TgAb on FNA-Tg, and determined the optimal cutoff value of FNA-Tg. Subjects and methods: We conducted a retrospective analysis of patients diagnosed as PTC with suspicious cervical lymph node between August 2015 and May 2023. Fine-needle aspiration (FNA) and FNA-Tg measurement were performed on suspicious lateral cervical lymph nodes. Final diagnose was determined by FNA cytology (FNAC) or histopathological examination. For FNAC negative lymph node, patients received follow-up for at least 1year. Results A total of 10,503 lateral cervical lymph nodes from 4259 patients were included in the study, with 2583 lymph nodes identified as metastatic. Receiver operating characteristic (ROC) curve analysis determined the optimal cutoff value for FNA-Tg to be 0.865 ng/mL for all patients, with a sensitivity of 80.0 % and specificity of 94.4 % respectively. When combining with FNAC and thyroglobulin ratio assessment, it achieved an overall diagnostic accuracy of 96.6 %. FNA-Tg was correlated with serum Tg and thyroid gland status ($p<0.001$), and no significant correlation was observed between FNA-Tg and serum TgAb ($P = 0.66$) or TSH ($P = 0.31$). Conclusion FNA-Tg demonstrates high accuracy in the diagnosis of metastatic lymph nodes, and the optimal cutoff value is related with serum Tg and thyroid glands status.

Keywords: Fine-needle aspiration washout fluids; Thyroglobulin; Papillary thyroid carcinoma; Lymph node metastases

25COASNOV04:

Title: Time to treatment initiation in primary extremity sarcomas: Determinants and oncological outcomes in a tertiary LMIC cancer center,

Anand Murali, Chandra Kumar Krishnan, Vivek Patel, Shrinivas Venkatesh, Gaurav Ravi Kumar,

European Journal of Surgical Oncology, Volume 51, Issue 11,2025,110449,
https://doi.org/10.1016/j.ejso.2025.110449.

Abstract: Time to treatment initiation (TTI) has emerged as a key quality control metric in oncology, with early treatment initiation translating to improved survival in certain malignancies. However, data is lacking for primary extremity sarcomas (PES). Hence, this study aimed to quantify TTI, identify factors influencing TTI, and evaluate its effect on oncological outcomes in PES. Methods This study was a retrospective analysis of patients with PES who received curative-intent treatment between 2011 and 2020. Various demographic details, tumor characteristics, treatment, healthcare variables, and oncological outcomes were analysed. Results Median TTI for primary bone sarcoma (PBS) was 24 days, and for primary soft tissue sarcoma (PSTS) was 35 days. Univariate analysis of PBS, age >20 years ($p < 0.001$), low-grade tumors ($p = 0.011$), chondrosarcoma as histology ($p < 0.001$), and surgery as the first treatment ($p < 0.001$) modality were associated with a delayed TTI. On multivariate analysis, only age ($p < 0.001$) and histology ($p = 0.002$) retained significance. In PSTS, age >20 years ($p = 0.018$) and non-affordability ($p = 0.019$) were significant in both univariate and multivariate analyses. Differences in TTI (early vs late) did not translate to changes in oncological outcomes, with similar overall survival rates at both 3-year and 5-year follow-up, for both PBS ($p = 0.719$) and PSTS ($p = 0.786$). Conclusion TTI is multifactorial. Though early treatment initiation did not impact survival rates, this study introduces a structured framework for auditing institutional workflows to identify bottlenecks and facilitate system-level improvements in the delivery of multidisciplinary sarcoma care.

Keywords: Sarcoma; Diagnosis; Quality control; Chemotherapy; Surgery

25COASNOV05:

Title: Contour-like model for precision risk stratification in gastric cancer patients underwent neoadjuvant therapy: A multicenter retrospective study,

Siwei Pan, Weiwei Zhu, Yanqiang Zhang, Ruolan Zhang, Qing Yang, Yizhou Wei,

European Journal of Surgical Oncology,Volume 51, Issue 11,2025,110455,
https://doi.org/10.1016/j.ejso.2025.110455.

Abstract: Lymph node metastasis (LNM) is a critical determinant of prognosis in gastric cancer (GC). Accurate evaluation of lymph node involvement enhances prognostic accuracy and informs postoperative strategies. Methods This retrospective study included 649 GC patients who received neoadjuvant chemotherapy followed by curative surgery at two centers between 2009 and 2019. An additional cohort of 292 patients was selected from the SEER database using matching criteria. Collected variables included the number of retrieved lymph nodes (rLNs), positive lymph nodes (pLNs), pathological T stage after treatment (ypT), and Tumor Regression Grade. A novel contour-like ypTN (Con-ypTN) model was constructed using a Gaussian process-augmented Cox regression approach to predict the overall prognosis. Model performance was evaluated through receiver operating characteristic curve analysis, the Delong test, calibration plots, and decision curve analysis. Results The Con-ypTN model demonstrated strong prognostic discrimination. AUC values were 0.853 (95 % CI: 0.807–0.900) in the training cohort. Calibration plots and Delong test results showed good agreement between predicted and actual outcomes across all datasets. Notably, the Con-ypTN model significantly outperformed all comparator staging systems ($P < 0.05$). Patients classified as high risk by the Con-ypTN model had significantly worse survival outcomes

than those in the low-risk group ($P < 0.05$). Conclusion The Con-ypTN model provides a robust and clinically relevant tool for prognostic stratification of GC patients treated with neoadjuvant chemotherapy. The model enables precise identification of high-risk individuals, offering improved guidance for postoperative clinical decision-making.
Keywords: Gastric cancer; Contour-like model; Neoadjuvant chemotherapy; Prognosis

25COASNOV06:
Title: Revisiting the paradigm: Asymptomatic high-grade endometrial cancer diagnosis is not associated with improved outcomes,
Ahmet Namazov, Limor Helpman, Ram Eitan, Zvi Vaknin, Ofer Lavie, Amnon Amit, Tally Levy,
European Journal of Surgical Oncology,Volume 51, Issue 11,2025,110427,
https://doi.org/10.1016/j.ejso.2025.110427.
Abstract: To compare the survival of women with high grade endometrial cancer between asymptomatic and women presenting bleeding symptoms. Design An Israel Gynecologic Oncology Group multi-center retrospective cohort study. Methods The study included women who underwent surgery for high-grade endometrial cancer. We compared outcomes between women presenting with postmenopausal bleeding and asymptomatic women diagnosed with high-grade endometrial cancer. Recurrence-free, disease-specific and overall survival were assessed using the Kaplan Meier method and compared using the log-rank test. Risk factors for recurrence and death were evaluated using Cox regression analysis; the primary exposure variable assessed was the presence of postmenopausal bleeding. Results Of the 584 women with high-grade histology, 498 (85.3 %) presented with postmenopausal bleeding and 86 (14.7 %) were asymptomatic. The median follow-up was 52 months (12–120 months). There was no difference in recurrence-free survival between women diagnosed with postmenopausal bleeding and asymptomatic women (70.1 % vs.64.6 % at 5 years, $p = 0.35$, respectively). There were no significant differences in disease-specific survival (66.3 % vs. 64.2 % at 5 years, $p = 0.83$) or in overall survival (56.4 % vs. 58 % at five years, $p = 0.55$) between study groups. The multivariate Cox regression analysis did not reveal any significant association between postmenopausal bleeding and survival. Conclusion In this study, the diagnosis of high-grade endometrial cancer in asymptomatic women was not associated with earlier disease stage at diagnosis. In women with incidental ultrasonographic findings of a thickened endometrium or polyp, routine invasive evaluation may be unnecessary.
Keywords: High-grade; Endometrial cancer; Asymptomatic; Survival

25COASNOV07:
Title: From conventional minimally invasive to robotic-assisted Ivor Lewis esophagectomy – A Nordic single-center retrospective study,
Tobias Hauge, Egil Johnson, Magnus Fasting, Dag Førland, Caroline Skagemo, Tom Mala,
European Journal of Surgical Oncology,Volume 51, Issue 11,2025,110417,
https://doi.org/10.1016/j.ejso.2025.110417.
Abstract: High-quality studies from Asia have demonstrated that robotic assisted minimally invasive esophagectomy (RAMIE) is a feasible and comparable alternative to conventional minimally invasive esophagectomy (MIE), evidence regarding its application to Western patients remains limited. This study evaluates the short-term outcomes during the initial

phase of RAMIE implementation in comparison to the previous standard MIE technique in a Nordic center. Methods A retrospective single center study of prospectively registered data, comparing short-term outcomes between the final 100 patients operated with MIE and the first 100 patients operated with RAMIE. The primary outcome was the total number of lymph nodes harvested. Secondary outcomes included postoperative pneumonia, anastomotic leakage, serious complications (Clavien Dindo ≥ 3), length of operation, length of hospital stay and resection margin status. An inverse probability weighting model and regression analysis was conducted. Results 200 patients were included (RAMIE n = 100, MIE n = 100). Matched groups (RAMIE n = 96, MIE n = 97) showed no difference in total number of lymph nodes harvested (RAMIE 22.1 vs. MIE 23.7, p = 0.50). RAMIE had higher postoperative pneumonia risk (OR = 2.3, p < 0.01), longer length of operation (+33.9 min, p < 0.01) and marginally increased risk of anastomotic leakage (OR = 2.4, p = 0.05). Comparing the last 50 patients operated with RAMIE to the MIE group, there was no difference in length of operation (OR = 10.3, p = 0.43). Conclusion The short-term oncological outcomes and safety remain secure even during the initial phases of RAMIE implementation in a Nordic cohort. The perioperative outcome for some measures after RAMIE were inferior to MIE, potentially related to learning curve aspects.
Keywords: Esophageal cancer RAMIE; MIE; Short-term outcome; Learning curve

25COASNOV08:

Title: A standardized surgical approach to multifocal locoregionally recurrent left-sided adrenocortical carcinoma,

Shruthi R. Perati, Alyssa V. Eade, Aaron Dinerman, Katherine M. Barrows, Rachael Lowney, Lindsay R. Friedman,

European Journal of Surgical Oncology, Volume 51, Issue 11,2025,110395,
https://doi.org/10.1016/j.ejso.2025.110395.

Abstract: Society guidelines recommend surgery for recurrent adrenocortical carcinoma (ACC) in selected patients; however, no standards exist to guide surgeons, and this may be particularly problematic in the management of multifocal locoregional recurrence. Materials and methods A standardized approach was developed for patients with multifocal locoregionally recurrent left-sided ACC as part of an NCI study (NCT05237934). En bloc resection included the distal pancreas, spleen, left kidney, portion of left diaphragm, and possibly a portion of the left lateral liver, greater curve of the stomach, and/or descending colon. Morbidity, survival, and quality of life (QoL) were assessed. Results From 2018 to 2024, ten patients (median age 59 years) underwent multi-visceral en bloc resections for multifocal locoregionally recurrent left-sided ACC. Prior to surgery, 90 % of patients had undergone systemic therapy and a median of one prior operation (range 1–4). Size of local recurrence(s) averaged 6.5 cm (range 1.9–12.2 cm) at largest diameter, with a median of 3 (range 2–8) foci of disease identifiable on pre-operative imaging. Two patients (20 %) developed a Grade 1B post-operative pancreatic fistula. There were no peri-operative mortalities. Median locoregional recurrence-free survival was 22.1 months at 19.3 months of median follow-up. 50 % of QoL survey respondents reported feeling recovered/back to baseline activity level within 4 months of surgery. Conclusion Locoregional control can be obtained with reasonable success and acceptable morbidity in select patients with multifocal locoregionally recurrent left-sided ACC using a standardized left upper quadrant en bloc

multi-visceral resection approach. Verification of the results of this technique is required in other experienced centers.

Keywords: Locoregional recurrence; Adrenocortical carcinoma (ACC); en bloc multi-visceral resection

25COASNOV09:

Title: Postoperative chemotherapy versus surgery alone in esophageal squamous cell carcinoma: A single-center propensity-matched survival analysis,

Youqiang Qiu, Peiyuan Wang, Hao He, Shuoyan Liu, Feng Wang,

European Journal of Surgical Oncology, Volume 51, Issue 11, 2025, 110441,
https://doi.org/10.1016/j.ejso.2025.110441.

Abstract: Current clinical guidelines lack a consensus regarding adjuvant chemotherapy (ACT) for esophageal squamous cell carcinoma (ESCC) patients undergoing primary surgical resection. Therefore, our study evaluates both the survival benefits and predictors in this specific population. Methods This retrospective study stratified 1039 ESCC patients into ACT and surgery-only groups. Propensity score matching (PSM) generated 311 matched pairs (n = 622) with balanced baseline characteristics. The endpoints were 5-year DFS and 5-year OS, analyzed by Kaplan-Meier methodology. Prognostic factors were identified through univariable and multivariable Cox regression analyses. Results With a median follow-up of 49 months, the post-PSM OS rates at the 1-, 3-, and 5-year were 89.7 %, 66.4 %, and 56.0 %, with DFS rates of 85.8 %, 63.6 %, and 53.9 %, respectively. ACT demonstrated significantly improved 5-year DFS (HR 0.69, 95 % CI 0.53–0.89; P = 0.004) and 5-year OS (HR 0.67, 95 % CI 0.51–0.87; P = 0.003) versus surgery alone. Subgroup analyses demonstrated significant DFS and OS improvements with ACT in patients with pN1-3 disease, pT3-4 tumors, and pT3N0 cases exhibiting either mid/upper thoracic location with moderate/poor differentiation or adverse pathological features (lymphovascular/perineural invasion; all P < 0.05). Multivariable Cox regression identified BMI ≥22 kg/m2, ACT, higher lymph node yield, lower metastatic nodal burden, earlier pT/N stages, and absence of LVI/PNI invasion as independent predictors of improved OS and DFS. Conclusions ACT demonstrated survival benefits in ESCC patients with advanced tumor burden (pathologically confirmed pT3-4 or pN1-3 disease) and those with pT3N0 cases harboring either mid/upper thoracic tumors with moderate/poor differentiation or adverse pathological features (LVI/PNI).

Keywords: Esophageal squamous cell carcinoma; Adjuvant chemotherapy; Survival benefits

25COASNOV10:

Title: Prognosis and clinical characteristics of signet ring cell colorectal peritoneal metastases – a Swedish population-based study,

Malin Enblad, Lana Ghanipour, Gabriella Palmer, Valentinus Valdimarsson, Elinor Bexe Lindskog, Peter Cashin,

European Journal of Surgical Oncology, Volume 51, Issue 11,2025,110429,
https://doi.org/10.1016/j.ejso.2025.110429.

Abstract: Signet ring cell (SRC) colorectal cancer is strongly associated with peritoneal metastases (PM), but the role of cytoreductive surgery (CRS) and hyperthermic intraperitoneal chemotherapy (HIPEC) remains uncertain due to poor prognosis. This study aimed to analyse the prognostic impact of SRCs, assess clinical characteristics, and evaluate

the risk of open-close laparotomy. Methods This Swedish population-based study included patients with colorectal PM accepted for initial CRS and HIPEC at four national centres between 2010 and 2023. Data were retrieved from the Swedish HIPEC registry. Tumours with ≥50 % and <50 % SRCs were included. Results Among 810 patients, 97 (12 %) had SRC tumours. SRC patients had a higher risk of open-close laparotomy (22 % vs. 13 %, p = 0.04) and worse 5-year overall survival (OS) compared to non-SRC patients (18 % vs. 32 %, p = 0.004). SRC patients were younger, more often had synchronous PM, regional lymph node metastases, higher peritoneal cancer index, and were less likely to receive neoadjuvant treatment or have synchronous liver metastases. At diagnosis, PM were more often an unexpected intraoperative finding, and SRC patients exhibited a stronger preoperative systemic inflammatory response, with a higher CRP/albumin ratio. Among those undergoing CRS and HIPEC, the 5-year OS was 24 % (95 % CI: 14–40) in SRC patients and 36 % (95 % CI: 32–42, p = 0.056) in non-SRC patients. Conclusion SRC colorectal PM is associated with a high risk of open-close laparotomy, poor prognosis, and distinct clinical features. These findings highlight the aggressive nature of SRCs but suggest that CRS and HIPEC should not be excluded for these patients.

Keywords: Signet ring cells; Colorectal cancer; Peritoneal metastases; Cytoreductive surgery; HIPEC

25COASNOV11:

Title: Discrepancy between mammographic and pathological sizing of screen-detected DCIS: Risk factors and impact on ipsilateral recurrence rates,

C.C. Kirwan, B. Hilton, K. Clements, D. Dodwell, S.E. Pinder, A. Shaaban, H. Stobart, M. Wallis,

European Journal of Surgical Oncology,Volume 51, Issue 11,2025,110431,
https://doi.org/10.1016/j.ejso.2025.110431.

Abstract: Discrepancy between mammographic and pathological sizing of DCIS can lead to surgical overtreatment, with poorer cosmesis or unnecessary mastectomy, or undertreatment and recurrence. Methods Within the UK Sloane Project prospective cohort study of screen-detected DCIS (2003–2012), we investigated factors associated with 'pathology larger (PL)' (pathological larger than mammographic size) or 'mammogram larger (ML)' (mammographic larger than pathologic size), size discrepancy and the impact on ipsilateral recurrence. Results Among 9937 patients (mean age 60; range 46–87), mammographic size remained constant at median 19 mm (IQR 10–35)mm whilst pathological size increased from 16(10–28)mm to 20(10–33)mm (p = 0.001)over the study. The mammographic and pathological size discrepancy decreased from 3.4 mm to 0.2 mm (p < 0.05). In patients undergoing BCS, size discrepancy of ≥5 mm was associated with increased 5-year ipsilateral recurrence if lesions were PL (odds ratio(OR) 1.37 (C.I. 1.03–1.82, p = 0.03) and if lesions were ML (OR 1.4 (C.I. 1.10–1.86, p = 0.008), compared to <5 mm discrepancy. Factors associated with PL by ≥ 5 mm were high grade (OR 1.9 [95 % CI 1.5–2.4, p < 0.001]) and mastectomy (OR 4.4 [C.I. 3.8–5.1, p < 0.001]) and for ML ≥ 5 mm was larger mammographic tumour size (>40 mm; OR 115.7 [C.I. 82.3–162.6], p < 0.001]). Conclusion Mammographic-pathological size discrepancy is associated with higher recurrence following BCS for DCIS.

25COASNOV12:

Title: Impact of sarcopenic obesity on postoperative complications and long-term survival in patients with gastric cancer,

Yulong Wang, Xijuan Liu, Xianhu Zhang, Peng Fan, Yunmeng Zong, Xiao Feng, Lili Huang,
European Journal of Surgical Oncology, Volume 51, Issue 11, 2025,110437,
https://doi.org/10.1016/j.ejso.2025.110437.

Abstract: Sarcopenic obesity (SO), defined as the coexistence of sarcopenia (low muscle mass with impaired function) and obesity, has been linked to adverse outcomes in several cancers, but its impact in gastric cancer (GC) remains unclear. Methods This retrospective cohort study included 502 GC patients who underwent curative gastrectomy. Body composition was assessed via preoperative CT at the L3 vertebral level. SO is conceptually the coexistence of sarcopenia-low muscle mass with impaired function-and obesity; in this cohort, lacking function tests, SO was operationally defined as low skeletal muscle index (SMI) plus high visceral fat area (VFA). Patients were categorized into four groups: normal composition, obesity, sarcopenia, and SO, with the normal composition group serving as the reference. Complications, overall survival (OS), and disease-free survival (DFS) were assessed via logistic and Cox regression. Results SO was present in 16.9 % of patients. The median follow-up time was 40 months (interquartile range [IQR]: 20–65 months), and the estimated 5-year OS was 45 %. Compared with the normal composition group, SO was independently associated with higher rates of postoperative complications (odds ratio [OR] = 2.63, 95 % CI: 1.91–4.90, P = 0.002), worse OS (hazard ratio [HR] = 1.88, 95 % CI: 1.32–2.67, P < 0.001), and poorer DFS (HR = 1.75, 95 % CI: 1.22–2.51, P = 0.002). SO outperformed sarcopenia or obesity alone in predicting adverse outcomes. Conclusions SO is an independent prognostic factor in GC and should be incorporated into preoperative evaluation. Early intervention strategies targeting SO may help improve postoperative and survival outcomes.

Keywords: Gastric cancer; Sarcopenic obesity; Complications; Overall survival; Disease-free survival

25COASNOV13:

Title: Adequate lymphadenectomy and adjuvant capecitabine warrant survival benefit in gallbladder cancer,

M. Di Martino, B. Ielpo, S. Cremona, F. Giuliante, J. Martinie, A. Ruzzenente, G. Torzilli, L. Aldrighetti,
European Journal of Surgical Oncology, Volume 51, Issue 11,2025, 110318,
https://doi.org/10.1016/j.ejso.2025.110318.

Abstract: Significant heterogeneity exists in the management of resectable gallbladder cancer (GBC), regarding the extent of lymphadenectomy and the role of adjuvant chemotherapy (aCTx). This study investigates outcomes of resected GBC according to contemporary surgical oncology principles. Methods The international database of the GBC Study Group was queried for patients with resected GBC between 2012 and 2022. Patients with ≥6 lymph nodes resected and aCTx were compared to those with inadequate lymphadenectomy or inadequate aCTX. Unadjusted and adjusted Cox regression models were employed to assess oncological outcomes. Results Out of 656 patients, 300 patients (45.7 %) had ≥6 lymph nodes resected, 240 (36.5 %) received any aCTx 323 and 118

(17.9 %) received capecitabine aCTx. Patients with adequate lymphadenectomy exhibited prolonged disease-free survival (DFS) (HR 0.69, p = 0.004 CI 95 % 0.55–0.89) and overall survival (OS) (HR 0.68, p = 0.002 CI 95 % 0.54–0.87) in pN0 but not in pN + cases. Patients receiving adjuvant capecitabine demonstrated prolonged DFS (HR 1.48, p < 0.001 95 %CI 1.20–1.83) and OS followed a similar pattern (HR 1.67, p < 0.001, 95 %CI 1.34–2.09). In the multivariable analysis, underlying hepatic disease (HR 2.75, p = 0.001, 95 %CI 1.49–5.07), adequate lymphadenectomy (HR 0.67, p = 0.020, 95 %CI 0.48–0.94), T stage (HR 2.14, p < 0.001, 95 %CI 1.60–2.86), R status (HR 1.88, p = 0.008, 95 %CI 1.18–3.00), and capecitabine aCTx (HR 1.27, p = 0.039 95 %CI 1.01–1.61) were identified as predictors of OS. Despite presenting with more aggressive disease, patients with adequate lymphadenectomy and aCTx with capecitabine presented prolonged OS (15 vs 7.5 months, HR 0.53, p = 0.038, 95 %CI 0.29–0.96) compared to those without lymphadenectomy or aCTx. Conclusions A significant proportion of patients still did not receive adequate lymphadenectomy and aCTx. Patients treated according to contemporary surgical oncology principles presented a survival benefit. These principles should be further evaluated considering the aggressiveness of GBC.

Keywords: Gabblader cancer; Biliary tract cancer; Capecitabine; Adjuvant chemotherapy; Surgical oncology; Liver resection; Lymphadenectomy

25COASNOV14:

Title: The financial impact of implementation of a prehabilitation program for colorectal cancer patients in the Netherlands: A budget impact analysis,

C.R. Sabajo, C.T.J. Michels, A. van der Hout, B. van den Heuvel, J.W. Dekker, J.M. Klaase, G.D. Slooter,

European Journal of Surgical Oncology, Volume 51, Issue 11, 2025,110375,
https://doi.org/10.1016/j.ejso.2025.110375.

Abstract: Prehabilitation is proven to be clinically effective, it has shown to decrease complication rate and length of hospital stay after colorectal cancer surgery. However, for broad implementation, information is needed on the financial impact of prehabilitation. This study evaluates the budget impact of a prehabilitation program for colorectal cancer surgery patients in the Netherlands. Methods This budget impact analysis was based on real world data from Dutch hospitals and available data in literature. It was assessed for a period of five years, considering an annual rate of approximately 10,500 colorectal cancer surgeries in the Netherlands. Several scenarios were assessed, varying population size, prehabilitation program cost, and uptake of prehabilitation. Results The total mean hospital admission costs per patient was €3060 for the prehabilitation program and €3636 for standard care. Calculated over a one-year period, this was €77.9 million for patients with a prehabilitation program, while the standard care costs €90.8 million. Conclusion Implementation of a prehabilitation program for colorectal cancer surgery patients in the Netherlands may reduce hospital costs. The program could generate savings of approximately €64.3 million over five years, supporting its broader adoption.

Keywords: Prehabilitation; Colorectal cancer; Surgery; Budget impact analysis; Preoperative care

25COASNOV15:

Title: Impact of tumor size on oncological and surgical outcomes in robot-assisted transaxillary surgery for papillary thyroid carcinoma,

Piermarco Papini, Leonardo Rossi, Leonardo Russo, Chiara Becucci, Andrea De Palma, Carlo Enrico Ambrosini, Marco Puccini, Gabriele Materazzi,

European Journal of Surgical Oncology, Volume 51, Issue 11, 2025,110422,
https://doi.org/10.1016/j.ejso.2025.110422.

Abstract: Robot-assisted transaxillary thyroidectomy (RATT) has emerged as a remote access approach for differentiated thyroid carcinoma (DTC), yet data on its oncological efficacy for tumors larger than 3 cm, particularly in European cohorts, remain scarce. This study aimed to evaluate surgical and oncological outcomes of RATT in patients with papillary thyroid carcinoma (PTC), stratified by tumor size. Materials and methods We retrospectively reviewed 270 patients with histologically confirmed PTC who underwent RATT between July 2012 and August 2022 at a single tertiary center. Patients were categorized into two groups based on tumor size: Group A (<3 cm, n = 226) and Group B (≥3 cm, n = 44). Surgical outcomes, complication rates, and oncological parameters—including serum thyroglobulin (Tg) levels, anti-thyroglobulin antibodies, and structural recurrence—were analyzed. Subgroup analysis was conducted based on radioiodine ablation (RAI) status. Results No significant differences were observed between groups in terms of operative time, hospital stay, or postoperative complications. Tg levels after RAI were comparable between Group A and Group B (p = 0.999), indicating similar biochemical response. Only one patient experienced structural recurrence during follow-up (mean: 48 ± 31 months). Patients who underwent lobectomy alone showed no evidence of recurrence regardless of tumor size. No independent predictors of Tg levels were identified. Conclusions RATT appears to be a safe and oncologically effective approach for PTC, even for tumors ≥3 cm. These findings support the broader use of RATT in selected patients, with outcomes comparable across tumor sizes. Further multicenter studies with longer follow-up are warranted to validate these results.

Keywords: Thyroid carcinoma; Differentiated thyroid cancer; Robot-assisted surgery; Oncological outcomes; Tumor size; Transaxillary approach

25COASNOV16:

Title: Long-term impact of preoperative radiotherapy for rectal cancer on testicular function,

Louise de la Motte, John Tapper, Stefan Arver, Torbjörn Holm, Josefin Segelman, Ravi Jasuja, Anna Martling, Christian Buchli,

European Journal of Surgical Oncology, Volume 51, Issue 11,2025,110458,
https://doi.org/10.1016/j.ejso.2025.110458.

Abstract: The aim was to assess long-term impact of preoperative radiotherapy (RT) for rectal cancer on testicular function, its clinical relevance regarding sexual function and cancer-related events. Materials and methods This analysis of an original cohort with longitudinal design included 163 men with rectal or prostate cancer stage I-III treated with surgery in Stockholm, Sweden, between 2010 and 2014. Exposure to RT (n = 91) was quantified by cumulative mean testicular dose. Repeated measurement of serum Testosterone (T), free T and Luteinizing hormone (LH) respectively questionnaires of sexual function

(IIEF and AMS) were collected before treatment (baseline), one and two years postoperatively. Data on cancer recurrence were collected from medical records during the standard five-year cancer follow-up. Association between hormone levels and patient reported outcome measures for sexual function was assessed by linear random-effect models with final analysis adjusted for age, BMI and ASA-score. Results Testicular dose was associated with a preoperative decline in T and free T, with a consecutive increase in LH and LH/T ratio during the study period. Not all androgen levels recovered within two years. Testosterone levels were associated with patient reported outcome measures for sexual function. Elevated LH one year after surgery for rectal cancer was associated with a three-times increased risk for cancer recurrence. Conclusion Endocrine testicular function is related to sexual symptoms in men treated for rectal- or prostate cancer. Monitoring of testicular function in these patients could be valuable to improve interventions for treatment-related sexual dysfunction. The association between elevated LH and cancer recurrence requires further investigation.

Keywords: Rectal cancer; Testicular function; Preoperative radiotherapy; Sexual function

25COASNOV17:

Title: Cross-cultural adaptation of the locally recurrent rectal cancer – Quality of life questionnaire,

Niamh McKigney, Jan M. van Rees, Stefi Nordkamp, Sophia Waldenstedt, Elisabeth Gonzalez,

European Journal of Surgical Oncology, Volume 51, Issue 11,2025,110363,
https://doi.org/10.1016/j.ejso.2025.110363.

Abstract: The Locally Recurrent Rectal Cancer – Quality of Life (LRRC-QoL) questionnaire was developed as a disease specific measure of health-related quality of life (HrQoL) in locally recurrent rectal cancer (LRRC), it has previously been validated for use in the UK and Australia. The aim of this study was to translate and cross-culturally adapt the LRRC-QoL to enable its use on an international platform. Materials and methods Cross-cultural adaptation of the LRRC-QoL was undertaken through a process of 1) Translatability Assessment (TA), 2) forward-backward translation, and 3) pre-testing interviews to establish content validity and conceptual equivalence across all versions. The QQ-10 measure was used to assess face validity and acceptability. The LRRC-QoL was translated into 13 languages: Danish, Dutch, French, Hindi, Italian, Mandarin, Marathi, Portuguese, Russian, Spanish, Swedish, Telugu, and Urdu. Results In total, 67 patients and 6 clinicians were recruited to pre-testing interviews across 12 countries: Brazil, Canada, Denmark, France, India, Italy, the Netherlands, New Zealand, Pakistan, Singapore, Spain, and Sweden. TA was also undertaken in the USA and Ireland, and translations were prepared in Russian, Marathi, and Telugu. The LRRC-QoL was found to demonstrate conceptual equivalence and content validity across all versions. Mean QQ-10 Value score 76.80 (SD 13.88) and mean Burden score 20.22 (SD 23.03), confirming face validity and acceptability in this international cohort. Conclusion The LRRC-QoL has now undergone cross-cultural adaptation to enable its use in 10 languages and 16 countries. Its psychometric properties will be further examined through external validation in an international cohort.

Keywords: Locally recurrent rectal cancer (LRRC); Health-related quality of life (HrQoL); Cross-cultural adaptation; Cultural equivalence

25COASNOV18:

Title: Impact of nutrition, comorbidity and complication on long term survival in gastric cancer following laparoscopic radical gastrectomy: A 10-year cohort study,

Hengyi Zhang, Siqi Tao, Yangyang Luo, Mengting Lu, Guoxin Li, Hao Liu,

European Journal of Surgical Oncology, Volume 51, Issue 11, 2025,110442,
https://doi.org/10.1016/j.ejso.2025.110442.

Abstract: Previous studies on perioperative influences in gastric cancer have largely relied on single scoring systems, overlooking the interaction between factors. This study utilized the Age-Adjusted Charlson Comorbidity Index (ACCI), Nutritional Risk Screening-2002 (NRS-2002), and Clavien-Dindo classification to assess the impact of key perioperative conditions on long-term survival in a large-scale cohort of gastric cancer patients. Method This study analyzed 2420 gastric cancer patients who underwent laparoscopic radical resection between January 2004 and December 2023 at Nanfang Hospital, Southern Medical University, Guangzhou, China. The analysis, based on postoperative complications, comorbidity burden, and nutritional status, was conducted using Clavien-Dindo classification, ACCI, and NRS-2002, and compared their impact on long-term survival. Result Patients with a low comorbidity burden have significantly higher survival rates compared to those with a high comorbidity burden (5-year: 72.5 %, 10-year: 64.4 %). Patients with better nutritional status also have higher survival rates than those with malnutrition (5-year: 72.6 %, 10-year: 65.0 %). However, postoperative complications do not significantly affect overall survival trends (P = 0.14). Among patients with the same ACCI score, those with malnutrition have significantly lower survival rates (5-year: 44.8 %, 10-year: 31.1 %). Furthermore, among patients with the same nutritional status, those with postoperative complications have markedly worse survival outcomes (5-year: 49.8 %, 10-year: 32.2 %). Conclusion A more precise assessment of the perioperative condition in gastric cancer patients would be recommended via integrating nutritional status with comorbidities or postoperative complications. Improving these conditions are expecting to enhance the long-term overall survival postoperatively.

Keywords: Gastric cancer; Long-term survival; Comorbidity; Postoperative complication; Nutrition

25COASNOV19:

Title: Clinicopathological features and survival differences between G/GEJ-CSC and GAC: A Propensity score-matched, large-scale cross-population retrospective study,

Kang Liu, Kailai Yin, Yubo Ma, Ruihong Xia, Yingsong Zheng, Li Yuan, Xiangdong Cheng, Zaisheng Ye, Zhengchen Jiang,

European Journal of Surgical Oncology, Volume 51, Issue 11, 2025, 110444,
https://doi.org/10.1016/j.ejso.2025.110444.

Abstract: Gastric squamous cell carcinoma and adenosquamous carcinoma, collectively termed gastric and gastroesophageal junction carcinomas containing squamous cells (G/GEJ-CSC).Due to low incidence and high heterogeneity, their clinicopathological features and prognostic patterns lack systematic investigation. Traditional views suggest greater aggressiveness but lack large-scale evidence. This study uses large-scale cohorts to compare G/GEJ-CSC with gastric adenocarcinoma (GAC), clarifying features, prognosis, and supporting personalized treatment. Methods Retrospectively analyzed the clinicopathological

features of eligible patients with G/GEJ-CSC and GAC from Zhejiang Cancer Hospital (2010–2024) and the SEER database (2004–2020). Propensity score matching was used to balance confounding factors. Kaplan-Meier method and Cox proportional hazards model were employed to evaluate survival differences. Results Compared with GAC patients, G/GEJ-CSC occurred more frequently in the gastric-esophageal junction and exhibited a significantly higher Epstein-Barr virus positivity rate, along with worse clinicopathological features. Multivariate Cox analysis showed that pathological type was an independent risk factor for overall survival (Chinese cohort:HR = 1.45,P = 0.044; SEER:HR = 1.23).Kaplan-Meier survival analysis revealed that OS was significantly inferior in G/GEJ-CSC patients compared with GAC (Chinese cohort: 5-year OS 33.0 % vs. 56.1 %, P < 0.001; SEER: 34.8 % vs. 42.7 %, P = 0.013), and this difference persisted after PSM adjustment (Chinese cohort: 5-year OS 36.4 % vs. 52.0 %, P = 0.034; SEER: 34.8 % vs. 44.1 %, P = 0.041). Stratified analysis further indicated a more pronounced survival gap in early-stage patients (Chinese cohort: 5-year OS43.1 % vs.84.1 %, P < 0.001; SEER: 45.4 % vs. 54.2 %, P = 0.002). Conclusion G/GEJ-CSC, a rare gastric cancer subtype, has unique aggressive biology and "early high-risk" prognosis. Need enhanced early identification and personalized treatment exploration.

Keywords: Gastric squamous cell carcinoma; Gastric adenosquamous carcinoma; Esophageal-gastric junction; Tumor staging; Prognosis

25COASNOV20:

Title: Robot-assisted radical nephroureterectomy for locally advanced upper tract urothelial carcinoma: a multicenter study by the Junior ERUS/YAU Working Group on Robot-assisted Surgery,

Fabrizio Di Maida, Carlo Andrea Bravi, Ruben De Groote, Federico Piramide, Filippo Turri, Mike Wenzel,

European Journal of Surgical Oncology, Volume 51, Issue 11,2025,110396,
https://doi.org/10.1016/j.ejso.2025.110396.

Abstract: Aim of the study was investigate outcomes of patients affected by locally advanced (pT3-pT4 and/or pN+) upper tract urothelial carcinoma (UTUC) and treated with robot-assisted radical nephroureterectomy (RNU). Materials and methods Clinical and surgical data of newly-diagnosed UTUC patients referring to 9 high-volume centres from January 2019 to March 2023 undergoing RNU were collected. Results 191 patients showed locally advanced disease. Da Vinci and Hugo RAS ™ System were employed in 95.8 % and 4.2 % of cases, respectively. Bladder cuff removal was carried out in 161 (84.3 %) patients, by using either an intravesical and extravesical approach in 50 (31.1 %) and 111 (68.9 %) respectively. Open and robotic approaches for bladder cuff removal were preferred in 107 (66.5 %) and 54 (33.5 %) patients, respectively. Lymph node dissection was performed in 55 % of patients. Median follow up was 19 (IQR 10–23) months and 31 (16.4 %) patients experienced bladder recurrence. On multivariate analysis, in those patients receiving RNU and bladder cuff removal, the approach for bladder cuff management (extravesical vs intravesical) was the only independent predictor of bladder recurrence (hazard ratio [HR]: 1.34; 95 % confidence interval [CI] 1.12–2.11; p = 0.03). Surgical approach for bladder cuff management (open vs robot) was not independently associated with bladder recurrence or tumor progression (both p > 0.05) Conclusions In experienced hands, the robotic approach

showed satisfactory survival outcomes also for the surgical treatment of pathological locally advanced UTUC. Extravesical approach for bladder cuff management may be burdened by a higher risk for bladder recurrence in locally advanced disease.

Keywords: Da vinci; Hugo RAS system; Nephroureterectomy; Robotic; Upper tract urothelial carcinoma (UTUC); Urothelial neoplasm

25COASNOV21:

Title: Influence of lymphadenectomy extent on the efficacy of immunotherapy in recurrent gastric cancer patients,

Danni Zhu, Zhuoran Fang, Teng Yang, Yiming Lu, Ke Shen, Xiu Zhu, Guangjun Jin, Qing Wei, Xiangdong Cheng,

European Journal of Surgical Oncology, Volume 51, Issue 11, 2025,110454,
https://doi.org/10.1016/j.ejso.2025.110454.

Abstract: Current guidelines recommend ≥16 lymph node (LN) dissection for gastric cancer, preferably >30. However, optimal LN count for immunotherapy after recurrence remains unclear. Methods Retrospective study of 147 gastric adenocarcinoma patients receiving immunotherapy for postoperative recurrence (2017–2023). Participants were grouped by dissected LN (DLN) count. Outcomes included progression-free survival (PFS), overall survival (OS), and response rate (ORR). Results We collected data from 147 patients and stratified them into three groups by DLN count. Stratification revealed: Group A (DLN≤15, 6.1 %, n = 9), Group B (16–30, 44.2 %, n = 65), and Group C (>30, 49.7 %, n = 73). The median disease-free survival (DFS) post-initial surgery was 19.0 months. PFS under immunotherapy differed significantly: Group A (6.0 months) had worse outcomes than B (8.0 months), while C showed intermediate results (7.0 months; P = 0.017). OS followed a similar trend, with Group B having the longest median survival (18.0 months vs. 14.0 for A and 13.0 for C; P = 0.223). ORR was 34.0 %, with progressive disease (PD) more frequent in Group C (30.1 % vs. 20.0 % in B; P = 0.244). Multivariate analysis confirmed DLN count as the sole independent predictor of outcomes. Conclusion DLN count exhibits a U-shaped association with immunotherapy efficacy: both insufficient (≤15) and excessive (>30) dissection correlate with poorer PFS/OS versus moderate resection (16–30). Inadequate lymphadenectomy may cause stage migration, while excessive dissection could disrupt antitumor immunity. Precision lymphadenectomy balancing oncologic radicality and immune preservation is advocated.

Keywords: Gastric cancer; Lymphadenectomy; Dissected lymph node count; Immunotherapy; Recurrence

25COASNOV22:

Title: Comparison of efficacy between the da Vinci surgical system and Toumai® robotic surgical systems for robot-assisted radical prostatectomy and robot-assisted partial nephrectomy,

Yiyang Chen, Zhenghong Liu, Bin Zheng, Xiaolong Qi, Qi Zhang, Feng Liu, Zujie Mao, Pu Zhang,

European Journal of Surgical Oncology, Volume 51, Issue 11,2025,110426,
https://doi.org/10.1016/j.ejso.2025.110426.

Abstract: The Toumai® surgical robot, a cutting-edge medical assistance robot, was developed and launched in China. Compare the effectiveness and safety of the da Vinci robotic surgical system and the Toumai® surgical robot in RARP and RAPN surgeries(the Toumai® -RARP versus the DV-RARP, the Toumai®-RAPN versus the DV-RAPN). Design, setting, and participants One randomized controlled trials were conducted among patients aged 18–77 years suspected of having T1a N0M0 renal cancer, and another randomized controlled trial was conducted among patients aged 55–79 years suspected of having T2 N0M0 prostate cancer. Reasults The clinical characteristics of the two groups of patients undergoing the same surgical procedure showed no significant differences. All surgeries were successfully completed without the need for conversion from laparoscopic to open surgery. The operative time in the Toumai® group was significantly longer. Additionally, there were no significant differences between the two groups in key indicators such as blood loss, length of hospital stay, complication rates, and functional outcomes. Conclusions This comparative study on the efficacy and safety between the Toumai® system and the da Vinci system demonstrates that the Toumai® surgical robot and the da Vinci robotic system achieve comparable safety profiles, surgical outcomes, and postoperative expectations when performing RAPN and RARP procedures, with no statistically significant differences observed.

Keywords: The Toumai® surgical robot; The da Vinci robotic surgical system; RARP; RAPN

25COASNOV23:

Title: Prognostic impact of myopenia and establishment of a nomogram for predicting survival following radical gastrectomy in patients with gastric cancer: A multicenter study,

Chang-Yue Zheng, Xiao-liang Huang, Ju Wu, Xian-tu Qiu, Bin Zu, Hui-bin Liu, Rui Xu, Han-he Chen, Wei Lin,

European Journal of Surgical Oncology, Volume 51, Issue 11,2025,110450,
https://doi.org/10.1016/j.ejso.2025.110450.

Abstract: The prognostic value of myopenia following radical gastrectomy (RG) remains controversial. Materials and methods Patients who underwent RG between January 2015 and December 2018 at two East Asian centers were retrospectively included. Myopenia was defined using sex-specific computed tomography-derived L3 skeletal muscle index, with cut-off values determined by X-tile software based on overall survival (OS). Cox regression models identified independent prognostic factors for OS and disease-free survival (DFS), whereas logistic regression identified risk factors for textbook outcomes (TO). A LASSO-based prognostic nomogram was developed, and its performance was evaluated using calibration curves, concordance index, time-dependent receiver operating characteristic, and decision curve analysis. Results Overall, 943 patients were included (211 and 732 with and without myopenia, respectively). The myopenia group had a significantly lower TO rate ($P = 0.003$), and myopenia was confirmed as an independent risk factor for TO failure ($P < 0.05$). Moreover, the myopenia group had significantly lower 5-year OS (45.5 % vs. 69.3 %, $P < 0.001$) and DFS (45.0 % vs. 66.8 %, $P < 0.001$), with myopenia independently associated with poor prognosis. The nomogram developed in this study outperformed the tumor-node-metastasis staging system in predicting 3- and 5-year OS (both $P < 0.05$),

demonstrating superior net clinical benefits across a threshold range of 10 %–80 %. Risk stratification effectively discriminated 5-year OS (94.3 % vs. 61.2 % vs. 24.2 %, P < 0.001). These results were reproduced in the validation cohort. Conclusions Myopenia independently predicts both short-term outcomes and long-term prognosis after RG. The myopenia-integrated nomogram showed strong predictive accuracy and clinical utility for individualized prognostic assessment of patients with gastric cancer.

Keywords: Myopenia; Gastric cancer; Multimodal treatment; LASSO; Nomogram

25COASNOV24:

Title: Pre-treatment S-index as a promising prognostic indicator of treatment response and survival in patients with synchronous colorectal liver metastases: A retrospective multi-center study,

Yiqiao Deng, Yuan Li, Rui Zhang, Zhijie Wang, Rui Guo, Xinyu Bi, Jianjun Zhao, Jianguo Zhou, Zhiyu Li, Rui Zhang, Qichen Chen, Hong Zhao,

European Journal of Surgical Oncology, Volume 51, Issue 11,2025,110371,
https://doi.org/10.1016/j.ejso.2025.110371.

Abstract: Patients with synchronous colorectal cancer liver metastasis (CRLM) often face sub-optimal outcomes from systemic therapy or resection. This study investigates the prognostic value of the pre-treatment S-index, a reliable non-invasive marker for liver fibrosis, for outcomes in synchronous CRLM patients. Methods This study included two populations of patients with synchronous CRLM: one population undergoing resection and another population receiving systemic therapy for unresectable CRLM. Pre-treatment S-index levels were assessed from blood samples. Patients were categorized into high and low S-index groups, and comparisons were made regarding outcomes: progression-free survival (PFS), early post-operative recurrence and fibrosis in liver metastases in the resection population, and treatment response in the systemic therapy population. Multiplex immunohistochemistry/immunofluorescence (mIHC/IF) was used to investigate the distribution of immunosuppressive T-cell subsets in liver metastases. Results For synchronous CRLM patients receiving resection (n = 1000), patients with high preoperative S-index demonstrated significantly worse PFS both before (HR = 1.556, 95 % CI: 1.255–1.929; P < 0.001) and after IPTW-adjusted Cox proportional hazards regression analysis (IPTW-adjusted HR = 1.439, 95 % CI: 1.094–1.894; P = 0.036). High S-index patients also exhibited an elevated risk of early recurrence, both before and after adjustment (OR = 1.556, 95 % CI: 1.255–1.929, P < 0.001; IPTW-adjusted OR = 1.439, 95 % CI: 1.094–1.894, P = 0.009). For synchronous CRLM patients receiving system therapy (n = 123), a high pre-treatment S-index (OR = 34.691, P = 0.005) was a significant predictor of progression disease in multivariate analyses. Further, the S-index showed an AUC of 0.814 (95 %CI: 0.762–0.866, P < 0.001) for detecting fibrosis in liver metastases, with a specificity of 0.928. mIHC/IF analysis revealed that inhibitory T cells, especially CD4+PD1+ T cells and CD4+FOXP3+ T cells, were significantly elevated in the liver metastases of the high S-index group. Conclusion This study contributed valuable evidence regarding pre-treatment S-index for association with outcomes among synchronous CRLM patients receiving resection or system therapy. Furthermore, it underscores a significant association between a high S-index and the presence of fibrosis in liver metastases, as well as more infiltration of immunosuppressive T cells in the tumor.

Keywords: Colorectal cancer liver metastasis; Pre-treatment S-Index; Recurrence; Treatment response; Fibrosis

25COASNOV25:

Title: Selection for local treatment and outcomes of surgical resection in patients with synchronous colorectal liver metastases: A nationwide population-based study,

Michelle R. de Graaff, Joost M. Klaase, Macel den Dulk, Dirk J. Grünhagen, R.-J. Swijnenburg,

European Journal of Surgical Oncology, Volume 51, Issue 11, 2025, 110411,
https://doi.org/10.1016/j.ejso.2025.110411.

Abstract: The aim of this study was to evaluate potential disparities in the probability of undergoing surgical treatment among patients with synchronous colorectal liver metastases (CRLM) and to investigate which non-tumour-related characteristics influenced postoperative outcomes. Methods This was a population-based study of all patients diagnosed with synchronous CRLM between 2015 and 2021 in the Netherlands. Data were retrieved from the Netherlands Cancer Registry (NCR) and data of patients who underwent surgical exploration were retrieved from the Dutch Hepato Biliary Audit (DHBA). The association between non-tumour-related factors, the chance of getting local treatment of CRLM and outcomes after resection were evaluated using multivariable logistic regression models. Results From the NCR, 14,047 patients with synchronous CRLM were included. Of these 2753 (20 %) patients underwent local treatment of CRLM. Non-tumour-related factors associated with a lower likelihood of local treatment of CRLM included age (OR 0.94 95 %CI 0.94–0.95) and female sex (OR 0.87, 95 %CI 0.78–0.97). Middle and high Socioeconomic status (SES) compared to low SES (respectively OR 1.35, 95 %CI 1.18–1.54 and OR 1.61, 95 %CI 1.41–1.84) and presentation in a hospital that performed liver surgery (OR 1.52, 95 %CI 1.26–1.84) were associated with a higher likelihood of getting local treatment. From the DHBA 2535 patients were included. Non-tumour-related factors associated with both major morbidity and mortality included age (OR 1.01 95 %CI 1.00–1.03 and OR 1.07, 95 %CI 1.02–1.11, respectively) and ASA-score ≥3 (OR 1.7,95 %CI 1.34–2.29 and OR 2.88, 95 CI 1.92–1.11) respectively. Conclusion In addition to tumour-related factors, non-tumour-related factors, including age, male sex, SES and hospital of presentation, all contributed to the likelihood of getting local treatment for CRLM. As not all these factors influence postoperative outcomes, healthcare systems should also focus on eliminating barriers to accessing appropriate care.

Keywords: Selection; Socio-economic status; Sex; Local treatment; Synchronous colorectal liver metastasis; Postoperative outcomes

25COASNOV26:

Title: Ideal outcomes in pancreatic neuroendocrine tumor vs. adenocarcinoma following resection: A nationwide study using ACS-NSQIP,

Jiage Qian, Sebastiaan Ceuppens, Nikhil V. Tirukkovalur, Kenneth K. Lee, Amer H. Zureikat, Alessandro Paniccia,

European Journal of Surgical Oncology, Volume 51, Issue 11,2025, 110438,
https://doi.org/10.1016/j.ejso.2025.110438.

Abstract: Prior evidence suggests higher postoperative complications in pancreatic neuroendocrine tumors (pNET) compared to ductal adenocarcinoma (PDAC). This study

refines the comparison using the Ideal Outcome (IO) metric and identifies predictors of IO. Methods A retrospective cohort study was performed using the 2014–2023 standard and pancreas-targeted ACS-NSQIP database to identify patients with PDAC or pNET who underwent pancreatoduodenectomy (PD) or distal pancreatectomy (DP). IO was defined as absence of clinically relevant postoperative pancreatic fistula (CR-POPF), prolonged length of stay (LOS), severe complications, reoperation, readmission, and mortality. Results A total of 25,290 PDAC and 4914 pNET patients were included. In PD, IO was lower in pNET (44.2 %) compared to PDAC (56.9 %, $p < 0.001$), with pNET having higher rates of severe complications (31.2 % vs. 19.0 %, $p < 0.001$), prolonged LOS (28.9 % vs. 25.8 %; $p = 0.004$), CR-POPF (26.7 % vs. 10.9 %; $p < 0.001$), and readmission (23.6 % vs. 15.3 %; $p < 0.001$). In contrast, pNET had higher IO after DP (60.1 % vs. 57.1 %; $p = 0.008$), with higher CR-POPF (19.2 % vs. 13.4 %; $p < 0.001$) but lower prolonged LOS (18.5 % vs. 26.4 %; $p < 0.001$). In PD, predictors of lower IO for both histologies included male sex (PDAC aOR 0.83; pNET 0.60), obesity (0.77; 0.63), hypertension (0.89; 0.79), small duct (0.81; 0.75), and soft gland (0.62; 0.57). In DP, minimally invasive surgery was associated with higher IO in both cancer types (PDAC aOR 1.71; pNET 1.52; all $p < 0.05$). Conclusion Compared to PDAC, IO rate for pNET was lower after PD but higher after DP. CR-POPF was consistently higher in pNET, while other components of IO varied by procedure.

Keywords: Pancreatic neuroendocrine tumors; Pancreatic ductal adenocarcinoma; Ideal outcome; Postoperative complications; Pancreatoduodenectomy; Distal pancreatectomy

25COASNOV27:

Title: Improving oncological outcomes for pelvic bone sarcomas: Is it possible?,

Minna K. Laitinen, Vineet J. Kurisunkal, Michael C. Parry, Guy V. Morris, Jonathan D. Stevenson, Lee M. Jeys,

European Journal of Surgical Oncology,Volume 51, Issue 11, 2025, 110416,
https://doi.org/10.1016/j.ejso.2025.110416.

Abstract: Pelvic bone sarcomas are rare, heterogeneous malignancies that present significant diagnostic and therapeutic challenges. Despite advances in imaging, surgical navigation, and multidisciplinary care, it remains unclear whether these innovations have improved outcomes across all histiotypes. Material and methods We conducted a retrospective cohort study of 475 patients surgically treated for primary pelvic bone sarcomas between 2003 and 2022. Patients were stratified into historical (2003–2012) and modern (2013–2022) cohorts. We assessed disease-specific survival (DSS), local recurrence-free survival (LRFS), surgical margin status, reconstruction trends, and adoption of navigation technologies. Results Chondrosarcoma (51 %) was the most common tumour, followed by Ewing sarcoma (16 %) and osteosarcoma (11 %). Use of navigation and patient-specific planning significantly increased in the modern cohort, correlating with reduced positive margin rates (8.5 % vs. 21 %; $p < 0.001$). DSS improved for chondrosarcoma ($p = 0.027$) and chordoma ($p = 0.040$), while LRFS improved for chondrosarcoma ($p = 0.003$), Ewing sarcoma ($p = 0.007$), and chordoma ($p = 0.045$). No significant DSS improvement was seen in osteosarcoma or Ewing sarcoma. Conclusion Advances in centralization, and technical advances have significantly improved local control and survival, particularly for chondrosarcoma and sacral chordoma. However, outcomes for osteosarcoma and ES remain constrained, highlighting the need for ongoing innovation and multidisciplinary strategies.

Keywords: Bone sarcoma; Pelvis; Survival rate; Treatment outcome

25COASNOV28:

Title: Sentinel lymph node biopsy in apparently early-stage ovarian cancer: beyond removal of green nodes and surgical experience,

Stefano Uccella, Anna Catozzo, Beatrice Cattin, Pier Carlo Zorzato, Anna Festi, Mariachiara Bosco, Simone Garzon,

European Journal of Surgical Oncology, Volume 51, Issue 11, 2025, 110394,
https://doi.org/10.1016/j.ejso.2025.110394.

Abstract: Systematic pelvic and para-aortic lymphadenectomy is the standard procedure for surgical staging in apparently early-stage ovarian cancer. The role of sentinel lymph node biopsy remains unclear. To evaluate the diagnostic accuracy, feasibility, and safety of sentinel lymph node biopsy when performed by a single operator with a standardized technique. Methods Case series of 36 patients with apparently early-stage ovarian cancer who underwent surgery performed by a single operator following the SELLY trial protocol. Sentinel lymph node mapping was performed by injecting the tracer into the infundibulopelvic and utero-ovarian ligaments. Sentinel node biopsy was followed by systematic pelvic and para-aortic lymphadenectomy. Results Thirty-six consecutive patients with apparently early-stage ovarian cancer were enrolled; 22 patients underwent immediate surgery and 14 delayed procedures after incidental diagnosis. 86.1 % of patients had successful mapping of at least one SLN, and 54.8 % had successful mapping in both pelvic and para-aortic regions. Three patients had isolated tumor cells (ITCs) and one patient had macro-metastasis in SLN. No cases of false negative SLN were observed. The sensitivity and negative predictive value were 100 %. We had five (13.9 %) postoperative complications not related to the SLN procedure itself. Conclusion SLN is a reliable and safe surgical procedure in apparent early-stage ovarian cancer regardless of immediate and delayed surgery, but strict protocol adherence and expert surgeons are mandatory. SLN mapping in apparent early-stage ovarian cancer is feasible and accurate in detecting lymph node metastasis.

Keywords: Early ovarian cancer; SLN (sentinel lymph node) mapping; Systematic lymphadenectomy; SLN detection rate; SLN sensibility

25COASNOV29:

Title: The impact of immediate lipofilling on oncological outcomes, complication rates and patient reported outcomes in breast conserving surgery: a systematic review and meta-analysis,

James Lucocq, Hassan Baig, J. Michael Dixon,

European Journal of Surgical Oncology, Volume 51, Issue 11, 2025, 110446,
https://doi.org/10.1016/j.ejso.2025.110446.

Abstract: There is concern from in-vitro studies that adipose-derived stem cells could promote cancer recurrence through their proliferative properties. The impact of immediate lipofilling (ILF) in the setting of breast conserving surgery (BCS) on oncological outcomes, complications and patient-reported outcomes are unknown. Methods A systematic search of Medline, Embase and Cochrane Central was conducted for studies investigating the impact of ILF in patients undergoing BCS. Random-effects meta-analysis were conducted for oncological outcomes (local [LR], regional [RR], distant [DR] and overall recurrence).

Results Six studies fulfilled the inclusion criteria including 252 patients. The pooled LR, RR, DR and overall recurrence rates were 2.38 %, 1.52 %, 3.03 % and 5.95 %, respectively (median follow-up, 39 months). A meta-analysis of studies comparing ILF (n = 170) with no-ILF (n = 362) found no difference in LR (OR, 0.77; 95 % CI, 0.19–3.17; p = 0.714), RR (OR 1.73, 95 % CI 0.36–8.21, p = 0.686), DR (OR 1.37, 95 % CI, 0.51–3.63; p = 0.627) or overall recurrence (OR 1.23, 95 % CI, 0.60–2.52; p = 0.569). Cancer-specific survival in the ILF group was 100 % compared to 98.7 % with no-ILF. Post-operative calcifications (12.9 % [21/163] vs. 0 %; [0/72], p = 0.002) and fat necrosis (7.8 % (17/217] vs. 2.8 % [8/283], p = 0.011) were significantly more common with ILF, but early complications (e.g. haematoma and infection) showed no difference (p > 0.05). Three studies reported superior Breast-Q scores in ILF compared to no-ILF. No randomised controlled trials have been conducted. Conclusion Immediate lipofilling following BCS appears oncologically safe, enhances aesthetic outcomes and causes minimal morbidity, but higher-quality studies are required.

Keywords: Lipofilling; Breast conserving surgery; Recurrence; Complications; Patient reported outcome measures

25COASNOV30:

Title: Exploring decision making for treatment in LARC and LRRC: A qualitative study,

Anwen Williams, Claire O'Neill, Hayley Hutchings, Aaron Quyn, Michael Duff, John Ian Jenkins, Claire Taylor, Ben Griffiths, Dean Harris, Martyn Evans, Deena Harji,

European Journal of Surgical Oncology, Volume 51, Issue 11, 2025, 110372,
https://doi.org/10.1016/j.ejso.2025.110372.

Abstract: Decision-making in locally advanced (LARC) and locally recurrent rectal cancer (LRRC) has transformed over recent years. Informed consent and shared decision making have allowed patients to consider what information and factors are individually important to them. There is a limited understanding of the complexities of decision-making in patients undergoing pelvic exenteration (PE) for rectal cancer. The aim of this study was to explore patients and clinicians' perceptions on factors important during the decision-making process. Methods A prospective, cross-sectional, qualitative study was undertaken using in-depth virtual telephone audio recorded interviews across five UK centres between January and October 2020 with both patients and healthcare professionals (HCPs). The transcripts were imported into NVIVO 12 (QSR International Pty Ltd., Melbourne, Australia) and coded using the principles of thematic content analysis. Results Thirty-three interviews (25 patients (76 %) and 8 HCPs (24 %)) were conducted. Thirteen males (52 %) and 12 females (48 %) with a median age of 59 years (range 36–73) were recruited. Median time elapsed between surgery and interview was 7 months (range 3–11). Six themes emerged relevant to decision-making including: communication, recovery, psychological impact, relationships, lifestyle, support. Healthcare professionals focus primarily on treatment expectations, recovery, and psychological impact. Discussion Our study highlights the differing perspectives of patient and HCPs priorities during the decision-making process for PE. Our findings have direct relevance to framing pre-operative counselling discussions in helping patients decide on individual treatment decisions. Policy makers and clinicians need to ensure we are meeting

patients' informational needs by investing into a standardised dedicated service throughout the UK.

Keywords: Pelvic exenteration; Locally advanced rectal cancer; Locally recurrent cancer; Qualitative study; Treatment decisions; Decision making

25COASNOV31:

Title: Feasibility of optical stereotactic navigation for rectosigmoid cancer with deep learning-supported 3D modelling,

Reinier ten Brink, Renske Schram, Gursah Kats-Ugurlu, Thomas Kwee, Patrick Hemmer, Klaas Havenga,

European Journal of Surgical Oncology, Volume 51, Issue 11, 2025, 110397,
https://doi.org/10.1016/j.ejso.2025.110397.

Abstract: The rate of incomplete resection in the surgical treatment of locally advanced primary rectal cancer and locally recurrent rectosigmoid cancer is high. The use of optical stereotactic navigation during surgery has the potential to reduce this risk. This study evaluates the feasibility of its implementation by assessing navigational accuracy and oncological outcomes. Methods In this prospective interventional cohort study, ten patients with either locally advanced cT4bN0–2 rectal cancer or locally recurrent rectosigmoid cancer underwent surgery supported by optical stereotactic navigation at a single tertiary referral centre. Real-time navigation was achieved via a tracked pointer or surgical instrument, using preoperative CT images fused with MRI-based segmentations of the tumour and adjacent structures, partially generated by trained deep learning models. Primary outcomes were navigation accuracy and the rate of R0 resection, defined as a tumour-free margin of ≥1 mm. Results Navigation demonstrated sub-millimetric accuracy with a median target registration error of 0.7 mm (IQR 0.5–1.1). An R0 resection was achieved in 7 of 10 patients (70 %). When analysing only planes where navigation was used, tumour-free margins were obtained in 8 of 10 cases (80 %). No navigation-related complications occurred. Median additional preparation time for navigation was 26 min (IQR 22–51). Surgeon satisfaction was consistently high. Conclusions The demonstrated feasibility and high accuracy support the potential value of this technique, particularly within a tertiary care setting where further refinement and evaluation can take place.

Keywords: Colorectal neoplasms; Colorectal surgery; Artificial intelligence; Surgical procedures; Operative; Oncologic surgery

25COASNOV32:

Title: Chest wall perforator flaps for partial breast reconstruction: An observational cohort study of 290 women to evaluate clinical and oncological outcomes,

Angus Reid, Lewis Sibbering, Isabel Burridge, Loraine Kalra, Adam Critchley, Robert Thomas,

European Journal of Surgical Oncology, Volume 51, Issue 11, 2025, 110430,
https://doi.org/10.1016/j.ejso.2025.110430.

Abstract: Partial breast reconstruction (PBR) using chest wall perforator flaps (CWPFs) is an oncoplastic technique utilised to facilitate breast conservation surgery (BCS). It is particularly applicable in women with a larger tumour-to-breast volume ratio requiring volume replacement rather than volume displacement. This single-centre retrospective cohort

study aimed to explore the safety and efficacy of PBR using CWPFs. Method All patients who underwent PBR using a CWPF following wide local excision between March 2016 and August 2024 were reviewed. Data was extracted from hospital electronic patient records and statistical analysis performed using R-Studio® (alpha = 0.05). Results Of 290 cases identified: 237 had invasive cancers and 53 ductal carcinoma in situ (DCIS). The median age at presentation was 59 years and the median tumour size 22 mm, with multifocal tumours in 22.1 % of cases and extensive DCIS in 27.0 % of invasive cancers. Overall, complication rates were low (n = 83, 28.6 %) with 6.9 % of patients requiring a return to theatre. Margins were involved in 17.8 %, with 15.6 % requiring re-excision. The locoregional recurrence (LRR) rate was 2.9 % and disease-free survival (DFS) 93.8 % with a median follow-up of 3.1 years (n = 276). A subset analysis of women receiving surgery before January 2020 (n = 96) with a follow-up of 5.1 years had a LRR of 4.2 %. Conclusion This study reports acceptable rates of complications, margin re-excision and LRR, demonstrating the safety and efficacy of utilising PBR with CWPFs for the treatment of breast cancer. CWPFs offer the opportunity to extend the boundaries of BCS to those women who may otherwise require a mastectomy.

25COASNOV33:

Title: Rethinking TNM: Tumor deposit-based prognostic models may improve N-staging in colorectal cancer,

Simon Lundström, Erik Agger, Marie-Louise Lydrup, Fredrik Jörgren, Pamela Buchwald,

European Journal of Surgical Oncology, Volume 51, Issue 11, 2025, 110420,
https://doi.org/10.1016/j.ejso.2025.110420.

Abstract: Tumor deposits are an important negative prognostic factor for long-term oncological outcomes in colorectal cancer patients, independent of lymph node status. Several novel models have been proposed to further integrate tumor deposits into the TNM-staging system, but their comparative performance remains unclear. The aim of this study was to identify, compare and validate novel prognostic models incorporating tumor deposits for N-stage classification. Methods A scoping literature review identified novel prognostic models that incorporated tumor deposits or tumor deposit count into N-staging. The identified models were validated using patient data from the Swedish Colorectal Cancer Registry, assessing overall survival, distant metastasis, and local recurrence. Prognostic performance was compared to the TNM N-staging using Kaplan-Meier curves for visual analysis, Harrell's C-index for discriminative ability, and Bayesian information criterion for model fit. Results Of 792 articles, seventeen met the inclusion criteria, resulting in ten unique models in addition to TNM. For the patient cohort, 26,970 patients remained after exclusion, of whom 3,312 (12 %) had tumor deposits. All models were superior to TNM with two models standing out; an integrated model combining lymph node and tumor deposit count, and a ratio model considering number of tumor deposits, positive lymph nodes, and total number of extracted nodal structures. All models provided prognostic value, but differences were modest. Conclusion This study demonstrated that although all models outperformed TNM, prognostic differences between the models were small. While tumor deposits provide valuable prognostic information for high-risk patients, additional risk factors are required to further enhance the staging system.

Keywords: Colorectal neoplasm; Extra nodal extension; Neoplasm staging; Lymph nodes; Prognosis

25COASNOV34:

Title: Comparison of long-term outcomes of 2.5- and 3-field lymph node dissections for esophageal squamous cell carcinoma,

Maohui Chen, Taidui Zeng, Yizhou Huang, Shuliang Zhang, Chun Chen, Bin Zheng,

European Journal of Surgical Oncology, Volume 51, Issue 11, 2025,110435,
https://doi.org/10.1016/j.ejso.2025.110435.

Abstract: Previous studies demonstrated that the mesoesophageal suspension technique is safe and effective for thoracoscopic lymph node dissection in esophageal squamous cell carcinoma (ESCC), but direct comparison with 3-field dissection is lacking. This study aimed to compare 2.5- and 3-field lymph node dissections in terms of survival benefits, recurrence patterns, and complications in patients with ESCC. Methods This was a retrospective study of patients with ESCC who underwent 2.5- or 3-field lymph node dissection (FLD). The outcomes included 30-day mortality, postoperative complications, overall survival (OS), disease-free survival (DFS), and recurrence pattern. Results A total of 353 patients with ESCC were included in this study. After propensity score matching, the frequency of all complications (27.8 % vs. 18.3 %, P = 0.072), recurrent laryngeal nerve injury (5.6 % vs. 0.8 %, P = 0.033) and respiratory complications (19.8 % vs. 11.9 %, P = 0.084) was higher in the 3-field group compared with the 2.5-field group. Smaller number of dissected lymph nodes (median, 31.5 vs. 41, P < 0.001) but comparable number of metastatic lymph nodes (median, 0 vs. 1, P = 0.143) was found in the 2.5-field group compared with the 3-field group. The rate of positive supraclavicular lymph nodes was 1.6 % in the 3-field group. There were no differences OS and DFS between the two groups, with median OS and DFS not reached in both groups. Recurrence pattern of all stage patients was similar between the two groups. Conclusion The 2.5- and 3-FLD have comparable survival benefits for patients with ESCC, while the 2.5-FLD has a lower risk of complications.

Keywords: Esophageal squamous cell carcinoma; Lymph node dissection; Long-term outcomes; Survival; Recurrence

25COASNOV35:

Title: A novel nomogram for predicting long-term survival in patients with esophageal squamous cell carcinoma after minimally invasive esophagectomy,

Jinlong Fang, Ziyang Han, Jingchuan Yu, Weiguang Zhang, Zhixin Huang, Peipei Zhang, Shaobin Yu, Mingqiang Kang,

European Journal of Surgical Oncology, Volume 51, Issue 11, 2025, 110443,
https://doi.org/10.1016/j.ejso.2025.110443.

Abstract: Esophageal cancer is the 7th most common cancer worldwide, while esophageal squamous cell carcinoma (ESCC) is the 4th leading cause of cancer-related deaths in China. Minimally invasive esophagectomy (MIE) is the employed as the primary treatment for ESCC. However, there is still a lack of specialized tools for evaluating postoperative outcomes in these patients. Methods Univariate and multivariate COX regression analyses were conducted to identify the prognostic factors. A nomogram was developed for predicting the survival probabilities at 1-, 3- and 5- year after MIE. The prediction performance of the developed nomogram was evaluated using the receiver operating characteristic (ROC) curve, concordance index (C-index), calibration curve, decision curve analysis (DCA) curve and risk stratification. Results A total of 709 patients were enrolled in the study. Age, vascular

invasion, pT stage and pN stage were independent predictors of the prognosis and were used to develop a nomogram model. The areas under the curve (AUC) values predicting overall survival (OS) at 1, 3 and 5 years were 0.814, 0.761 and 0.794 in the training cohort and 0.703, 0.751 and 0.780 in the validation cohort. Furthermore, the calibration plot revealed good agreement between the predicted results and actual observations. The DCA curve confirmed that the nomogram achieved higher clinical value compared to other indicators. Further, we stratified the entire patient population into low-risk group, medium risk group and high-risk group. A significant difference in survival was observed between the three groups ($P < 0.001$) Conclusions A novel nomogram for predicting ESCC patient's survival outcomes after MIE. The accuracy of the proposed nomogram exceeded that of the Union for Union for International Cancer Control(UICC)/American Joint Committee on Cancer(AJCC) 8th staging systems.

Keywords: Esophageal squamous cell carcinoma (ESCC); Minimally invasive esophagectomy (MIE); Nomogram; Survival

25COASNOV36:

Title: Prognostic significance of early on-treatment evolution of circulating tumor DNA in advanced ER-positive/HER2-negative breast cancer,

A. Mamann, Y. Pradat, F.C. Bidard, S. Delaloge, L. Cabel, I. Faull, S. Marques, T. Bachelot, F. Dalenc,

Annals of Oncology, Volume 36, Issue 11, 2025, Pages 1342-1355,
https://doi.org/10.1016/j.annonc.2025.06.015.

Abstract: Patients with advanced estrogen receptor-positive, HER2-negative breast cancer commonly develop resistance to treatment with hormone therapy and cyclin-dependent kinase 4/6 (CDK4/6) inhibitors. Responders cannot be distinguished from nonresponders after the first cycle of treatment under current practice. We assessed circulating tumor DNA (ctDNA) measures at early timepoints as prognostic markers. Patients and methods Paired plasma samples were collected at baseline and early on-treatment (median 28 days) from 369 patients with advanced ER-positive/HER2-negative breast cancer treated in the PADA-1 trial with hormone therapy and a CDK4/6 inhibitor. Cell-free DNA was profiled with a 497-gene panel (Guardant360 LDT). Results Baseline ctDNA levels, including the mean variant allele frequency (VAF) [progression-free survival (PFS) hazard ratio (HR) 1.07, 95% confidence interval (CI) 1.05-1.09), $P < 0.001$; overall survival (OS) HR 1.08, 95% CI 1.05-1.11, $P < 0.001$] and the number of driver somatic mutations (PFS HR 1.13, 95% CI 1.07-1.19, $P < 0.001$; OS HR 1.16, 95% CI 1.07-1.24, $P < 0.001$) were prognostic. Early on-treatment ctDNA dynamics were also associated with outcomes, including the number of driver somatic mutations with VAF > 0.5% at both timepoints (PFS HR 1.39, 95% CI 1.27-1.53, $P < 0.001$; OS HR 1.51, 95% CI 1.35-1.68, $P < 0.001$) and the number of driver somatic mutations with a VAF increase (PFS HR 1.31, 95% CI 1.19-1.44, $P < 0.001$; OS HR 1.10, 95% CI 1.02-1.18, $P = 0.02$). A ctDNA-based risk model incorporating baseline and dynamic ctDNA features was independently prognostic from RECIST in multivariable models (test set: OS HR 4.10, 95% CI 1.93-8.72, $P < 0.001$; PFS HR 1.86, 95% CI 1.16-2.97, $P = 0.009$). The integration of ctDNA features into a clinical model improved survival discrimination for PFS [C-index 64.7% (± 2.5%) for a ctDNA and clinical model versus 59.3% (± 2.2%) for a clinical-only model, $P = 0.027$] and for OS [C-index 70.0% (± 3.4%) versus 60.3% (± 4.2%),

P = 0.035]. Conclusions Early on-treatment evolution of ctDNA is prognostic for both PFS and OS in advanced ER-positive/HER2-negative breast cancer. A ctDNA-based risk model improves upon traditional RECIST and clinical parameters, advocating for ctDNA as a prognostic biomarker in clinical practice.

Keywords: ER+/HER2− advanced breast cancer; circulating tumor DNA; on-treatment dynamics; survival analysis; prognostic model; risk score

25COASNOV37:

Title: Re-examining post-operative chemoradiotherapy in head and neck cancer: an updated long-term combined analysis of RTOG 9501/EORTC 22931,

Z.S. Zumsteg, M. Luu, C. Fortpied, J.K. Jang, M.M. Chen, J. Mallen-St. Clair, E. Walgama, Q.T. Le,

Annals of Oncology, Volume 36, Issue 11, 2025,Pages 1379-1388,
https://doi.org/10.1016/j.annonc.2025.07.004.

Abstract: Post-operative chemoradiation (CRT) is generally recommended for head and neck cancer patients with extranodal extension (ENE) and/or positive margins, but not for patients without these features, based on a post hoc analysis of Radiation Therapy Oncology Group (RTOG) 9501 and European Organisation for Research and Treatment of Cancer (EORTC) 22931. However, this analysis lacked tests of interaction necessary to identify a predictive biomarker. In addition, updated data are now available. Patients and methods This study assessed 744 patients enrolled on RTOG 9501 and EORTC 22931, randomized trials that compared CRT with radiation (RT) following surgery. Overall survival (OS) was analyzed with Cox regression. Cancer-specific mortality (CSM), other-cause mortality (OCM), and recurrence outcomes were analyzed with competing risks methodology. Tests of interaction assessed for differential benefits of CRT in various subgroups. Results Median follow-up was 6.9 years. Among all patients, CRT improved OS [hazard ratio (HR) 0.81, 95% confidence interval (CI) 0.68-0.97, P = 0.026]. Although CRT improved OS in the subgroup with ENE and/or positive margins (HR 0.71, 95% CI 0.57-0.89, P = 0.003) and not in those without these features (HR 0.94, 95% CI 0.68-1.30, P = 0.7), tests of interaction showed no evidence of a differential effect of CRT in these subgroups (P-interaction = 0.17). There was also no evidence of interaction when analyzing other outcomes, or when assessing ENE and margin status individually. While CRT significantly reduced CSM (HR 0.68, 95% CI 0.55-0.83, P < 0.001), it also significantly increased OCM (HR 1.51, 95% CI 1.07-2.12, P = 0.018). Post-operative CRT improved locoregional recurrence (HR 0.64, 95% CI 0.48-0.85, P = 0.002), but not distant metastasis (HR 0.83, 95% CI 0.64-1.08, P = 0.17). Conclusions Concurrent chemotherapy improved OS in head and neck cancer patients undergoing post-operative radiotherapy in the combined populations of EORTC 22931 and RTOG 9501. ENE and/or positive margins are not predictive biomarkers, and patients without these features may still benefit from CRT. CRT improved CSM, but this was partly offset by higher OCM. Refining the population most likely to benefit from post-operative CRT, taking into consideration both oncologic and patient-related factors, needs further exploration.

Keywords: head and neck cancer; chemoradiation; post-operative

25COASNOV38:

Title: Risk of disease progression in first-line metastatic colorectal cancer therapy to guide disease reassessments—analysis of 11 trials by AIO and GONO☆,

M.M. Germani, V. Heinemann, D. Rossini, L. Fischer von Weikersthal, F. Pietrantonio, K. Heinrich,

Annals of Oncology, Volume 36, Issue 11, 2025, Pages 1307-1318,
https://doi.org/10.1016/j.annonc.2025.08.001.

Abstract: We evaluated the distribution and risk of disease progression (PD) in first-line therapy of unresected metastatic colorectal cancer (mCRC) patients receiving chemotherapy + biologics. The aim of the analysis is to provide guidance for the timing of disease reassessments during first-line therapy. Patients and methods Individual data of 2939 unresected patients from TRIBE, MOMA, TRIBE2, VALENTINO, ATEZOTRIBE, TRIPLETE, FIRE-3, XELAVIRI, PANAMA, FIRE-4 and FIRE-4.5 were analyzed. The frequency and risk of PD events were calculated for individual timepoints during therapy. RAS/BRAF profiling, tumor sidedness, type of therapy and early tumor shrinkage (ETS) were used to identify subgroups for risk assessment. A Cox regression model to predict first-line progression-free survival (PFS) was built. Results In the overall population, the maximum frequency of PD events was observed at 7.6 months, with an absolute PD risk of 19%. Then, the PD risk flattened, achieving a maximum of 23% at 14 months in RAS/BRAF-wild-type patients (n = 1786), 25% at 10 months in RAS-mutant patients (n = 973) and 35% at 8 months in BRAF-mutant patients (n = 180). Eastern Cooperative Oncology Group performance status >0, right-sidedness, initially unresected primary tumor, higher number of organs involved by metastases and BRAF mutation were independently associated with a higher risk of PD in first line. The impact of baseline characteristics on PFS was mitigated after incorporation of ETS in the model. Conclusions The distribution of PD events does not follow a Gaussian pattern, with the highest density observed between the third and fourth reassessment of a bimonthly surveillance schedule. In clearly unresectable patients, restaging should focus on the interval between 6 and 10 months and not on the initiation of systemic therapy. Our model might be helpful to schedule radiological reassessments according to baseline characteristics, early response and the expected duration of each treatment efficacy.

Keywords: metastatic colorectal cancer; first-line chemotherapy; radiological surveillance

25COASNOV39:

Title: Fracture-related hospitalisations in newly diagnosed high-risk localised or metastatic hormone-sensitive prostate cancer: secondary analysis of the STAMPEDE phase III trials of docetaxel and zoledronic acid using healthcare systems data,

C. Jones, P. Dutey-Magni, L.R. Murphy, M.L. Murray, J.E. Brown, E. McCloskey, M. Brown, C.L. Amos,

Annals of Oncology, Volume 36, Issue 11, 2025,Pages 1331-1341,
https://doi.org/10.1016/j.annonc.2025.07.005.

Abstract: Androgen deprivation therapy (ADT), the mainstay systemic treatment for high risk non-metastatic (M0) and metastatic (M1) prostate cancer is associated with bone loss and increased fracture risk. The STAMPEDE trial tested the addition of zoledronic acid (ZA) ± docetaxel (with prednisolone) to ADT. Both regimens may impact bone health. However, long-term fracture incidence remains uncertain. Patients and methods Health systems data

were obtained for patients recruited from England and randomised to standard-of-care (SOC) ADT compared with SOC plus ZA or docetaxel or both docetaxel and ZA. ICD10 diagnosis and OPCS procedure codes from inpatient hospital admissions were used to identify fracture-related hospitalisations. Flexible parametric competing risks models were used to estimate 5- and 10-year cumulative incidence and sub-distribution hazard ratios (SDHR). Results 2140 of 2705 (79%) patients recruited from trial sites in England were eligible for this secondary analysis. Linked data were available for 2042/2140 (96%) pts (734 M0, 1308 M1). 5-year cumulative incidence of fracture for M0 and M1 patients treated with SOC only was 11% [95% confidence interval (CI), 8% to 15%] and 23% (95% CI, 19% to 28%), respectively. 10-year cumulative incidence in M0 patients was 26% (95% CI, 20% to 33%). Allocation to ZA significantly reduced the risk of fracture in M1 patients (SDHR 0.73, 95% CI 0.55-0.97; P = 0.015) but not M0 patients (SDHR 0.88, 95% CI 0.59-1.32; P = 0.549). Docetaxel had no clear effect on the risk of fracture in M0 (P = 0.570) or M1 (P = 0.264) patients. Conclusions High cumulative incidence of fracture was observed in both M0 and M1 prostate cancer patients receiving ADT. The addition of ZA to ADT ± docetaxel significantly reduced long-term fracture risk in M1 participants but had no clear effect in M0 disease. These data support the use of bone protective agents to reduce fracture risk in men with M1 prostate cancer undergoing ADT.

Keywords: prostate cancer; androgen deprivation therapy; fracture; zoledronic acid; docetaxel; health systems data

25COASNOV40:

Title: Incidence trends and long-term survival in early-onset colorectal cancer: a nationwide Swedish study,

S. Barot, A. Liljegren, C. Nordenvall, J. Blom, C. Radkiewicz,

Annals of Oncology, Volume 36, Issue 11,2025,Pages 1400-1408,
https://doi.org/10.1016/j.annonc.2025.07.019.

Abstract: Early-onset colorectal cancer (EOCRC, diagnosis before age 50) is increasing globally. Survival comparisons with late-onset colorectal cancer (CRC) are inconsistent, however, and long-term excess mortality remains poorly understood. This Swedish population-based study aimed to evaluate trends in incidence, survival, and long-term excess mortality in early- versus late-onset CRC. Materials and methods We identified all incident colorectal adenocarcinomas recorded in the Swedish National Cancer Register from 1993 to 2019. Incidence trends were quantified using annual percentage changes and relative survival differences were assessed using excess mortality rate ratios, both from Poisson regression models with 95% confidence intervals (CIs). Results A total of 47 864 right-sided colon, 40 664 left-sided colon, and 47 082 rectal cancer cases were included. EOCRC patients were more frequently diagnosed with metastatic disease, compared with late-onset CRC. EOCRC incidence increased across all subsites, with annual percentage changes ranging from 2.04 (95% CI 1.51-2.56) for rectal to 2.64 (95% CI 2.02-2.37) for right-sided colon cancer, while an increase among late-onset cases was observed only for right-sided colon cancer. Crude 5-year relative survival was similar across age groups, but after full adjustment (including metastatic stage), EOCRC was associated with better survival, with excess mortality rate ratios ranging from 0.76 (95% CI 0.68-0.84) for rectal cancer to 0.83 (95% CI 0.74-0.92) for right-sided colon cancer. Notably, excess mortality remained elevated 5-10 years after

diagnosis in both age groups. Conclusions EOCRC incidence is increasing in Sweden, aligning with global trends. Although younger patients were more often diagnosed at an advanced stage of disease, they had similar crude survival and better stage-adjusted survival, compared with older patients. The persistent long-term excess mortality in both groups, even during periods when CRC patients are typically considered statistically cured, highlights the need for extended follow-up and tailored survivorship care.

Keywords: early-onset colorectal cancer; incidence trends; long-term survival

25COASNOV41:

Title: Prediction of survival after de-escalated neoadjuvant therapy in HER2-positive early breast cancer: a pooled analysis of three WSG trials,

M. Graeser, O. Gluz, C. Zu Eulenburg, S. Kuemmel, R. von Schumann, M. Christgen, R. Wuerstlein,

Annals of Oncology, Volume 36, Issue 11, 2025,Pages 1366-1378,
https://doi.org/10.1016/j.annonc.2025.07.016.

Abstract: We analyzed outcomes and survival predictors in three West German Study Group (WSG) randomized de-escalation trials (ADAPT-HR−/HER2+, ADAPT-TP, TP-II) in human epidermal growth factor receptor 2 (HER2)-positive early breast cancer (eBC) investigating short (12-week) neoadjuvant treatments with or without chemotherapy. Patients and methods A total of 713 patients were analyzed; neoadjuvant chemotherapy (paclitaxel plus pertuzumab plus trastuzumab): n = 149, neoadjuvant chemotherapy-free (pertuzumab plus trastuzumab, trastuzumab-only)/antibody–drug conjugate (ADC, trastuzumab emtansine) treatment: n = 564. Patients with pathological complete response (pCR, ypT0/is ypN0) were allowed to omit further chemotherapy; chemotherapy was mandatory after non-pCR. The primary endpoint of each trial was pCR; survival was the secondary endpoint. Survival was analyzed using the Kaplan–Meier method and Cox regression. Results Median follow-up was 60.7 months. In total, 10 (7%) and 74 (13%) invasive disease-free survival (iDFS) events, 8 (5%) and 51 (9%) distant DFS (dDFS) events, and 6 (4%) and 34 (6%) deaths occurred in the neoadjuvant chemotherapy and chemotherapy-free/ADC groups, respectively; the respective 5-year survival rates were 96% [95% confidence interval (CI) 92% to 99%] and 88% (95% CI 85% to 91%) for iDFS (hazard ratio 0.56, 95% CI 0.29-1.08, P = 0.083) and 98% (95% CI 93% to 99%) and 97% (95% CI 95% to 98%) for overall survival (hazard ratio 0.88, 95% CI 0.36-2.11, P = 0.775). The 5-year iDFS rates in patients with pCR were 98% (95% CI 91% to 99%) after chemotherapy and 94% (95% CI 89% to 97%) after chemotherapy-free/ADC treatment (hazard ratio 0.76, 95% CI 0.27-2.12, P = 0.609). iDFS was comparable between patients with and without adjuvant chemotherapy after pCR to chemotherapy-free/ADC treatment (hazard ratio 1.25, 95% CI 0.39-4.00, P = 0.712). In multivariable analysis, node-negative status and pCR were favorably associated with iDFS in the chemotherapy-free/ADC group. Conclusions This pooled analysis demonstrates that neoadjuvant de-escalation trials with further pCR-adapted treatment (de-)escalation are feasible and appear safe for HER2-positive eBC patients. Twelve-weekly neoadjuvant paclitaxel plus HER2 blockade is effective and well tolerated. Neoadjuvant chemotherapy-free/ADC treatments can be viable alternatives for stage I-II eBC. Excellent survival after pCR to neoadjuvant chemotherapy-free/ADC treatment lays the groundwork for further de-escalation strategies.

Keywords: breast neoplasms; survival; neoadjuvant therapy; paclitaxel; chemotherapy; adjuvant

25COASNOV42:

Title: Pooled analysis of trastuzumab deruxtecan retreatment after recovery from grade 1 interstitial lung disease/pneumonitis,

H.S. Rugo, E. Tokunaga, H. Iwata, V. Petry, E.F. Smit, Y. Goto, D.-W. Kim, K. Shitara, J.F. Gruden,

Annals of Oncology, Volume 36, Issue 11, 2025, Pages 1389-1399,
https://doi.org/10.1016/j.annonc.2025.07.015.

Abstract: Trastuzumab deruxtecan (T-DXd), an antibody-drug conjugate treatment for multiple solid tumors, carries risk of interstitial lung disease/pneumonitis (ILD). Management guidelines generally mandate interrupting T-DXd treatment for grade 1 ILD, with possible retreatment following resolution of imaging findings. This pooled analysis examined T-DXd retreatment duration and ILD recurrence following recovery from grade 1 ILD. Patients and methods Data were pooled from nine clinical trials of patients with various human epidermal growth factor receptor 2 (HER2)-positive, HER2-low, or HER2 (ERBB2)-mutant solid tumors treated with T-DXd (5.4-8.0 mg/kg). ILD events were reported and graded by investigators and confirmed as drug related by an independent ILD adjudication committee. Patients who recovered from a first investigator-assessed grade 1 and adjudication committee-confirmed drug-related ILD event (ILD1) could receive T-DXd retreatment. Patients were evaluated until disease progression or data cut-off. Results Among 2145 pooled patients, 9% (193/2145) had grade 1 ILD1, of which 23.3% (45/193) were retreated with T-DXd. Median retreatment duration was 85 days (range 1-848 days); 17.8% (8/45) of patients received T-DXd retreatment for ≥1 year. ILD recurrence (ILD2) occurred in 33.3% (15/45) of retreated patients; median time to ILD2 from T-DXd retreatment was 64 days (range, 22-391 days) and were low-grade events (grade 1, n = 6; grade 2, n = 9; no grade ≥3 or fatal events). Reasons for T-DXd retreatment discontinuation were disease progression [33.3% (15/45)]; ILD recurrence [20% (9/45)]; non-ILD adverse events [17.8% (8/45)]; and physician's decision [4.4% (2/45)]. At the analysis cut-off, 24.4% (11/45) of retreated patients were still receiving treatment, and most patients with ILD2 [60% (9/15)] had recovered with/without sequelae. Conclusions This first large-scale pooled analysis demonstrates the safety of T-DXd retreatment after recovery from grade 1 ILD. ILD recurred in one-third of patients; all recurrence events were grade 1/2 and manageable using existing treatment guidelines. T-DXd retreatment following resolution of grade 1 drug-related ILD has potential to maximize therapeutic benefit.

Keywords: interstitial lung disease; ILD; pneumonitis; trastuzumab deruxtecan; T-DXd; retreatment

25COASNOV43:

Title: Impact of anthracyclines in genomic high-risk, node-negative, HR-positive/HER2-negative breast cancer,

N. Chen, J.Q. Freeman, S. Yarlagadda, A. Atmakuri, K. Kalinsky, L. Pusztai, J.A. Sparano, D. Huo, R. Nanda, F.M. Howard,

Annals of Oncology,Volume 36, Issue 11,2025,Pages 1356-1365,

https://doi.org/10.1016/j.annonc.2025.08.002.

Abstract: The benefit of anthracyclines for patients with high 21-gene recurrence score (RS) is unclear, despite the widespread use of RS to guide adjuvant chemotherapy treatment for hormone receptor (HR)-positive /human epidermal growth factor receptor 2 (HER2)-negative breast cancer. This study aimed to assess whether patients with RS ≥ 31 would have improved outcomes with the addition of anthracyclines to taxane-based chemotherapy. Patients and methods We included patients from TAILORx with RS ≥ 11 who received treatment with either taxanes with cyclophosphamide (TC) or taxane with anthracyclines/cyclophosphamide (T-AC). Distant recurrence-free interval (DRFI), distant recurrence-free survival (DRFS), and overall survival (OS) were compared, controlling for age, tumor size and grade, receptor status, and RS. Spline regression was used to estimate adjusted hazard ratio (aHR) for receipt of T-AC (versus TC) for these endpoints as a function of RS. Results A total of 2549 patients who received either T-AC or TC were included in the primary analysis. In patients with RS ≥ 31, receipt of T-AC was associated with improved DRFI (5-year rate of 96.1% with T-AC versus 91.0% with TC, aHR 0.31, P = 0.006), DRFS (95.4% versus 89.8%, aHR 0.49, P = 0.032), and a trend toward improved OS (adjusted 5-year rate 97.3% versus 93.6%, aHR 0.67, P = 0.31). Spline regression demonstrated increasing anthracycline benefit with increasing RS. Conclusion Patients with early-stage, HR-positive/HER2-negative breast cancer with the highest genomic risk disease (RS ≥ 31) may benefit from the addition of an anthracycline to taxane-based adjuvant chemotherapy. Genomic RS testing may predict anthracycline benefit more accurately than clinicopathological factors such as nodal status.

Keywords: breast cancer; HR-positive/HER2-negative; recurrence score; anthracyclines

25COASNOV44:

Title: Ten-year survival rates by PSA nadir in patients with metastatic hormone-sensitive prostate cancer: long-term survival analysis from the ECOG-ACRIN 3805 (CHAARTED) trial☆,

A. Tripathi, Y. Chen, D.F. Jarrard, J.A. Garcia, R. Dreicer, G. Liu, M.H. Hussain, D.H. Shevrin, M. Cooney,

Annals of Oncology,Volume 36, Issue 11,2025,Pages 1409-1413, ISSN 0923-7534,
https://doi.org/10.1016/j.annonc.2025.08.004.

Abstract: The CHAARTED trial investigated the long-term survival of patients with metastatic hormone-sensitive prostate cancer (HSPC) treated with androgen deprivation therapy (ADT) with or without docetaxel (Taxotere). This analysis focuses on 10-year overall survival (OS) stratified by disease volume and on-therapy prostate-specific antigen (PSA) levels at 6 months. Patients and methods OS was calculated using the Kaplan–Meier method from randomization to death or last known alive date. Patients were grouped based on baseline disease characteristics [high-volume (HV) or low-volume (LV)] and PSA levels at 6 months (<0.2 ng/ml versus ≥0.2 ng/ml). Multivariable Cox regression analysis was used to evaluate correlation of PSA nadir with OS adjusted for treatment arm, disease volume, Gleason score, and prior local therapy. Results Of 790 patients, 225 were without recorded death after a median follow-up of 10 years. The 10-year OS was 25.9% (ADT + docetaxel) versus 22.5% [ADT; hazard ratio (HR) 0.78, P = 0.004]. HV patients treated with docetaxel had significantly higher OS (20.9% versus 11.4%, P < 0.0001). PSA <0.2 ng/ml at 6 months

was associated with improved median OS in both ADT + docetaxel (100.3 versus 45.4 months, P < 0.0001) and ADT (116.8 versus 31.8 months, P < 0.0001) arms. PSA nadir <0.2 ng/l at 6 months was an independent predictor of improved OS (HR 0.41, P < 0.0001) adjusting for disease volume, prior local therapy, Gleason score and treatment arm. Conclusions Long-term follow-up confirms that ADT + docetaxel significantly improves OS in metastatic HSPC patients with HV disease. PSA nadir <0.2 ng/ml at 6 months is a strong prognostic marker for OS, supporting its use in response-adapted de-escalation strategies.

Keywords: prostate cancer; PSA; docetaxel; androgen deprivation therapy; treatment intensification

25COASNOV45:

Title: Final overall survival and safety analyses of the phase III PSMAfore trial of [177Lu]Lu-PSMA-617 versus change of androgen receptor pathway inhibitor in taxane-naive patients with metastatic castration-resistant prostate cancer,

K. Fizazi, K.N. Chi, N.D. Shore, K. Herrmann, J.S. de Bono, D. Castellano, J.M. Piulats, A. Fléchon,

Annals of Oncology, Volume 36, Issue 11, 2025,Pages 1319-1330,
https://doi.org/10.1016/j.annonc.2025.07.003.

Abstract: In PSMAfore, [177Lu]Lu-PSMA-617 (177Lu-PSMA-617) prolonged radiographic progression-free survival (rPFS) in taxane-naive patients with metastatic castration-resistant prostate cancer (mCRPC), with a favourable safety profile, versus a change in androgen receptor pathway inhibitor (ARPI). We report the final overall survival (OS) analysis and updated safety data. Patients and methods PSMAfore (NCT04689828) was an open-label, international, phase III trial. Patients with prostate-specific membrane antigen (PSMA)-positive mCRPC who had experienced disease progression once on a previous ARPI and were candidates for ARPI change were randomized 1 : 1 to 177Lu-PSMA-617 or ARPI change to abiraterone or enzalutamide. Crossover from ARPI change to 177Lu-PSMA-617 was allowed after centrally confirmed radiographic progression. Endpoints included rPFS (primary), OS (key secondary), and safety (secondary). Results Patients were randomized to 177Lu-PSMA-617 or ARPI change (n = 234 each): 141/234 participants (60.3%) randomized to ARPI change crossed over (75.4% of those with centrally confirmed radiographic progression). The median OS was 24.48 months [95% confidence interval (CI) 19.55-28.94 months] with 177Lu-PSMA-617 versus 23.13 months (95% CI 19.61-25.53 months) with ARPI change [hazard ratio (HR) 0.91, 95% CI 0.72-1.14, P = 0.20] based on the intention-to-treat (ITT) principle; the crossover-adjusted OS HR by inverse probability of censoring weighting modelling was 0.59 (95% CI 0.38-0.91). For 177Lu-PSMA-617 versus ARPI change, exposure-adjusted incidences of grade ≥3 and serious treatment-emergent adverse events were 60.8 versus 85.1 and 32.5 versus 49.9 per 100 patient-treatment years, respectively. Dry mouth occurred in 135/227 participants (59.5%; 2/227 grade ≥3) and anaemia in 62/227 (27.3%; 14/227 grade ≥3) in the 177Lu-PSMA-617 arm. Conclusions OS analyses did not show a statistically significant difference between the 177Lu-PSMA-617 and ARPI arms based on the ITT principle; results were likely confounded by the high rate of crossover. The safety profile of 177Lu-PSMA-617 was favourable with no new safety signals identified.

Keywords: metastatic castration-resistant prostate cancer; radioligand therapy; taxane-naive; 177Lu-PSMA-617; overall survival; safety

25COASNOV46:

Title: Association Between Social Vulnerability Index and Time to Treatment in Resectable Non-Small Cell Lung Cancer,

Arsalan A. Khan, Savan K. Shah, Wara Naeem, Minha Ansari, Gillian C. Alex, Nicole M. Geissen,

The Annals of Thoracic Surgery,Volume 120, Issue 5,2025,Pages 937-945,
https://doi.org/10.1016/j.athoracsur.2025.04.018.

Abstract: Social determinants of health, including race, education, and insurance status, have been linked to delays in non-small cell lung cancer (NSCLC) treatment, although quantification has been challenging. This study investigated whether the social vulnerability index (SVI), a quantitative measure of social determinants of health, is associated with time to treatment. Methods Patients with surgically resected NSCLC at a single institution from 2010 to 2021 were identified. Non-Illinois residents, patients with incomplete addresses, and patients receiving neoadjuvant therapy were excluded. Time to treatment was defined as the interval from chest computed tomographic scan prompting surgery to the surgery date. SVI, ranging from 0 to 100, was calculated using the Centers for Disease Control and Prevention census-tract-level tool. Univariable and multivariable linear regressions assessed the relationship between SVI and time to treatment, with adjustment for demographics and comorbidities. Results Of 890 patients, 55.6% were female and 78.8% were White, with a median age of 71 years (interquartile range [IQR], 64-76 years). The median SVI was 0.31 (IQR, 0.15-0.60), and median time to treatment was 35 days (IQR, 23-67 days). Overall, 13% of patients experienced 30-day major morbidity or mortality, 36% died during the follow-up period, and 26% experienced disease recurrence. Multivariable analysis confirmed that higher SVI ($\beta = 1.18$; $P < .001$), dual Medicaid and Medicare coverage ($\beta = 43.85$; $P < .001$), and lack of insurance ($\beta = 79.21$; $P = .003$) independently predicted delays in time to treatment. Conclusions Higher SVI, Medicaid and Medicare coverage, and uninsured status are associated with increased time to treatment. SVI may help to identify patients at risk for delays in treatment.

25COASNOV47:

Title: Skeletal maturation in patients with cleft lip and palate and normal population analyzed by CVM analysis and the fusion of sphenooccipital synchondrosis,

Qianchuan Ding, Jiangling Sun, Huan He, Haijian Zhu, Binjie Xie, Hongchao Feng, Reinhard E. Friedrich,

Journal of Cranio-Maxillofacial Surgery, Volume 53, Issue 11,2025, Pages 2031-2042,
https://doi.org/10.1016/j.jcms.2025.08.007.

Abstract: The Cervical Vertebral Maturation(CVM) of normal population and cleft lip and palate population was measured by cone beam computed tomography (CBCT). The fusion of sphenooccipital synchondrosis(SOS)was staged, and the correlation between CVM and SOS fusion staging was analyzed. The reliability of CVM in the diagnosis of SOS joint staging provides some reference for clinical evaluation of the growth and development stage of patients. Methods 100 patients with cleft lip and palate and 100 normal people were

randomly selected from January 2020 to December 2023 in Guiyang Stomatological Hospital. There were 121 males and 79 females. The CBCT data of patients were imported into Dolphin software to complete three-dimensional reconstruction and CVM measurement as well as SOS fusion for staging. The experimental results were statistically analyzed by software SPSS25 0.0. The correlation between CVM and SOS fusion staging was analyzed by Spearman analysis. The reliability of CVM diagnosis of SOS fusion staging was calculated by positive likelihood ratio (PositiveLikelihoodRatio,LR+). Results Spearman rank correlation analysis was used to analyze the consistency of CVM and SOS fusion staging. The results are as follows: 1. The correlation between CVM staging and SOS fusion staging and age was studied in normal group A: male group and female group. The results showed that the two staging methods were highly correlated. The Spearman rank correlation coefficient between CVM staging and SOS fusion stage was 0.922. ($p < 0.01$). The correlation coefficient of Spearman grade between SOS fusion degree and age was 0. 842 ($p < 0$ 0.01). 2. Group B: the correlation coefficient of Spearman grade between CVM stage and age was 0.781 ($p < 0$ 0.01). The correlation coefficient of Spearman grade between the fusion degree of SOS and age was 0.765 ($p < 0$ 0.01). Study on the reliability of CVM in the diagnosis of cranial base suture maturity: in group A, CVM1 could diagnose SOS fusion stage 1, CVM2 could diagnose SOS fusion stage 2, CVM3 could diagnose SOS fusion degree 3, CVM4 could diagnose SOS fusion degree 4, while in group B, CVM2 diagnosed SOS fusion stage 3, CVM3 and CVM4 diagnosed SOS fusion stage 4. It can be seen that the degree of CVM and SOS fusion in group B is later than that in group A. Conclusion CVM staging and SOS fusion staging in cleft lip and palate patients were later than those in normal subjects. In normal people and cleft lip and palate people, CVM stage was highly correlated with the degree of SOS fusion, and gradually fused with the increase of age, female SOS fusion earlier than male.In the normal population, there is a clear correlation between CVM (Cervical Vertebral Maturation) stages and the fusion stages of the spheno-occipital synchondrosis. This standardized diagnostic criterion provides important clinical reference for determining orthodontic treatment timing or surgical intervention. However, the situation differs in individuals with cleft lip and palate, as this population may exhibit overall delayed or abnormal skeletal development patterns, making them unsuitable for application of general standards.If accurate discrimination of age is needed, it needs to be confirmed by auxiliary diagnostic methods.

Keywords: CBCT; Cervical vertebral maturation; Spheno-occipital synchondrosis; Jaw development

25COASNOV48:

Title: Mandibular positioning using patient-specific guides and osteosynthesis implants in bimaxillary orthognathic surgery with maxilla-first approach. A 3D-analysis,

Mario Scheurer, Johannes Schulze, Thomas Lins, Tobias Daut, Robin Kasper, Frank Wilde, Alexander Schramm, Marcel Ebeling, Andreas Sakkas,

Journal of Cranio-Maxillofacial Surgery, Volume 53, Issue 11, 2025, Pages 1935-1945,
https://doi.org/10.1016/j.jcms.2025.08.002.

Abstract: The aim of this study was to evaluate the accuracy of a fully 3D planned digital workflow for bimaxillary osteotomies, utilizing patient-specific osteotomy and drill guides (PSDOG) and osteosynthesis implants (PSOI), within a maxilla-first approach. Emphasis was

placed on the accuracy of guided mandibular positioning. This retrospective study included 30 patients undergoing bimaxillary orthognathic surgery [bimaxillary PSDOG/PSOI (Group 1; n = 11) versus maxillary PSDOG/PSOI (Group 2; n = 19)]. 3D CT datasets were used for accuracy assessment. Primary outcome parameter was the accuracy of the intraoperative mandibular transfer evaluated on cephalometric landmarks. Secondary outcome parameter was the 3D accuracy of mandibular positioning. Cephalometric analysis revealed significant vertical undercorrections and lateral deviations in the positioning of proximal mandibular segments (adj. $p < 0.05$). 3D analysis revealed a trend towards lower maximal deviations at the left ascending ramus in Group 1 ($p = 0.058$). Moderate positional accuracy was observed, with the largest vector deviations occurring in the latero-inferior-anterior direction. Iatrogenic injuries and bad splits were lower in Group 1 ($p \geq 0.52$). Duration of surgery did not differ significantly between groups ($p = 0.21$). Fully guided and patient-specific orthognathic procedures enable precise and reproducible mandibular repositioning and may contribute to a reduction in intraoperative complication rates. However, control of the proximal segments, particularly condylar positioning, remains limited.

Keywords: Virtual orthognathic surgery; Sagittal split osteotomy; Patient-specific drill and osteotomy guide; Patient-specific osteosynthesis implant; CAD/CAM; 3D slicer

25COASNOV49:

Title: Postoperative assessment of forehead contouring in facial feminization surgery,

Sead Abazi, Till Schatzmann, Michel Beyer, Lukas Seifert, Neha Sharma,
Journal of Cranio-Maxillofacial Surgery, Volume 53, Issue 11, 2025, Pages 1966-1973,
https://doi.org/10.1016/j.jcms.2025.08.014.

Abstract: Facial feminization surgery (FFS) is essential for transgender women seeking alignment between facial appearance and gender identity. Frontal bone and sinus reshaping is a key component of FFS to achieve a more traditionally feminine contour. This retrospective study evaluates the effectiveness of frontal debossing by comparing pre- and postoperative volumetric and morphometric data. Sixteen patients who underwent frontal debossing at the University Hospital Basel between 2020 and 2024 were included. Preoperative and postoperative CT or CBCT scans were used to assess volume changes in the frontal bone, frontal sinus, and bilateral supraorbital rims. Additionally, changes in the nasofrontal angle were measured. Significant volume reductions were observed in all analyzed structures: left supraorbital rim (mean reduction 792.28 mm3), right supraorbital rim (726.19 mm3), frontal bone (2930.81 mm3), frontal sinus (2508.84 mm3), and combined frontal structures (3251.83 mm3). The nasofrontal angle increased by an average of 21.71°, indicating a substantial improvement in upper facial contour. These results support the clinical value of frontal debossing as an effective and safe component of FFS, providing quantifiable improvements in facial morphology and symmetry. This study further underscores the importance of individualized planning and outcome assessment in gender-affirming craniofacial surgery.

Keywords: Facial feminization surgery; Image processing; Maxillofacial surgery; Precision medicine

25COASNOV50:

Title: Head and neck free flap reconstruction: A prospective case series with the Symani® surgical system,

Johannes Spille, Jörg Wiltfang, Henning Wieker,

Journal of Cranio-Maxillofacial Surgery, Volume 53, Issue 11, 2025, Pages 1957-1961,
https://doi.org/10.1016/j.jcms.2025.08.009.

Abstract: Robotic surgery has undergone steady evolution in recent years. Until now, there has been no suitable robotic system for plastic reconstruction. With the Symani Surgical System, anastomoses of free flaps in the head and neck region can be performed efficiently and accurately. This prospective single-centre study aims to describe and investigate the use of robotic reconstructions in the head and neck region by oral and maxillofacial surgeons for the first time. 93 patients after ablative tumor surgery who required a free flap for reconstruction in the head and neck region were included in the study; 73 had oral squamous cell carcinoma (78.5 %). Radial forearm flap 28 (30.1 %), ulnar forearm flap 28 (30.1 %), and fibula flap 22 (23.7 %) were used most frequently. Three revision surgeries were performed, and one free flap was lost. Robotic microsurgery has a steep learning curve and can be used effectively to perform anastomoses in free flap reconstructions. The surgical spectrum of microsurgical techniques has not yet been fully explored and should be further investigated. Supermicrosurgery could benefit from the Symani robotic system in the long term.

Keywords: Robotic; Oral cavity; Microsurgery; Free flap; Head and neck

25COASNOV51:

Title: Selegiline as an innovative drug for the treatment of inferior alveolar nerve injury: a randomized clinical trial,

Bruno Silva Mesquita, Ana Cláudia Amorim Gomes, Belmiro Cavalcanti Egito Vasconcelos,

Journal of Cranio-Maxillofacial Surgery, Volume 53, Issue 11, 2025, Pages 1974-1980,
https://doi.org/10.1016/j.jcms.2025.08.015.

Abstract: Inferior alveolar nerve (IAN) injuries are common complications of mandibular orthognathic surgery. Selegiline has demonstrated neuroprotective effects in preclinical studies. To evaluate the effect of oral selegiline hydrochloride on neurosensory recovery following bilateral sagittal split osteotomy. Methods A randomized, double-blind, controlled trial was conducted with 40 patients. Participants received either selegiline (5 mg/day for 30 days) or a combination of uridine 5′-triphosphate (UTP), cytidine-5′-monophosphate (CMP), and hydroxycobalamin (three times daily). Neurosensory assessments included two-point discrimination, directional perception, and 1-point sensitivity, evaluated at six time points. Pain was assessed using a visual analog scale (VAS). Results The selegiline group showed earlier improvement in some parameters, especially in 1-point tactile sensitivity of the lower lip at day 15 ($p < 0.05$). Differences in two-point discrimination and directional perception were not consistent. Pain scores were lower in the selegiline group at day 15 ($p < 0.05$). By day 90, both groups had similar recovery levels. Conclusion Selegiline hydrochloride may contribute to early neurosensory recovery after IAN injury, particularly in the lower lip. However, these benefits were limited to specific parameters and time points. Further studies are needed to validate its therapeutic potential.

Keywords: Selegiline; Mandibular osteotomy; Peripheral nerve injuries; Nerve regeneration; Sensory thresholds; Randomized controlled trial

25COASNOV52:

Title: Robotic surgery: The convergence of digital innovations in head and neck surgery,

Yue Liu, Xue Zhao, Chengbi Xu, Dan Yu, Xueshibojie Liu,

Journal of Cranio-Maxillofacial Surgery, Volume 53, Issue 11, 2025, Pages 2005-2011,
https://doi.org/10.1016/j.jcms.2025.08.018.

Abstract: To investigate the application value, technical advantages, clinical efficacy, educational impact, and challenges in promotion of the Da Vinci robotic surgical system (Transoral Robotic Surgery, TORS) in complex head and neck surgeries, providing a reference for the advancement of precise and intelligent surgery in this field. Methods The technical principles and evolution of the Da Vinci system were analyzed. Its clinical application data in laryngeal, oropharyngeal, obstructive sleep apnea (OSA), nasal cavity, and thyroid surgeries were reviewed. The supporting role of digital technologies (AI, 3D visualization, VR, 3D printing) was assessed. Challenges related to cost and training requirements were summarized. Results Leveraging advantages such as instrument flexibility, high-definition 3D visualization, tremor filtration, and precise manipulation, the Da Vinci system significantly enhanced outcomes in head and neck surgery: precise resection of laryngeal cancer reduced operative risks; efficient treatment of early-stage oropharyngeal squamous cell carcinoma (OPSCC) was achieved with fewer complications; favorable long-term survival rates were observed for OPSCC; OSA symptoms were effectively improved; and it demonstrated both minimally invasive benefits and therapeutic efficacy in recurrent nasal cavity cancers and thyroid surgeries. Digital technologies enhanced surgical precision and medical training efficiency. However, high unit costs and stringent training requirements limit its adoption in small and medium-sized hospitals. Conclusion The Da Vinci system, integrated with digital technologies, significantly improves the safety, precision, and patient prognosis in head and neck surgery, while elevating medical education standards. High costs and intensive training needs are issues for why it is not widely used. Future tasks should emphasize cost-cutting to enhance patient care access and improve quality across the medical spectrum.

Keywords: Robotic surgical system; Head and neck surgery; Medical graduate education

25COASNOV53:

Title: Sagittal split ramus osteotomy-enhanced mandibular distraction osteogenesis: A biomechanically superior approach for three-dimensional reconstruction in severe micrognathia,

Xiang Li, Tianyu Zhao, Zhuoga Baima, Kan Li, Siyong Gao, Huanzhong Ji, Wei Sun, Xiang Gao, Guangsen Zheng, Guiqing Liao,

Journal of Cranio-Maxillofacial Surgery, Volume 53, Issue 11, 2025, Pages 1946-1956,
https://doi.org/10.1016/j.jcms.2025.08.005.

Abstract: Mandibular distraction osteogenesis (MDO) remains essential for severe micrognathia correction. The clinical adoption of conventional osteotomy techniques has been constrained by complications including non-union, inferior alveolar nerve injury, and

dental germ damage, compounded by suboptimal occlusal relationships and compromised facial aesthetics. Critical considerations in MDO execution encompass neural structure preservation, osteotomy gap integrity, and achieving three-dimensional skeletal augmentation to enhance both functional stability and craniofacial proportions. Methods Between January 2020 and September 2024, ten patients with severe micrognathia underwent MDO via sagittal split ramus osteotomy (SSRO) or vertical transversal osteotomy (VTO). A subset of patients subsequently underwent staged orthognathic procedures to optimize facial balance. Results SSRO-based MDO (SSRO-DO) demonstrated superior clinical outcomes relative to VTO-DO, evidenced by 3-fold greater osteotomy surface area ($p < 0.01$) and thus 33 % superior central ossification area ratio (COAR) ($p = 0.02$). Postoperative enhance was confirmed with SSRO, achieving significant transverse expansion of mandibular body ($p = 0.02$). SSRO-DO group demonstrated significant improvement in sagittal advancement of mandibular body as well as facial contour against VTO-DO group. Conclusions SSRO-DO demonstrates potential advantages over current VTO-DO. This technique facilitates primary deformity correction and preserves anatomical foundations for subsequent orthognathic refinement. Further studies and long-term follow-up are needed.
Keywords: Distraction osteogenesis; Vertical transversal osteotomy; Sagittal split ramus osteotomy vertical transversal osteotomy micrognathia deformity

25COASNOV54:

Title: Reconstructing complexity: Indications for simultaneous and chimeric free flaps in extensive maxillofacial defects,

Jakob Fenske, Philipp Lampert, Henri Kreiker, Claudius Steffen, Steffen Koerdt, Christian Doll, Norbert Neckel, Max Heiland, Carsten Rendenbach, Kilian Kreutzer,
Journal of Cranio-Maxillofacial Surgery, Volume 53, Issue 11, 2025, Pages 2043-2048,
https://doi.org/10.1016/j.jcms.2025.09.003.

Abstract: Reconstructing complex head and neck defects using multiple simultaneous or chimeric microvascular free flaps is rare, with no established guidelines on indications. This study evaluates the indications, flap combinations, outcomes, and complications associated with these techniques in maxillofacial reconstruction. A retrospective analysis was conducted on patients who underwent either two simultaneous free flaps or chimeric free flaps for head and neck defects between February 2018 and December 2024. Flap success rates and complication rates were assessed. Twenty-two patients received simultaneous free flaps, with a flap-level success rate of 91 % and a complication rate of 55 %. The most common combination was a fibula free flap with an anterolateral thigh flap. Thirty-six patients underwent chimeric flap reconstruction, achieving a success rate of 94 % and a complication rate of 39 %. Indications for these reconstructions fell into three broad categories: extensive composite defects, complex extraoral defects requiring additional bone reconstruction, and defects involving compromised tissues due to prior radiotherapy or multiple surgeries. Chimeric flaps are a viable option for addressing complex defects in more vulnerable patients, while simultaneous free flaps are feasible for selected cases. Despite acceptable success rates, the elevated complication risks associated with simultaneous flaps necessitate vigilant postoperative monitoring.
Keywords: Microvascular free flap; Simultaneous free flaps; Synchronous free flaps; Chimeric free flaps; Maxillofacial reconstruction; Complex defects

25COASNOV55:

Title: Clinical efficacy of subsequent microvascular free flaps in head and neck reconstructive surgery,

Friedrich Mrosk, Emilia Schott, Victoria Vertic, Maximilian Richter, Jan Oliver Voß, Christian Doll,

Journal of Cranio-Maxillofacial Surgery, Volume 53, Issue 11, 2025, Pages 2026-2030,
https://doi.org/10.1016/j.jcms.2025.09.004.

Abstract: Microvascular free flap reconstruction is a standard technique in head and neck surgery with high success rates. Nevertheless, complications like early flap loss, locoregional recurrence of head and neck cancer and osteoradionecrosis may require further flap procedures. This study aims to assess outcomes and challenges associated with subsequent free flap procedures. In this retrospective cohort study, all patients who received subsequent free flaps between January 2013 and December 2022 were assessed and examined by explorative descriptive analysis. Furthermore, one exemplary case is presented. Overall, 69 patients with 150 free flaps were included, with up to 4 subsequently performed flaps. Reasons for subsequent flaps included early failure, local cancer recurrence, osteoradionecrosis and wound healing disorders. After early failures, subsequent flaps were successful in 97 % of this cohort. The more flaps were performed, the more likely the contralateral neck was used for vascular anastomosis and the more likely vein grafts were used. Subsequent free flap procedures are safe and viable options in head and neck reconstruction, even in cases of previous flap failure. Even if previous surgeries, already harvested flaps and radiation therapy might complicate the choice of reconstruction, this should not be a deterrent to achieve consistent rehabilitation of the patient.

Keywords: Subsequent flaps; Multiple flaps; Free flap; Flap success

25COASNOV56:

Title: Technical note: Supine harvesting of subscapular system of flaps combined with the pull-through technique,

Kazuki Hasegawa, Hideo Miyamoto, Tomokazu Sawada, Yoshio Ohyama,

Journal of Cranio-Maxillofacial Surgery, Volume 53, Issue 11,2025,Pages 1962-1965,
https://doi.org/10.1016/j.jcms.2025.08.011.

Abstract: Traditionally, tumor ablation and reconstruction using the subscapular system of flaps require two patient position changes. Consequently, ablation and harvesting cannot be performed simultaneously by two teams, which is a considerable disadvantage of the subscapular flap system. We harvested these flaps using the pull-through technique in the lateral decubitus position to decrease position changes. Even with this procedure, a positioning change was required. Following the 2004 report on supine flap elevation, we adopted a supine approach combined with the pull-through technique, eliminating the need for repositioning and repeated field preparation, and significantly reducing operative time. Overall, 121 subscapular system of flaps were harvested in the supine position employing the pull-through technique wherein flap elevation preceded tumor ablation. Tumor ablation and donor-site closure were then performed simultaneously by two surgical teams. During tumor ablation, the elevated flap remained vascularized by the subscapular vessels, minimizing the ischemic time and allowing continuous monitoring. The risks of patient repositioning under general anesthesia were eliminated. All flaps showed stable vascularity, and harvesting was

uneventful. The combination of supine harvesting and the pull-through technique offered significant advantages in reconstructive procedures utilizing the subscapular system of flaps.
Keywords: Subscapular system of flaps; Supine harvesting; Pull-through technique; Head and neck reconstruction; Simultaneous procedure by two surgical teams

25COASNOV57:
Title: The molecular mechanism of human beta-defensin 1 in inhibiting the progression of head and neck squamous cell carcinoma: The role of the IL-17B/IL-17RB/TRAF6/NF-κB signaling axis,
Shaonan Hu, Simin Li, Wenhao Chen, Guangqin Dai, Xiuhong Huang, Tao Tian, Yaxin Rao, Wanchen Ning,
Journal of Cranio-Maxillofacial Surgery,Volume 53, Issue 11,2025,Pages 1981-1994,
https://doi.org/10.1016/j.jcms.2025.08.016.
Abstract: The present study aimed to investigate the regulatory functions and mechanisms of human β-defensin 1 (hBD-1) in head and neck squamous cell carcinoma (HNSCC) through comprehensive bioinformatics analyses and experimental validation. Comprehensive bioinformatics analyses of TCGA database samples were performed, including DEFB1 expression profiling, clinical correlation analysis, prognostic evaluation, and pathway enrichment studies. The results demonstrated that DEFB1/hBD-1 expression was significantly downregulated in tumor tissues and negatively correlated with key genes in the IL-17 signaling pathway, while being associated with reduced lymph node metastasis and improved overall survival. Immunohistochemical validation confirmed low hBD-1 protein expression in HNSCC tissues. Assessment of hBD-1 expression across multiple HNSCC cell lines revealed consistently downregulated hBD-1 mRNA and protein levels. Functional experiments using stable hBD-1-overexpressing cell models demonstrated that hBD-1 overexpression significantly inhibited cell metabolic activity, clone formation, invasion, and migration while effectively inducing apoptosis. Mechanistic studies revealed that hBD-1 suppressed the IL-17B/IL-17RB/TRAF6/NF-κB signaling pathway by downregulating IL-17B and IL-17RB expression, inhibiting TRAF6 ubiquitination, and decreasing NF-κB pathway protein phosphorylation levels. In vivo xenograft experiments validated that hBD-1 overexpression significantly reduced tumor growth, volume, cell proliferation, and increased apoptosis. These findings collectively demonstrate that DEFB1/hBD-1 functions as a tumor suppressor in HNSCC through suppression of the IL-17B/IL-17RB/TRAF6/NF-κB axis, positioning it as a potential prognostic biomarker and therapeutic target for HNSCC management.
Keywords: Human β-defensin 1 (hBD-1); DEFB1 gene; Head and neck squamous cell carcinoma (HNSCC); IL-17B/IL-17RB/TRAF6/NF-κB signaling pathway; Tumor suppression; Apoptosis

25COASNOV58:
Title: Clinical and radiographic outcomes of dynamic navigation-assisted and freehand zygomatic implant surgery: a retrospective study with an average follow-up of 5 years,
Houzuo Guo, Donghao Wei, Tiziano Testori, Ping Di, Xi Jiang, Ye Lin,
Journal of Cranio-Maxillofacial Surgery,Volume 53, Issue 11,2025,Pages 1995-2004,
https://doi.org/10.1016/j.jcms.2025.08.017.

Abstract: Little evidence was available regarding the long-term clinical outcomes of zygomatic implants placed with dynamic navigation assistance compared to freehand zygomatic implants placement. The study aimed to evaluate the clinical and radiographic outcomes of dynamic navigation-assisted and freehand zygomatic implant placement over an average observation period of 5 years. Zygomatic implants were placed in patients with dynamic navigation assistance or by freehand. Immediate provisionalization was completed within 24 h postoperatively. Permanent restorations were placed for all patients 6–12 months after surgery. Subsequently, annual follow-ups were conducted. Implant survival, mechanical and biological complications, and patient-reported outcomes (PROs) were recorded. Meanwhile, the area of bone-to-implant contact (A-BIC), the implant angle, the implant exit section, the distances to the infraorbital margin (DIO), and the distances to the infratemporal fossa (DIT) were measured on postoperative radiographic images. A total of 28 patients with 52 zygomatic implants completed an average follow-up period of 60.29 ± 11.16 months. The implant survival rates were 96.15 % in both groups. The incidence of paresthesia was significantly higher in the freehand group (11.54 %) compared to the dynamic navigation group (3.85 %). Statistically differences were found between the groups in A-BIC, implant angle, and DIO ($p = 0.007$, $p = 0.011$, and $p = 0.032$). In the freehand group, 3 zygomatic implants (11.54 %) exited to the infratemporal fossa, while no implants in the dynamic navigation group did. The PROs of the two groups showed comparable results. Zygomatic implants exhibited promising long-term survival rates. Limited by a retrospective study design, dynamic navigation-assisted surgery offered potential advantages including significantly reduced complications for patients and a greater bone-to-implant contact area.
Keywords: Zygomatic implant; Dynamic navigation; CBCT imaging; Survival

25COASNOV59:

Title: Fibula free flap reconstruction: improving the accuracy of virtual surgical planning using titanium inserts,

C. Coppen, T. Verhoeven, T.J. Snoeijink, W.L.J. Weijs, A. Verhulst, J.G. van Rijssel, T.J.J. Maal, E.A. Dik,

International Journal of Oral and Maxillofacial Surgery,Volume 54, Issue 11,2025,Pages 1037-1042,
https://doi.org/10.1016/j.ijom.2025.04.1141.

Abstract: Although advancements in three-dimensional (3D) modelling techniques have significantly reduced deviations between planned and actual clinical outcomes in fibula free flap reconstructions, discrepancies between the virtual surgical plan (VSP) and postoperative results persist. In this study, three head and neck surgeons performed 10 fibula osteotomies using conventional cutting templates and 10 osteotomies using more rigid cutting templates with titanium inserts. Differences in 3D angles and segment lengths between the planned and achieved osteotomy planes were calculated. The use of the titanium inserts resulted in a decrease in 3D angular deviation by 0.5° and a reduction in fibula segment length deviation by 0.2 mm for both the short and long sides. The use of the inserts enhanced guidance of the saw and diminished the risk of creating a false route, resulting in a better alignment with the VSP. This may lead to better reconstructive results, decreased operation times, and a potential reduction in complications in a cost-effective manner.

Keywords: Fibula; Free tissue flaps; Plastic surgery procedures; Osteotomy; Surgical oncology

25COASNOV60:

Title: Comparison of a third surgical protocol for the treatment of unilateral cleft lip and palate: a multidisciplinary systematic review and meta-analysis,

V.L. van Roey, S.L. Versnel, A. Heliövaara, S. Alaluusua, S.T.H. Tjoa, E.B. Wolvius, A.B. Mink van der Molen, I.M.J. Mathijssen,

International Journal of Oral and Maxillofacial Surgery,Volume 54, Issue 11,2025,Pages 1043-1070,
https://doi.org/10.1016/j.ijom.2025.04.008.

Abstract: This systematic review and meta-analysis builds upon our previous publication on the outcomes of patients with unilateral cleft lip and palate (UCLP) treated with Oslo protocols (OP; vomerplasty during lip closure vs delayed hard palate closure protocols (DHPCP), comparing the outcomes of these two protocols with those of one-stage palatoplasty protocols (OSPP). A systematic search of the Embase, MEDLINE/PubMed, Web of Science, Cochrane, and Google Scholar databases was conducted until August 2024. In total, 162 articles (156 study groups) were reviewed, including 4040 UCLP patients following OSPP, 1632 following OP, and 791 following DHPCP. The results suggest that intrinsic maxillofacial growth disturbances are common in UCLP patients, regardless of the timing or type of palatal closure. The incidence of velopharyngeal insufficiency was significantly higher in OP (24%) when compared to DHPCP (9%), with OSPP showing an intermediate incidence (14%). However, these findings are of very low certainty due to evident non-reporting bias and limited data. In contrast, OP and OSPP showed lower oronasal fistula (ONF) rates (7% for OP, 10% for OSPP) compared to DHPCP (20%). Altogether, OSPP and OP are favoured over DHPCP due to the lower incidences of ONF, better overall speech outcomes, and fewer primary surgeries.

Keywords: Cleft lip; Cleft palate; Operative surgical procedures; Oral surgical procedures; Treatment outcome

25COASNOV61:

Title: The role of artificial intelligence in implant dentistry: a systematic review,

G. Vázquez-Sebrango, E. Anitua, I. Macía, I. Arganda-Carreras,

International Journal of Oral and Maxillofacial Surgery, Volume 54, Issue 11,2025, Pages 1098-1122,
https://doi.org/10.1016/j.ijom.2025.04.005.

Abstract: The aim of this systematic review was to comprehensively analyse recent studies on the application of artificial intelligence (AI) in dental implantology. The PRISMA guidelines were followed. Five databases were accessed: Scopus, Web of Science, MEDLINE/PubMed, IEEE Xplore, and JSTOR. Documents published between 2018 and October 15, 2024 relating to AI and implantology were considered. Exclusions encompassed reviews, opinion articles, books, conference references, studies using AI as a supplementary method, AI for teaching implant dentistry, and AI for implant fabrication, prothesis, or design. A total of 120 relevant papers were included. Risk of bias was assessed using PROBAST. Findings demonstrated extensive utilization of AI in various aspects of dental

implantology: guided surgery, diagnosis, classification of oral structures, bone classification, classification of dental restorations, implant classification, implant planning, and implant prognosis. Deep learning algorithms were employed in 89.2% of studies, predominantly utilizing image data (72.0% two-dimensional images and 28.0% three-dimensional images). Publications doubled in 2022 compared to the previous year and have remained consistent since. Despite growth, the field remains relatively underdeveloped. However, with advancements in technology and data quality, substantial progress is anticipated in forthcoming years. Remarkably, 11 studies were found to have a high risk of bias.

Keywords: Artificial intelligence; Dental implants; Dental implantation; Neural networks (computer); Machine learning; Systematic review

25COASNOV62:

Title: Splintless maxillomandibular advancement for edentulous sleep apnoea patients: surgical accuracy and efficacy,

J.P.T.F. Ho, N. Zhou, T.C.T. van Riet, C. Klop, R. Schreurs, A.G. Becking, J de Lange,
International Journal of Oral and Maxillofacial Surgery,Volume 54, Issue 11,2025,Pages 1080-1087,
https://doi.org/10.1016/j.ijom.2025.03.013.

Abstract: The primary aim of this study was to assess the accuracy and predictability of a splintless treatment protocol for edentulous patients with moderate to severe obstructive sleep apnoea (OSA) undergoing maxillomandibular advancement (MMA). Ten consecutive edentulous patients treated with MMA were enrolled in this retrospective study. All cases were virtually planned, followed by computer-aided design of individual osteotomy cutting guides and patient-specific implants. For the maxilla, the mean discrepancy between the planned and achieved right to left, posterior to anterior, and cranial to caudal translations was 0.3 ± 0.2 mm, 1.0 ± 0.6 mm, and 0.8 ± 0.6 mm, respectively. There was a mean discrepancy of 0.5° ± 0.5°, 2.5° ± 2.0°, and 0.3° ± 0.4° for roll, pitch, and yaw of the maxilla, respectively. The mean discrepancy of the mandible osteotomy gap was 1.2 ± 1.0 mm on the right side and 0.8 ± 0.5 mm on the left. Surgical success was achieved in nine patients, one of whom met the criteria for surgical cure. On average, the apnoea–hypopnea index was reduced by 72%. The results of this study indicate that the splintless treatment protocol for MMA applied in edentulous OSA patients is highly accurate, predictable, and effective in the treatment of OSA.

Keywords: Orthognathic surgical procedures; Obstructive sleep apnea; Edentulous jaw; Health care outcome assessment; Computer-aided design

25COASNOV63:

Title: Beta-tricalcium phosphate patient-specific gap implants in bilateral sagittal split osteotomy: an innovative treatment method to enhance the mandibular border contour. Part 1: concept and workflow,

G.R.J. Swennen, A. Aksu, F. Reinauer, L. Pottel, Y. Weinberg,
International Journal of Oral and Maxillofacial Surgery,Volume 54, Issue 11,2025,Pages 1071-1079,
https://doi.org/10.1016/j.ijom.2025.01.004.

Abstract: Antegonial notching can occur after bilateral sagittal split osteotomy (BSSO) and may lead to unpleasant aesthetic outcomes in both young and older patients. This clinical study presents a new concept to potentially overcome this problem and describes the workflow. Beta-tricalcium phosphate patient-specific gap implants (β-TCP gap-PSIs) are biocompatible and resorbable bone grafts that are placed in the space of the osteotomy gap during orthognathic procedures; they are virtually planned and printed in 3D. Between July 9, 2017 and July 31, 2018, 14 patients received bilateral β-TCP gap-PSIs during BSSO procedures. Nine were female (64.3%) and five were male (35.7%); mean age at surgery was 32.4 ± 12.7 years and the mean sagittal advancement gap was 9.4 ± 1.74 mm. The immediate postoperative position of the β-TCP implants, as well as early and long-term complications were evaluated; the clinical follow-up was 5 years. Intraoperative placement of the β-TCP implants was achieved without early complications, and the mandibular border contour was rated as very good or good in 82.1% of sides. Two minor long-term complications occurred, resulting in a total grafting success rate of 92.9%. In conclusion, this initial study (part 1) showed the potential of the β-TCP gap-PSI concept in BSSO procedures to prevent antegonial notching, which is currently underestimated and underreported. However, further extensive quantitative assessment is mandatory and will be presented in part 2.
Keywords: Mandibular osteotomy; Bone transplantation; Calcium phosphates; Bone substitutes; Treatment outcome; Cone-beam computed tomography

25COASNOV64:

Title: Immunohistochemical expression of Ki67, CD10, BRAF, and α-SMA tumour markers in ameloblastoma and odontogenic keratocyst,

C. Chen, T. Taheri, M. Batstone, N. Johnson,

International Journal of Oral and Maxillofacial Surgery,Volume 54, Issue 11,2025,Pages 1023-1030,
https://doi.org/10.1016/j.ijom.2025.06.012.

Abstract: Certain tumour markers may play a role in the pathogenesis of ameloblastoma and odontogenic keratocyst (OKC), and may aid the initial diagnostic assessment in selected cases, or possibly serve as prognostic indicators. An immunohistochemical (IHC) study was undertaken to observe the staining patterns of Ki67, CD10, BRAF, and α-SMA tumour biomarkers in relation to ameloblastoma and OKC. Patients treated for ameloblastoma or OKC at the Royal Brisbane and Women's Hospital between January 1, 2008 and December 31, 2020, inclusive, were included. Selected paraffin tissue blocks were retrieved, and slides underwent IHC staining for Ki67 and CD10 (both OKC and ameloblastoma cases) and for BRAF and α-SMA (ameloblastoma cases). Differences were observed in CD10 expression between lesions, with inflammation influencing increased expression in OKC, while unicystic ameloblastoma was usually CD10-positive (87.5%) regardless of inflammation. CD10 and BRAF demonstrated significant differences in location, both presenting higher in mandibular than maxillary ameloblastoma. The study findings suggest that some tumour markers may assist as diagnostic tools in odontogenic lesions; however, tumour marker expression did not demonstrate utility as a prognostic biomarker in ameloblastoma or OKC, where treatment decisions likely played a larger role in the risk of recurrence.
Keywords: Ameloblastoma; Odontogenic tumors; Odontogenic cysts; Immunohistochemistry; Biomarkers; Tumor; Local neoplasm recurrence

25COASNOV65:

Title: Indications and limitations of CAD/CAM splints in Le Fort I osteotomy,

S. Yamamoto, R. Iwadate, K. Maeda, N. Taniike,

International Journal of Oral and Maxillofacial Surgery,Volume 54, Issue 11,2025,Pages 1088-1097,
https://doi.org/10.1016/j.ijom.2025.04.007.

Abstract: The surgical outcome of planned Le Fort I osteotomy (LFI) is important for successful orthognathic surgery. The aim of this study was to evaluate the accuracy of LFI using a CAD/CAM intermediate splint by performing a three-dimensional (3D) comparison of the planned and postoperative maxillary positions. This retrospective study evaluated 31 patients who underwent LFI with a CAD/CAM intermediate splint. The patients were classified into three skeletal malocclusion types: Class III, Class II, and facial asymmetry. Five maxillary reference points and two axes were measured using computed tomography obtained pre-surgery and at 4 days post-surgery and on the preoperative virtual operation 3D images. The 'movement by simulation' and 'deviation from simulation' of the maxilla were analysed by surface superimposition of the virtual LFI osteotomy segments. The deviation from simulation of Class II in the anteroposterior direction, ranging from 1.11 ± 1.05 mm (at PNS) to 3.24 ± 1.09 mm (at U1) (mean ± standard deviation values for the reference points), was significantly more forwards than that of Class III ($P < 0.001$). A detailed 3D study of the accuracy of LFI using CAD/CAM splints revealed high accuracy and good indication for Class III, but low accuracy, with deviation that exceeded the clinically acceptable range, in Class II and facial asymmetry.

Keywords: Orthognathic surgery; Le Fort osteotomy; Dimensional measurement accuracy; Computer-aided design; Occlusal splints

25COASNOV66:

Title: Clinicopathological study of invasion patterns and late cervical lymph node metastasis in pT1/T2 oral squamous cell carcinoma,

Y. Oikawa, M. Fukuda, Y. Noguchi, K. Ito, H. Igarashi, H. Takano,

International Journal of Oral and Maxillofacial Surgery,Volume 54, Issue 11,2025,Pages 1011-1018,
https://doi.org/10.1016/j.ijom.2025.06.010.

Abstract: Despite early-stage oral squamous cell carcinoma (OSCC) often being treated effectively with surgery or radiation, 20–40% of patients develop late cervical lymph node metastasis (LCLM), significantly impacting survival rates. This clinicopathological study was performed to investigate the association between invasion patterns and LCLM with pT1/T2 OSCC, treated surgically without preoperative chemotherapy or radiation; 145 patients were included, of whom 21 developed LCLM. Various histopathological factors were analysed, including depth of invasion (DOI), grade, pattern of invasion (POI), and the Yamamoto–Kohama classification. Multivariable analysis revealed that grade and POI were independent prognostic factors for LCLM; higher grade (hazard ratio 3.49, $P = 0.043$) and POI (hazard ratio 9.35, $P = 0.007$) were associated with an increased metastasis risk. Notably, 88.9% of cases with worst pattern of invasion-5 (WPOI-5) demonstrated LCLM. The study suggests that a combination of POI and grade should be considered for more accurate prediction and management of the LCLM risk, potentially guiding decisions on elective neck dissection to

improve patient outcomes. However, WPOI-5 is difficult to identify from biopsy specimens, highlighting the need for a comprehensive approach combining multiple factors to accurately identify cases with a poor prognosis.

Keywords: Squamous cell carcinoma of head and neck; Lymphatic metastasis; Neoplasm invasiveness; Lymph node dissection; Surgical pathology

25COASNOV67:

Title: Robotic modified radical neck dissection for thyroid carcinoma using a gas-insufflation one-step single-port transaxillary (GOSTA) approach,

Young Woo Chang, Dohoe Ku, Da Young Yu, Seung Yeon Ko, Hye Yoon Lee, Gil Soo Son,
Asian Journal of Surgery,Volume 48, Issue 11,2025,Pages 6684-6690,
https://doi.org/10.1016/j.asjsur.2025.07.182.

Abstract: To evaluate the feasibility, safety, and surrogate oncologic markers of robotic modified radical neck dissection (MRND) using the gas-insufflation one-step single-port transaxillary (GOSTA) approach compared with conventional open MRND. Methods Between January 2018 and December 2024, 69 patients with papillary thyroid carcinoma (PTC) underwent MRND, with 39 patients receiving open MRND (OMRND) and 30 undergoing robotic MRND (RMRND) using the GOSTA approach. Data on clinical and pathological characteristics, perioperative outcomes, and complications were analyzed using statistical tests to compare both groups. Results The mean operative time was significantly longer in the RMRND group than in the OMRND group (297.8 ± 95.8 min vs. 237.2 ± 128.5 min, p = 0.03). However, there were no significant differences in postoperative hospital stay, unstimulated thyroglobulin (Tg) levels before first RAI, or stimulated Tg levels at the first radioactive iodine (RAI) therapy. The number of harvested and metastatic lateral lymph nodes was comparable between the groups (p = 0.51 and p = 0.31, respectively). The complication rates were similar, with no significant differences in transient or permanent recurrent laryngeal nerve palsy, hypoparathyroidism, or other surgical complications. Conclusion Robotic MRND using the GOSTA approach is a feasible and safe alternative to open MRND, providing comparable oncologic outcomes with enhanced cosmetic benefits.

Keywords: Follicular thyroid carcinoma; Papillary thyroid cancer; Thyroidectomy; Thyroid neoplasm; Robotic surgical procedure

25COASNOV68:

Title: Survival outcome with liver resection versus percutaneous radiofrequency ablation in patients with 2–3 cm single hepatocellular carcinoma,

Yi-Hao Yen, Yueh-Wei Liu, Sheng-Nan Lu, Tsung-Hui Hu, Jing-Houng Wang, Chao-Hung Hung,
Asian Journal of Surgery, Volume 48, Issue 11, 2025, Pages 6691-6698,
https://doi.org/10.1016/j.asjsur.2025.07.186.

Abstract: Previous studies have yielded inconclusive results regarding the efficacy of percutaneous radiofrequency ablation (RFA) versus liver resection (LR) in patients with early-stage hepatocellular carcinoma (HCC), specifically those classified as Barcelona Clinic Liver Cancer (BCLC) stage A with a single 2.0–3.0 cm tumor. To date, only one study has applied propensity score matching (PSM) to investigate this comparison; however, its findings are limited by the lack of data on liver function reserve and BCLC staging, which

incorporates performance status (PS) as a key component. Methods Between 2011 and 2021, we enrolled 378 patients who underwent LR and 238 patients who underwent RFA for BCLC stage A HCC with a single 2.0–3.0 cm tumor and Child–Pugh class A liver function. PSM was performed based on age, sex, alpha-fetoprotein level, Charlson Comorbidity Index, hepatitis B surface antigen (HBsAg), anti-hepatitis C virus (anti-HCV) status, receipt of antiviral therapy, and clinically significant portal hypertension. Overall survival (OS) and recurrence-free survival (RFS) were analyzed using the Kaplan–Meier method. Results Before PSM, LR was associated with significantly better survival outcomes compared to RFA (five-year OS: 83 % vs. 61 %, $p < 0.001$; five-year RFS: 62 % vs. 30 %, $p < 0.001$). After PSM, LR continued to demonstrate a significant survival advantage (five-year OS: 80 % vs. 60 %, $p = 0.001$; five-year RFS: 58 % vs. 32 %, $p < 0.001$). Conclusions LR provides a superior survival benefit compared to RFA in patients with early-stage HCC presenting with a single 2.0–3.0 cm tumor.

Keywords: Hepatocellular carcinoma; Percutaneous radiofrequency ablation; Liver resection

List of Serials
Abstracted in COAS
COAS, Volume- 2 Issue No. 11, 2025

1. American Journal of Roentgenology, Volume-225, Issue- 4, 2025
2. Annals of Oncology, Volume-36, Issue - 10 and 11, 2025
3. Annals of Oncology,Volume 36, Issue 11, 2025
4. Anticancer Research, Volume- 45, issue 11, 2025
5. Archives of Pathology and Laboratory Medicine, Volume-149, Issue -10, 2025
6. Asian Journal of Surgery,Volume 48, Issue 11, 2025
7. Biochimica Et Biophisica Acta (BBA) Review of Cancer, Volume- 1880, Issue 6, 2025
8. Blood , Volume-146, Issue- 8 and 9, 2025
9. British Journal of Anaesthesia,Volume 135, Issue 5,2025
10. Cancer Cytopathology, Volume-133, Issue -11, 2025
11. Cancer Gene Therapy, Volume- 32, Issue 11, 2025
12. Cancer, Volume -131, Issue 19,20,21,22, 2025
13. European Journal of Surgical Oncology,Volume 51, Issue 11, 2025
14. International Journal of Cancer, Volume-157 , Issue- 6 and 7, 2025
15. International Journal of Oral and Maxillofacial Surgery,Volume 54, Issue 11, 2025
16. JAMA Oncology , Volume-11, Issue- 7 and 8, 2025
17. Journal of American Chemical Society, Volume -147, Issue 40,41,42,43,44,45, 2025
18. Journal of Cardiothoracic and Vascular Anesthesia, Volume 39, Issue 11, 2025
19. Journal of Clinical Anesthesia, Volume 107, 2025
20. Journal of Clinical Oncology, Volume 43, Issue- 18,19,20,21 and 22. 2025
21. Journal of Clinical Pathology, Volume- 78, Issue- 11, 2025
22. Journal of Cranio-Maxillofacial Surgery,Volume 53, Issue 11, 2025
23. Journal of Intensive Care Medicine, Volume 40, Number 11, 2025
24. Journal of Pain and Symptom Management, Volume 70, Issue 5, 2025
25. Medical Oncology, Volume- 42, Issue- 10, 2025
26. Nature Cell Biology, Volume -27, Issue 10, 2025
27. New England Journal of Medicine, Volume- 393, Issue- 11 and 12, 2025
28. The American Journal of Surgical Pathology, Volume-49, Issue- 11 , 2025
29. The Annals of Thoracic Surgery,Volume 120, Issue 5, 2025
30. Toxicology Letter, Volume- 413, 2025

November 2025, Volume 2 Issue 11

Current Oncological Abstract Service (COAS)

Chittaranjan National Cancer Institute
(An Autonomous Body under Govt. of India, Ministry of Health & Family Welfare)
1st Campus,Hazra: 37,S.P.Mukherjee Road, Kolkata-700026
2nd Campus,New Town: Street Number 299, DJ Block, Action Area I,New Town, Kolkata-700160